EFFECT OF ROOFTOP GREENERY ON OUTDOOR MEAN RADIANT TEMPERATURE IN THE TROPICAL URBAN ENVIRONMENT

TAN CHUN LIANG

(B.Arch. (Hons.), NUS; M.Arch., NUS)

A000355Y

A THESIS SUBMITTED
FOR THE DEGREE OF DOCTOR OF PHILOSOPHY

DEPARTMENT OF BUILDING
SCHOOL OF DESIGN AND ENVIRONMENT
NATIONAL UNIVERSITY OF SINGAPORE

2015

DECLARATION

I hereby declare that this thesis is my original work and it has been written by me in its entirety. I have duly acknowledged all the sources of information which have been used in the thesis.

This thesis has also not been submitted for any degree in any university previously.

……………………………………………………………

Tan Chun Liang

22/06/2015

ACKNOWLEDGEMENTS

I would like to express my immense and sincere gratitude to Professor Wong Nyuk Hien, who has been a guiding light to my journey in exploring urban greenery. Associate Professor Tan Puay Yok and Associate Professor Nalanie Mithraratne for their expert guidance and willingness to enrich me with their knowledge and experience.

Dr. Steve Kardinal Jusuf, whose brilliance I can only try to emulate. This thesis would not have been possible without him, as well as expert advice and guidance from Mr Marcel Ignatius, Ms Lee Seu Quin, Ms Religiana Hendarti, Mr Daniel Hii, Mr Alex Tan, Ms Norishahaini Binti Mohamed Ishak and Ms Erna Tan.

Mr Komari, Mr Zaini and Mr Guna for their technical assistance and always accommodating to my numerous requests.

Mr Chiam Zhiquan, Mr Sim Yong Xiong, Mr Zheng Kai, Ms Alvina Au-Yong and Ms Chia Pei Yu for enduring my physically and mentally demanding requests for field measurement and data analysis.

Mr Zac Toh of Chop Ching Hin Pte Ltd, whose introduction was nothing short of divine intervention. I hope our aspirations for urban greenery can be realized in good time.

Ms Natalie He, who has been an unwavering pillar of support in my most trying moments.

This study would not have been possible without any one of them.

In the five years, I have learned many things and experienced countless epiphanies, the most important being a staunch respect for nature. Nature speaks to us through science, and this thesis is but a modest testimony to her splendor.

Tan Chun Liang

EXECUTIVE SUMMARY

Urbanization has been widely acknowledged to be a major contributory factor to many environmental issues. Some issues include global warming and pollution. Rising temperature due to climate change and the Urban Heat Island (UHI) effect has led to intensive research into adaptive and mitigative strategies to improve thermal comfort.

The implementation of urban greenery has become a widely accepted way of mitigating effects of climate change and the Urban Heat Island effect. In view of this, there is a need for the formulation of an objective framework for selection and allocation of urban vegetation. This will ensure sensible design and planning practices that do not adhere chiefly to aesthetics, and that ecosystem resources can be optimised.

With the main focus of quantifying air (t_a) and mean radiant temperature (t_{mrt}) attenuation profiles of rooftop greenery, the proposed research seeks to achieve the following objectives:

1. To quantify characteristics of rooftop greenery and measure their effects on t_a and t_{mrt}; and
2. To develop a model framework for selection and allocation of greenery in the urban environment.

This is done by correlating changes in temperature with vegetative attributes such as plant evapotranspiration rate and shrub albedo.

A regression model is established using data of this study. The model substantiates the need to evaluate plants based of quantifiable traits and sets the framework for plant selection and allocation based on their heat reduction potential.

LIST OF FIGURES

LIST OF TABLES

ABBREVIATIONS

AE	Actual Evapotranspiration Rate
ALB	Average Surface Albedo
ASHRAE	American Society of Heating, Refrigeration, and Air-Conditioning Engineers
ASL	Atmospheric Surface Layer
BCA	Building and Construction Authority
BPR	Building Plot Ratio
BR	Bowen Ratio
BREB	Bowen Ratio and Energy Balance
CBD	Central Business District
DEMs	Digital Elevation Model
ET	EvapoTranspiration rate
ETTV	Envelope Thermal Transfer Value
GIS	Geographical Information Systems
GPR	Green Plot Ratio
IBM SPSS	IBM Statistical Package for the Social Sciences
ISO	International Organisation Standardization
LAD	Leaf Angle Distribution
LAI	Leaf Area Index
LRA	Landscape Replacement Area
NParks	Singapore National Parks Board
PAR	Photosynthetically Active Radiation
PE	Potential Evapotranspiration
PET	Physiological equivalent temperature
PT model	Priestley-Taylor model
PVC	Polyvinyl Chloride
SET	Standard Effective Temperature
SVF	Sky View Factor
TAS	Thermal Analysis Simulation
UGS	Urban Green Spaces
UHI	Urban Heat Island
UNGI	Urban Neighbourhood Green Index
UTCI	Universal Thermal Climate Index
WBGT	Wet Bulb Globe Temperature

TABLE OF CONTENTS

1 INTRODUCTION

Modern civilisation has improved our lives in many ways. It has also produced a new environment, creating issues of adaptation. These issues include global warming, industrial waste, and pollution. As urban population increases at the global scale, more people will be affected by these issues (UN, 2004). Towards the end of the 21st century, average surface temperature increase is projected to be between 0.3 °C to 6.5 °C (IPCC, 2007). The rise in temperature will have a severe impact on thermal comfort of urbanised outdoor areas.

Outdoor spaces are important as it encompasses pedestrian traffic as well as various outdoor activities. Increased outdoor activity in urbanised areas can generate many positive attributes (Hakim et al., 1998; Jacobs, 1961). Therefore, it is important for outdoor spaces to be properly designed. The outdoor microclimate is an important factor that determines quality of outdoor urban spaces as it affects thermal comfort and subsequent usage (Nikolopoulou and Lykoudis, 2007).

Methods used to curb the rise in temperature are often categorised into mitigation or adaptation strategies (Smit, 1993). Mitigation is an effort to deal with the causes of changes in climate. Adaptation strategies are concerned with finding appropriate responses to effects of climate change. It may be autonomous (for example, intuitive action by individuals) or fostered (for example, by policy). Both adaptation and mitigation are needed and are mutually complementary (Figure 1). Provision of greenery into the urban landscape can be considered, to a certain extent, as both an adaption and mitigation strategy.

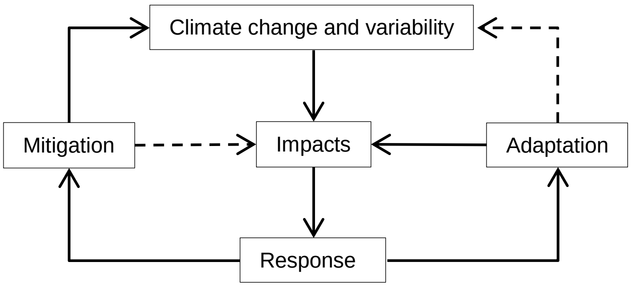

Figure 1. Mitigation and adaptation (Smit, 1993)

1.1 Urban greenery

The outdoor urban environment is different from the rural landscape, with vastly different proportions of built-up area and vegetation (Johansson, 2006; Shashua-Bar and Hoffman, 2003). These factors can affect urban microclimate via the UHI effect, which is an increase in night time air temperature in the city. The UHI effect is aggravated by loss of outdoor greenery, as it can help to improve the built environment microclimate, adapt to changes in the climate and lower energy consumption (Ali-Toudert and Mayer, 2007; Eliasson, 2000; Kurn et al., 1994; Oke, 2006; Oke et al., 1989). Benefits of vegetation in cities continue to be validated around the world. Many studies have confirmed the reduction of air temperature and improvement of outdoor thermal comfort due to introduction of greenery in the urban environment (Berkovic et al., 2012; Correa et al., 2012; Hwang et al., 2010; Hwang et al., 2011; Lin et al., 2010; Lin et al., 2012b; Mahmoud, 2011; Makaremi et al., 2012; Nasir et al., 2012; Ng and Cheng, 2012; Picot, 2004; Shashua-Bar and Hoffman, 2000; Shashua-Bar and Hoffman, 2003; Yan et al., 2012). Savings in building cooling load have also been documented in many studies (Akbari et al., 1997b; Donovan and Butry, 2009; Rosenfeld et al., 1998; Sander et al., 2010). Shade provided by trees can help to reduce a significant amount of incident solar radiation, thereby lowering surface temperature of the building envelope (Papadakis et al., 2001; Tooke et al., 2011). Ground level vegetation can serve as windbreaks and decrease wind-induced loading for low-rise buildings (Stathopoulos et al., 1994). Studies have also shown an inverse relationship between crime rate and greenery coverage (Troy et al., 2012), as well as the potential of trees for carbon sequestration and emissions trading (McHale et al., 2007).

The temperature reducing effect of vegetation in urban microclimates is simulated in many studies. Simulation enables architects and urban planners to predict potential savings in cooling load due to addition of greenery as well as to aid in design decisions such as street orientation and placement of ground level vegetation (Ali-Toudert and Mayer, 2007; Gulyás et al., 2006; Jesionek and Bruse, 2003; Matzarakis et al., 2010; Raeissi and Taheri, 1999; Shashua-Bar and Hoffman, 2002; Shashua-Bar and Hoffman, 2004; Simpson, 2002; Wang, 2006).

Recognising the benefits of urban vegetation, several major cities have incorporated the provision of greenery in their urban planning policy (Greater London Authority, 2004; HKSAR Government, 2010; NYC, 2011; Sydney, 2011; Tan et al., 2013b; Zhao, 2011). There are several ways of incorporating greenery into the urban landscape. At the larger scale, green zones can be identified within city limits and strategically sited to provide thermal comfort for its inhabitants (Gómez et al., 2001). At the micro scale, suitable tree species will be identified and planting site conditions assessed to ensure a conducive environment for growth and species diversity (Jim, 1999; Jim and Zhang, 2013). Urban spatial quality can be evaluated by means of thermal comfort or heat stress indices (Nikolopoulou and Steemers, 2003), or by a critique of landscape elements such as visual quality of tree forms (Müderrisoğlu et al., 2006).

Evaluation of urban greenery can be done in many ways. Vegetation can be analysed in tandem with thermal comfort indices to determine the impact of greenery on outdoor thermal comfort (Lin et al., 2008). The Leaf Area Index is one of the factors used to quantify tree canopy and solar insolation (Fahmy et al., 2010). LAI is defined as a 'dimensionless value of the total upper leaves area of a tree divided by the tree planting ground area' (Jonckheere et al., 2004). Higher values of LAI will result in higher levels of shade, as shown in studies that have quantified the LAI of different tree canopies and effective shade coverage (Kotzen, 2003; Shahidan et al., 2010). Computer modelling of trees can be done to observe the quality of the radiant environment due to their placement (Kotzen, 2003; Lindberg and Grimmond, 2011; Shahidan et al., 2012; Shahidan et al., 2010). The amount of greenery can be varied and its effect on air temperature quantified by empirical models (e.g. Green CTTC model (Shashua-Bar et al., 2010)). Height and physical dimensions of trees, as well as configuration of tree clusters can be varied using computer modelling to determine optimal daylight provision (Hongbing et al., 2010).

1.2 Optimizing ecosystem services

An ecosystem service is defined as the processes through which a natural ecosystem aids in sustaining and improving anthropogenic needs. Ecosystem services maintain biodiversity and production of ecosystem goods such as seafood, biomass fuels and pharmaceuticals (Daily, 1997).

Ecosystem services can be categorized in numerous ways and can be grouped according to numerous functional attributes (De Groot et al., 2002). Ecosystems influence climate locally as well as globally. At the mesoclimatic scale, vegetative ecosystems aid in carbon sequestration. At the microclimatic precinct scale, changes in greenery coverage can influence humidity and temperature. Urban greenery can be considered to be an ecosystem service that aids in climate regulation.

The concept of urban greenery as an ecosystem service is essential for a healthy urban environment. Application of urban greenery to improve the urban environment is analogous to the concept of streamlining processes of building design and construction for optimal performance. In the design and construction of a building, decisions on placement and orientation can be made in view of prevailing wind conditions. Building materials can be selected for their heat transmission attributes. Similarly, deployment of plants in the urban environment can also be done with an emphasis on how different types of plants and their placement can improve outdoor conditions. It is in this light that the full potential of urban greenery design as an ecosystem service can be realised.

1.3 Research question

Urban environments comprise mainly built-up areas, leaving little space for proper landscaping. Therefore, there is a need to realise the cooling potential of every bit of urban greenery. The decision to site the next tree or shrub should take into consideration factors such as plant species, planting location, physical dimensions, etc. What is the impact of the increased usage of rooftop greenery in the city landscape? There is a need to quantify traits inherent in urban vegetation that contribute to the reduction of temperature and to develop a framework for the objective selection and placement of plants in the urban environment. This leads to the research question:

What are the factors that contribute to the reduction of mean radiant temperature by rooftop greenery in the tropical urban landscape, and how do we test for these factors?

1.4 Objectives and scope of research

The implementation of urban greenery has become a common way of mitigating effects of temperature rise in the urban environment. There is therefore a need for the formulation of an objective framework for selection and allocation of urban vegetation. This will ensure sensible design and planning objectives that do not adhere solely to aesthetics, and that ecosystem resources can be optimised.

In this study, the criteria to which temperature reduction potential of plants is assessed is through evaluation of mean radiant temperature (t_{mrt}).The t_{mrt} is one of the main factors affecting outdoor thermal comfort, as shown in studies that have confirmed the high dependence on both long and short wave fluxes from the surroundings (Mayer, 1993; Mayer and Höppe, 1987).

With the main focus of quantifying t_{mrt} attenuation profiles of urban vegetation, the proposed research has the following objectives:

1.4.1 Objective 1

To quantify the effect of rooftop greenery on temperature in the tropical outdoor environment.

1.4.2 Objective 2

To identify plant traits that influence the reduction of temperature in the tropical outdoor environment.

1.4.3 Objective 3

To develop a model framework for selection and allocation of greenery in the tropical urban environment.

This is done by correlating changes in temperature with vegetative attributes such as:

1. Plant evapotranspiration rate; and
2. Shrub Albedo.

The scope of this study is restricted to plants that are commonly found in the tropical urban environment and recommended by the National Parks Board of Singapore for use in rooftop greenery.

1.5 Thesis structure

Chapter 1 highlights how greenery can be utilised to mitigate the issue of rising temperature in the urban environment, and the need for this process to be optimised. Objectives and scope of this thesis are elaborated.

Chapter 2 reviews literature on the role of vegetation in the urban environment. The first part looks into the microclimate of Singapore. The second part explores the impact of greenery on the built environment. The third part presents methods of measuring effects of greenery on the environment. The fourth part highlights aspects of plant physiology and processes that can influence the thermal environment. The fifth part illustrates the role of mean radiant temperature in establishing thermal comfort. The knowledge gap is subsequently identified.

Chapter 3 elaborates on the hypotheses and research methodology used for this study. The process of recalibrating the existing ASHRAE t_{mrt} formula for use in the tropical urban environment is described in this chapter. Final deliverables and potential contribution to science are outlined. Limitations of this study are discussed.

Chapter 4 presents results and analyses from the main study on the effect of rooftop greenery on t_{mrt}.

Chapter 5 introduces the mean radiant temperature reduction regression model based on plant attributes, using data collected from the preceding chapter. A series of sensitivity analyses are performed with the model. A plant selection chart is derived using the regression model.

Chapter 6 explores applicability of the regression model. The importance of plant selection for rooftop greenery is elaborated in this chapter. A hypothetical design scenario is presented to illustrate application of the landscape planning framework derived from findings of this study.

Chapter 7 serves to conclude the thesis. Limitations to the study as well as future directions for research are identified.

In addition to field measurement data, the appendix contains information on additional studies conducted with intent to better understand the impact of greenery on mean radiant temperature in the tropical urban environment. The studies are as follows:

- Large scale urban mapping of mean radiant temperature;
- Impact of plant height stratification on mean radiant temperature;
- Impact of vertical greenery on mean radiant temperature;
- Analysis of similar plant types in horizontal and vertical setup; and
- Review of the role of greenery in green building rating tools.

2 LITERATURE REVIEW

2.1 Urban microclimate of Singapore

Urban Heat Island (UHI) is a phenomenon where temperature in an urbanised region is drastically higher than rural areas around it. This may be due to the reduction of green spaces, low wind speed arising from high built-up density and albedo of urban surfaces (Takahashi et al., 2004). More heat is trapped by buildings and asphalt surfaces, which results in an increased demand for air conditioning, leading to higher temperatures (Crutzen, 2004). Figure 2 shows air temperature profiles across different parts of an urban area for both night and day of a city suffering from the UHI effect (Voogt, 2004).

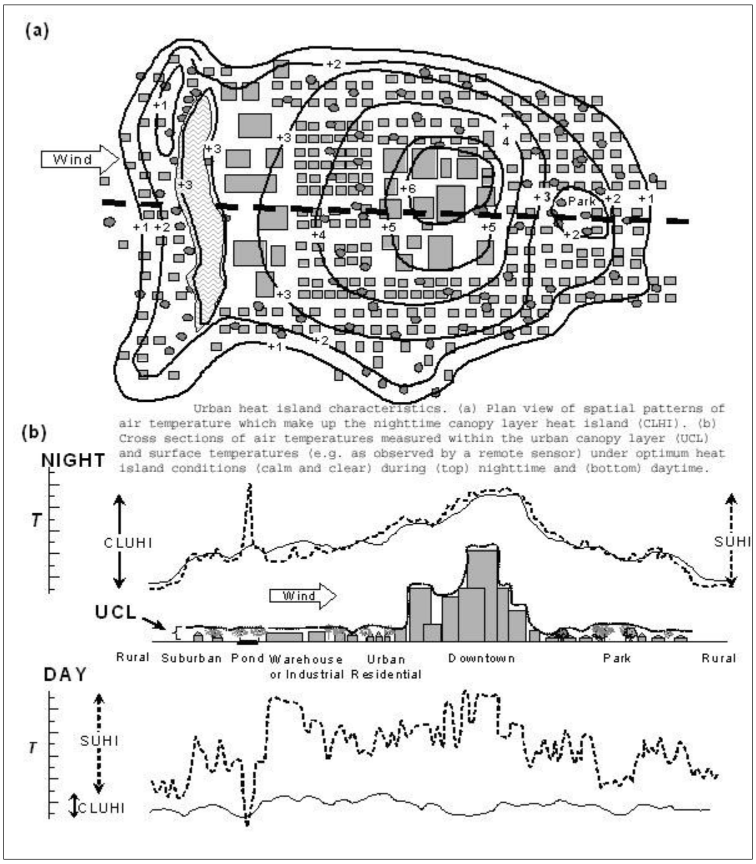

Urban heat island characteristics. (a) Plan view of spatial patterns of air temperature which make up the nighttime canopy layer heat island (CLHI). (b) Cross sections of air temperatures measured within the urban canopy layer (UCL) and surface temperatures (e.g. as observed by a remote sensor) under optimum heat island conditions (calm and clear) during (top) nighttime and (bottom) daytime.

Figure 2. Urban heat island characteristics (Voogt, 2004).

The UHI phenomenon is also prevalent in Singapore. A study conducted using satellite imagery shows that surface temperature is significantly higher in industrial and commercial areas. Areas with lower temperature can be found in parks and forested areas (Wong et al., 2002).

A separate study shows that a 3.5 °C difference in temperature between the central business district and areas with large amounts of greenery can be found (Nieuwolt, 1966). The drastic difference in temperature between the urbanised and rural area is believed to be caused by increased solar insolation and reduced evapotranspiration in the city. Remote sensing technology shows that a temperature difference of 4.0 °C was recorded for city and rural areas (Nichol, 1994). Diurnal UHI measurement in 2001 show that night time heat island temperature differences of up to 4.0 °C can be observed in densely populated areas (Roth et al., 1989).

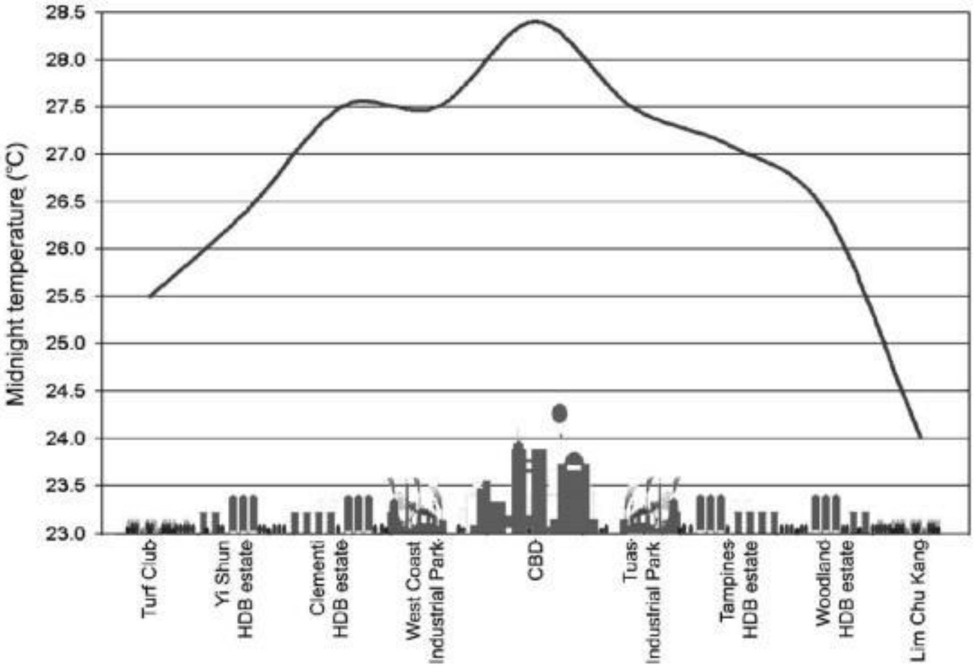

Figure 3. UHI profile in Singapore (Wong and Chen, 2005)

Wong and Chen (2005) analysed surface temperature via thermal satellite imagery and mobile survey. The satellite image shows that the UHI effect during daytime and hot areas can be observed for built-up areas such as industrial and commercial zones while cool areas can be observed in parks. Figure 3 shows the temperature profile between different land uses.

2.2 Role of greenery in the urban microclimate

Vegetation can play a crucial role in the climate of cities and the microclimate of buildings. Besides providing a conducive environment for social activity (Gobster, 1998; Maas et al., 2009; Troy and Grove, 2008), promotion of mental health (Grahn and Stigsdotter, 2010; Korpela and Hartig, 1996; Takano et al., 2002), the introduction of greenery is a useful mitigation strategy for rising temperature due to climate change and the UHI effect. For densely built-up urban environments, greenery can help to cool the air and provide shade. It can also lower energy usage by reducing heat gain into buildings.

Urban greenery can bring about benefits to the microclimate through several physical processes (Dimoudi and Nikolopoulou, 2003; Wilmers, 1991):

- Shading from plants and trees lower solar heat gain on the building envelope;
- Terrestrial (long wave) radiation is reduced due to lower surface temperature through shading;
- Evapotranspiration of plants help to lower dry-bulb temperature; and
- Latent heat of cooling is increased due to added moisture to the air via evapotranspiration.

The cooling effect of greenery has been validated worldwide (Ca et al., 1998; Chen et al., 2009; Chudnovsky et al., 2004; Dimoudi and Nikolopoulou, 2003; Emmanuel et al., 2007; Gill et al., 2007; Giridharan et al., 2008; Honjo and Takakura, 1991; Jauregui, 1991; Jonsson, 2004; Lin et al., 2008; Nichol and Wong, 2005; Sad de Assis and Barros Frota, 1999; Saito et al., 1991; Shashua-Bar and Hoffman, 2004; Weng and Yang, 2004; Wong and Chen, 2005). Urban greenery can be categorised in a variety of ways. Some examples include the Green Plot Ratio (GPR), a concept developed by combining the concepts of Leaf Area Index and Building Plot Ratio (Ong, 2003). The Urban Neighbourhood Green Index (UNGI) can be used by planners to quantify the proximity to greenery for each neighbourhood (Gupta et al., 2012). Park provision ratio and per capita green cover are urban planning benchmarks that have been used in countries such as Singapore (Tan et al., 2013b). Provision of Urban Green Spaces (UGS) also acts as urban lungs, helping to absorb pollutants and releasing oxygen, providing clean air (Hough, 2004; Levent and Nijkamp, 2004).

The primary metric for greenery is land cover. This metric is sometimes further delineated into lawns and shrubs-and-trees. The cooling effect exhibited by plants is a result of its metabolic processes, such as photosynthesis and evapotranspiration. The intensity of such processes is generally related to the amount of bio-mass (e.g. leaves) available (Jones, 1992).

2.3 Impact of greenery on the built environment

2.3.1 Outdoor air and surface temperature

Many studies have shown significant reductions in outdoor air and building surface temperature due to the presence of greenery. Ca (1998) measured temperature around a park in Tokyo and observed that temperature above greenery could be up to 2.8 °C lower compared to temperature above built-up surfaces.

Streiling and Matzarakis (2003) observed that temperature reduction is evident even in the presence of one single tree. Air temperature differences of up to 2.2 °C can be observed between areas with and without trees. Measurements of air temperature were 0.1 °C higher under the single tree when compared to a tree cluster. Measurements of Physiological Equivalent Temperature (PET) showed that comfort levels in the presence of trees are much better.

Wong and Chen (2006b) observed that urban parks are able to provide cooling for their surroundings. A difference of 1.3 °C could be observed at different spots around the parks. Deviations of temperature measured in the park are smaller compared to built-up areas, suggesting the ability of vegetation to stabilize temperature fluctuations (Figure 4). Temperature measured within parks also exhibited a high correlation with plant Leaf Area Index. Results derived from Thermal Analysis Simulation (TAS) show energy savings of up to 10% for buildings sited close to parks. Envi-MET simulation shows that the park provides cooling to its surroundings throughout the day.

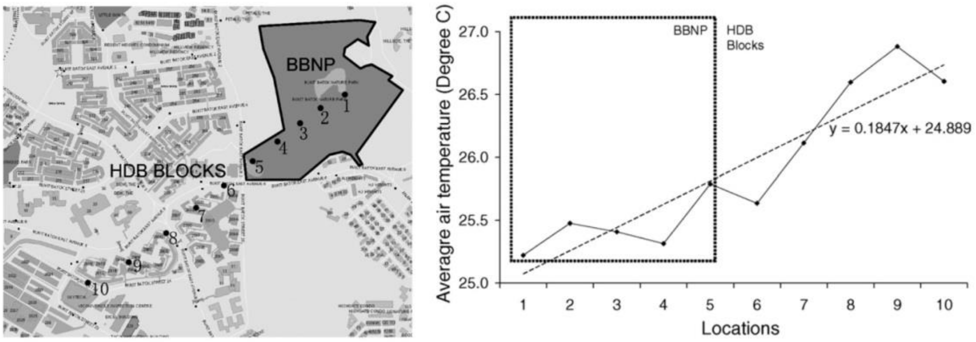

Figure 4. Average air temperatures measured from park to the built environment (Wong and Chen, 2006b)

Kawashima (1991) observed via satellite imagery that lower surface temperatures can be observed in forested areas while higher temperatures are prevalent on built-up surfaces in daytime Tokyo. It is noted that the cooling potential of greenery is less effective in urbanised areas than in suburban areas.

Wong and Chen (2006a) measured the impact of rooftop greenery on buildings and their surrounding environment. Results show that rooftop greenery can provide benefits to the building as well as outdoor ambient temperature. Reductions of up to 31.0 °C in surface temperature and 1.5 °C in air temperature were observed. In the absence of plants, the metal roof surface (experiment control) recorded temperature of up to 70.0 °C during daytime and lower than 20.0 °C at night. With vegetation, the range is limited to between 24.0 °C to 32.0 °C. The study showed that plant density was significant in influencing temperature fluctuation. The mean surface temperature reduction values of surfaces below weeds, sparse and dense vegetation are 1.4 °C, 1.9 °C and 4.7 °C respectively.

Radiation absorption by a single tree was measured using a Whirligig (Green, 1993). Transpiration rate of the tree was estimated by the Penman-Monteith (PM) model. Net photosynthetic rate was estimated by combining a photosynthetic light response curve with total PAR absorbed by the foliage. It was concluded that the evapotranspiration process accounted for up to two-thirds of total solar radiation captured was eventually converted into latent heat.

2.3.2 Outdoor radiation

Trees can have both a direct and indirect impact on outdoor radiation conditions. Brown and Gillespie (1990) noted that air temperature underneath a single tree may be the same as in the open, but radiant conditions may vary significantly. The study interprets solar transmissivity values of trees, into values of radiation received by a person under the trees and into resultant thermal comfort levels. Quantification of radiation received by person under specific trees enables the objective selection of trees that have inherently better shading characteristics (Figure 5).

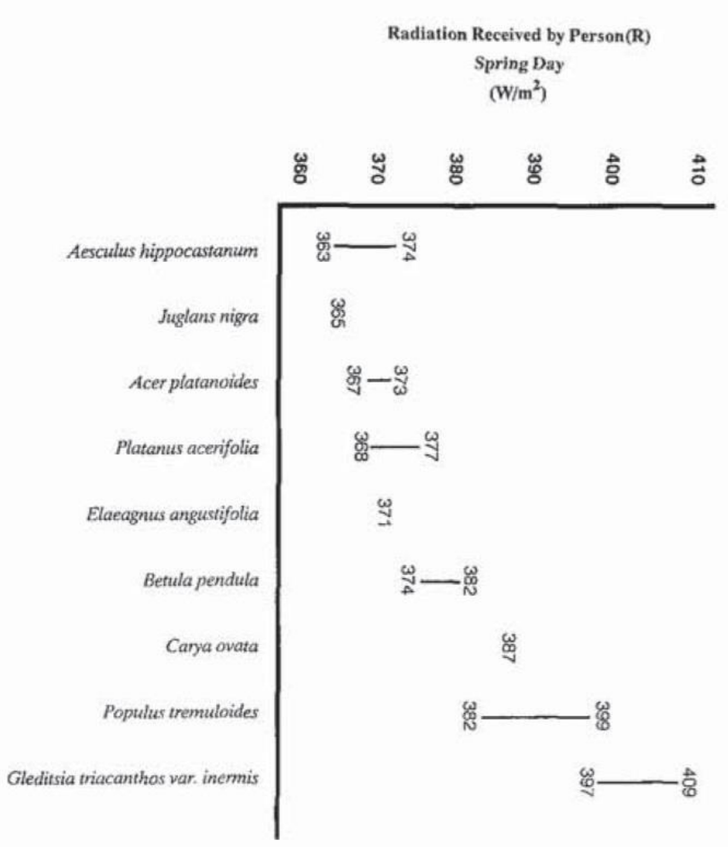

Figure 5. Estimated solar radiation exposure under selected shade trees (Brown and Gillespie, 1990)

Papadakis (2001) compared physical parameters of a wall that simultaneously contained shaded and unshaded parts. Parts shaded by trees exhibited a significant reduction in net solar irradiance as well as wall surface temperature (Figure 6). It is also observed that night-time radiation is lower for unshaded areas, which may be justified by the trees blocking longwave radiation emitted by hard surfaces.

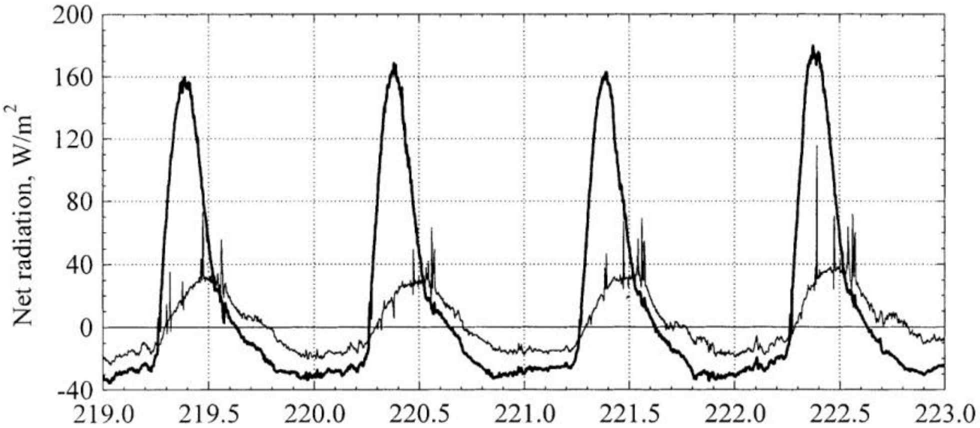

Figure 6. Net radiation in the shaded area (thin line) and in the unshaded area (thick line) (Papadakis et al., 2001)

2.3.3 Energy usage

Tsiros (2010) noted that tree covers may reduce summer time cooling load during the day by up to 8.6 %. The impact of shading from trees is considered to be the biggest factor for energy reduction.

Parker (1981) showed that savings in 50 % for cooling load can be achieved by adding shrubs and trees near a building. Akbari et al. (1997a) analysed peak-power and cooling loads of two houses in California. The two houses are well-shaded by trees. It was observed that average savings of 3.6 kWh and 4.8 kWh per day could be achieved. Peak-demand savings were about 27 % savings in one house and 42 % in the other.

Rudie Jr and Dewers (1984) studied the impact of on cooling load in College Station, Texas. Tree shade on roofs were observed from 1977 to 1979 (June to September). Tree height was measured as a means to approximate shade cast, at hourly intervals. It was observed that roof and wall colour, as well as shade provide by trees significantly affect total energy consumption.

Remote sensing techniques were used by Jensen et al. (2003) to approximate LAI at randomly allocated locations in Indiana. Values of LAI obtained were compared with energy consumption for the relevant areas. Regression analysis shows that daily electricity usage decreases by 4.17 kWh for every unit increase in LAI.

2.3.4 Strategic placement of greenery

Heisler (1986a) highlighted the important fact that trees around buildings do not always save energy. Instead, it is the strategic placement and proper management of trees that saves energy. The positioning of trees, in addition to aesthetics, should be considered for optimal energy efficiency (Figure 7). The study argues that optimum arrangement of trees for the purpose of energy conservation could yield up to 25 % in annual savings of energy consumption.

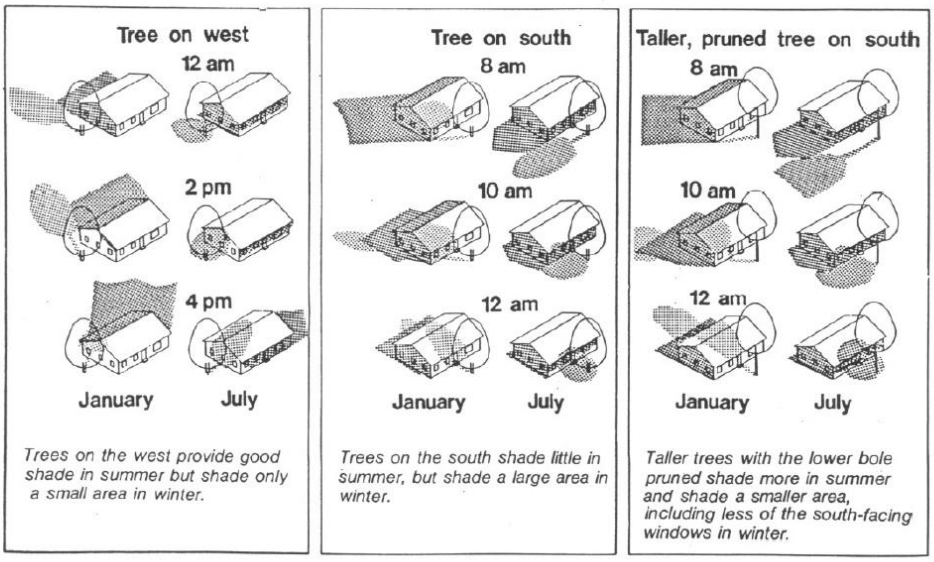

Figure 7. Analysis of tree position for optimal shade (Heisler, 1986a)

Simpson and McPherson (1996) observed that trees blocking the western sun provide the highest cooling potential. The study recommends trees to be placed westwards to provide maximum shading. Additional trees may be located to shade windows on the west and southwest sides first, followed by the east. The study also noted that the shade provided tends to diminish as building-to-tree distance is increased. Therefore, tree planting in landscape design should be done such that the edge of the canopy is as close to the building wall as possible as the tree matures. Tree planting in the south, resulting in additional shading during winter, should be avoided.

Donovan and Butry (2009) analysed electricity bills from houses in California and observed that electricity consumption in summer is reduced when trees are placed on western and southern sides of the house but may increase when trees are placed on the northern side of the house. Similar reductions in electricity consumption can be observed for a tree that is placed about 12 m on the south and for the same tree to be placed about 18 m on the western side. The study acknowledges that due to high land prices, many homeowners are unable to allocate plants in optimal locations and advocates the provision of strategic tree planting during development and planning stage, not simply as an afterthought.

Gómez-Muñoz et al. (2010) studied the effect of tree shadowing on buildings. Simplified models of three types of trees were analysed. Shadow projections were compared against blocked solar radiation on walls, and subsequently linked to energy savings indoors. The study concluded that it is more expensive to plant young trees than to plant more mature trees to begin with.

2.3.5 Alternate forms of urban greenery

Roof gardens and vertical greenery are often employed as alternative forms of green cover for densely built-up cities that do not have adequate land to provide for Urban Green Space (UGS). Countries with high population density such as Hong Kong and Singapore, are characterized by their compact city form and land scarcity (Ganesan and Lau, 2000; Neville, 1993). Rooftop and vertical greenery can provide numerous benefits to the urban landscape without the need for ground level space. Singapore, for instance, has paid particular attention to maximising available real estate to create a 'Vertical Garden City', via the introduction of rooftop gardens, vertical greenery and sky terraces (Tan, 2012).

There are many studies done on the benefits of vertical greenery. Most studies focus on temperature reduction through the use of vertical greenery (Chen et al., 2013; Cheng et al., 2010; Perini et al., 2011; Wong et al., 2010a). Vegetation can reduce impact of the UHI effect through shade provision and the plant evapotranspiration process (McPherson et al., 1994). Vegetation can also reduce diurnal temperature fluctuation from direct sunlight (Dunnett and Kingsbury, 2008). Surface temperatures of green walls are lower than common building materials such as concrete and metal surfaces (Bass and Baskaran, 2003). This reduction in surface temperature can lead to lower cooling load for the building interior (Alexandri and Jones, 2008; Mazzali et al., 2013; Papadakis et al., 2001; Peck et al., 1999; Pérez et al., 2011; Wong et al., 2009). Numerous studies have also shown vertical greenery to be able to improve acoustics insulation (Van Renterghem et al., 2012; Wong et al., 2010b).

Many studies on green roofs have focused on surface temperature of roofs as well as quantification of cooling energy savings for the building (Akbari and Konopacki, 2005; Rosenfeld et al., 1998). Research into green roofs often focuses on the quantification of roof surface temperature. There are also studies into various aspects of rooftop greenery such as types of plants used, growth substrates, acoustic performance, air quality and maintainability (Baik et al., 2012; Parizotto and Lamberts, 2011; Saadatian et al., 2013). Various feasibility studies have been undertaken to determine structural and logistical considerations in green roof implementation (Castleton et al., 2010).

2.4 Measuring the effects of greenery on the built environment

2.4.1 Shade

Studies on tree shade have focused on comparing different types of trees within an objective framework. Kotzen (2003) demonstrates how short, large canopy trees tend to provide more shading than a taller tree (Figure 8).

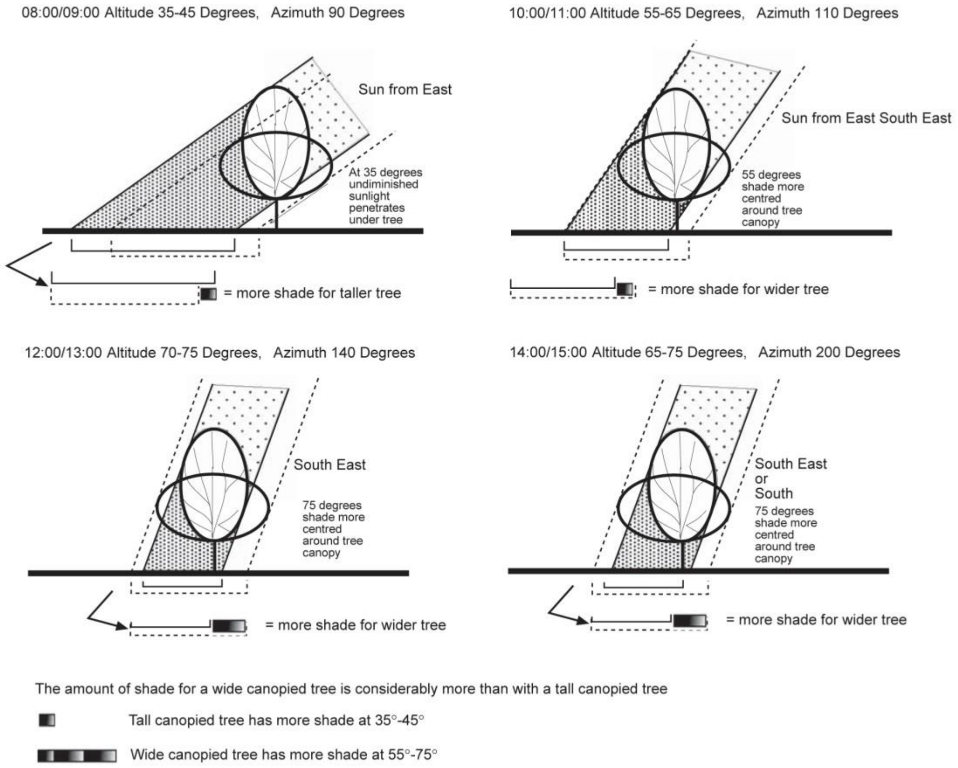

Figure 8. Comparison of shade generated by trees of different shapes (Kotzen, 2003)

The shade of six native trees from the Negev desert are quantified and results indicate a general trend of increased shade provided by broad shaped canopies over the entire duration of the day, especially during summer midday. The study concludes that canopy size is more significant than tree height in terms of shade provision and that a systematic evaluation of the shading properties of trees is possible to go beyond the fundamental knowledge that trees provide shade.

Shahidan et al. (2010) studied the effects of shade casted by trees during the day. The methodological framework consists of the use of simulation via Autodesk Ecotect and the measurements of actual shade cast by two trees, namely *Mesua ferrea* L. and *Hura crepitans* L. (Figure 9). The study systematically compared the shading potential of two types of tree species by analysing their radiation modification characteristics.

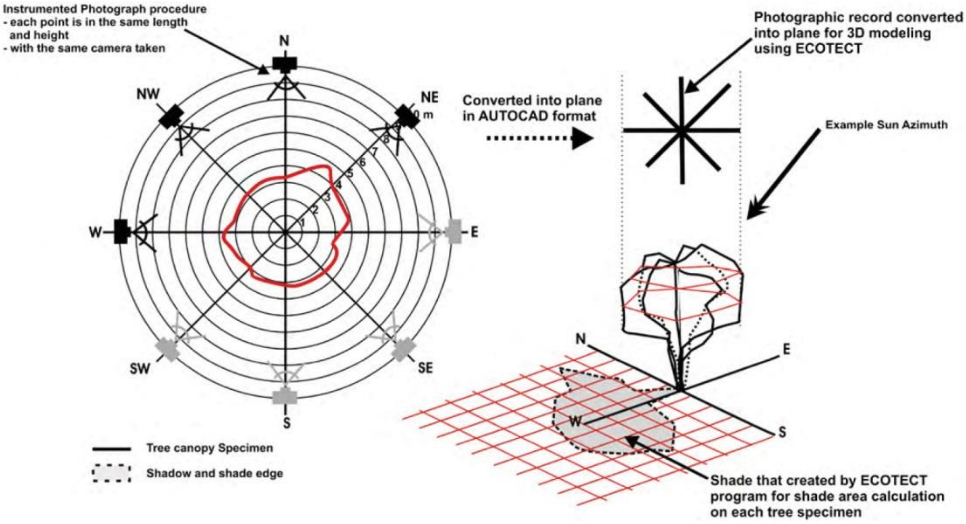

Figure 9. Simulation of tree shade using Ecotect (Shahidan et al., 2010)

Results show that *Mesua ferrea* L. provides more shading than *Hura crepitans* L., with 93 % average filtration. Therefore, *Mesua ferrea* L. is objectively proven to be more effective in blocking direct soar radiation than *Hura crepitans*. This is attributed to its substantial branch structure, high LAI of 6.1 and low canopy transmission. A strong correlation is also exhibited between thermal radiation filtration and LAI values of *Mesua ferrea* L. and *Hura crepitans* L. (R^2 = 0.96 and 0.95).

The conclusion that reduction in canopy transmission will result in lower surface temperature beneath the tree and subsequently lesser emittance of long wave radiation is consistent with the studies with Brown and Gillespie

(1995) and Kotzen (2003). Results of this study may be made applicable to architects and urban planners as a tool for improving outdoor thermal comfort. Heisler (1986b) measured the crown size and visual density of a sample of four trees and analysed the effects of shading on a house for a year using a Heliodon model. Pyranometers are used to measure solar insolation and attenuation. Measurements are made for trees with and without leaves, and insolation is categorised as desirable during winter and undesirable during summer. Results indicate that for mid-sized deciduous trees located in the west provided more desirable insolation reductions than the south of the house throughout the year.

2.4.2 Temperature

Wong and Chen (2006b) measured the air temperature of city parks by installing air temperature sensors in two urban parks. Results show that there is a maximum difference of 1.3 °C from the parks to residential areas. It was also observed that compared to built-up areas, vegetation can reduce temperature fluctuations more effectively on a diurnal basis.

Bogren et al. (2000) measured the effects of heat attenuation on surface temperature due to tree shade on road surfaces. Results show that a drop in temperature can be observed almost immediately when a site is screened. A maximum temperature difference of 10.0 °C is evident at 14:00 hrs. The act of transition from non-shade to shade results in a decrease in surface temperature of 7.5 °C in under an hour. The study also shows that a surface temperature during the day is required to produce a significant temperature differential after sunset. Measurements indicate that during January, surface temperature difference of about 2.0 °C results in no difference in surface temperature after sunset. In mid-February, the surface temperature difference during the day is 6.5 °C, which results in a temperature difference of 2.0 °C at sunset and 1.5 °C four hours later.

2.4.3 Simulation

Van Elsacker et al. (1983) used photography exclusively to simulate the profile of trees and to quantify the subsequent interception of short wave radiation. This technique eliminated requirements for solar insolation data.

McPherson and Rowntree (1988) studied different types of shapes that best represent trees to be used for simulation. Photographic samples were taken and simplified to generic shapes (e.g. cone, paraboloid, sphere, etc). A statistical comparison showed significant correlation between the estimated tree canopy profiles and photographic samples. The mean percentage difference between the areas for the sample was only 1.3 %.

McPherson et al. (1988) performed simulation on typical single-storey ranch homes using the MICROPAS building energy simulation program and SPS shading simulator. Results show that space cooling costs were most significant to roof and west wall shading from vegetation. This indicates that there are specific areas that benefit more from intervention, and that placement of vegetation may be most effective when considered using simulation.

Gulyás et al. (2006) used the RayMan simulation tool to generate the Physiological Equivalent Temperature (PET) indices as well as the t_{mrt} of a section of the town of Szeged, located in the southern part of Hungary. In the RayMan software, information on vegetation can be inserted as input parameters. This includes the type of tree (Deciduous, Coniferous), the tree location, dimensions of the tree (height, crown radius, trunk length and diameter), albedo and emission coefficient (Figure 10). Different scenarios were simulated (Only buildings, buildings and trees, and trees only). Results show that the PET exhibits stronger correlation with t_{mrt} than with air temperature in summer. The PET index differential amongst these places due to varying solar exposure can be as high as 15.0 °C to 20.0 °C. In particular, the planting of deciduous trees provides more shading and reduces heat stress in the summer afternoon, while the leafless trees reduce cold stress while maximising low-angle solar irradiance in winter.

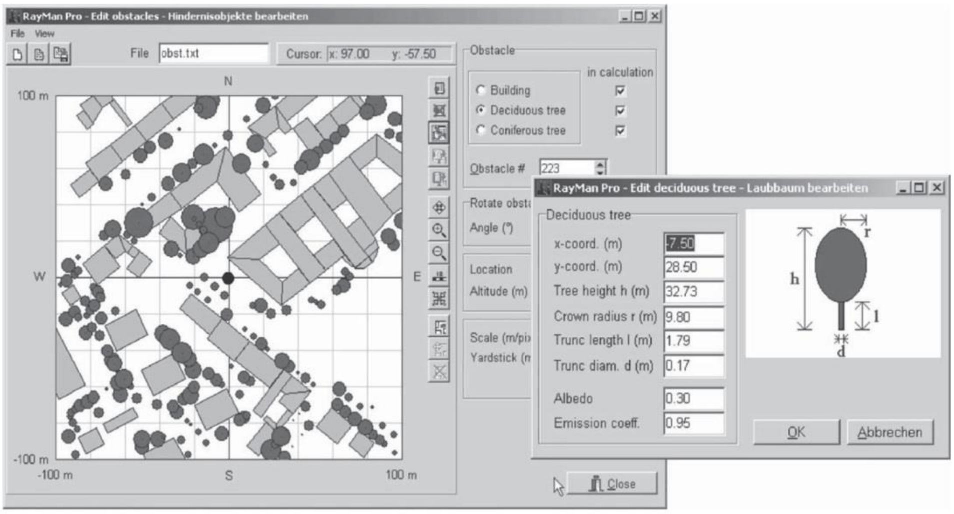

RayMan Pro - Edit obstacles - Hindernisobjekte bearbeiten

File obst.txt

Cursor: x: 97.00 y: -57.50

Obstacle

○ Building ☑

● Deciduous tree ☑

○ Coniferous tree ☑

Obstacle # 223

RayMan Pro - Edit deciduous tree - Laubbaum bearbeiten

Deciduous tree

x-coord. (m) -7.50

y-coord. (m) 28.50

Tree height h (m) 32.73

Crown radius r (m) 9.80

Trunc length l (m) 1.79

Trunc diam. d (m) 0.17

Albedo 0.30

Emission coeff. 0.95

Figure 10. Tree input parameters in RayMan (Gulyás et al., 2006)

Matzarakis and Rutz (2005) used the RayMan software to simulate PET and t_{mrt} of potential tourist spots to identify areas that are not adequate in providing thermal comfort. The study showcases the possibility of planning for dwellings that provide passive cooling and thermal comfort-inducing facilities for hotels and resorts. It can be utilised shade analysis for the purpose of creating comfortable thermal conditions in tourism areas and resorts. The RayMan software has been validated by field measurements (Matzarakis et al., 2000).

Yoshida (2006) introduced the concept of the three dimensional plant canopy model to study the drag force of trees, shading effects on long and shortwave radiation and the transpiration properties of the plant canopy (Figure 11). The t_{mrt} and Standard Effective Temperature (SET) are also simulated to deduce outdoor human thermal comfort.

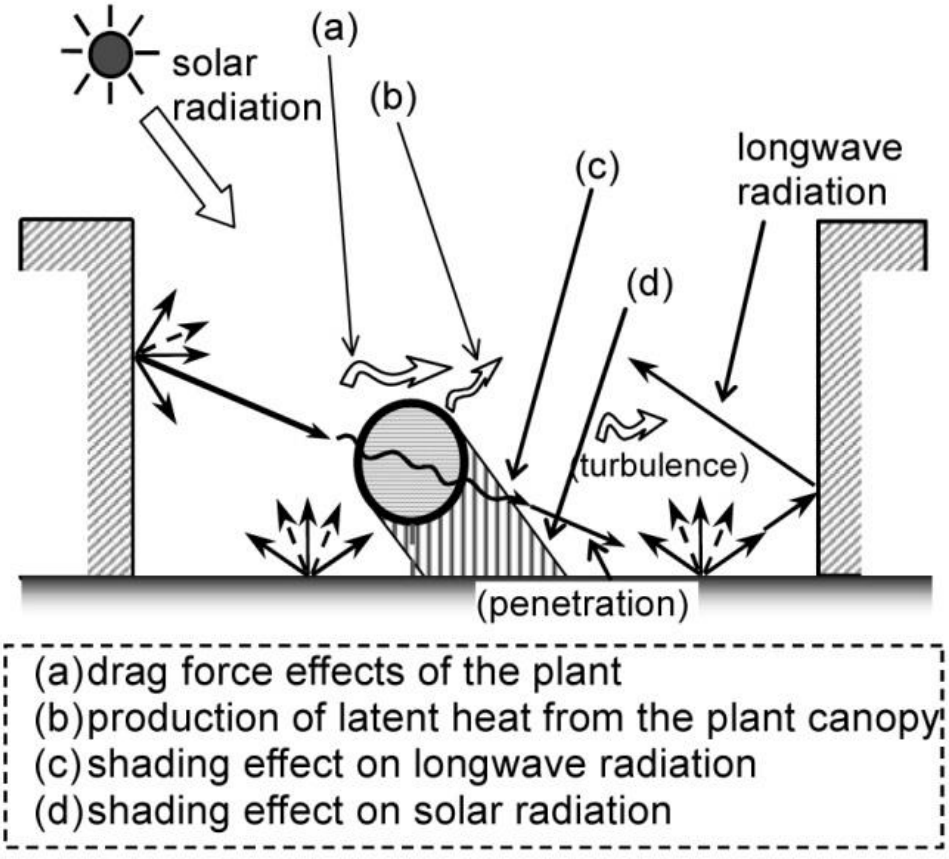

Figure 11. Effects of plant canopy on outdoor thermal environment (Yoshida, 2006)

Results show that increasing the turf area improves outdoor thermal conditions during summer. However, excessive planting tends to worsen outdoor thermal conditions due to reduction of air velocity. This is mainly due to the effect of drag force of the plant canopies. This study emphasises the need for an objective framework for landscape planning, and challenges the popular notion that the planting of trees is always beneficial.

Akbari et al. (1997a) simulated cooling energy savings in two houses (T1 and T2) by shading them with sixteen trees. DOE-2.1E building energy analysis was used for simulation. Trees were modelled as rectangular forms, with a transmissivity value of 0.10. Results show that cooling load savings at both sites are 47 % for T1 and 26 % for T2. Peak cooling power usage was reduced by 0.8±0.1 kW at T1, and by 0.6±0.1 kW at T2. Simulation results show the ability of trees to reduce energy loads.

Lindberg et al. (2008a) developed a mean radiant temperature simulation program, SOLWEIG, which considers the effects of long and shortwave radiation fluxes in complex urban settings. The program was further refined (Lindberg and Grimmond, 2011) to include vegetation, namely trees and shrubs. The main function of this introduction is to project shadows casted by vegetation. Digital Elevation Models (DEMs) are used to represent vegetation. Three types of vegetation can be inserted: coniferous trees, deciduous trees, and bushes. Simulations effectively highlight the t_{mrt} reduction potential of vegetation both on ground level as well as on the buildings (Figure 12).

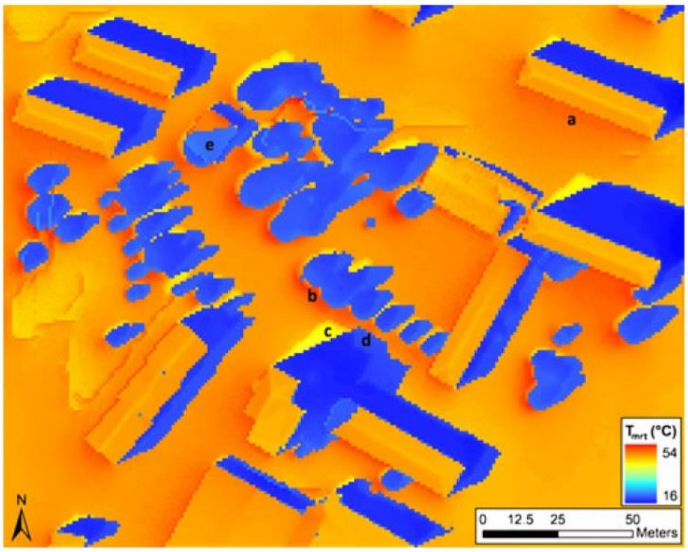

Figure 12. Spatial variations of t_{mrt} simulated using SOLWEIG v2 (Lindberg and Grimmond, 2011)

2.5 Plant physiology and biotic processes

2.5.1 Evapotranspiration

Evapotranspiration is a process in which water vapour moves into the atmosphere through plants and soil. It describes water loss through a vegetated surface via the process of plant transpiration as well as water evaporation from the soil.

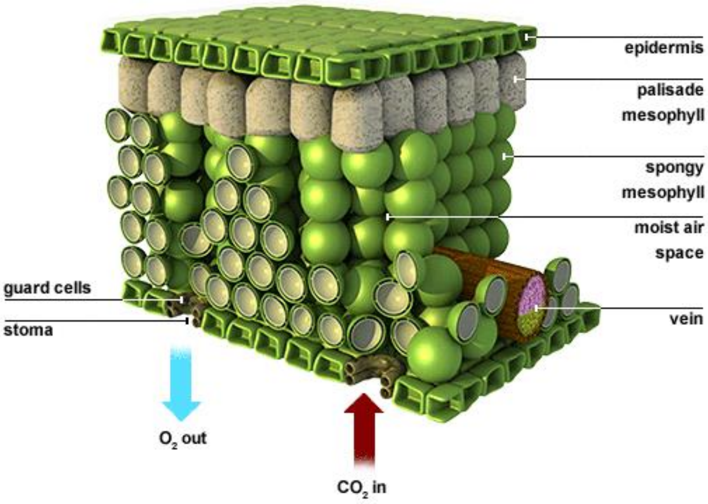

Figure 13. Sectional perspective of a leaf (BBC, 2013)

Figure 13 shows a section of a leaf. During transpiration, a large portion of water is passed through the stomata, which are tiny pores on the leaf that facilitates the flow of gasses during the photosynthetic process. Transpiration is controlled by opening or closing the stomata (Allen et al., 1998; Hillel, 1980).

Evaporation and transpiration occur simultaneously. Evaporation from a cropped soil is dependent on solar insolation. Irradiance decreases as the plant grows and overshadowing of the soil occurs. Figure 14 illustrates the separation of EvapoTranspiration rate (ET) into evaporation and transpiration. Initially, almost all of the measured ET is attributed solely to evaporation. When the plant is well-grown and fully covers the soil, most of the measured ET can be attributed to transpiration.

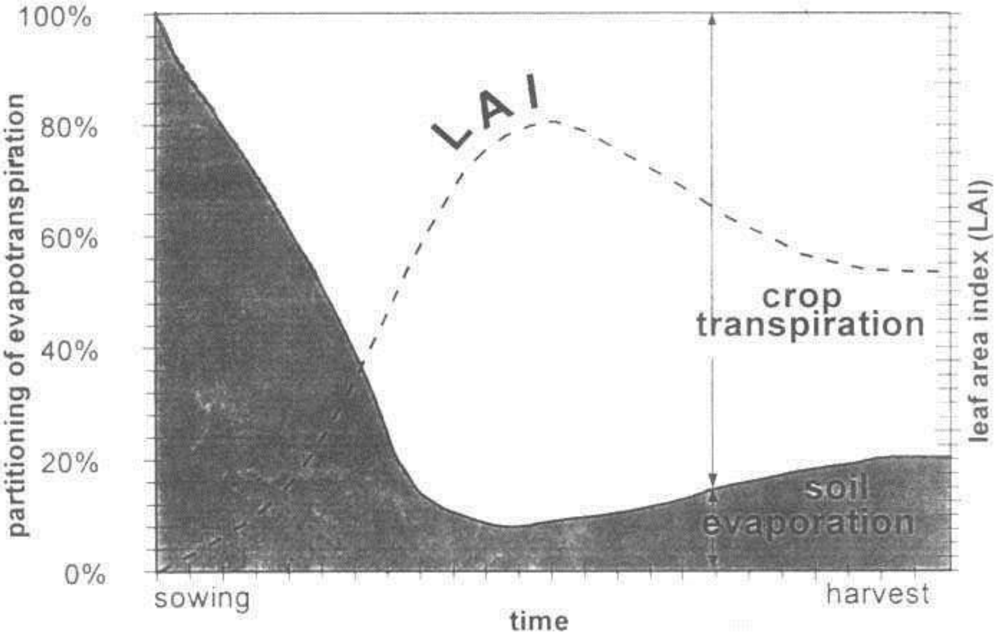

Figure 14. Evapotranspiration rate and plant development (Allen et al. 1998)

Energy is needed to turn water from liquid to gas. This energy is provided by the sun. The cooling effect due to plants is the result of an energy balance mechanism in which the evapotranspiration process of plants is in effect. Takebayashi and Moriyama (2007) states that sensible heat flux on a vegetated surface decreases due to an increase in latent heat flux from the evapotranspiration process. The ambient temperature, therefore, can be reduced through this process. Niachou et al. (2001) showed that ambient temperature can decrease by 10.0 °C on the insulated roof constructed from green roof. Wong et al. (2003a) observed that the surrounding ambient temperature of rooftop gardens could be reduced by around 4.0 °C.

Factors that influence the rate of evapotranspiration in plants are as follows (Allen et al., 1998):

1. Solar radiation

Solar radiation is a major factor in plant evapotranspiration. Maximum ET occurs under clear sky conditions, and is at its minimal under cold and cloudy conditions. Location, latitude, sun altitude and azimuth as well as atmospheric pollution are determinants for net radiant energy exposure.

2. Wind

Wind maintains vapour pressure gradients above the vegetation surface by removing water molecules from the canopy. It serves as a heat transport medium and accelerates evaporation by removing water from the plant to the atmosphere. Wind has a higher influence on ET when t_a is low.

3. Vapour pressure gradient

Vapour pressure gradient is determined by immediate surface conditions. Lack of moisture above a surface will limit continuity of the evapotranspiration process. This will result in a decline for actual evapotranspiration, below the potential evapotranspiration rate. This is a common occurrence when the soil is dry and will result in a moisture deficit. Subsequently, plants will be vulnerable to moisture stress and nutrients deficiencies.

4. Humidity and air temperature

Humidity and air temperature are determinants for dryness of the atmosphere. Air temperature affects the potential of solar and wind factors in vaporizing water.

5. Crop characteristic

Evapotranspiration rates can be different due to the influence of crop characteristics such as type, variety, resistance to transpiration, height, roughness and root, even when other conditions are kept identical.

6. Management and environmental aspects

The evapotranspiration process may be adversely affected by land fertility as well as soil management practices. Some factors that may affect ET include plant density, soil type and water availability.

2.5.1.1 Measurement and estimation of plant evapotranspiration rate

There are 4 approaches for evapotranspiration rate (ET) measurements:

1. Hydrology

- Soil water balance

ET can be derived based on the principle of mass conservation (one dimensional). The average rate of ET in mm per day is ascertained by recording changes in soil water volume over time (Rana and Katerji, 2000):

$$P + I + W - ET - R - D = \pm[\Delta S]_0^r \quad [1]$$

Where,

P = Precipitation (mm·day^{-1})

I = Irrigation (mm·day^{-1})

W = Contribution from water table upward (mm·day^{-1})

R = Surface runoff (mm·day^{-1})

D = Drainage (mm·day^{-1})

ΔS = Soil water storage in the soil layer (mm·day^{-1})

Precipitation, irrigation and surface runoff can be measured easily. However, measurement of drainage and soil moisture content is complex. Therefore, this method can be used only on a large scale, long-term basis where it can be assumed that drainage to bedrock is balanced by water release from spring seepage and where the change in soil moisture content is negligible (Smithson et al., 2002).

- Weighing lysimeters

In this direct measurement method, a container is used to measure the movement of water over a specified area. The ET is determined by changes in water mass. Lysimeters can be grouped into (Allen et al., 2011):

1. Non-weighing, constant water-table lysimeters. These are used when the water table is sufficiently high and at similar levels outside the lysimeter.
2. Non-weighing, percolation lysimeters. Small samples are taken for the precise measurement of water mass.
3. Weighing lysimeters. Changes in water content are measured by weighing with a scale or load cell. This method can provide the most accurate data for short measurement frequencies of 30 min. However, data obtained from a lysimeter may only represent the ET of just one specific location of the field (Grebet and Cuenca, 1991) due to variance in vegetation density, soil and plant height. Especially in arid environments, neighbouring crops in close proximity may also affect measurement (Allen et al., 1991).

2. Energy balance

This approach considers evapotranspiration in terms of energy usage for turning water inside the vegetation into vapour. This change in energy is termed latent heat. Approaches to estimate latent heat flux (Rana and Katerji, 2000) are as follows:

- The Bowen Ratio and Energy Balance (BREB) method

Latent heat flux is calculated by means of balancing the energy budget of the plant. As latent heat flux cannot be measured directly, the BREB method is used to provide an indirect estimate.

The Bowen Ratio (BR) can be determined by measurements of air temperature and vapour pressure gradients near the plant (Bowen, 1926). The temperature and vapour pressure gradient are generally measured around 0.3 m above dense foliage. Net radiant measurement should consider the ratio between the fetch and the height of the equipment to gain a representative surface condition. Fetch is defined as the distance of the field edge to the location of the BR equipment. Measurement of soil heat flux is typically conducted between 0.05 m to 0.15 m below the surface (Allen et al., 2011).

The BREB method does not require aerodynamic data and provide reliable measurements of ET over a wide variety of vegetation surfaces. However, homogeneous condition of the surface has to be established to avoid a large error in calculation. In order to achieve equilibrium condition, Panofsky and Townsend (1964) stated that the ratio of fetch to the highest position of BR measurement for temperature and humidity gradient could be from 10:1 to 200:1. Subsequently, Heilman et al. (1989) confirmed that a fetch-to-height ratio of 20:1 still provides reliable estimations of the Bowen ratio. This study also supports the calculation of Yeh and Brutsaert (1971) which reported that BR estimation is insensitive to fluctuating fetch conditions as long as the Bowen ratio is small.

- Aerodynamic method

Calculation of latent heat flux (λE) using this method is described by the following equation (Rana and Katerji, 2000):

$$\lambda E = -\lambda \rho u q \qquad [2]$$

Where,

λE = Latent heat flux (Wm^{-2})

ρ = Density of air (kgm^{3})

u = Friction velocity (ms^{-1})

q = Specific air humidity (kgkg^{-1})

Another approach conducted by Pieri and Fuchs (1990) to avoid difficulties in measuring water vapour gradients is by determining sensible heat flux by means of measuring flux-gradients (Equation 3). Latent heat flux is estimated using the equation:

$$H = -\rho c_P u \cdot T \qquad [3]$$

Where,

H = Latent heat flux ($\mathrm{Wm^{-3}}$)

ρ = Density of air ($\mathrm{kgm^{-3}}$)

u = Friction velocity ($\mathrm{ms^{-1}}$)

c_p = Specific heat of air ($\mathrm{kJ(kgK)^{-1}}$)

T = Temperature (°C)

The friction of velocity is obtained by wind speed and profile measurements. The stability function is calculated through an iterative process and requires measurements of at least three levels (Webb, 1965).

- Eddy covariance

This method takes into account turbulent fluxes that occur with the confines of the atmospheric boundary layer. Measurement is used to estimate heat, water, CO_2 exchange and other gasses. The measurement takes instantaneous vertical air speed, air temperature, vapour density and statistical covariance (correlation) data to derive flux values, especially for sensible heat and evapotranspiration measurement (Uddin et al., 2013). A high speed measurement system, usually at frequencies of 5- 20 Hz, is recommended (Allen et al., 2011).

The statistical relationship for evaporation rate is as follows (Swinbank, 1951):

$$E = \rho_a \overline{W'q'} = \frac{0.622}{P} \rho_a \overline{W'e'} \qquad [4]$$

Where,

ρ_a = Density of moist air (kgm^{-3})

P = Atmospheric pressure (Pa)

q' = Instantaneous deviation of specific humidity from mean specific humidity (kgm^{-1})

e' = Instantaneous deviation of vapour pressure from mean vapour pressure (Pa)

W' = Instantaneous deviation of vertical wind velocity from mean vertical wind velocity (ms^{-1})

E = Evaporation rate (kgm^{-2}s^{-1}).

3. Plant physiology

- Sap flow method

This method measures water flow in the plant xylem in two ways (Allen et al., 2011):

1. Speed of heat pulse being moved away from specified heat source; and
2. Rate of heat dissipation in plant from convection heat transfer.

This method only measures the plant transpiration component of the evapotranspiration process as it does not measure the evaporation over a heterogeneous surface. Cohen et al. (1988) noted that the sap flow method seemed to be inaccurate when used on plants with low transpiration rates and that calibration is required for each species being measured.

This method takes into account conductive losses upstream (q_u), downstream (q_d) and radially (q_r) away from the heat source (Allen et al., 2011):

$$q_f = P_w - q_u - q_d - q_r \qquad [5]$$

Where,

q_f = Convective heat loss (W)

P_w = Total power provided by heater (W)

q_u = Upstream heat flux (W)

q_d = Downstream heat flux (W)

q_r = Radial heat flux (W)

This method can only be implemented for branches less than 50 mm in diameter, since the portion of branch being measured must first be uniformly heated to yield valid results.

- Chambers system.

The chamber system was firstly described by Reicosky and Peters (1977) where latent heat flux can be estimated via the gradient of vapour density against time, latent heat of vaporisation, area of soil surface and volume of chamber (Dugas et al., 1991). The chamber was made from a clear plastic and was covered by a square metal frame, but was later modified into clear glass to reduce solar irradiance (Reicosky et al., 1983).

Stannard (1988) constructed a chamber for a small area with different types of vegetation which also has been studied and implemented by Mcleod et al. (2004). This method is sensitive to surrounding conditions. The major environmental conditions affecting measurement are air temperature and wind velocity, which could affect the plant transpiration process (Rana and Katerji, 2000).

4. Statistical Analogy

The estimation models for the evapotranspiration rate based on analytical approach are as follows:

- Penman-Monteith model

This model is originally suggested by Penman (1948) to eliminate the measurement of surface temperature difference, so that it is possible to write an expression for the sensible heat flux between the air and surface. The volumetric heat capacity of dry air used to approximate the heat capacity of air. In summary, the Penman-Monteith model for evaporation becomes:

$$E = \frac{\{s(\emptyset_n - G) + \rho_a c_p \mathrm{gH} \delta_e\}}{\lambda[s + \left(\frac{\gamma \mathrm{gH}}{\mathrm{gW}}\right)]} \qquad [6]$$

Where,

s = Slope of the curve relating saturation vapour pressure to temperature (kPa°C^{-1})

$\emptyset_n$ = Net radiant (Wm^{-2})

G = Soil heat flux (Wm^{-2})

ρ_a = Air density (kgm^{-3})

c_p = Specific heat capacity (J(kgK)$^{-1}$)

gH = Heat conductance (molm^{-2}s^{-1})

δ_e = Water vapor deficit (kPa)

γ = Psychrometer constant (kPaK^{-1})

gW = Water conductance (Sm^{-1})

λ = Latent heat of vaporization (Jg^{-1})

This equation can also be expressed with different forms, such as by using the value of the resistance and is described as follows (Zhang et al., 2008):

$$\lambda E = \frac{s(\emptyset_n - G) + (\frac{\rho_a c_p D}{r_a})}{\mathrm{s} + \gamma[1 + \left(\frac{r_c}{r_a}\right)]} \qquad [7]$$

Where,

r_a = Aerodynamic resistance (sm^{-1})

r_c = Surface canopy resistance (sm^{-1}), depends on climate factors and availability of soil water

This model indicates that evaporation (E) increases with increasing radiant energy and with increasing vapour pressure deficit of the ambient temperature as well as with the increasing of total water vapour conductance.

- Priestley-Taylor (PT) model

The PT model can be considered to be a simplified version of the PM model and is derived from the equilibrium evaporation concept (Amarakoon et al., 2000; Penman, 1948; Slatyer and McIlroy, 1961). Equilibrium evaporation defined as a condition in which the vapour pressure (*e*) tends to be equal to the saturation vapour pressure at air temperature (*e'*).

The model can be expressed as follows (Priestley and Taylor, 1972):

$$ET = \alpha PT \frac{S(\emptyset_n - G)}{S + \gamma} \qquad [8]$$

Where,

αPT = Priestly-Taylor coefficient with the value of 1.26

S = Slope of the curve relating saturation vapour pressure to temperature (kPa $°C^{-1}$)

$\emptyset_n$ = Net radiation (Wm^{-2})

G = Soil heat flux (Wm^{-2})

γ = Psychrometer constant (kPa $^oC^{-1}$)

In practice, PT coefficient varies according to vegetation type, soil moisture condition and strength of advection (Flint and Childs, 1991). Gunston and Batchelor (1983) reported that both PM and PT model provides a satisfactory equation for estimating the evapotranspiration rate in humid tropical climates. The PT coefficient, 1.26, was confirmed to be suitable for the tropical climate if conditions remain homogeneous or free from advection, relatively high humidity and low wind speed. While Li et al. (2012) reported that this model with the coefficient of 1.26 is not suitable for a desert region since the results was an overestimation of 5.1 times of the observed eddy covariance. For arid environments, the modified PT model by Ding et al. (2013) showed a good agreement with their observation using eddy covariance measurement methods.

2.5.1.2 Energy budget of the evapotranspiration process

The principle of energy conservation can be applied to predict plant evapotranspiration rate. At any instant, the total energy reaching any surface has to be equal to the total energy that is leaving it.

The energy balance of green roofs is describe in Equation (9) (Hillel, 1998; Nobel, 1983):

$$R_n = ET + Q_s + Q_c + S_t + M \qquad [9]$$

Where,

R_n = Sum of all incoming radiation fluxes minus all outgoing radiation. (Wm^{-2}) This includes all long and shortwave radiation

ET = Latent heat flux or heat converted in the evapotranspiration process (Wm^{-2})

Q_s = Convective heat flux (Wm^{-2})

Q_c = Conduction heat flux from green roof into the building (Wm^{-2})

S_t = Thermal storage for substrate and plants (Wm^{-2})

M = Metabolic storage of photosynthesis and respiration (Wm^{-2})

In Equation (9), M is assumed to be negligible, as it consists of only a very small portion of overall radiation (Jones, 1992). Therefore, the equation can be further elaborated as:

$$Q = LE + H + G \qquad \text{or} \qquad R_n = \lambda ET + H + G \qquad [10]$$

$$\lambda ET = R_n - H - G \qquad [11]$$

Where,

Q = R_n = Net radiation (Wm^{-2})

H = Sensible heat flux (Wm^{-2})

G = *S*oil heat flux (Wm^{-2})

λET = Latent heat flux (Wm^{-2})

Figure 15 illustrates the relationship between all heat fluxes.

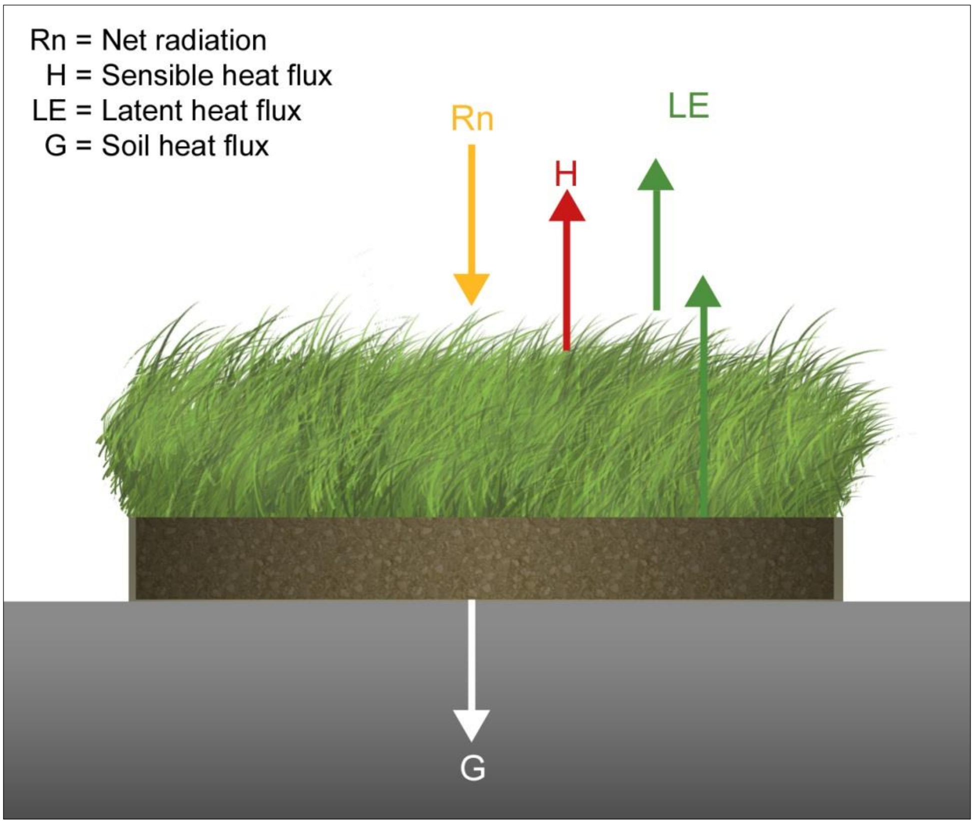

Figure 15. The mechanism of Energy balance at the vegetated surface

Equation (11) also explains that net radiation flux entering the crop environment is use for evaporation, soil and air heating. Latent heat flux (λET), which is a description of the evapotranspiration process, can be determined if data for all other variables are available. Meteorological variables such as soil heat flux and net radiation can be measured directly. Latent heat flux is often measured indirectly through calculation of the Bowen ratio (β), which is defined as the ratio of sensible to latent heat flux ($H/\lambda ET$). The Bowen ratio is proportional to the ratio of the air temperature gradient (ΔT) to the vapour pressure gradient (Δe) over a specified vertical distance above the crop canopy (Fritschen and Simpson, 1989):

$$\beta = \frac{H}{\lambda ET} = \gamma \frac{\Delta T}{\Delta e} \qquad [12]$$

Where,

β = Bowen ratio

H = Sensible heat flux (Wm^{-2})

λET = Latent heat flux (Wm^{-2})

ΔT = Air temperature gradient (°C)

Δe = Vapour pressure gradient (Pa)

The value of λET can be estimated as follows:

$$\lambda ET = \frac{R_n - G}{1 + \beta} \qquad [13]$$

Where,

λET = Latent heat flux (Wm^{-2})

R_n = Net radiation (Wm^{-2})

G = Soil heat flux (Wm^{-2})

β = Bowen ratio

The advantages of employing the BREB method are that it can provide continuous diurnal measurement and wind speed data is not required. Tanner (1960) observed that the Bowen ratio provides advantages for calculating latent heat flux because:

1. It does not require data on wind speed; and
2. Limitations of fetch do not affect measurements significantly.

Measurements of evapotranspiration from lysimeters and those derived from energy balance methods showed good agreement in humid regions with plants that are well-irrigated. Estimates of Bowen ratio in arid regions are less accurate due to severe advection. Xing et al. (2008) observed similar concerns regarding the accuracy of the BR method on the semi-arid, advective environments.

The BREB method makes several assumptions without significantly compromising its accuracy. Measurement sensors are assumed to be located in a region where energy fluxes are constant with respect to height. The entire vegetative surface is assumed to be homogeneous in terms of energy fluxes and aerodynamic characteristics. Flux movement is assumed to be one-dimensional.

2.5.2 Plant canopy

2.5.2.1 Leaf Area Index

Leaf Area Index is defined as the ‘total one-sided area of leaf tissue per unit ground surface area or the ratio of the total area of all leaves on a plant to the area of ground covered by the plant’ (Watson, 1947). For instance, the LAI of a plant would be 1 it has only one layer of leaves and they are placed next to each other without gaps, covering one square meter. LAI is the key parameter that influences both canopy microclimate both above and below the canopy, light attenuation and gas exchange (Chason et al., 1991).

Direct measurement of LAI can be done by obtaining a statistically significant sample of leaves from a vegetative canopy, measuring all available leaf area and dividing the area by the total surface area (Wilson, 1959). LAI can also be determined indirectly by measuring canopy shape (cone, sphere, etc) or correlation with light attenuation (Marshall and Waring, 1986; Rhoads et al., 2004).

2.5.2.2 Leaf Angle Distribution

Foliage is distributed differently between different plant types. For instance, Heliconia plants have leaves are hung vertically while Wedelia plants have leaves that spread horizontally. The Leaf Angle Distribution (LAD) is a statistical description of the approximated angles of leaves distributed within a canopy. For the same plant, LAD may change throughout the day as leaves may re-orientate themselves to face the Sun.

The LAD of a plant canopy is important because it determines total solar insolation for leaf surfaces and the entire plant canopy (Falster and Westoby, 2003). This directly affects the amount of transpiration and water loss experienced by plants (Ehleringer and Werk, 1986). Plants with leaves that are vertically hung tend to receive less direct solar radiation during midday. This results in lesser heat gain and water usage by plants.

Leaf Angle Distribution can be measured in two ways:

1. Direct measurement – Measuring individual leaves (Lang, 1973; Ranson et al., 1981; Wilson, 1965).
2. Indirect measurement – Using a light interception model. The mean inclination angle of foliage is estimated by measurements of light interception by the canopy (Norman et al., 1989). For computer modelling, mathematical models are often used to approximate LAD (Campbell, 1986, 1990; Goel and Strebel, 1984).

Measurement of LAD can be conducted in the following ways (Kucharik et al., 1998):

- Direct measurement

Direct measurements of LAD can be done with a protractor, compass and metre rule (Norman and Campbell, 1989). The protractor is used to measure leaf inclination angle. The compass is used to measure leaf azimuth angle. The ruler is used to determine distance of the leaf from a pre-determined reference point such as the substrate level. For this method to be effective, sample size needs to be in the hundreds and selection should cover the entire plant canopy. This method does not consider plant effects such as plant heliotropism, movement due to moisture or wind. Lang (1973) developed an instrument to measure LAD directly, by using potentiometers linked to mechanical arms. The angle of each arm is measured as it rotates to match the orientation of the leaf being measured (Lang et al., 1990). Using the instrument, leaf position, azimuth and inclination angle can be measured (Daughtry et al., 1990). This method is seen to be the most accurate and convenient way to obtain direct measurements of LAD (Pearcy et al., 1989).

- Indirect measurement

Indirect measurements of LAD can be done with measurements of light attenuation as light travels through the plant canopy. This method is also known as the gap-fraction inversion technique (Norman and Campbell, 1989). Canopy gap-fraction can be measured by:

1. The LAI-2000 plant canopy analyser;
2. Quantum sensors (Chen and Black, 1992); and
3. Hemispherical (fish-eye) photography (Rich, 1990),

Chen et al. (1997) highlights some issues with gap-fraction measurements, such as overlapping penumbra from leaves and non-randomness in the plant canopy, which may lead to measurement errors.

2.5.2.3 Leaf and canopy reflectance

Leaf reflectance affects the total amount of sunlight absorbed and temperature of the leaf. It is often measured in relation to crop growth and yield (Carlson and Yarger, 1971; Kraft et al., 1996; Woolley, 1971). Measurement of leaf reflectivity can be done using a spectroradiometer. There is a significant difference between canopy reflectance and leaf reflectance. Reflectance of a leaf tends to be higher than the entire canopy because a portion of solar radiation incident on a canopy will be transmitted into the porous canopy structure (Campbell and Norman, 1998). Canopy reflectance can be measured by remote sensing methods (Kobayashi et al., 2007).

2.5.2.4 Albedo of vegetative surfaces

Solar radiation incident to a vegetative surface can be absorbed, reflected or transmitted by plants. The albedo of a surface is a description of the portion of incident radiation that is reflected from the surface. It can be considered to be a ‘measure of the overall reflecting potential of a surface’ (Ahmad and Lockwood, 1979). Albedo can be differentiated into spectral (specific wavelength) and total (all wavelengths) albedo (Dobos, 2006).

Albedo values can range from 0 to 1. A theoretical blackbody has an albedo of 0 as all the radiation are absorbed while the inverse is true for an ideal reflector of absolute white surface, where all the radiation are reflected (Figure 16). In actuality, surface albedo is not defined by a single number but by a range of values.

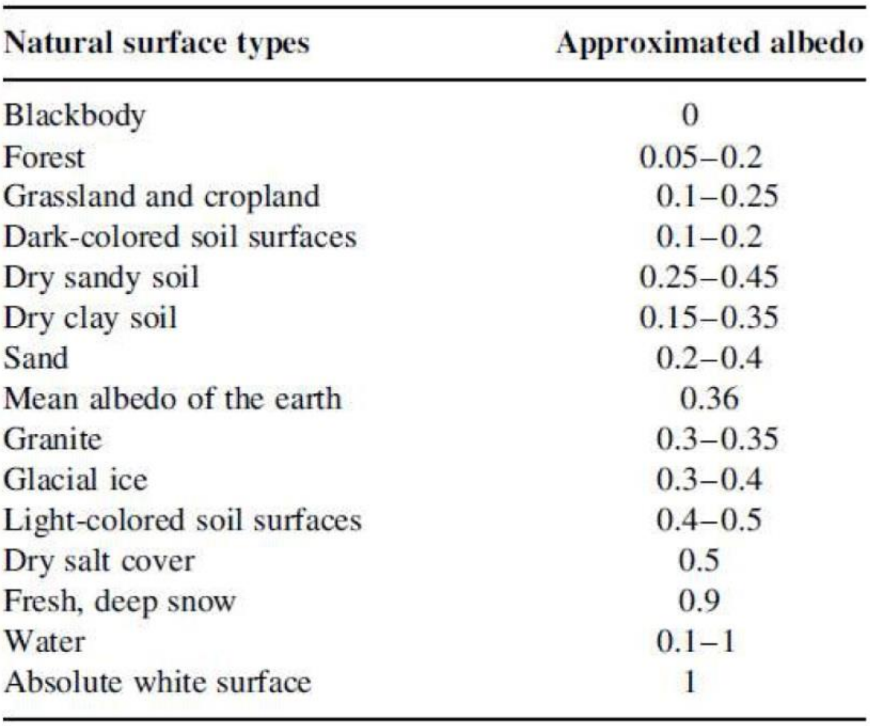

Natural surface types	Approximated albedo
Blackbody	0
Forest	0.05–0.2
Grassland and cropland	0.1–0.25
Dark-colored soil surfaces	0.1–0.2
Dry sandy soil	0.25–0.45
Dry clay soil	0.15–0.35
Sand	0.2–0.4
Mean albedo of the earth	0.36
Granite	0.3–0.35
Glacial ice	0.3–0.4
Light-colored soil surfaces	0.4–0.5
Dry salt cover	0.5
Fresh, deep snow	0.9
Water	0.1–1
Absolute white surface	1

Figure 16. Range of albedo of natural surfaces (Dobos, 2006)

Surface albedo is influenced by surface condition, sun position, sky condition and angle of surface to the horizontal (Ahmad and Lockwood, 1979). Surfaces that are dry, light-colored and smooth are often associated with high albedo while surfaces that are wet, dark-colored and rough are associated with low albedo. In Figure 16, dry clay soil has an albedo of 0.15 to 0.35 while dry sandy soil has an albedo of 0.25 to 0.45. This is because clayey soil can maintain a higher moisture content than sandy soil and smaller particle size of the sandy soil creates a relatively smooth surface which reflects more radiation. Sun zenith angle will influence diurnal variations, while sky condition refers to cloud cover characteristics. An overcast day with uniform and heavy clouds would lessen total solar insolation. In terms of albedo of vegetative surfaces, they are further affected by crop parameters such as LAI, height of plant canopy, temperature and moisture conditions (Doughty et al., 2011).

2.5.2.4.1 Measurement of albedo

Albedo can be measured using an albedometer or similar high-quality instruments such as a pyranometer. The pyranometer has to be oriented in both upward and downward directions such that readings are collected simultaneously for both directions. The upward-facing pyranometer measures the incident radiation while the downward-facing measures the reflected radiation. The setup is simple but has several problems as identified by Dobos (2006). The measurement of the surface albedo is complex under natural condition as the incident radiation includes diffused light from other directions. It is difficult to ensure that the incident radiation is solely from the radiation source. Additionally, the measured surfaces do not reflect radiation in all directions equally and evenly. Readings might vary at different parts of a same surface. Also, the sensors are only able to gather light from a specific range of angles.

2.5.2.4.2 Diurnal variation of albedo

The reflection of radiation from vegetative surfaces is complex as it composes of reflected radiation from plants as well as surrounding surfaces (Ahmad and Lockwood, 1979). As shown in Figure 17, the albedo of vegetative surfaces on a sunny day exhibits a typical bowl-shaped curve due to the diurnal variations of the sun zenith angle (Ahmad and Lockwood, 1979). This is also observed by Monteith and Szeicz (1961), Graham and King (1961) and Stewart (1971) who had studied different vegetation such as grass, maize and pine forests. Albedo values are at the minimum in the midday with most of the incident radiation directly from overhead. Little amount of radiation is reflected as most of them are trapped within the canopy. In this case solar radiation penetrates into the shrubbery and is reflected multiple times between the leaves. However, albedo increases the sun gets closer to the horizon. This is because more solar irradiance is reflected from the plant surface and there is less radiation is trapped inside the shrubbery.

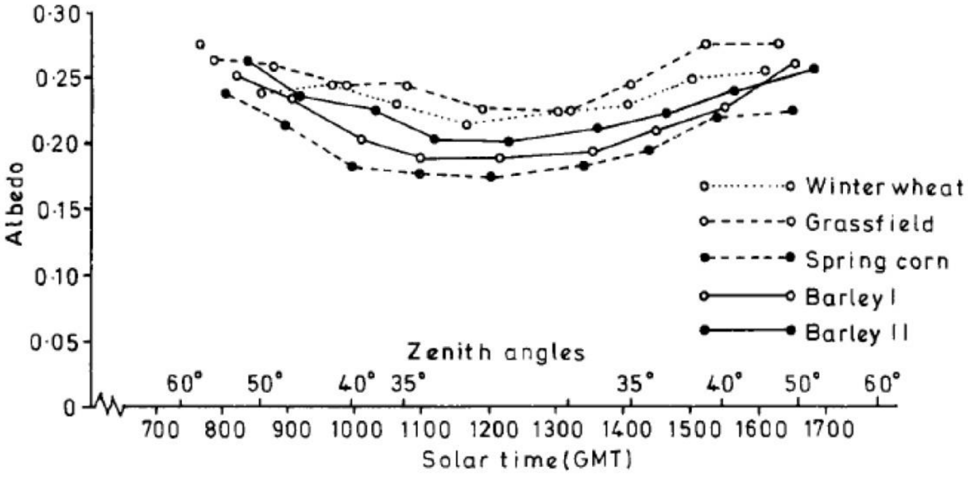

Figure 17. Diurnal variations of albedo (Ahmad & Lockwood, 1979)

Nkemdirim (1972) concluded that albedo values showed a clear correlation to sun zenith angle under clear sky conditions. Under overcast sky conditions, little variation in albedo values was observed. Similar results were observed by Ahmad (1978), where diurnal variation in albedo is more noticeable as cloudiness decreases. It was also observed that the values of albedo before noon are generally lower than after noon for similar zenith angles. According to Song (1998), this asymmetry is because of solar ray asymmetric variation and canopy reclination which is caused by strong prevailing winds.

2.5.3 Plant functional traits

Plant functional traits can be defined as plant features (physiological, morphological, etc) that are representative of their response to environmental influences. The variations in traits are useful in ecological pattern and processes, which includes opportunities and constraints similar plants face in different habitats (Grime, 1979; Southwood, 1977). Results can be used to develop dynamic global vegetation models, carbon models, water budget and land management models, forecast impacts of environmental change, plant effects on ecosystem function and resilience and examine evolutionary and phylogenetic relationships among species, fundamental trade-offs in plant design and eco-physiology (McGill et al., 2006; Reich et al., 2003; Westoby et al., 2002; Westoby and Wright, 2006).

Plant functional traits can be broadly classified into five main categories, as summarized in Table 1 (Pérez-Harguindeguy et al., 2013). Within these categories are specific traits which can be further explored. Most traits can be measured quantitatively but some has to be measured qualitatively due to methodological or logistical limitations. Some traits are more difficult to measure than others, as they require long period of measurements or experimental manipulations (Weiher et al., 1999).

Table 1. Classification of plant functional traits (Pérez-Harguindeguy et al., 2013)

Whole-plant traits	**Leaf traits**	**Stem traits**	**Below-ground traits**	**Regenerative traits**
Life history	Specific leaf area	Stem-specific density	Specific root length	Dispersal mode
Life form	Area of a leaf	Twig dry-matter content	Root-system morphology	Dispersule size and shape
Growth form	Leaf dry-matter content	Bark thickness	Nutrient uptake strategy	Dispersal potential
Plant height	Leaf thickness	Xylem conductivity		Seed mass
Clonality	pH of green leaves or leaf litter	Vulnerability to embolism		Seedling morphology
Spinescence	Leaf nitrogen and phosphorus concentrations			Resprouting capacity
Branching architecture	Physical strength of leaves			
Leaf to sapwood area	Leaf lifespan and duration of green foliage			
Root-mass fraction	Photosynthetic pathway			
Salt-tolerance traits	Vein density			
Relative growth rate	Light-saturated photosynthetic rate			
Water-flux traits	Leaf dark respiration			
	Electrolyte leakage			
	Leaf water potential			
	Leaf palatability			
	Litter decomposability			

2.5.3.1 Plant height

The height of a plant is defined as the 'shortest distance between soil or substrate level and the upper boundary of the main photosynthetic tissues on a plant' (Pérez-Harguindeguy et al., 2013). Maximum plant height (H_{max}) is defined as 'maximum height achieved by a typical mature individual plant species in a particular environment' (Pérez-Harguindeguy et al., 2013). Studies have shown H_{max} to be associated with plant growth, potential lifespan, position of the species with respect to light availability and competitive vitality (Gaudet and Keddy, 1988; Thomas, 1996).

2.5.3.2 Measurement of plant height

Measurement of plant height can be categorised as follows (Pérez-Harguindeguy et al., 2013):

1. Short plant species – Measurements of plant height should be taken for at least 25 plants for each species;
2. Tall plant species (trees) – Measurements of at least 5 of the tallest mature individual plants per species ; and
3. Tall plant species (trees) where time and resources are available - Measurements of at least 25 of the tallest mature individual plants per species.

The recorded height should be representative of general plant canopy, and should excluded inflorescences (flowers), outlying braches or leaves.

Measurement for short plant species can be conducted with the use of sticks or rulers with decimetre marks. Measurements for tall plant species can be used either with either a telescopic measuring stick with decimetre marks, or using the following trigonometric function:

$$H = d \times [\tan(\alpha) + \tan(\beta)] \quad [14]$$

Where,

H = Plant Height (m)

d = Horizontal distance from plant to measurement point (m)

$\boldsymbol{\alpha}$ = Angle between horizontal plane and plant canopy (°)

$\boldsymbol{\beta}$ = Angel between horizontal plane and plant base (°)

2.5.3.3 Leaf area

The leaf area (LA) is defined as the area (or projected area) of an individual leaf (one-sided only). Measurement of LA has been correlated with climatic variation, water-loss efficiency, growth form and radiation exposure (Givnish, 1987; Parkhurst and Loucks, 1972; Royer et al., 2008).

2.5.3.4 Measurement of leaf area

Prior to measurement, each leaf has to be cut from the stem. The inclusion of petioles should be based on research agenda. All leaves should be patted dry before measurement. Samples of at least 4 specimens from 10 individuals are recommended.

Measurement of leaf area can be categorised to the following (Pérez-Harguindeguy et al., 2013):

1. Using specialised leaf-area meters – Calibration is necessary. This is done using pieces of known length and area. The entire leaf is to be positioned within the scanning area and has to be flat;
2. Using a digital camera – Leaf samples are recommended to be secured under a glass plate. Images are to be taken with a ruler for the purpose of calibration. The camera is to be mounted on a tripod

with adequate lighting. The use of flash photography is not recommended ; and

3. Using a flatbed scanner – This method has the added advantage of capturing other features of interest such as leaf veins at high resolution. Leaves may be cut to facilitate scanning. Post-processing software such as Leafarea (Price et al., 2011) can be used to calculate leaf area.

2.6 Mean radiant temperature (t_{mrt}) and thermal comfort

There are several methods of determining the quality of both the indoor (Fanger, 1972; Gagge, 1971) and outdoor (Höppe and Mayer, 1987) microclimate. The use of biometeorological indices has enabled quantification of thermal comfort and assessment in tandem with behavioural aspects. Useful heat stress indices have also been developed to describe thermal stress (d'Ambrosio Alfano et al., 2011b; Epstein and Moran, 2006; Parsons, 2003). According to Parsons (2003), evaluations of thermal environments by means of a suitable comfort or stress index require the measurement of wind speed, relative humidity, air and mean radiant temperature. Among them, one of the main factors contributing to the thermal response of man to his surrounding environment is the mean radiant temperature (t_{mrt}). This quantity plays a crucial role not only in indoor situations but also outdoors as indicated in several studies which have stressed that outdoor thermal comfort is highly dependent on radiative heat transfer from its surroundings (Mayer, 1993; Mayer and Höppe, 1987). Estimation of t_{mrt} can be done by two-sphere radiometers, globe thermometers, constant-air-temperature sensors (ISO 7726, 1998). Calculation of t_{mrt} is also possible using radiant fluxes and the angle factors of surrounding surfaces (ISO 7726, 1998; Palmer and

Chapman, 2000). The calculation of t_{mrt} can be done with the ASHRAE formula:

$$t\text{mrt} = \left[(tg + 273.15)^4 + \frac{1.1 \times 10^8 Va^{0.6}}{\varepsilon D^{0.4}} \times (tg - ta)\right]^{0.25} - 273.15 \quad [15]$$

Where,

t_g = Globe temperature (°C) , measured by a temperature sensor placed inside the globe

V_a = Air velocity (ms^{-1}) , measured at the level of the globe

t_a = Air temperature (°C) , measured near the globe

D = Globe diameter (m)

ε = Globe emissivity

In some cases, the mean convective coefficient of the globe thermometer has to be recalibrated to suit the contextual outdoor conditions (Thorsson et al., 2007).

The effects of t_{mrt} can be studied through numerical modelling (Ali-Toudert and Mayer, 2006; La Gennusa et al., 2005). This method is useful when used for iterative studies such as the comparison of width-to-height ratios and orientations of street canyons. However, model geometry and ambient conditions are often simplified. Recent developments in solar and long wave environmental irradiance modelling takes into account large-scale urban geometry as well as important urban components such as tree and shrubs (Lindberg and Grimmond, 2011).

The estimation of radiant temperature is often an integral component to the assessment of thermal environments. Common thermal assessment indices such as the Physiological Equivalent Temperature (PET) and the recently developed Universal Thermal Climate Index (UTCI) are evaluated with t_{mrt} as a variable component (Höppe, 1999; Jendritzky et al., 2012; Lin et al., 2012a). Other heat stress indices such as the Wet Bulb Globe Temperature (WBGT) consider radiant temperature in the form of the globe surface temperature (Gaspar and Quintela, 2009; Lemke and Kjellstrom, 2012). Fluctuating radiation fluxes due to complex environments have contributed to the uncertainty in t_{mrt} estimation, and studies have shown that it can affect the overall thermal assessment in some temperature ranges (Weihs et al., 2012). Therefore, it is important that the estimated t_{mrt} can accurately reflect the prevalent conditions of radiation fluxes of the measured space.

2.7 Knowledge Gap

A review of the literature has uncovered several crucial knowledge gaps in the study of measuring the cooling effect of urban greenery. They are as follows:

- Globe thermometer used for outdoor t_{mrt} measurement needs to be calibrated for the tropical outdoor conditions;
- Studies on the measurement of outdoor t_{mrt} in the tropics at the diurnal scale are lacking;
- Studies on the cooling effect of outdoor greenery are largely on parks and large trees. There is little knowledge on the effects of outdoors t_{mrt} due to specific types of urban greenery systems such as shrubs and rooftop greenery;
- On the subject of cooling effect of plants, there is no distinction between the cooling due to reduction of radiant heat flux from plant shade and cooling due to evapotranspiration of plant;
- Reflectivity of a plant (shrub) is not considered in its entirety, but is ascertained by measuring the reflectivity of individual leaves and defining the Leaf Area Distribution; and
- There are no scientific criteria for the selection and placement of plants for rooftop greenery design.

3 HYPOTHESES AND RESEARCH METHODOLOGY

3.1 Hypotheses

Based on reviewed literature, it is found that:

- Addition of greenery in the urban environment can significantly lower the ambient temperature; and
- The cooling effect of outdoor greenery has been largely attributed to shade provision of trees and the plant evapotranspiration process.

For rooftop greenery, which has more exposure to direct sunlight, the opportunity for the shade provision by tree canopy is significantly reduced. The plant evapotranspiration rate, reflectance of short wave and long wave radiation as well as emission of terrestrial (long wave) radiation is hypothesized to be significant factors in the contribution of radiant heat flux.

Hence, the hypothesis can be rationalized as follows:

The overall cooling effect of plants comprises the plant evapotranspiration rate and albedo of the said plants.

$$\boldsymbol{Cooling\ effect\ of\ rooftop\ garden\ plants} \qquad [16]$$

$$= f\begin{pmatrix} Plant\ attributes\ causing\ a\ reduction\ in\ air\ temperature, \\ Plant\ attributes\ causing\ a\ reduction\ in\ radiant\ temperature \end{pmatrix}$$

$$= f\ (Plant\ Evapotranspiration\ Rate, Shrub\ Albedo)$$

Since t_{mrt} is a function of the air and surface temperature of its surroundings, it can be used to measure the overall reduction in temperature due to greenery. This gives us the equation:

$$\boldsymbol{Reduction\ in\ tmrt\ due\ to\ presence\ of\ plants} = f(Plant\ Evapotranspiration\ Rate, Shrub\ Albedo) \quad [17]$$

The rationale for proposing the following variables are shown in Table 2 and Figure 18.

Table 2. Influence of hypothesized variables on t_{mrt}

Variable	**Influence on t_{mrt}**
Plant EvapoTranspiration Rate (ET)	Increased ET will reduce surrounding air temperature through increased latent heat of vaporization. This will also result in cooler leave surfaces than will reduce longwave emission
Shrub Albedo	Albedo of shrub is a representation of leaf angle and shrub reflectivity. A lower albedo will result in higher thermal absorption for the shrub and subsequent increase in thermal emission to its surroundings

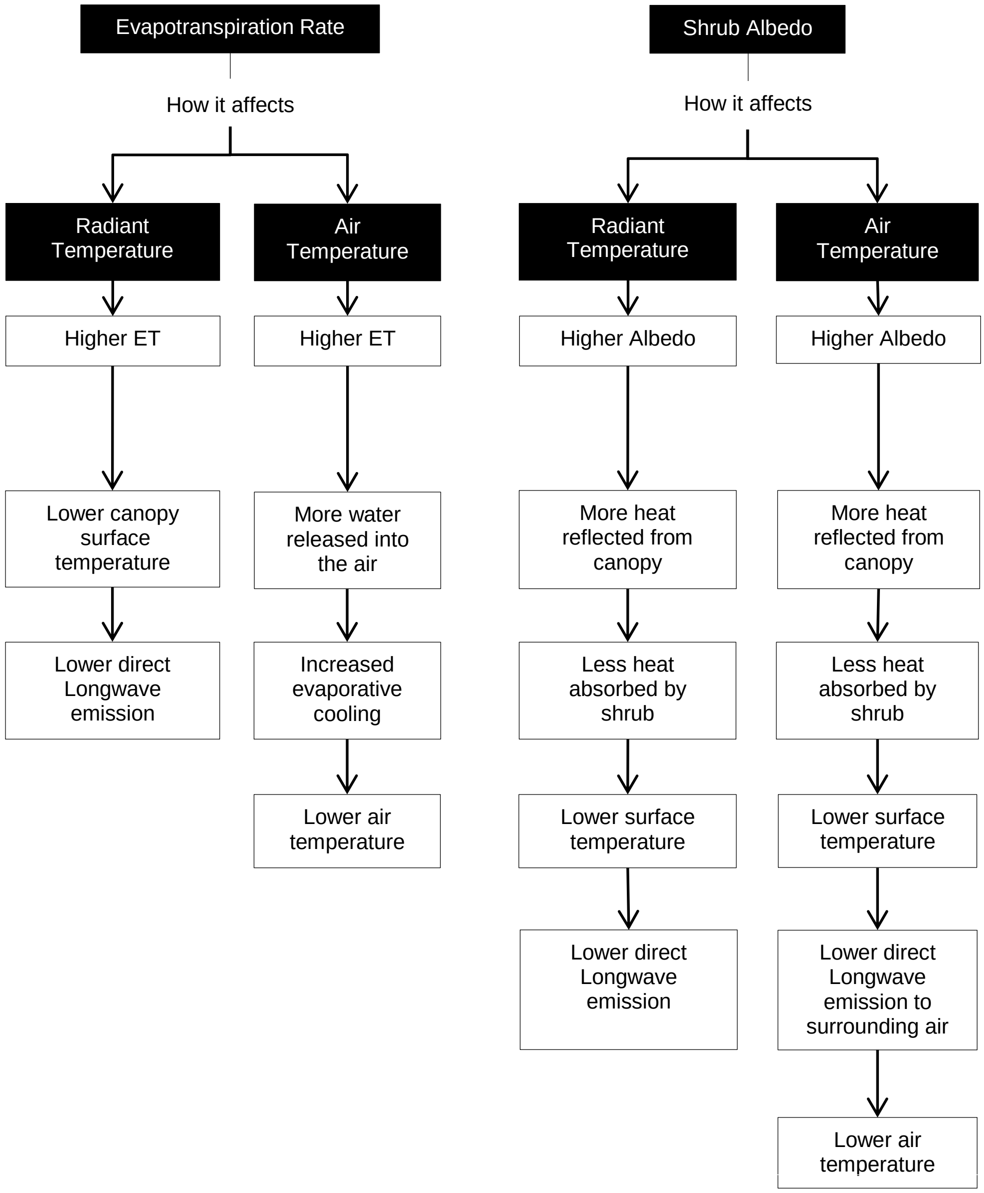

Figure 18. Hypothesised effects of ET and SA on t_{mrt}

Equation (17) forms the basis of the proposed hypothetical model on optimized landscape design (Figure 19).

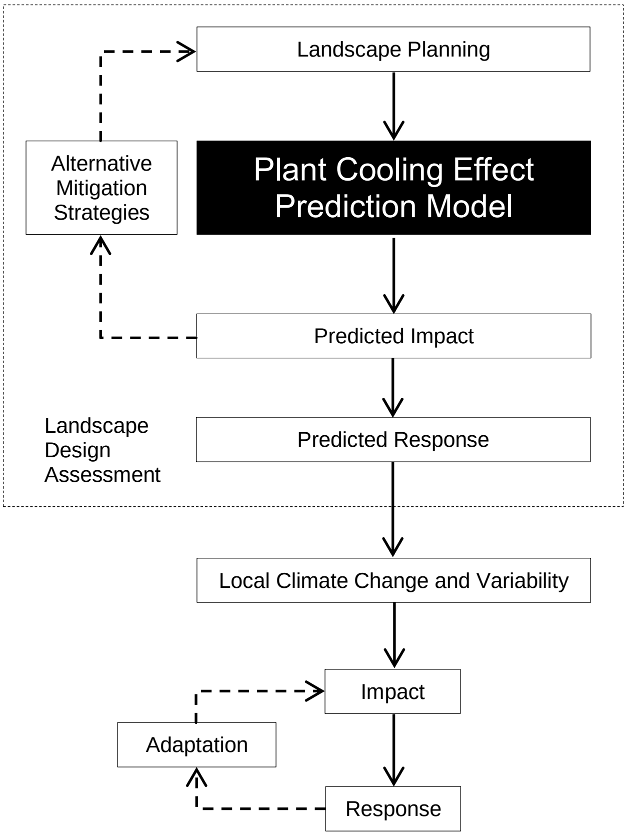

Figure 19. Hypothetical model on landscape design assessment in the mitigation and adaptation model

3.2 Methodology

The overall research methodology is illustrated in Figure 20. Studies on rooftop greenery will be conducted with different plants. Three quarters of all relevant data collected will be used for analysis and construction of a regression model for estimating t_{mrt} based on plant characteristics. The remaining quarter of data collected will be used for the purpose of validation.

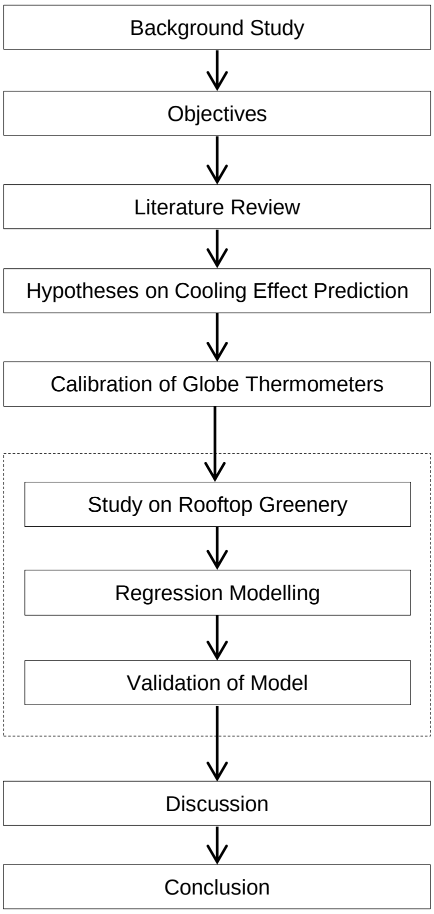

Figure 20. Research methodology

Quantification of the cooling effect of plants will be done through field measurement. Therefore, a series of measurements is proposed with the aim of quantifying plant evapotranspiration rates, radiant and functional attributes of plants used for rooftop greenery. The variables to be measured are shown in Table 3.

Table 3. Hypothesized variables

Variable	**Corresponding measurement**
Mean radiant temperature	Globe temperature, air temperature, wind velocity
Plant evapotranspiration rate	Water loss rate
Shrub albedo	Albedo

1. Calibration of the globe thermometer

The 38 mm globe thermometer will first be calibrated for use in the tropical outdoor urban environment. This is to enable accurate diurnal measurement of t_{mrt} near the plant canopy. The calibration process is documented in Chapter 3.2.1.

2. Measurement of plants in a roof garden setting

Measurements are proposed for a typical roof garden setting. Attributes of different plants that are hypothesized to be significant variables for cooling will be measured. The variables include plant evapotranspiration rate and shrub albedo (Figure 21). The complete list of measured variables is shown in Table 7.

Measurements from the hypothesized variables will be analysed to deduce their correlation with t_{mrt}.

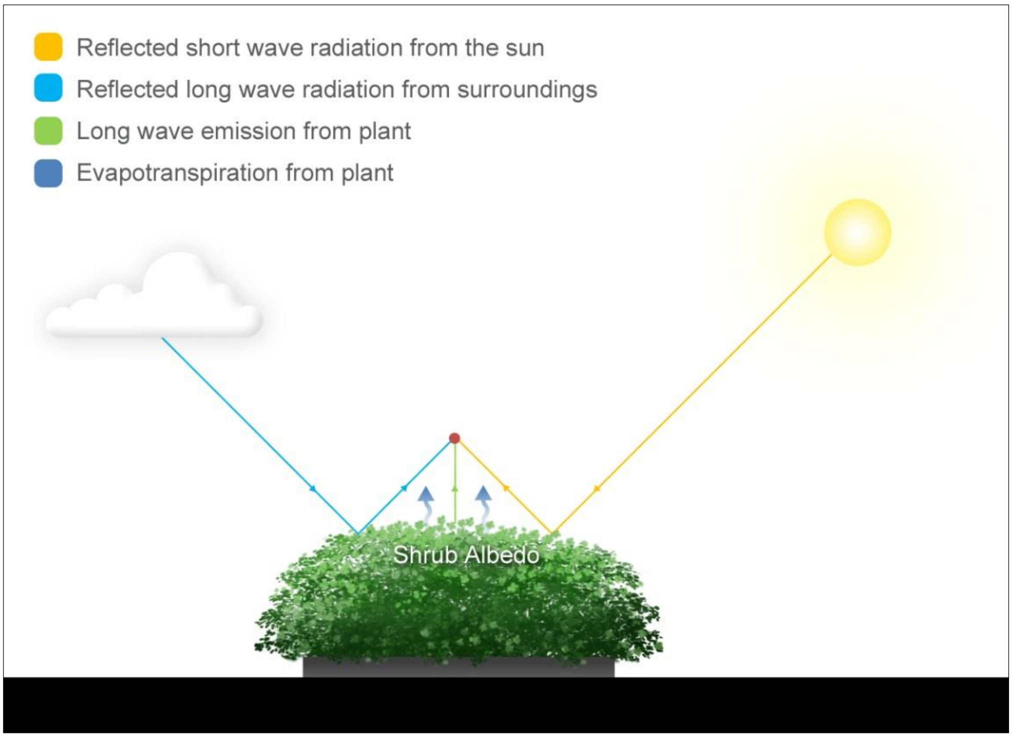

Figure 21. Effect of rooftop greenery on temperature at a given point

3.2.1 Calibration of globe thermometers for use in the tropical urban environment

Content from Chapter 3.2.1 (Pages 71 to 87) has been published in the Journal of Building and Environment, for which I am the main author:

Tan, C.L., Wong, N.H., Jusuf, S.K., 2013, Outdoor mean radiant temperature estimation in the tropical urban environment, *Building and Environment* 64:118-129.

3.2.1.1 Objectives

The objective of this study is to assess the feasibility of deploying customised 40 mm globe thermometers for outdoor t_{mrt} measurement in the tropics. Calibration of the mean convection coefficient in the ASHRAE t_{mrt} formula is performed to ensure accuracy of estimation.

3.2.1.2 Methodology

Customized globe thermometers are used to estimate the t_{mrt} outdoors to ensure the accuracy of t_{mrt} estimation, readings from the customized globe thermometers are first estimated against readings from a net radiometer. The mean convection coefficient of the formula used for t_{mrt} estimation is recalibrated for use in the local context. The mean radiant temperature is defined as the 'uniform temperature of an imaginary enclosure in which the radiant heat transfer from the human body equals the radiant heat transfer in the actual non-uniform enclosure' (ASHRAE, 2001a). It is often used as a parameter to estimate thermal comfort. Mean radiant temperature can be measured with a globe thermometer (De Dear, 1987; Keuhn et al., 1970; Nikolopoulou et al., 1999; Vernon, 1932). It can be used for indoor and outdoor conditions (Nikolopoulou and Lykoudis, 2006). The Vernon globe is a black copper sphere of 75 mm radius with a thermometer positioned in the middle of the sphere. For convenience, smaller globes were developed. The 38 mm globe thermometer is a common option as the globe used is a table tennis ball, which can be readily purchased and conveniently replaced (Humphreys, 1977). Accuracy of the 38 mm globe thermometer can be adjusted to cater to outdoor conditions by recalibrating the mean convection coefficient. This method has been tested in Sweden (Thorsson et al., 2007) and shown to be effective in outdoor conditions. To ensure validity of the t_{mrt} estimation for this study, the mean convection coefficient of the formula for t_{mrt} estimation via the globe thermometer is recalibrated. This is done by comparing the estimates from the customised globe thermometer to the long wave and short wave readings from a net radiometer. Two sets of measurements are made, one at each of the study areas (Table 4).

Two different methods for measuring the t_{mrt} outdoors are put to comparison:

1. Method A - Radiant flux measurements, where t_{mrt} calculation is based on short wave and long wave angular factors for a sphere;
2. Method B – 40 mm globe thermometer with t_{mrt} equation from ISO 7726:1998 (ISO 7726, 1998).

Table 4. Measurement period

	Study Area 1 Green Technology Laboratory rooftop	**Study Area 2 School of Design and Environment Block 1 rooftop**
Measurement date	28/02/2011 to 18/03/2011 30/03/2011 to 12/04/2011	13/08/2011 to 13/09/2011
No. of days measured	33	32
Purpose of measurement	Recalibration of mean convection coefficient	Validation of recalibrated mean convection coefficient
No. of days used for recalibration of mean convection coefficient	33	-
No. of days used for validation of mean convection coefficient	-	32

Results are used to recalibrate the t_{mrt} formula for Method B, so that the mean convection coefficient in the t_{mrt} equation will be representative of local outdoor conditions. Recalibration is done via statistical analysis using the IBM SPSS software.

Measurements are then made in another area with Methods A and B. The t_{mrt} formula used for the second measurement will be with the recalibrated mean convection coefficient. This is done to ensure validity of the recalibration.

Measurements are taken at the frequency of one minute, and averaged to five minute intervals (Thorsson et al., 2007). Data gathered from Methods A and B will be used to recalibrate the globe thermometer to improve the accuracy of the globe thermometer with respect to radiant flux measurements. Table 8 shows the measured variables and equipment used.

Figure 22 shows the measurement setup. A net radiometer with three integrated pyranometer and pyrgeometer arms (Kipp and Zonen, CNR 4) is used to measure long and shortwave radiation for the following directions:

- North
- East
- South
- West
- Upper hemisphere
- Lower hemisphere

The newly purchased net radiometer was factory calibrated. The pyranometers were calibrated side by side to a reference CMP 3 pyranometer according to ISO 9847:1992 annex A.3.1. The pyrgeometers were calibrated side by side to a reference CG(R) 3 pyrgeometer (Kipp, 2008).

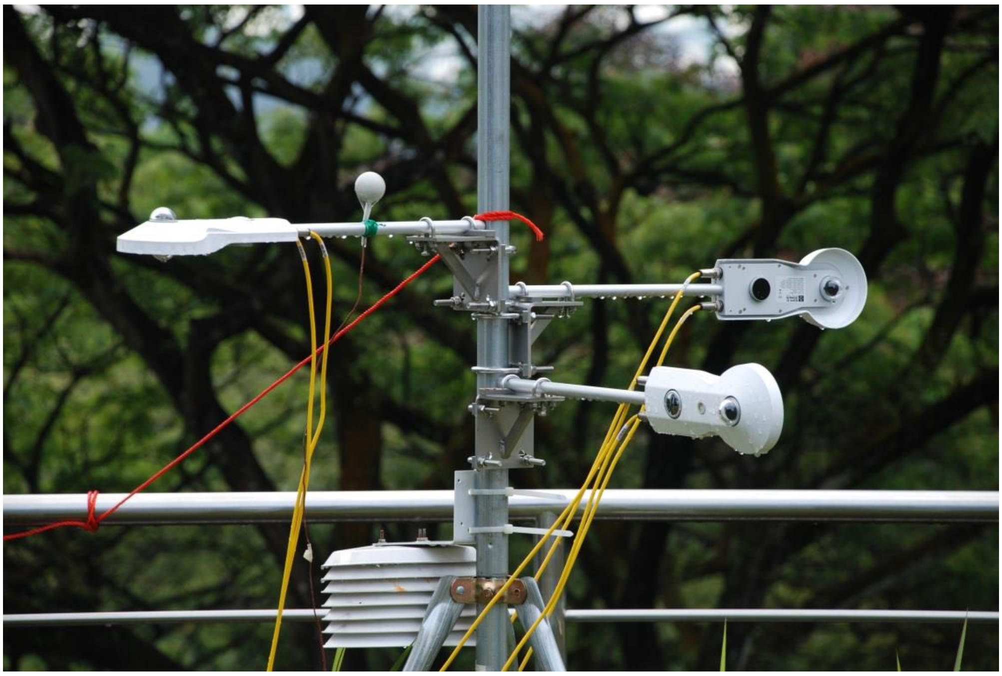

Figure 22. 40 mm globe thermometer mounted on net radiometer

In a previous study conducted in Sweden (Thorsson et al., 2007), the globe thermometer used consisted of a grey acrylic sphere that is 38 mm in diameter with a Pt100 sensor (De Dear, 1987; Humphreys, 1977; Nikolopoulou et al., 1999).

In this study, the globe thermometer is made of a 40 mm ping pong ball with a HOBO thermocouple wire at its centre. The ping pong is coated in flat grey paint (Phylox Nippon 144 dove grey). The 40 mm ping pong ball is preferred over the original 38 mm due to the decrease in availability of 38 mm ping pong balls (ITTF, 2009). The globe thermometer is secured on the arm of one of the net radiometer sensors to ensure accuracy of readings for both methods of t_{mrt} calculation. A total of nine other customised globe thermometers are set up near the globe thermometer to ensure measurement consistency. All thermocouple loggers and Type-T Copper-Constantan thermocouple sensors used for this study are new and factory calibrated. The globe thermometers are positioned such that they will not experience any effects of overshadowing from the mounting structure.

3.2.1.3 Results and discussion

3.2.1.3.1 Validation of customised globe thermometers

Calculation of t_{mrt} can be done for Method A using the following method (Thorsson et al., 2007):

1. Estimate mean radiant flux density (S_{str})
2. Estimate t_{mrt} using value of S_{str}

Estimation of S_{str} is done using Equation (18) (VDI, 1994):

$$Sstr = \alpha_{\mathrm{k}} \sum_{i=1}^{6} K_{\mathrm{i}} F_{\mathrm{i}} + \varepsilon_{\mathrm{p}} \sum_{i=1}^{6} L_{\mathrm{i}} F_{\mathrm{i}} \qquad [18]$$

Where,

K_i = Short wave radiation (Wm^{-2})

L_i = Long wave radiation (Wm^{-2})

F_i = Angular factors between observer and external surrounding
Value of 0.167 used (Fanger, 1972; Thorsson et al. 2007)

α_k = Absorption coefficient for short wave radiation. Value of 0.7 is used (Thorsson et al. 2007)

ε_p = Emissivity of the human body. Value of 0.97 is used (Thorsson et al. 2007)

The t_{mrt} (°C) can be calculated from the Stefan–Boltzmann equation:

$$Tmrt = \sqrt[4]{\left(\frac{Sstr}{\varepsilon p\sigma}\right)} - 273.15 \qquad [19]$$

Where,

S_{str} = Mean radiant flux density (Wm^{-2})

σ = Stefan–Boltzmann constant (5.67 • 10^{-8} Wm^{-2}K^{-4})

ε_p = Emissivity of the human body. Value of 0.97 is used (Thorsson et al. 2007)

Estimation of t_{mrt} can be done for Method B using Equation (15) from ISO 7726 (1998):

$$Tmrt = \left[(Tg + 273.15)^4 + \frac{1.1 \times 10^8 Va^{0.6}}{\varepsilon D^{0.4}} \times (Tg - Ta)\right]^{0.25} - 273.15 \qquad [15]$$

Where,

t_g = Globe temperature (°C)

V_a = Air velocity (ms^{-1})

t_a = Air temperature (°C)

D = Globe diameter (m)

ε = Globe emissivity

Mean convection coefficient of the globe (1.1 X 10^8 $V_a{}^{0.6}$) comprises of the wind exponent as well as an empirically derived constant.

Values of t_{mrt} for Method B are calculated using Equation (19).

A total of 65 days of field data from the two study areas are measured (Table 5). A typical clear sunny day is used for analysis of the diurnal tmrt profile at Study Area 1. The 18th of March 2011 was a sunny day with clear skies. The mean near-surface air temperature was 27.3 °C, the minimum near-surface air temperature recorded was 24.2 °C and the maximum near-surface air temperature recorded was 31.0 °C. The mean wind speed was 3 ms^{-1}. The sun rose at 07:10 hrs and set at 19:16 hrs. The sun reached its maximum altitude of 87.5° at 13:13 hrs. Mean wind speed was measured with a weather station that was placed within 10 m of the mean radiant temperature measurement site.

Figure 23 shows the short wave and long wave radiation fluxes for six directions. K_{NORTH}, K_{SOUTH}, K_{EAST} and K_{WEST} represents the short wave radiation fluxes from the North, South, East and West respectively. K_{UP} represents short wave radiation from the sky (upper hemisphere), and K_{DOWN} represents short wave radiation from the ground (lower hemisphere).

Direct solar radiation K_{UP} peaked at 1142 Wm^{-2} at 14:10 hrs. Its value is most significantly affected by the position of the sun. The reflected short wave radiation K_{DOWN} follows a similar pattern to that of K_{UP} but with significantly lower values. It peaked at 133 Wm^{-2} at 14:10 hrs. K_{EAST} peaked at 351 Wm^{-2} in the morning (10:00 hrs). Thereafter, readings remained low. In contrast, K_{WEST} remained low in the morning and increased slowly until it reached its peak of 684 Wm^{-2} (almost twice the peak value of K_{EAST}) at 16:25 hrs. This is due to exposure to more intense direct solar radiation from the West. K_{NORTH} and K_{SOUTH} remained low throughout the day. K_{NORTH} peaked at 291 Wm^{-2} at 16:25 hrs. K_{SOUTH} peaked at 246 Wm^{-2} at 12:50 hrs. There is negligible short wave radiation activity in the absence of sunlight.

L_{NORTH}, L_{SOUTH}, L_{EAST} and L_{WEST} represents the long wave radiation fluxes from North, South, East and West respectively. L_{UP} represents long wave radiation from the sky (upper hemisphere), and L_{DOWN} represents long wave radiation from the ground (lower hemisphere).

The long wave fluctuations for all six directions follow a similar pattern. The L_{UP} profile is notably lower than the other profiles. This is due to the fact that L_{UP} is facing the sky and not directly at any objects. L_{UP} peaked at 465 Wm^{-2} at 14:15 hrs. L_{DOWN} exhibited the highest profile, due to the fact that it is facing downwards and has maximum exposure to objects and surfaces. The difference between the other points is most evident during periods of intense exposure to sunlight. L_{DOWN} peaked at 546 Wm^{-2} at 13:50 hrs. L_{EAST} increased steadily until 14:00 hrs. L_{WEST} does not exhibit a similar trend. This may be because there is a wall on the West side of the net radiometer, and it is exposed to direct sunlight after 14:00 hrs. L_{EAST} peaked at 519 Wm^{-2} at 16:30 hrs and L_{WEST} peaked at 498 Wm^{-2} at 14:10 hrs. L_{WEST}, L_{NORTH} and L_{SOUTH} showed similar trends in fluctuation throughout the day. L_{NORTH} peaked at 499 Wm^{-2} at 14:10 hrs and L_{SOUTH} peaked at 497 Wm^{-2} at 13:50 hrs. The minimum value for all long wave radiation ranges from 433 Wm^{-2} to 440 Wm^{-2} at 06:40 hrs. There are slight fluctuations in the absence of sunlight.

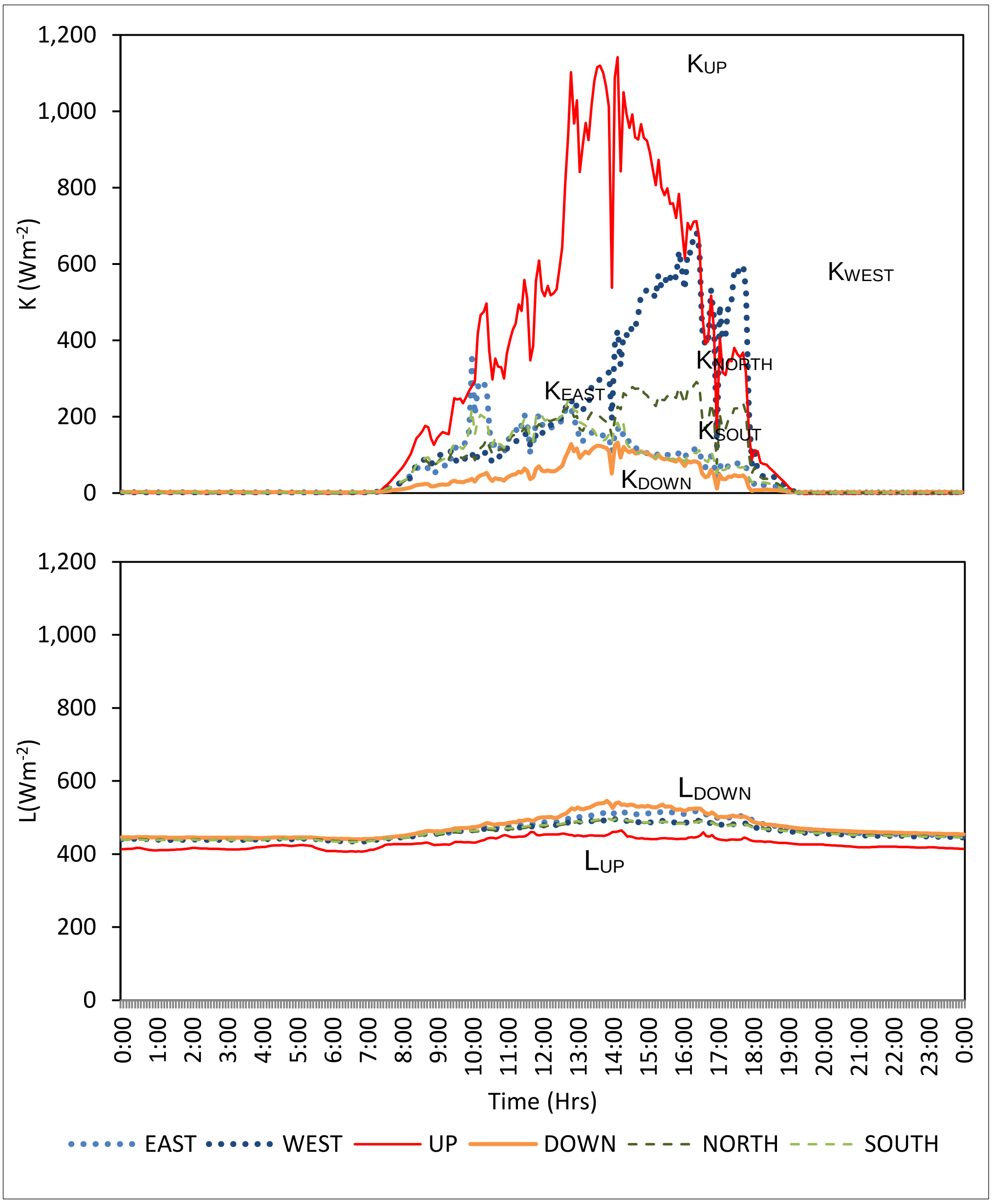

Figure 23. Diurnal short wave (K) and long wave (L) profile for 18th March 2011

Measurements using Method A (Net radiometer) are used to plot the diurnal t_{mrt} profile for 18th March 2011. The plot is overlaid with a plot of diurnal t_{mrt} using Method B. The t_{mrt} profile generated is similar to that of K_{UP}, indicating the high relevance of direct solar radiation to t_{mrt}. Figure 24 shows that the calculation of t_{mrt} using the globe thermometer (Method B) differs from the values obtained via the net radiometer (Method A) drastically.

Results show that measurement of t_{mrt} using the customised globe thermometers and Equation (15) is highly unsuited for use in the given context. There is a slight overestimate of t_{mrt} in the absence of sunlight and a drastic underestimate during sunlit hours. Any measurement of outdoor t_{mrt} using the customised globe thermometers using Equation (15) would be highly inaccurate.

Figure 24 shows that the calculation of t_{mrt} using the globe thermometer (Method B) differs from the values obtained via the net radiometer (Method A) drastically. This is due to the mean convection coefficient used for the t_{mrt} formula (Equation 15) that does not adequately represent the convective conditions found in the tropical outdoor climate.

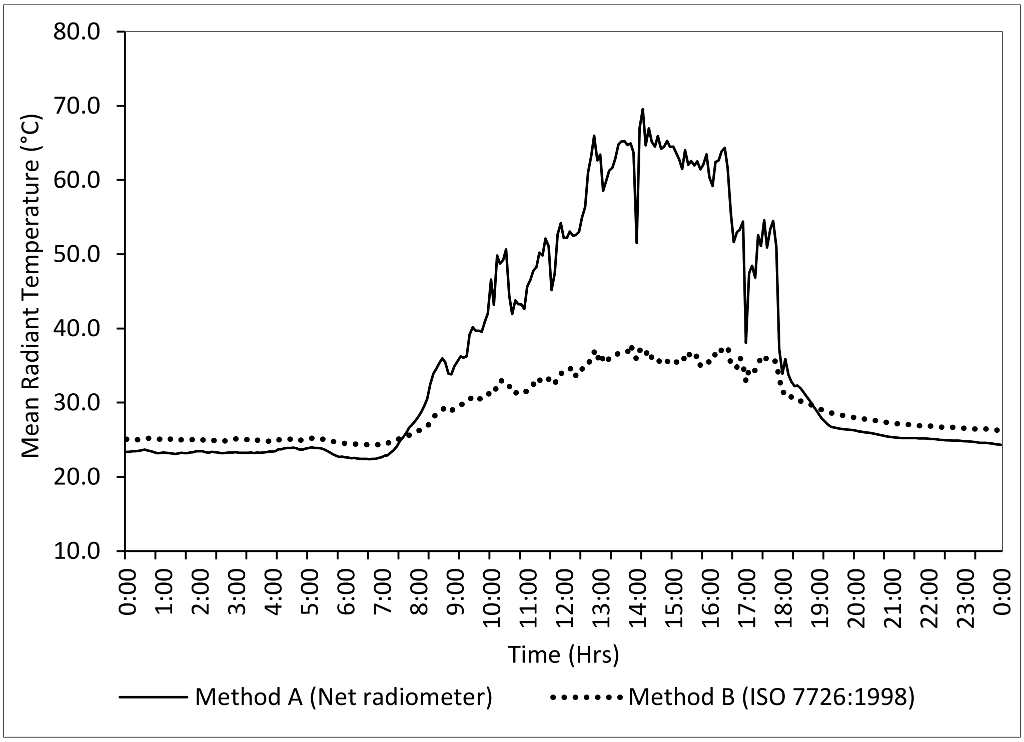

Figure 24. Calculation of t_{mrt} using Method A and B (ISO 7726:1998) – 18th March 2011

In order to utilise the formula in this context, the mean convection coefficient of 1.1 X $10^8Va^{0.6}$ is recalibrated. This is done by considering the field measurements of the following variables:

- Mean radiant temperature (°C)
- Globe temperature (°C)
- Air temperature (°C)
- Air velocity (ms^{-1})

Only measurements taken from Study Area 1 are used for the calibration. A total of 33 days, which consists of diverse weather conditions, are used. The best fit curve generated gives the new mean convection coefficient of 2.20 X $10^8Va^{0.119}$, giving us the recalibrated equation:

$$Tmrt = \left[(T\mathrm{g} + 273.15)^4 + \frac{2.20 \times 10^8 V\mathrm{a}^{0.119}}{\varepsilon D^{0.4}} \times (T\mathrm{g} - T\mathrm{a})\right]^{0.25} - 273.15 \quad [20]$$

Where,

t_g = Globe temperature (°C)

V_a = Air velocity (ms^{-1})

t_a = Air temperature (°C)

D = Globe diameter (m)

ε = Globe emissivity

The derived values are significant at 95% confidence interval.

A re-plot of the t_{mrt} profile for 18th March 2011 with Equation (20) shows the new t_{mrt} profiles. The new profile is much closer to that of the t_{mrt} profile generated by Method A (Figure 25). There is still a slight underestimation for certain periods during the day. The slight overestimation of t_{mrt} during night time is reduced to match the t_{mrt} of Method A. The profiles of the two methods show that the 40 mm globe thermometer has a response time of less than 5 minutes, which is similar to the 38 mm globe thermometers used in previous indoor tests (Höppe, 1999). There is a general trend of underestimation of t_{mrt} with increasing short wave radiation. This suggests that the albedo of the globe may be slightly higher than desired, and may be reduced further by using a darker shade of grey.

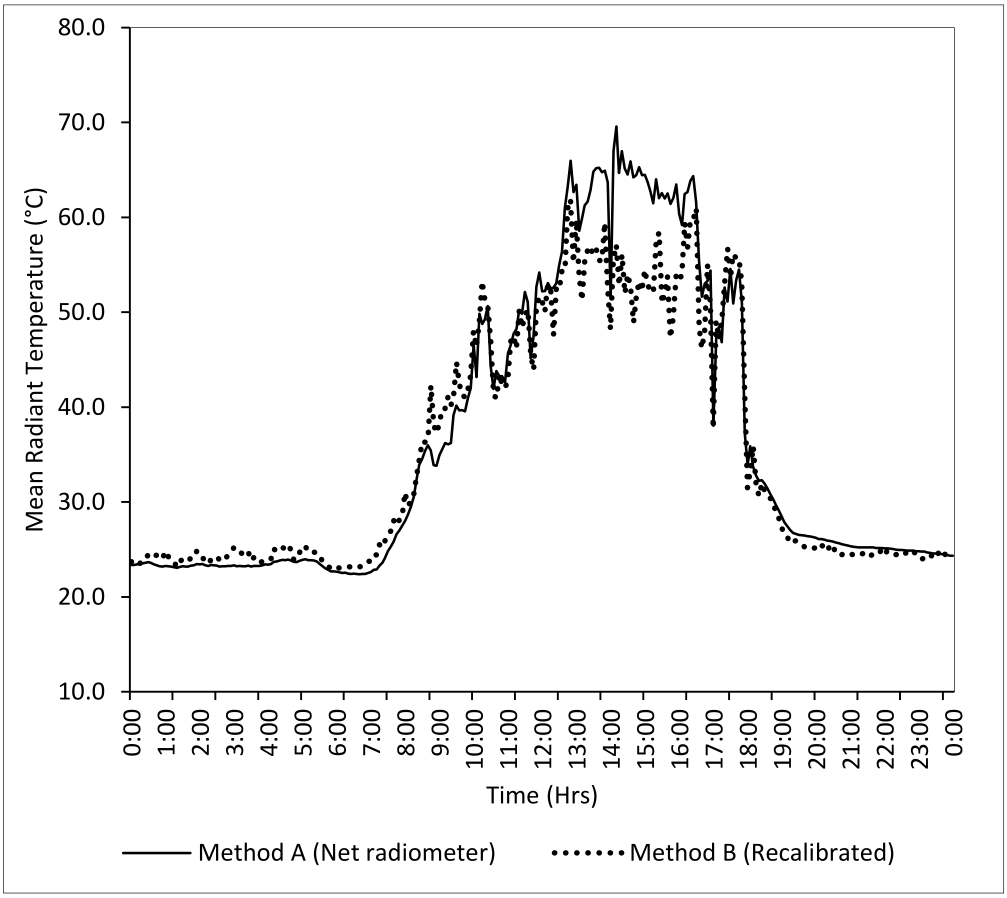

Figure 25. Calculation of t_{mrt} using Method A and B(Recalibrated) – 18th March 2011

To validate the new mean convection coefficient, Equation (20) is used to calculate the t_{mrt} of the same 40 mm globe thermometer at Study Area 2. A typical clear sunny day is chosen for analysis. A plot of the t_{mrt} profile for 16th August 2011 with Equation (20) shows the new t_{mrt} profile. Similar to the previous re-plot, the new profile is much closer to that of the t_{mrt} profile generated by Method A (Figure 26).

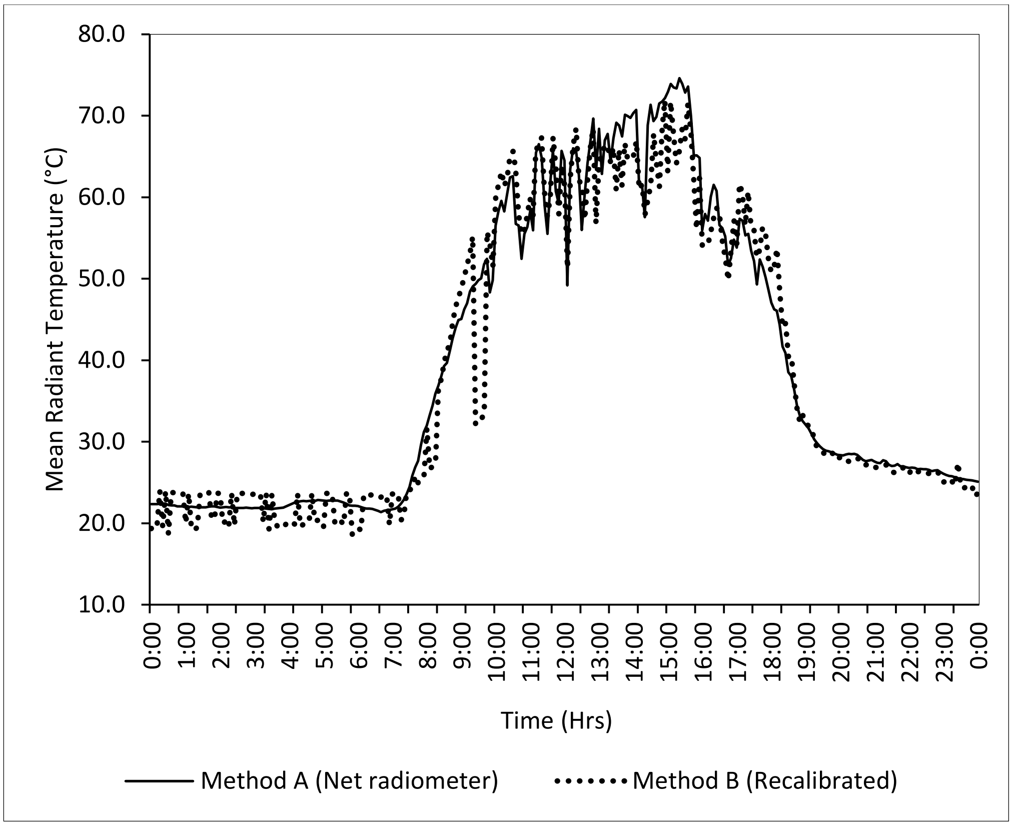

Figure 26. Calculation of t_{mrt} using Method A and B(Recalibrated) – Study Area 2, 16th August 2011

Figure 27 shows the whisker plot for the difference between t_{mrt} values derived from Method A and Method B. The median is approximately -0.4 °C, the inter-quartile range is approximately between 0.5 °C and -1.4 °C and the extreme values lie between 3.4 °C and -4.3 °C. This shows that most of the t_{mrt} values derived from Method B do not differ from that of Method A by 4.0 °C.

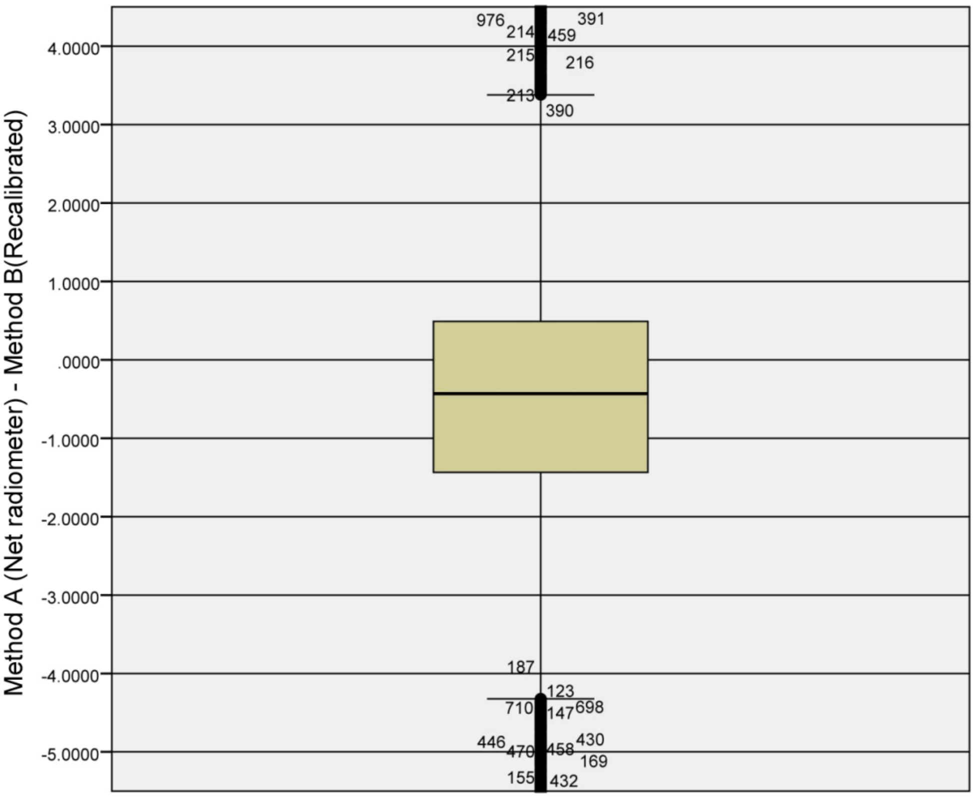

Figure 27. Whisker plot for Study Area 2 (Method A – Method B)

The 40 mm globe, together with the HOBO thermocouple data logger, can provide a good diurnal t_{mrt} profile that can be comparable to that of one derived through radiant flux measurements via a net radiometer (Figure 25 and Figure 26). The size of the globe does not demonstrate any significant impediment to its response time.

3.2.1.4 Conclusion

3.2.1.4.1 Recalibration of globe thermometer for use in the tropical urban environment

The objective of this study is to assess the feasibility of deploying 40 mm globe thermometers outdoors for t_{mrt} measurement in the tropics. The 40 mm ping pong ball is preferred over the original 38 mm due to the decrease in availability of 38 mm ping pong balls. Two methods are used to collect t_{mrt} measurements. Method A involves radiant flux measurements via a net radiometer, Method B involves using the 40 mm grey globe thermometer with a mean convection coefficient as stated in ISO 7726:1998. 5 minute mean values are used to compare readings from the two methods. The advantage of using Method A is that long wave and short wave radiation can be measured and analysed in different directions. Method B, while unable to measure long wave and short wave radiation, can provide estimates of t_{mrt} if air temperature and wind velocity data are provided.

Initial comparisons indicate that the t_{mrt} values obtained via the customised globe thermometers and ISO 7726:1998 deviated acutely from measurements obtained via the net radiometer. By redefining the mean convection coefficient of the 40 mm globe thermometer, a recalibrated Equation (20) for the 40 mm grey globe thermometer is obtained. The difference between Method A and Method B with the recalibrated formula is generally small. By conducting the measurement at two different sites, results show that Equation (20) is valid for typical outdoor conditions in Singapore. The air velocity ranges between 0 ms^{-1} and 4 ms^{-1}, and the incoming solar radiation of up to 1300 Wm^{-2}. Remaining errors may be attributed to instrumentation errors from the net radiometer and the 40 mm grey globe thermometers (e.g. location of sensors, etc.). The albedo of the 40 mm grey globe may have caused the slight underestimation of short wave radiation, and it is recommended that a darker shade of grey (lower albedo) be tested for improved results.

In this study, a net radiometer is used for the calibration of the customised globe thermometer. One area of concern is the level of uncertainty in measuring t_{mrt} with this method due to the fluctuating nature of radiation fluxes as well as the sensitivity of the net radiometer. A previous study has shown that measurement results from different net radiometers may vary significantly due to equipment specifications alone (d'Ambrosio Alfano et al., 2013). This variation, while in compliance to ISO standards, will affect the subsequent results of thermal comfort indices when used as input variables (d'Ambrosio Alfano et al., 2011a; Gaspar and Quintela, 2009). Dell'Isola et al. (2012) concluded from a study of measurement uncertainties on thermal environment assessment that the globe thermometer and net radiometer only produced similar results for the Predicted Mean Vote (PMV) only in conditions of low radiation asymmetry (Dell'Isola et al., 2012). Since the customised globe thermometer for this study is meant for outdoor deployment and will be subjected to high levels of short wave radiation, further validation using different t_{mrt} measurement methods is recommended.

This study has validated the application of the 40 mm grey globe thermometer in the tropical urban environment. Net radiometers can be used for accurate measurements of t_{mrt} but the equipment is bulky and requires a constant AC power source. The availability and portability of the customised globe thermometer makes it a convenient tool for outdoor t_{mrt} measurements. Since the values of air velocity, globe and air temperature are needed for Equation (20), usage of the 40 mm grey globe thermometers on a large scale for extended periods would entail the concurrent deployment of anemometers and air temperature sensors.

The revised mean convection coefficient provides the possibility of outdoor deployment of the 40 mm globe thermometer together with a data-logger for an extended period of time at an urban scale. Moreover, the availability and portability, coupled with relative ease of deployment makes it an ideal tool for outdoor field measurements.

To assess the deployability of recalibrated globe thermometers, an urban scale mapping of t_{mrt} is conducted after recalibration of the t_{mrt} formula with the intention of understanding the diurnal t_{mrt} profile of highly urbanized areas. Measurement areas are categorized into the following:

- Area with high density commercial buildings;
- Area in close proximity to a large water body;
- Area with high density residential buildings;
- Park.

Results of the urban scale mapping of t_{mrt} are shown in Appendix 10.1.

3.2.2 Sampling

The chief variable for this study is plant type. The objective is to sample plants commonly used for outdoor landscaping.

Tan and Sia (2009) categorised a list of 300 of the most commonly used landscape plants in Singapore into five major groups (Table 5).

Table 5. Summary of main plant groups (Tan and Sia, 2009)

Component		**Sub-Category**	**LAI**
Tree	Includes angiosperms and gymnosperms	Dense Canopy	4.0
		Intermediate Canopy	3.0
		Open Canopy	2.5
Shrubs	Includes monocots and dicots	Monocot	3.5
		Dicot	4.5
Palms	Include single-stemmed and multi-stemmed plants	Solitary	2.5
		Cluster	4.0
Turf	Refers to grass species	Planted Area	2.0

Plants that are categorised have the highest populations in landscaped areas managed by the National Parks Board of Singapore. Two methods are used to measure the LAI of plants in the various groups. This includes direct measurement of leaf area through partial sampling of the leaves, and indirect measurement using the plant canopy analyser LAI-2000 (under diffuse light conditions). At least three measurements are made for every specimen.

Since plants used for rooftop greenery are from the shrubs category, various shrubs of differing characteristics will be selected for measurement. The criteria for selection are based on:

1. Sub-category (Monocot/Dicot)
2. Physical characteristics of plant

Three different plant species is used for the study. Plants that are selected are commonly used in landscaping and provide a variety of LAI, leaf area and plant height values (Table 6).

Table 6. Plant selection and attributes

Plot	Plant	LAI (Nparks)	Estimated Leaf Area (m^2)	Estimated Plant Height (m)
1	Phyllanthus cochinchinensis	4.5	0.0005	0.5
2	Heliconia ‘American Dwarf’	3.5	0.0140	1.5
3	Sphagneticola trilobata	4.5	0.0020	0.3

Plot 1 - Phyllanthus cochinchinensis

Plot 2 - Heliconia ‘American Dwarf’

Plot 3 - Sphagneticola trilobata

3.2.3 Measurement setup

The proposed measurement setups are discussed in this section. Measurement will be conducted on the rooftop of SDE1, National University of Singapore. Measurements for rooftop greenery will be done with 3.0 m by 3.0 m roof garden plots (Figure 28). The proposed setup is derived from reviewed literature (DiGiovanni et. al, 2013; Jim, 2012) and customized to suit the objectives of this study. Mean radiant temperature and shrub albedo is measured 0.3 m above the center of the plot canopy to ensure homogenous conditions above the canopy surface as well as reliable measurements of albedo (Akbari et al., 1998; ASHRAE, 2001b; Townsend, 1964).

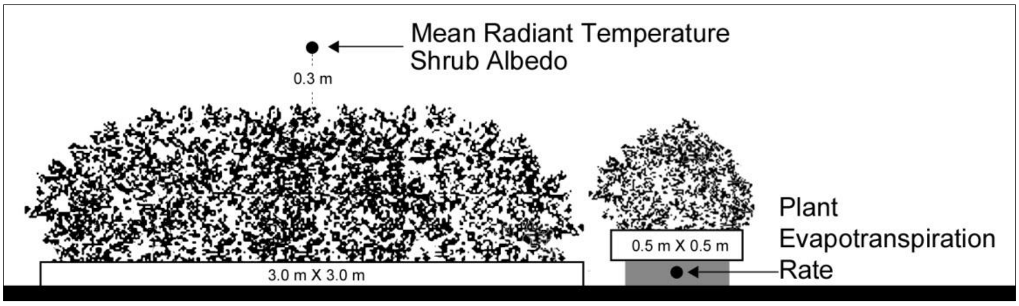

Figure 28. Rooftop greenery measurement setup

Location of all measurement points are shown in Figure 29. Measurement period and days used for analysis are shown in Table 7.

Not all data obtained was used for analysis. For Chapter 4, results shown are representative of typical clear or overcast sky conditions. Rainy days are not used for analysis unless no suitable alternatives are available.

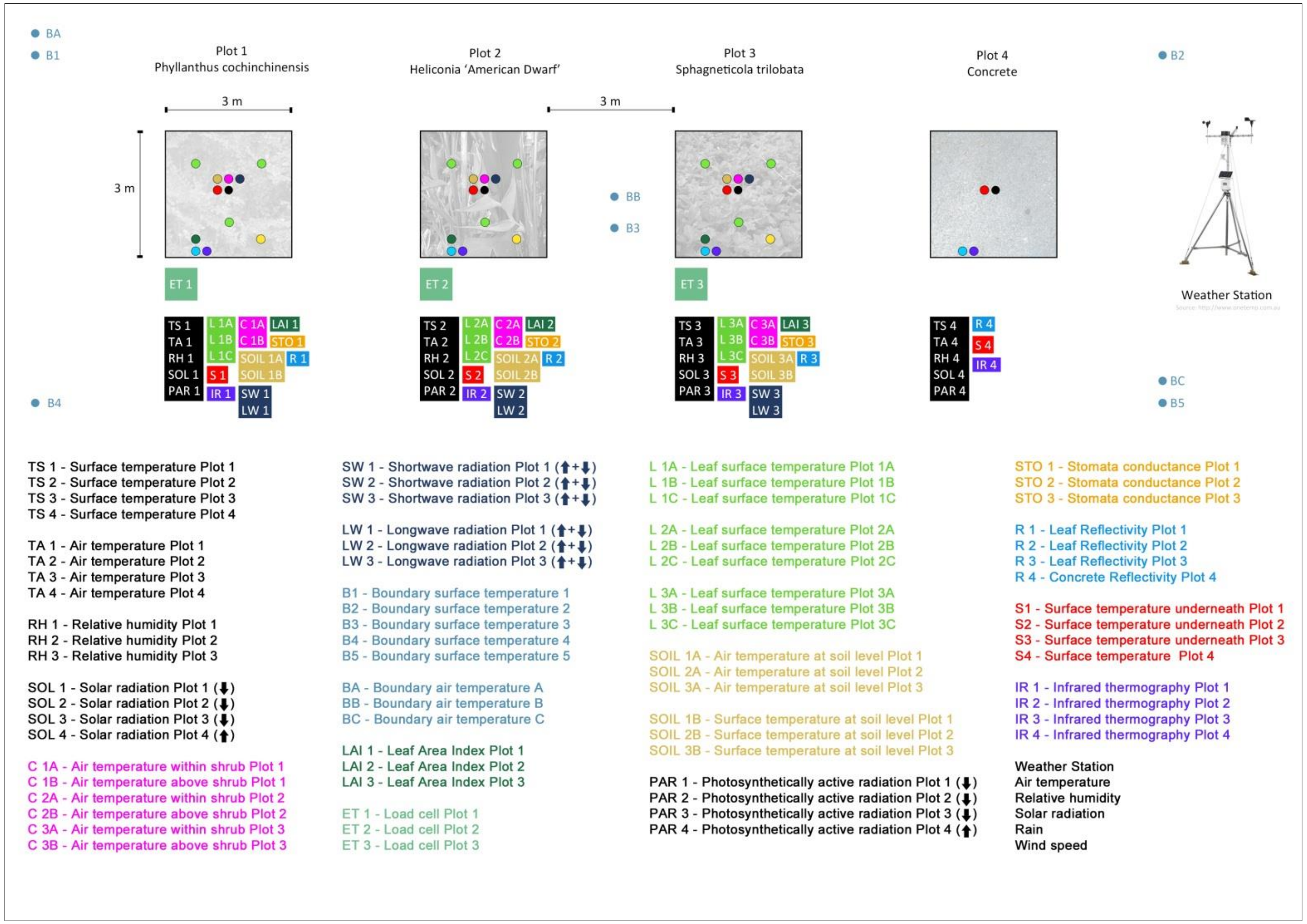

Figure 29. Rooftop measurement points

Table 7. Measurement variables and period

Measurement variable	**From**	**To**	**No. of days**
Mean radiant temperature	10/05/2014	31/12/2014	236
Air temperature of soil	26/06/2014	31/12/2014	189
Air temperature within canopy	26/06/2014	31/12/2014	189
Air temperature above canopy	26/06/2014	31/12/2014	189
Solar radiation	10/05/2014	31/12/2014	236
Photosynthetically Active Radiation	10/05/2014	31/12/2014	236
Relative humidity	10/05/2014	31/12/2014	236
Plant evapotranspiration rate	10/05/2014	31/12/2014	236
Shrub albedo	10/05/2014	31/12/2014	236
Leaf Area Index	-	-	-
Leaf reflectance	-	-	-
Stomatal conductance	28/05/2014 03/06/2014 09/06/2014 02/07/2014 10/07/2014	-	5
Leaf surface temperature	20/05/2014	31/12/2014	226
Leaf infrared thermography	28/05/2014 03/06/2014 09/06/2014 10/06/2014 02/07/2014 04/07/2014	-	6
Soil temperature	18/06/2014	31/12/2014	197
Temperature of concrete under roof plots	20/05/2014	31/12/2014	226
Longwave and shortwave radiation	19/06/2014	16/07/2014	28
Boundary surface temperature	20/05/2014	31/12/2014	226
Boundary air temperature	10/05/2014	31/12/2014	236

Measurement details for the hypothesized variables are as follows:

1. Plant EvapoTranspiration rate (ET)

Measurement are conducted for t_{mrt}, air temperature and ET. ET is obtained by measuring the water loss with a load cell. An extensive roof garden tray of 0.5 m by 0.5 m filled with the relevant plant is used. Surface temperature, air temperature and air velocity will be measured at 1 minute intervals at the homogenous level. Load cells will be placed next to each roof garden plot and on each rack measured (Figure 30). The weight of substrate is standardized at 10.0 Kg to ensure that the capacity for water absorption is the same throughout all plots. The bottom and sides of the tray are insulated with extruded foam to minimize effects due to advection.

Logging of load cell weight is done every 20 seconds. Data is processed to 1 minute intervals and averaged to hourly intervals.

Calculating of ET is performed in the following manner:

$$ET\ (Time) = \left(\frac{Wa - Wb}{10\ minutes}\right)\ x\ \frac{1}{A_{Plot}} \qquad [21]$$

Where,

ET = Plant evapotranspiration rate (mm·min^{-1})

T = Time (min)

W_a = Weight of load cell 5 minutes before (Kg)

W_b = Weight of load cell after 5 minutes after (Kg)

A_{Plot} = Area of plot (m^2)

For instance,

$$ET\ (12{:}00\ hrs) = \left(\frac{Weight\ @\ 11{:}55\ hrs - Weight\ @\ 12{:}05\ hrs}{10\ minutes}\right)\ x\ \frac{1}{0.25} \qquad [22]$$

Figure 30. Measurement of plant evapotranspiration rate with load cell

2. Leaf Area Index

Measurement of LAI is done by removing all the leaves in a 0.5 m by 0.5 m area for each plot and green wall (Figure 31). Leaves are scanned and digitally processed. Leaf pixel will be totaled and LAI is estimated by dividing total leaf pixel area by total scanned area in the 0.5 m by 0.5 m plot.

Figure 31. Measurement of Leaf Area Index

3. Shrub Albedo

Shrub albedo is defined as the ratio of reflected radiation from the shrub over global solar radiation. The measured albedo will provide data on the average leaf angle as well as shrub reflectivity. Pyranometers will be used to measure radiation exposure. One pyranometer will be directed towards the sky to measure global solar radiation. Subsequent pyranometers will be directed towards the shrub to measure reflected radiation (Figure 32). The pyranometers will be placed within 0.5 m of the canopy of the shrubs (Akbari et al., 1998; ASHRAE, 2001b).

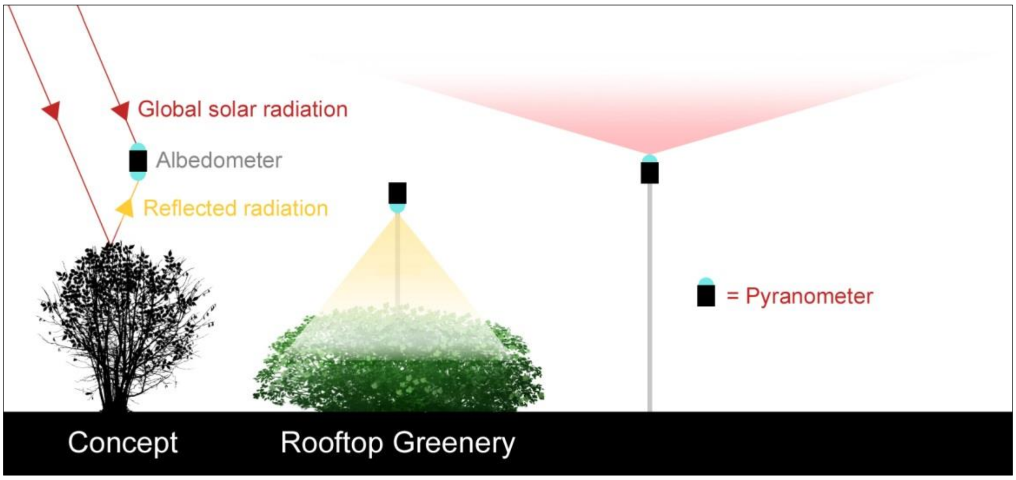

Figure 32. Measurement of Shrub Albedo

Concurrent measurements of t_{mrt} as well as albedo at a nearby location without the influence of rooftop greenery will also be made to serve as a control for the experiment.

3.2.4 Equipment

Equipment used for all measurements are shown in Table 8:

Table 8. Equipment list

Variable	Equipment	Measurement Range	Accuracy
Air temperature, t_a	*HOBO U12-012 Temp/RH data logger*	-20 °C – 70 °C	±0.35 °C from 0 °C – 50 °C, to a maximum of +/- 3.5%
	HOBO U23 Pro v2 External Temperature data logger – U23-004	-40 °C – 100 °C	±0.21 °C from 0 °C – 50 °C
Evapotranspiration Rate (ET)	*HBM Z6FC3 load cell and Quantum X logger*	0 to 200 kg	0.0018 % of full span
Globe temperature, t_g	*HOBO Thermocouple Data Logger*, U12-014 with Type-T Copper-Constantan thermocouple sensors and 40 mm diameter ping pong ball	-200 °C – 100 °C	±1.5 °C
Leaf Area Index, LAI	*Canon All-In-One Printer,* MP276	Optical Resolution: 1200 x 2400dpi	-
	LAI 2200 Plant Canopy Analyzer	Wavelength Range: 320-490 nm.	-
Reflectivity	*SHIMADZU Spectrophotometer*, UV-3150 UV-VIS-NIR	190 nm to 3200 nm	UV/VIS region: ±0.2 nm NIR region: ±0. 8 nm
Relative Humidity, RH	*HOBO U12-012 Temp/RH data logger*	5 % to 95 % RH	±2.5 % typical, 3.5 % maximum, from 10 to 90 % RH
Solar Irradiance	*Onset S-LIB-M003 Silicon Pyranometer* *Onset S-LIA-M003 PAR sensor*	0 to 1280 W/m^2 0 to 2500 umol/m^2/sec	±10 W/m2 or ±5%, whichever is greater in sunlight. Additional temperature induced error ±0.38 W/m^2 /°C from 25°C

Variable	Equipment	Measurement Range	Accuracy
Shading characteristics	Close-circuit television	-	-
Shrub Height	Measuring pole	0 to 2 m	0.001 m
Short and long wave radiation, K, L	*Kipp & Zonen,* CNR 4 With Integrated pyranometer, pyrgeometer, Pt-100 and thermistor	Pyranometer: 0 Wm^{-2} – 2000 Wm^{-2} Pyrgeometer: -250 Wm^{-2} – 250 Wm^{-2} Pt-100: -200 °C to 600 °C Thermistor: -40 °C to 300 °C	Pyranometer: < 5% uncertainty (95 % confidence level) Pyrgeometer: < 10% uncertainty (95 % confidence level) Pt-100 / Thermistor: ±0.7 °C
Sky View Factor, SVF	*Nikon D80* Digital SLR camera	Effective pixels:10.2 million	Sensitivity:100 to 1600 (ISO equivalent) in steps of 1/3 EV, plus HI-0.3, HI-0.7 and HI-1
Sky View Factor, SVF	*Nikon D80* Digital SLR camera	Effective pixels:10.2 million	Sensitivity:100 to 1600 (ISO equivalent) in steps of 1/3 EV, plus HI-0.3, HI-0.7 and HI-1
Stomata conductance	*Decagon* SC-1 Porometer	*0 to 1000* $mmolm^{-2}s^{-1}$	10 %
Surface Temperature, t_s	*Fluke Thermal Imager*	-20 °C to 150 °C (-4 °F to 302 °F)	±2 °C or 2 % (whichever is greater)
Surface temperature, t_s	*HOBO Thermocouple Data Logger*, U12-014 with Type-T Copper-Constantan thermocouple sensors	-200 °C – 100 °C	±1.5 °C
Surface temperature, t_s	*Yokogawa* DX230 DAQ Station, T type	-200 °C – 400 °C	±1.5 % of reading + 0.5 °C
Wind speed, V_a	*Onset Wind Speed Smart Sensor*, S-WSA-M003	0 ms^{-1} – 45 ms^{-1}	±1.1 ms^{-1} or ±4% of reading, whichever is greater

3.3 Final deliverables

The proposed deliverables for this research are as follows:

1. A prediction model for the overall cooling effect of rooftop greenery based on plant characteristics such as plant evapotranspiration rate and shrub albedo.
2. Guidelines for plant selection for rooftop greenery based on the objective of maximum reduction in t_{mrt}.

3.4 Importance and potential contribution of research

The prediction model will enable architects, urban and landscape designers to practice landscape design and allocate plants within an objective framework. Crucial areas that require more and appropriate plantings can be identified and redundancies can be avoided. This will help achieve the overall concept of optimizing vegetation ecosystem services and mitigating the effects of climate change as well as the UHI effect.

3.5 Limitations

Limitations of this research are as follows:

1. Structure of the substrate for shrubs on green roofs differs significant from shrubs at ground level. The depth of the substrate at green roofs is typically much shallower than conventional plantings at ground level (Extensive roof garden plots). This will have an impact on the overall evapotranspiration rate for plants.
2. Studies are conducted in the tropical urban environment. Due to differences in aridity and solar exposure, results may not be valid for temperate regions.
3. The study assumes all plants of the same genus to have statistically similar physiological attributes.

4 MEASUREMENT OF MEAN RADIANT TEMPERATURE IN A ROOF GARDEN SETTING

4.1.1 Results

4.1.1.1 Diurnal mean radiant temperature profiles

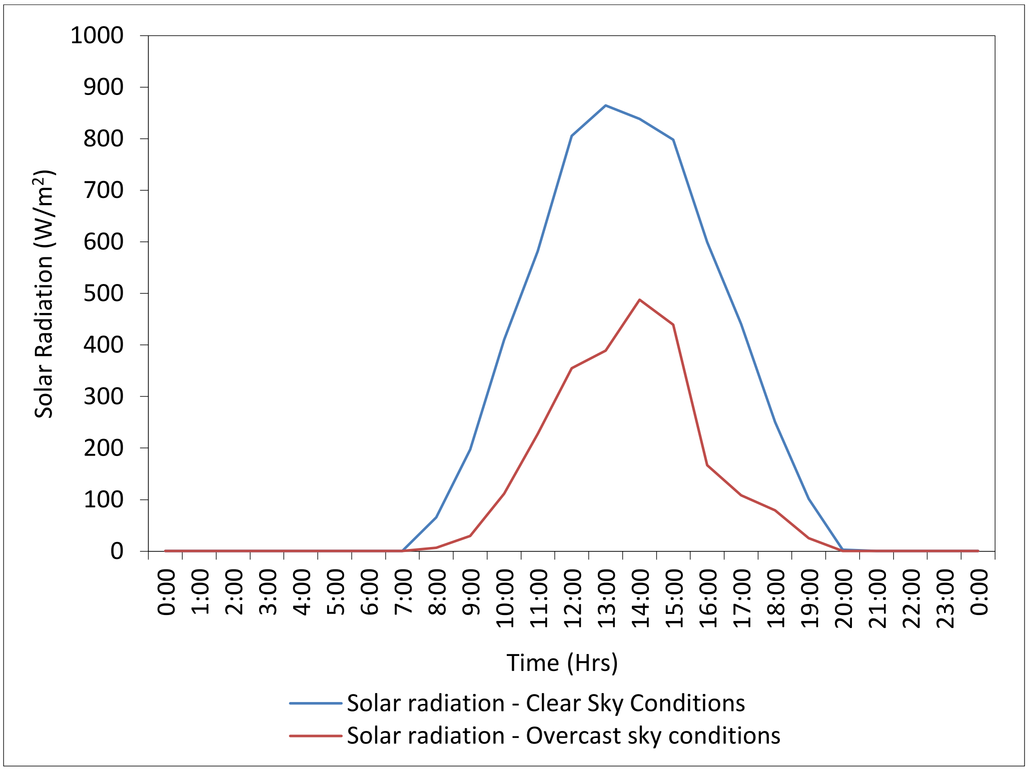

Figure 33. Typical clear (13th June 2014) and overcast (5th July 2014) sky solar irradiance profiles

Figure 33 shows the typical solar irradiance profile on days with clear sky and overcast sky conditions. The overall peak solar irradiance for a clear sky day was observed at 13:00 hrs with an approximate value of 900 Wm^{-2}. In comparison, the overall peak solar irradiance for an overcast day occurs at 14:00 hrs with a value of 500 Wm^{-2}. Both profiles show that the first solar irradiance is recorded at around 7:00 hrs when the Sun rises and decreases to 0.6 Wm^{-2} when the Sun sets between 19:00 hrs to 20:00 hrs. Results in the following section are generally classified as observations made under the two different sky conditions.

4.1.1.1.1 Clear sky conditions

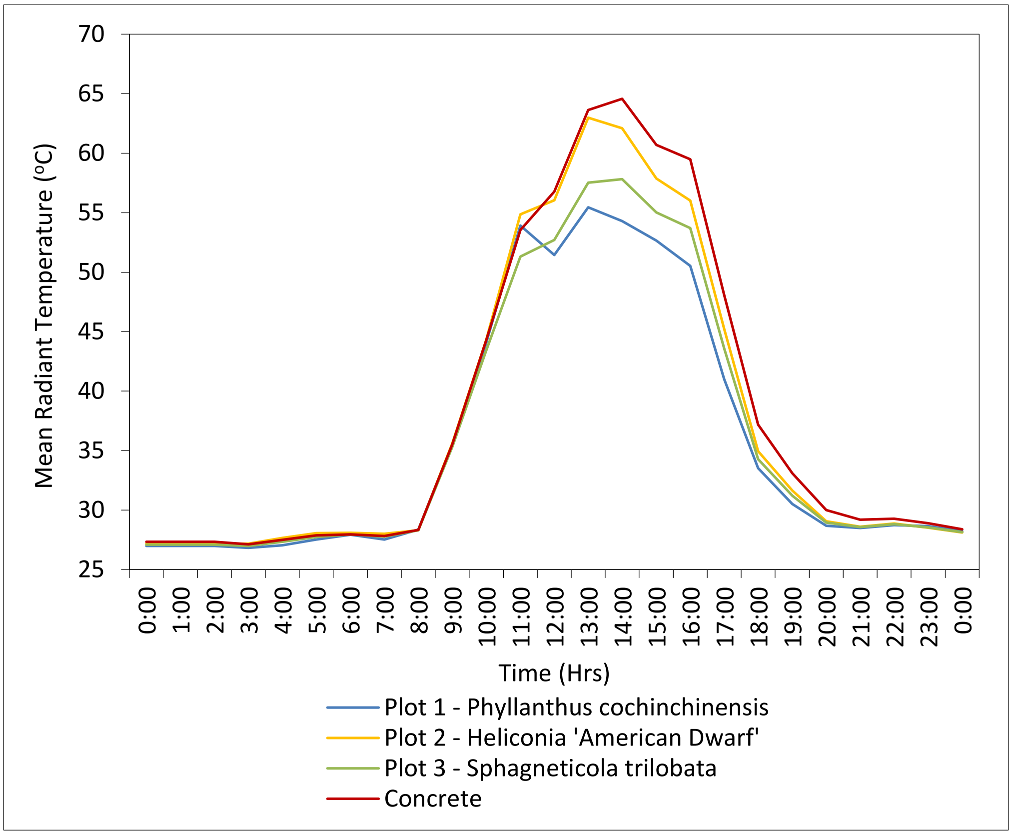

Figure 34. Mean radiant temperature profile for clear sky conditions (13th June 2014)

Figure 34 shows the mean radiant temperature profile for a typical day with clear sky conditions. Peak temperature can be observed at 14:00 hrs where concrete has the highest temperature recorded of 64.6 °C, followed by Plot 2, Plot 3 and Plot 1. The maximum temperature difference observed is between the concrete and Plot 1 with a difference of 10.0 °C at the peak. The temperature of concrete is generally higher than the plots.

4.1.1.1.2 Overcast sky conditions

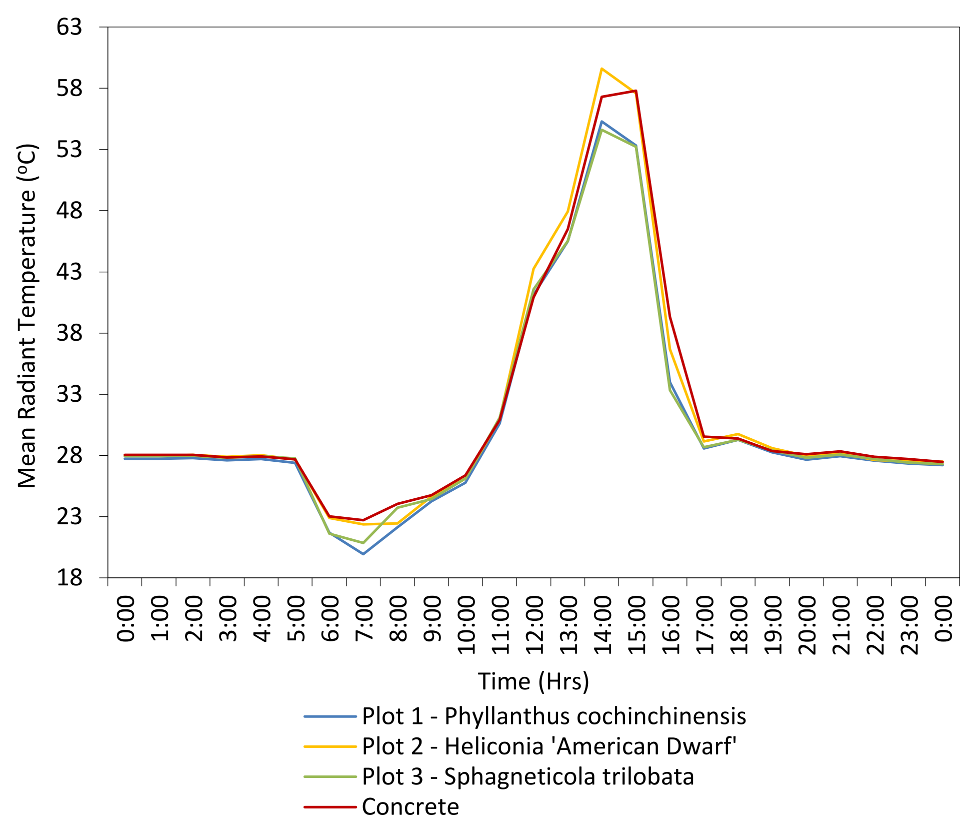

Figure 35. Mean radiant temperature profile for overcast sky conditions (5th July 2014)

Figure 35 shows the mean radiant temperature profile for a typical day with overcast sky conditions. Overall peak temperatures for all the plots and concrete are lower than those observed under clear sky conditions. Peak temperature can be observed at 14:00 hrs with Plot 2 being the highest at 59.6 °C, followed by concrete, Plot 1, and Plot 3. The maximum temperature difference is between Plot 2 and Plot 3 with a temperature of 5.0 °C.

4.1.1.2 Diurnal ambient temperature profiles

4.1.1.2.1 Clear sky conditions

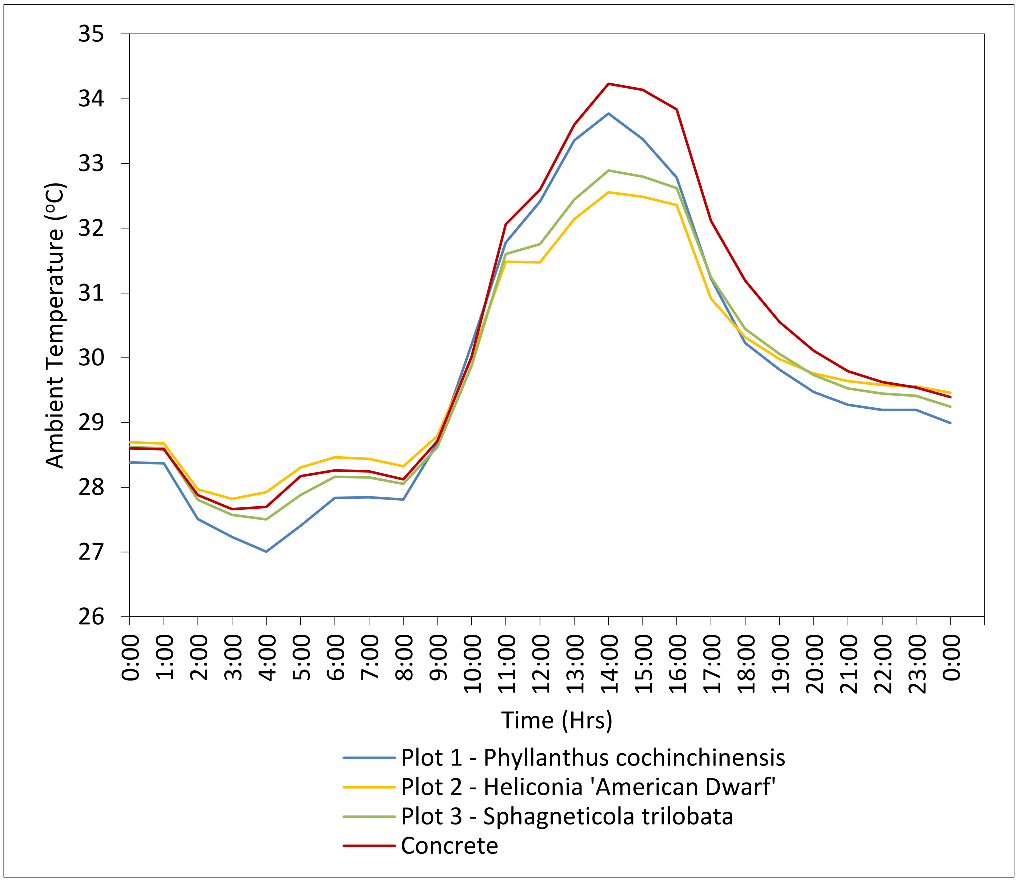

Figure 36. Air temperature profile for clear sky conditions (13th June 2014)

Figure 36 shows the air temperature profile for a typical day with clear sky conditions. Peak air temperature can be observed at 14:00 hrs where concrete has the highest temperature of 34.2 °C. This is followed by Plot 1, Plot 3 and Plot 2 which has the lowest peak temperature of 32.6 °C. There is a maximum difference of 1.6 °C between Plot 1 and Plot 2 at peak temperature. It can also be observed that Plot 1 has the lowest air temperature before 9:00 hrs and after 18:00 hrs while the air temperatures for Plot 2, Plot 3 and concrete are similar before 9:00 hrs and after 21:00 hrs.

4.1.1.2.2 Overcast sky conditions

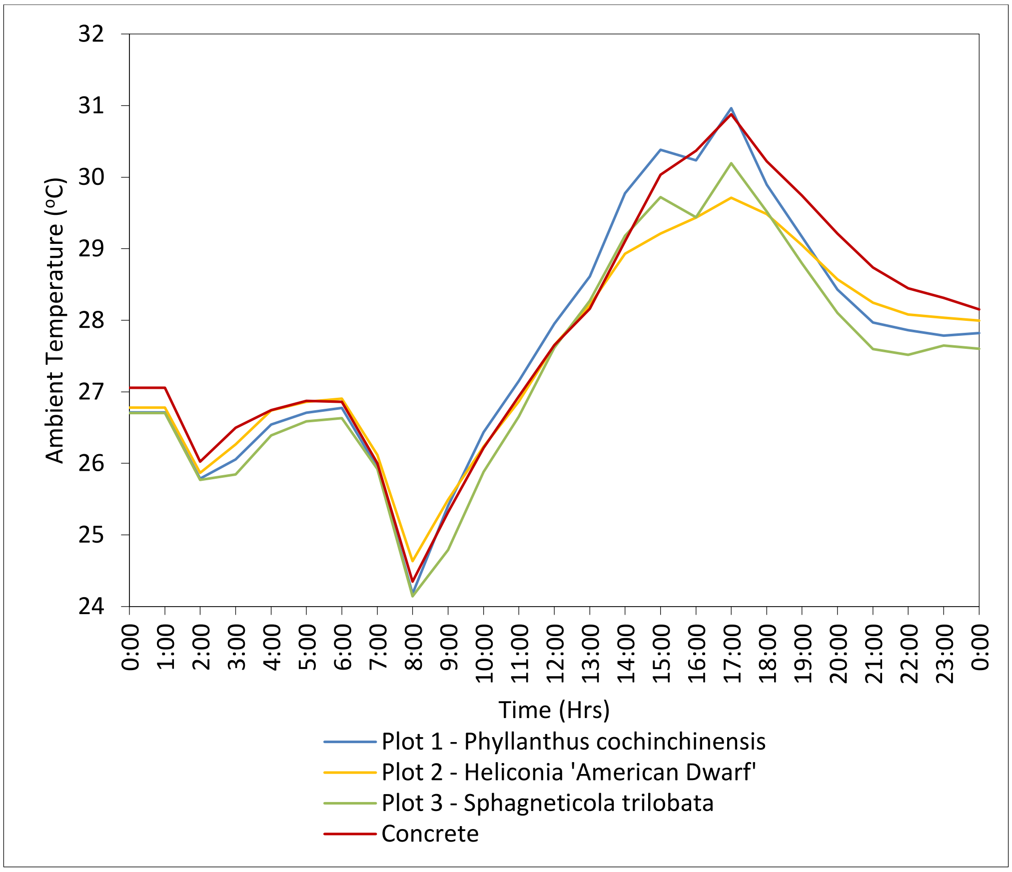

Figure 37. Air temperature profile for overcast sky conditions (12th July 2014)

Figure 37 shows the air temperature profile for a typical day with overcast sky conditions. A dip in air temperature was observed at 8:00 hrs and is likely due to a short period of rain. The peak temperature can be observed at 17:00 hrs where Plot 1 and concrete recorded a temperature of 31.0 °C. In comparison, Plot 2 has the lowest air temperature at 17:00 hrs and its difference with Plot 1 and concrete is 1.3 °C.

4.1.1.3 Stratification – soil layer, within shrub, above shrub

Measurement of air temperature was conducted at the soil, within and above the plant canopies of Plots 1 to 3. Schematic location of the points is shown in Figure 38.

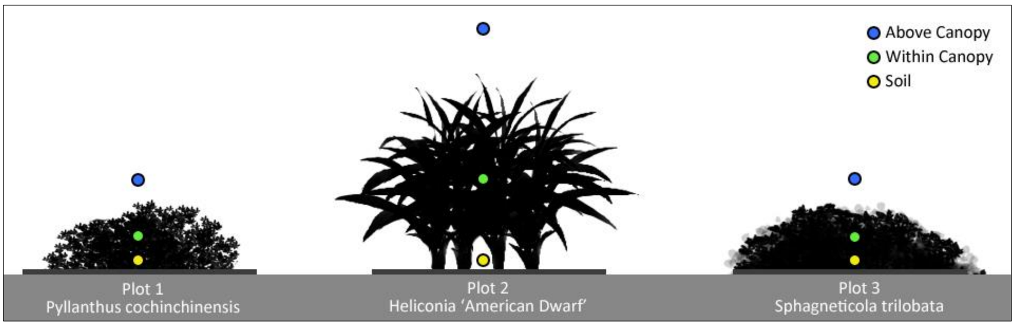

Figure 38. Location of air temperature probes

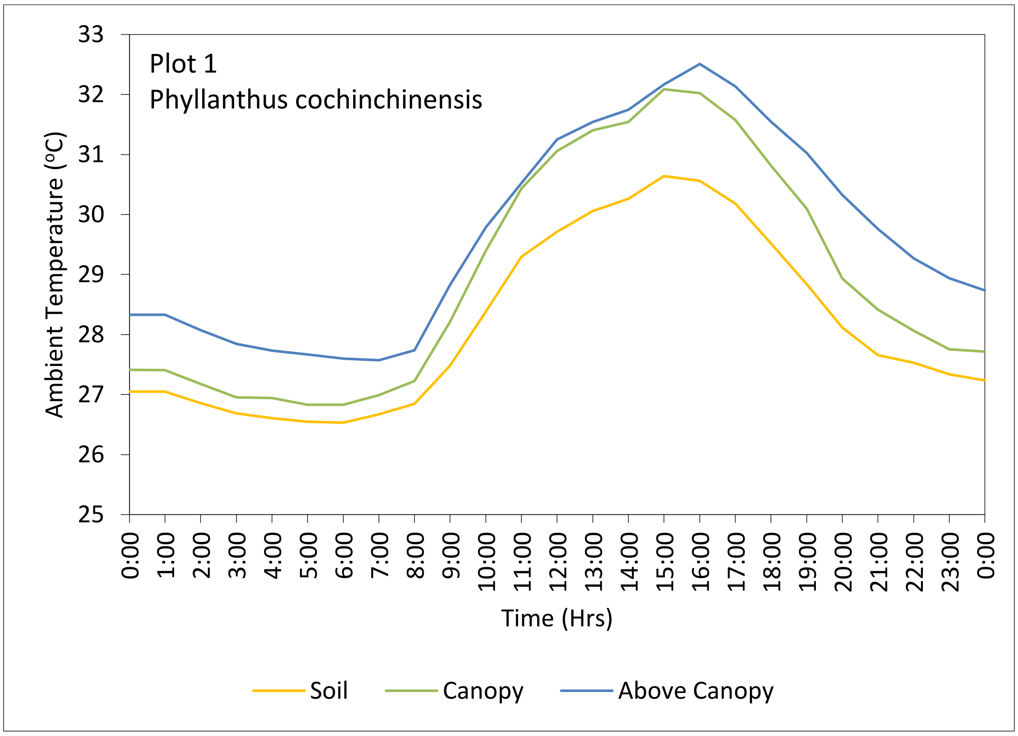

Figure 39. Stratified air temperature profile for Plot 1 (26th July 2014)

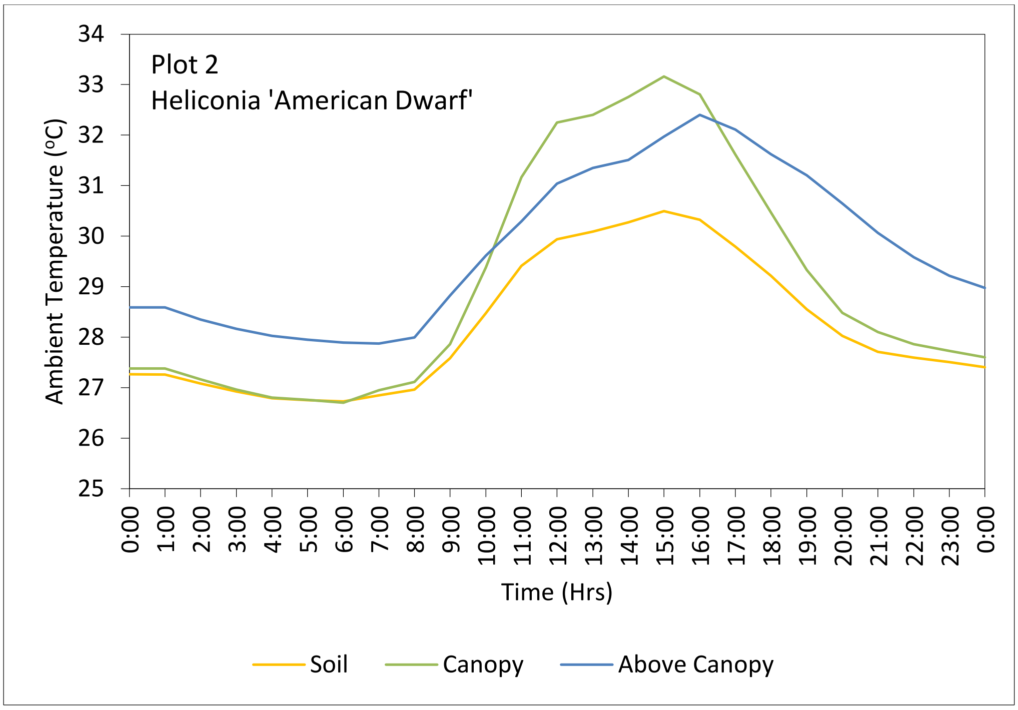

Figure 40. Stratified air temperature profile for Plot 2 (26th July 2014)

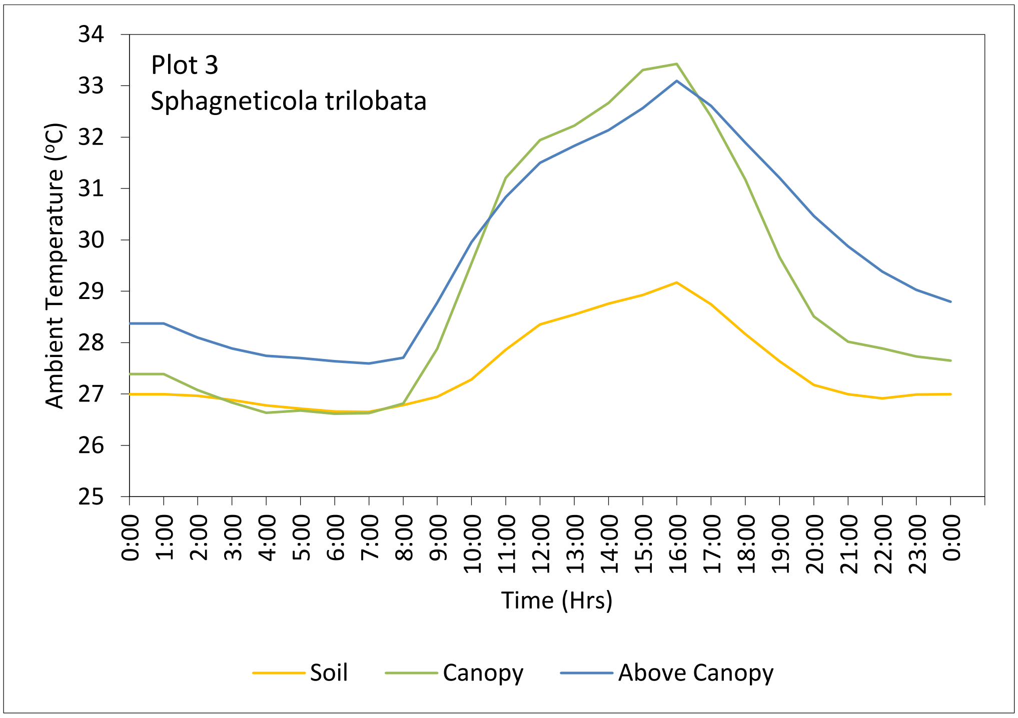

Figure 41. Stratified air temperature profile for Plot 3 (26th July 2014)

Figure 39, Figure 40 and Figure 41 show stratified air temperature profiles for Plot 1, Plot 2 and Plot 3 on a typical clear day condition respectively. Soil temperature for all three plots is generally lower compared to canopy and above-canopy air temperature.

Stratified air temperature profile for Plot 1 in Figure 39 shows a peak temperature of 32.5 °C at 16:00 hrs above the plant canopy while peak temperature for soil and canopy temperature graph occurs at 15:00 hrs. There is a difference of 2.0 °C between air temperature at soil level and air temperature above the plant canopy.

In comparison, the above canopy temperatures for both Plot 2 and Plot 3 (Figure 40 and Figure 41) have the highest temperature of approximately 33.0 °C and peaked at 16:00 hrs. The soil temperatures for these two plots were 30.5 °C and 29.1 °C at peak temperature. This would also represent a difference in 2.5 °C and 4.0 °C between the canopy and soil temperature.

Comparison of the stratified air temperature profiles for all 3 Plots show that air temperature above the canopy is slightly lower than within the canopy for Plot 2 and Plot 3. Air temperature within the canopy for Plot 1 is slightly lower than above it. This may be explained by the fact that Phyllanthus cochinchinensis has many small leaves that occupy the entire volume of the shrub, while Plot 3, in comparison, has its leaves only at the outermost portions of the canopy and only has stems within the inner regions of the canopy.

4.1.1.4 Meteorological variables

4.1.1.4.1 Solar radiation

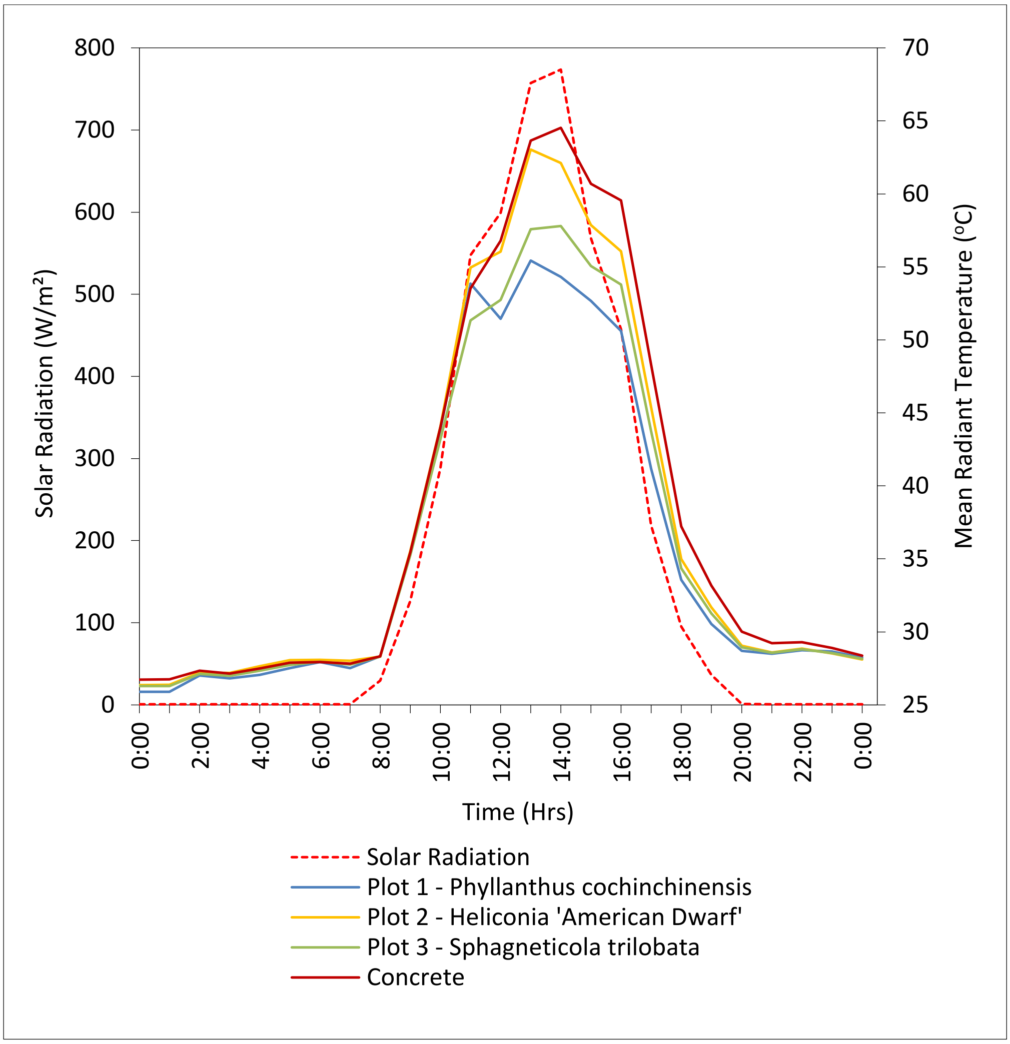

Figure 42. Solar radiation against mean radiant temperature profile (13th June 2014)

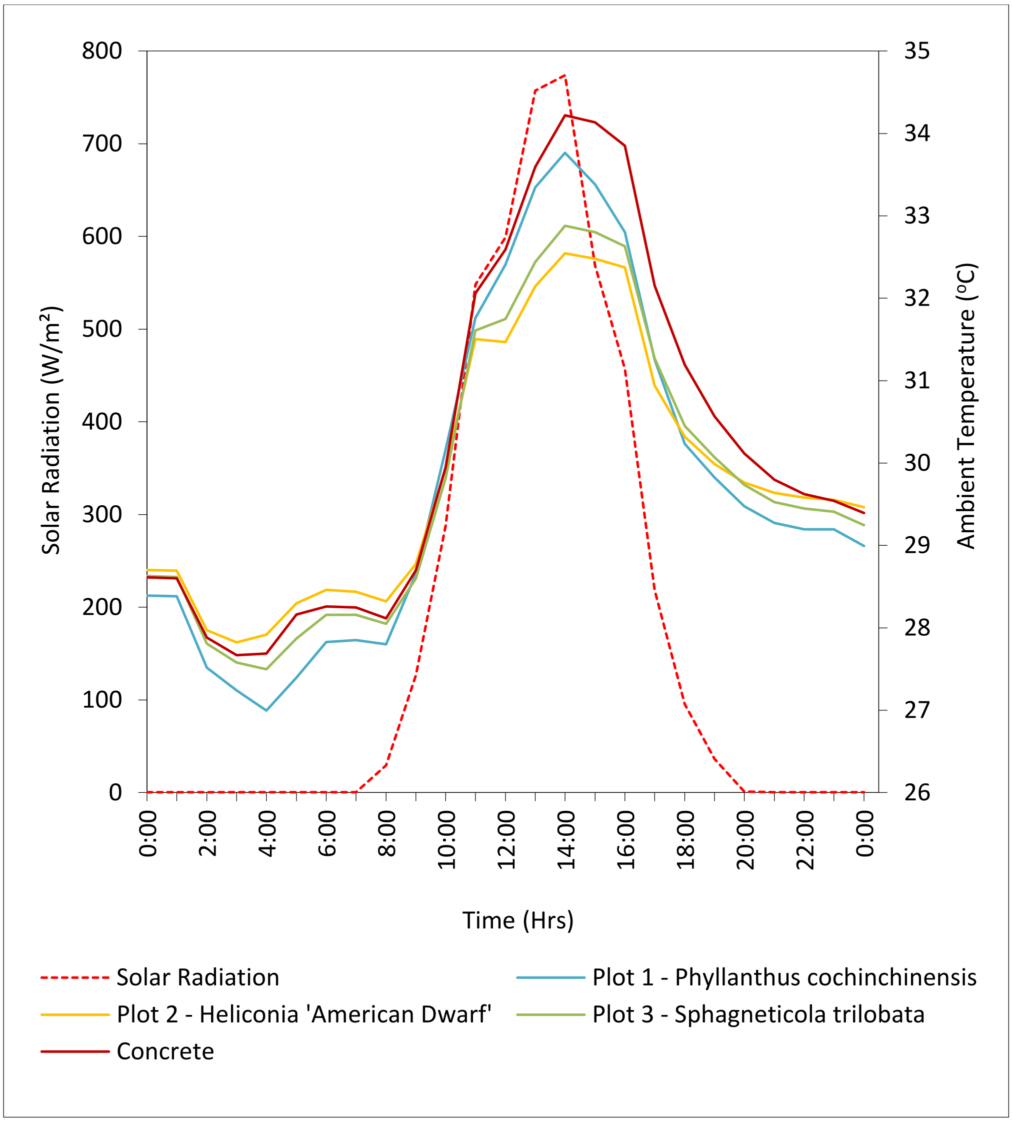

Figure 43. Solar radiation against air temperature profile (13th June 2104)

Figure 42 and Figure 43 show the diurnal t_{mrt} and solar irradiance profile for 13th June 2014 (clear sky conditions). The profiles follow a similar curve, peaking at 14:00 hrs. The highest solar radiation observed is 773.8 Wm^{-2}. It can be observed that both air and t_{mrt} profiles are directly proportional to solar irradiance.

4.1.1.4.2 Photosynthetically Active Radiation (PAR)

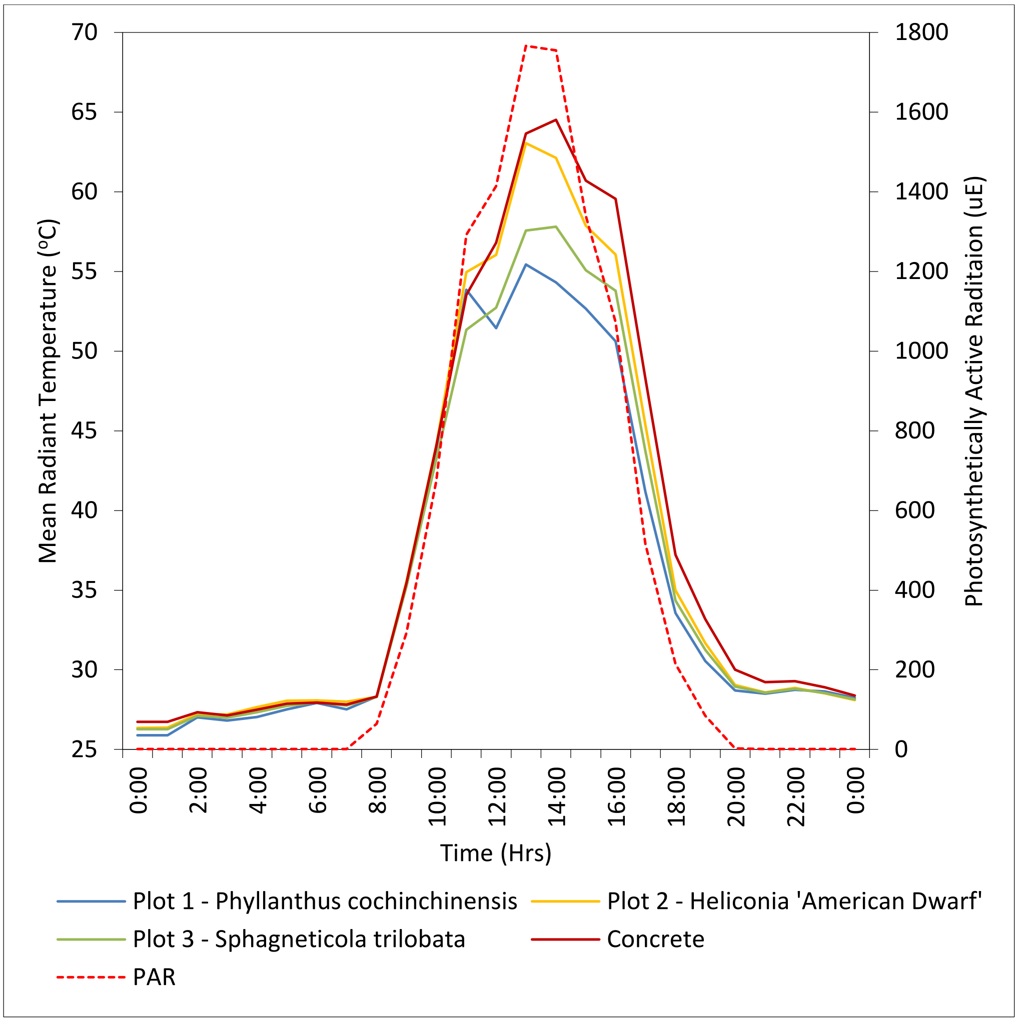

Figure 44. Photosynthetically Active Radiation against mean radiant temperature profile (13th June 2014)

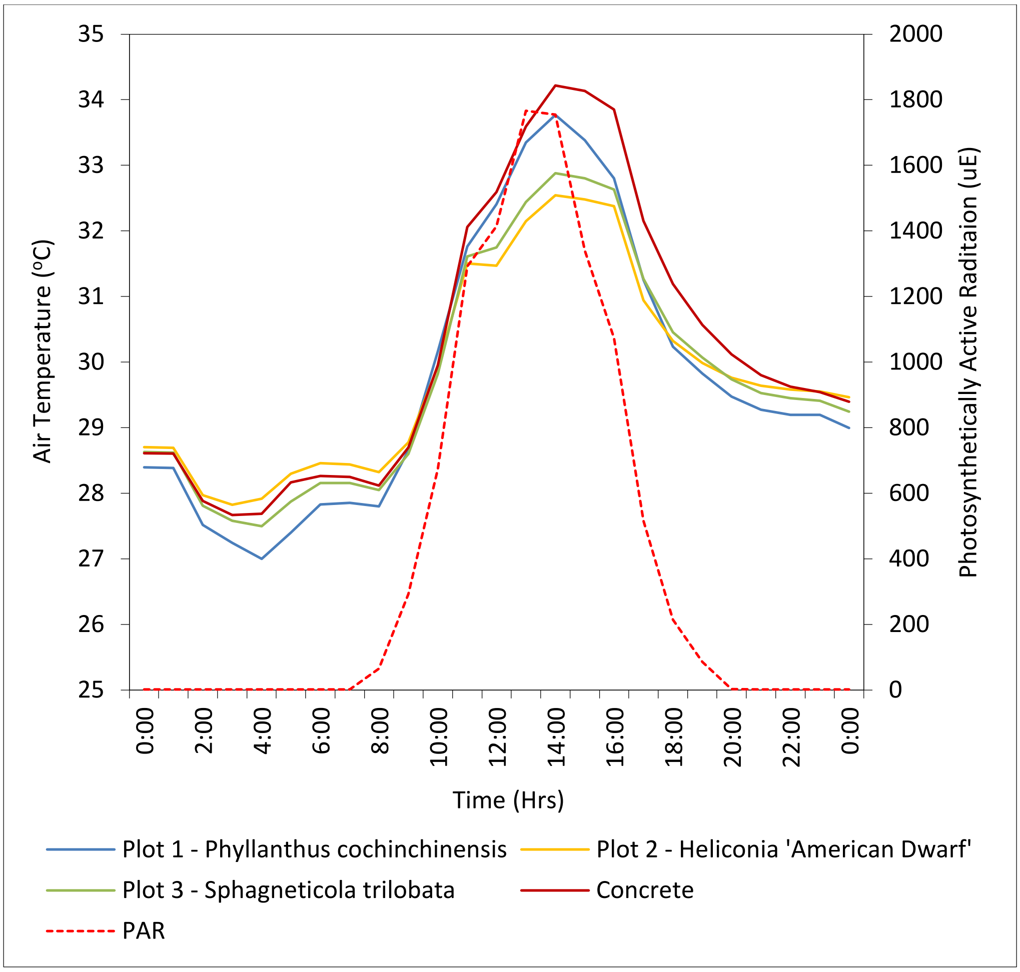

Figure 45. Photosynthetically Active Radiation against air temperature profile (13th June 2014)

Figure 44 and Figure 45 show the diurnal t_{mrt} and air temperature with solar irradiance profile for 13th June 2014. The profiles follow a similar curve, peaking at 13:00 hrs. The highest PAR observed is 1765.8 µE. Similar to the profiles of solar irradiance, both PAR profiles are directly proportional to t_{mrt} and air temperature.

4.1.1.4.3 Relative humidity (RH)

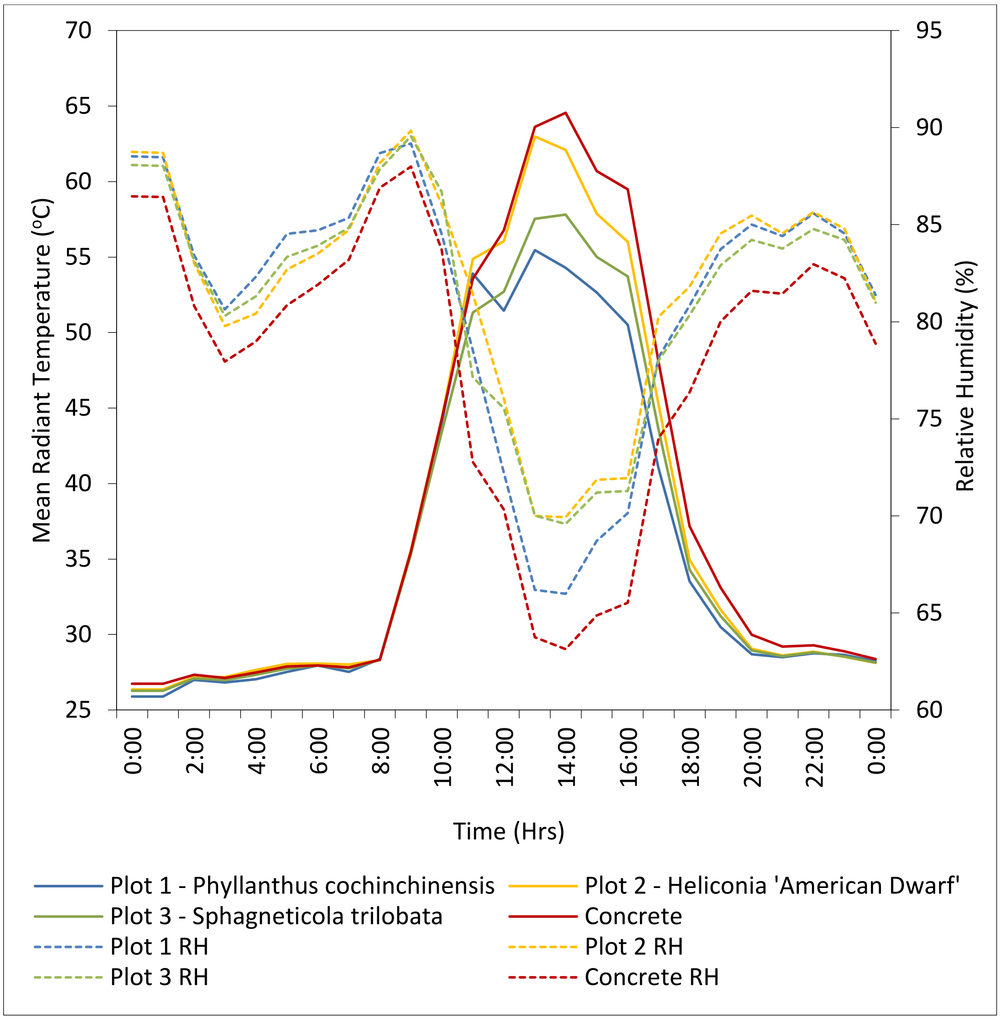

Figure 46. Relative Humidity against mean radiant temperature profile (13th June 2014)

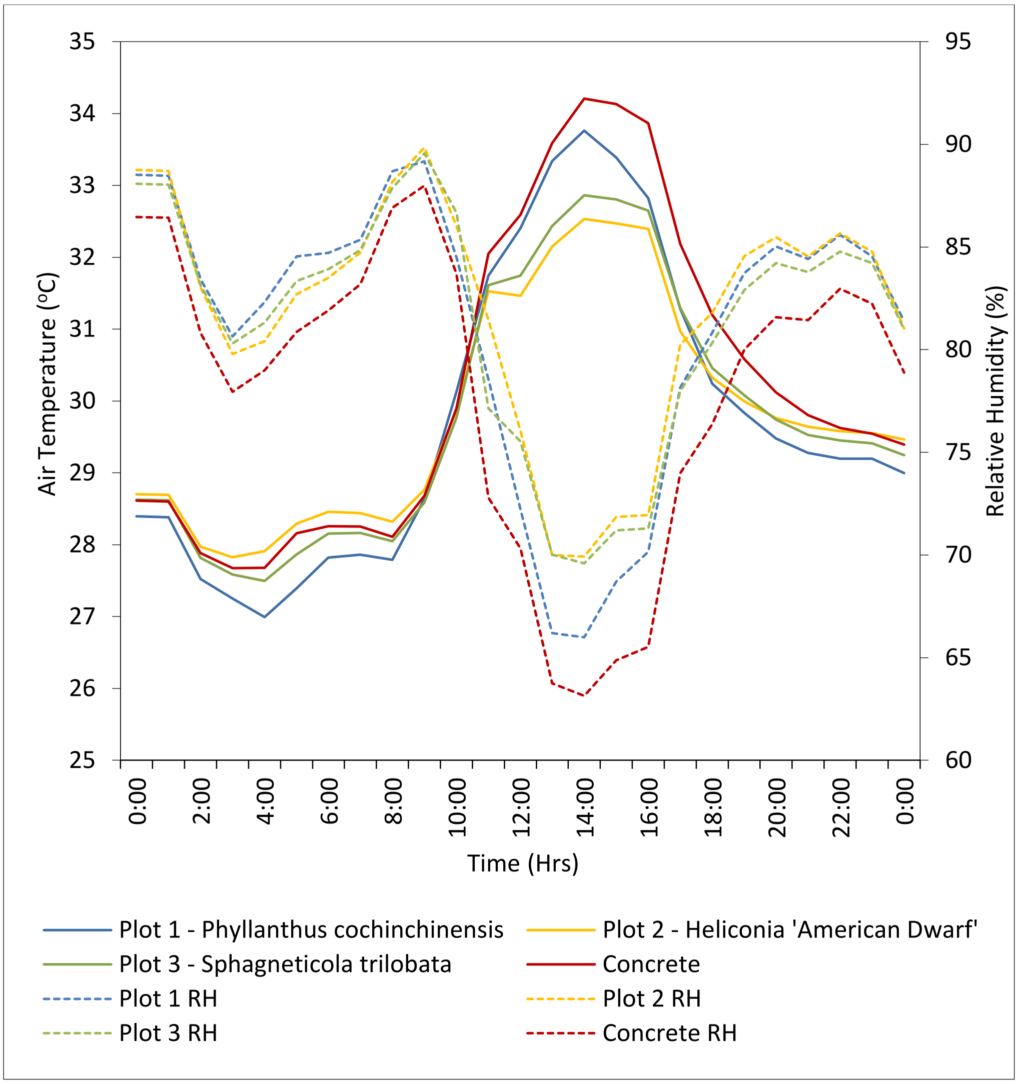

Figure 47. Relative Humidity against air temperature profile (13th June 2014)

Figure 46 and Figure 47 show the diurnal t_{mrt} and air temperature with relative humidity (RH) for 13th June 2014. The RH profiles are inversely proportional to t_{mrt} and air temperature profiles. The lowest RH recorded was at 14:00 hrs for concrete (63.1 %) followed by Plot 1 (65.9 %), Plot 3 (69.6 %) and Plot 2 (69.6 %) under clear sky conditions. There is a difference of approximately 6.5% between the concrete and Plots 2 and 3.

4.1.1.5 Shrub characteristics

4.1.1.5.1 Evapotranspiration rate

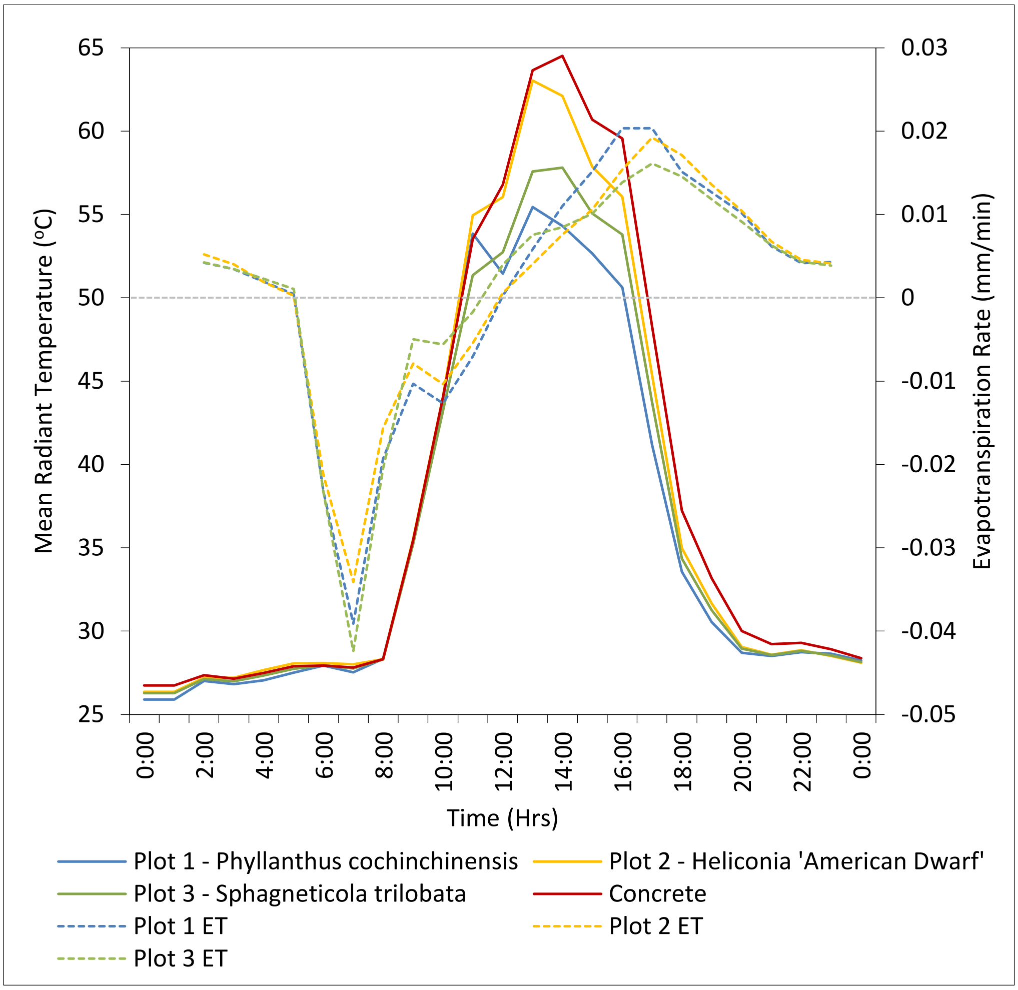

Figure 48. Evapotranspiration rate against mean radiant temperature profile (13th June 2014)

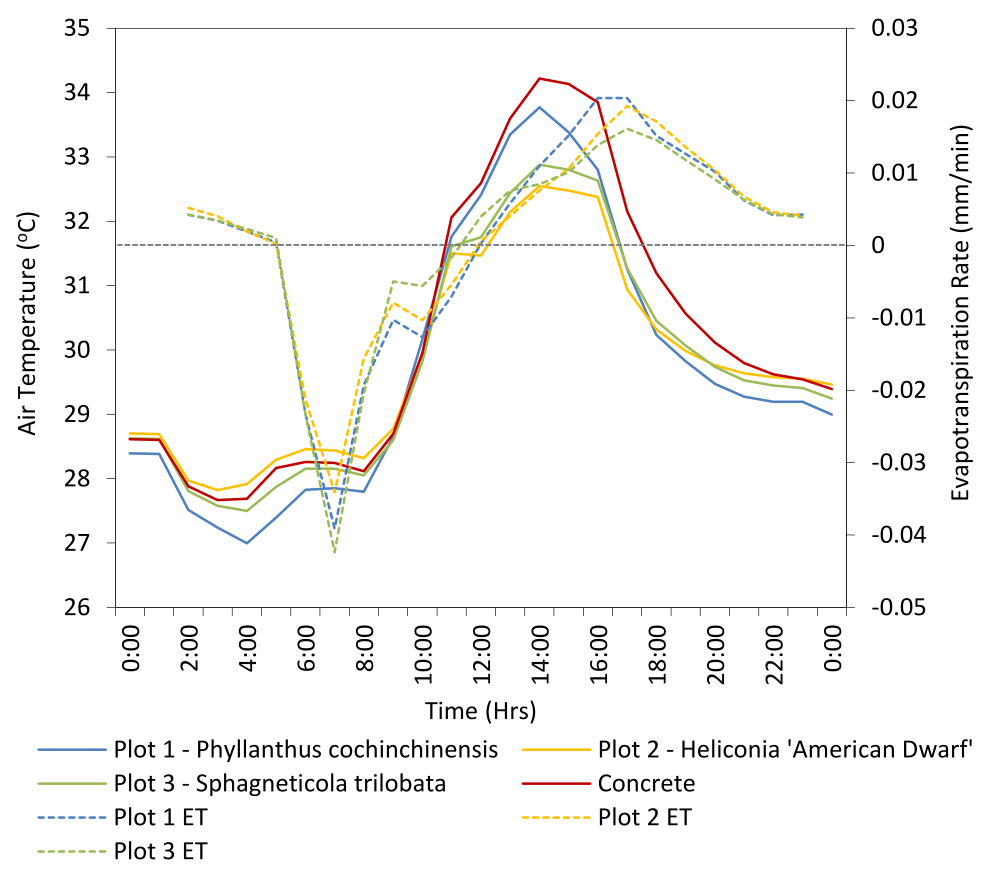

Figure 49. Evapotranspiration rate against air temperature profile (13th June 2014)

Figure 48 and Figure 49 show the diurnal evapotranspiration (ET) profile for 13th June 2014. There is a sharp dip in ET from 06:00 hrs to 07:00 hrs due to the plot irrigations. The ET rate for Plot 1 is low in the morning but picks up in the afternoon and has a highest value of 2.4 mmmin^{-1}. In comparison, Plot 3 has the highest ET rate in the morning period but gets lower than plot 2 in the late afternoon (17:00 hrs). The ET rates for Plot 2 and 3 peaked at 17:00 hrs with a value of 1.9 mmmin^{-1} and 1.7 kgmin^{-1} respectively. Generally, the ET rate is above zero from 11:00 hrs for Plot 3 and 12:00 hrs for Plot 1 and 2.

4.1.1.5.2 Shrub albedo

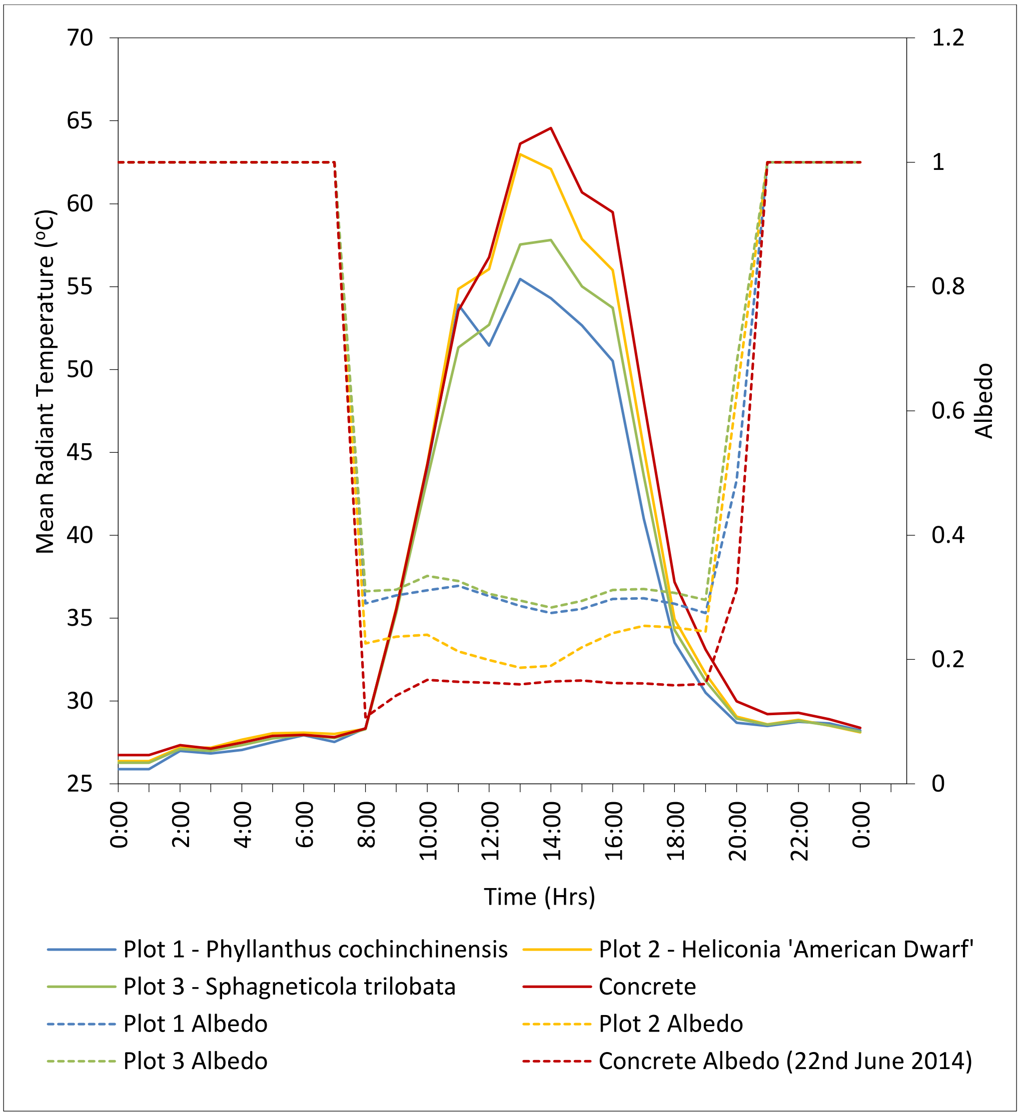

Figure 50. Albedo against mean radiant temperature profile (13th June 2014)

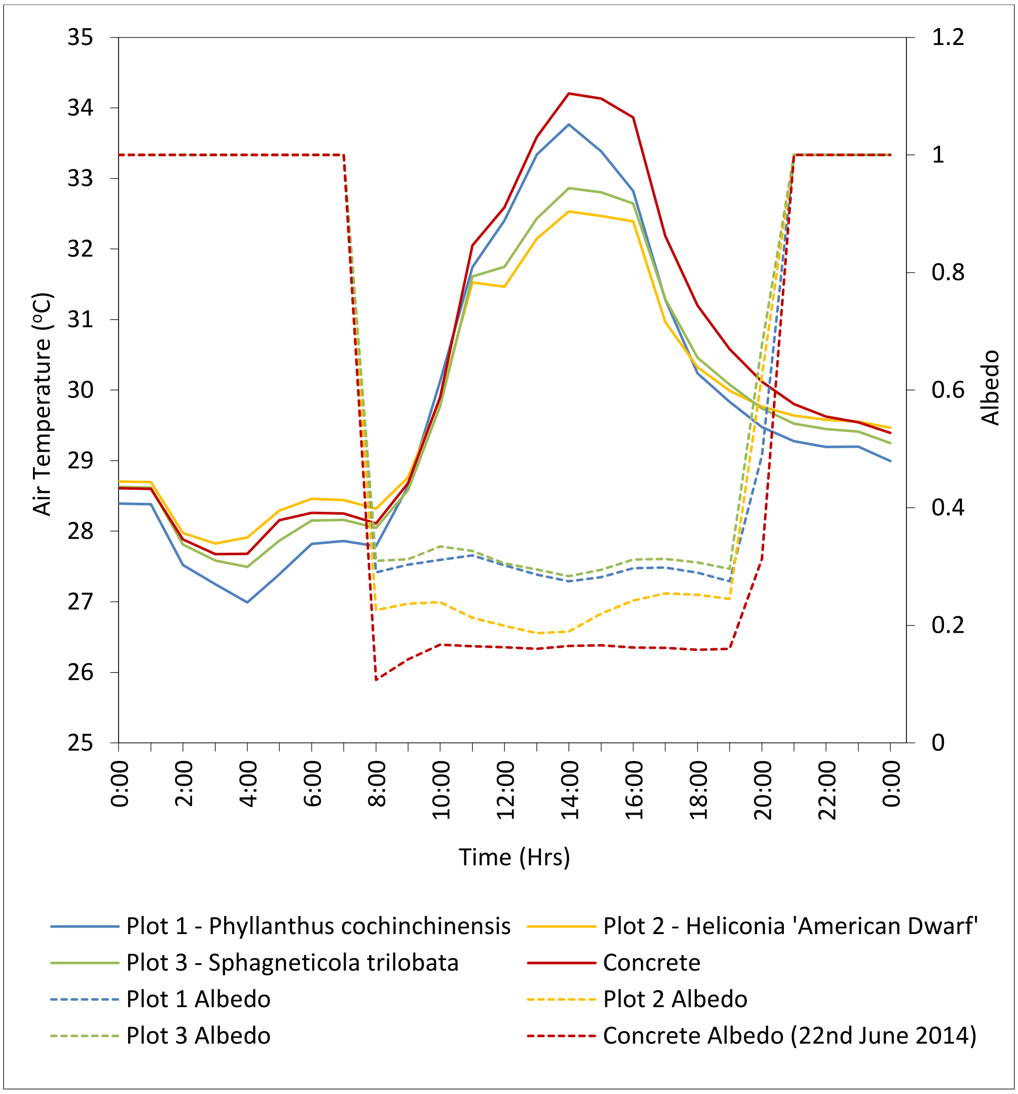

Figure 51. Albedo against air temperature profile (13th June 2014)

Figure 50 and Figure 51 show the diurnal albedo profile for 13th June 2014 and 22nd June 2014. Albedo of concrete in the day is constant at 0.17. It is lower than the albedo for the shrubs throughout the day.

Albedo values of Plots 1 to 3 are relatively consistent. The lowest albedo value is at peak temperature around 14:00 hrs. Plot 2 has a lower albedo than Plot 1 and Plot 3. Their average values are 0.16, 0.28 and 0.28 respectively.

4.1.1.5.3 Leaf Area Index (LAI)

Leaf area index was measured and estimated using the following methods:

1. Indirect measurement: Measurement of light attenuation due to plant canopy with the LAI-2000 (Figure 52).
2. Direct measurement: Plucking out leaves within a 0.5 m by 0.5 m area, and tabulating the total green area (Outlined in Section 3.2.3).
3. Literature reference: From the National Parks Board (Nparks) published handbook on LAI (Tan and Sia, 2009).

Figure 52. LAI-2000 canopy analyzer. (Source: http://www.licor.com)

Table 9. Averaged Leaf Area Indices for Plot 1 to Plot 3

Plot		LAI measurement method					
		Indirect measurement (Using LAI-2000)				Direct measurement (Plucking out leaves in 50 x 50 cm plot, pixel calculation)	Nparks handbook (Tan and Sia, 2009)
		1	2	3	Average		
1	Phyllanthus cochinchinensis Shrub (Dicot)	4.65	4.22	4.16	4.34	2.78	4.5
2	Heliconia American Dwarf Shrub (Monocot)	3.14	3.69	3.58	3.47	7.21	3.5
3	Sphagneticola trilobata Ground cover	4.70	4.28	4.83	4.60	3.59	4.5

Table 9 shows measured LAI of the plots and the corresponding LAI for each plant provided by the NParks (Tan and Sia, 2009). Using the indirect measurement method, Plot 3 has the highest LAI of 4.60, followed by Plot 1 at 4.34 and Plot 2 at 3.47. However, when direct measurements are conducted, the results are reversed. Plot 2 shows the highest LAI at 3.47 whereas Plot 3 and Plot 1 have a lower LAI at 3.59 and 2.78 respectively. The difference in both methods may be due to the excess direct shading captured by the LAI-2000 plant canopy analyzer to obtain measurement using the indirect measurement method.

4.1.1.5.4 Leaf Reflectance

Leaf reflectance was measured by first plucking out fresh leaves from Plots 1 to 3, and measuring the reflectance using a photospectrometer. Leave samples used for measurement are shown in Figure 53.

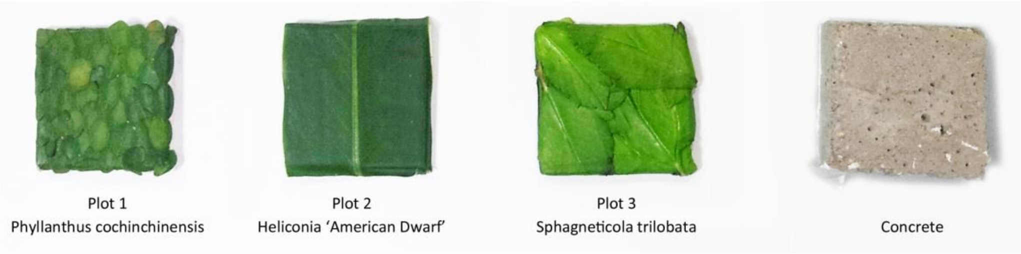

Figure 53. Leaf samples used for reflectance measurement (5 cm X 5 cm)

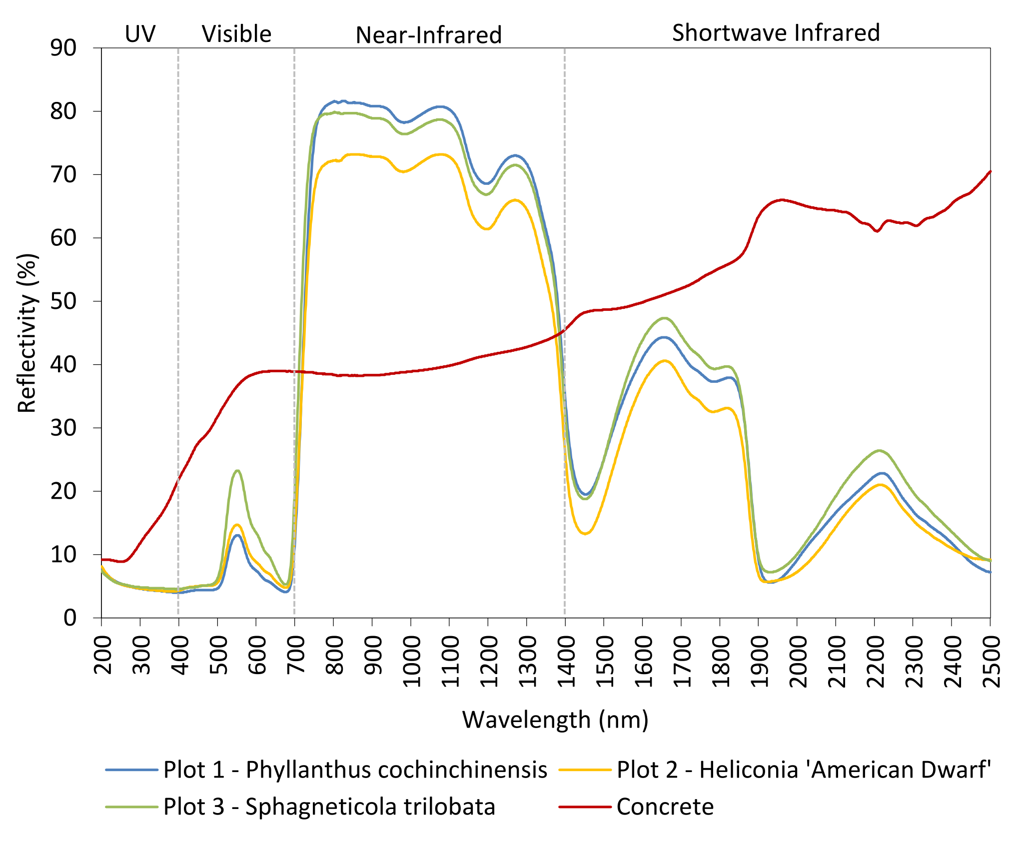

Figure 54. Reflectivity results

Figure 54 shows the reflectivity of the leaves taken from Plots 1 to 3. Under visible light which spans approximately 400nm to 700nm, reflectivity of concrete can be up to 40.4 %. Vegetation under visible light displayed a relatively lower reflectivity at the peak of 21.6 % (Plot 3), 14.5 % (Plot 1) and 13.8 % (Plot 2). At approximately 800 nm, reflectivity of leaves is higher than that of concrete. Plot 1 has the highest value of 85.9 %, followed by Plot 3 (85.0 %), Plot 2 (83.3 %) and concrete (42.2 %).

4.1.1.5.5 Stomatal conductance

Stomatal conductance was measured for Plots 1 to 3 with a porometer (Figure 55). Measurements were conducted on an hourly basis and a total of four leaves were measured for each plot. Averaged values from all four leaves are used for analysis.

Figure 55. Decagon leaf porometer (Source: http://www.decagon.com)

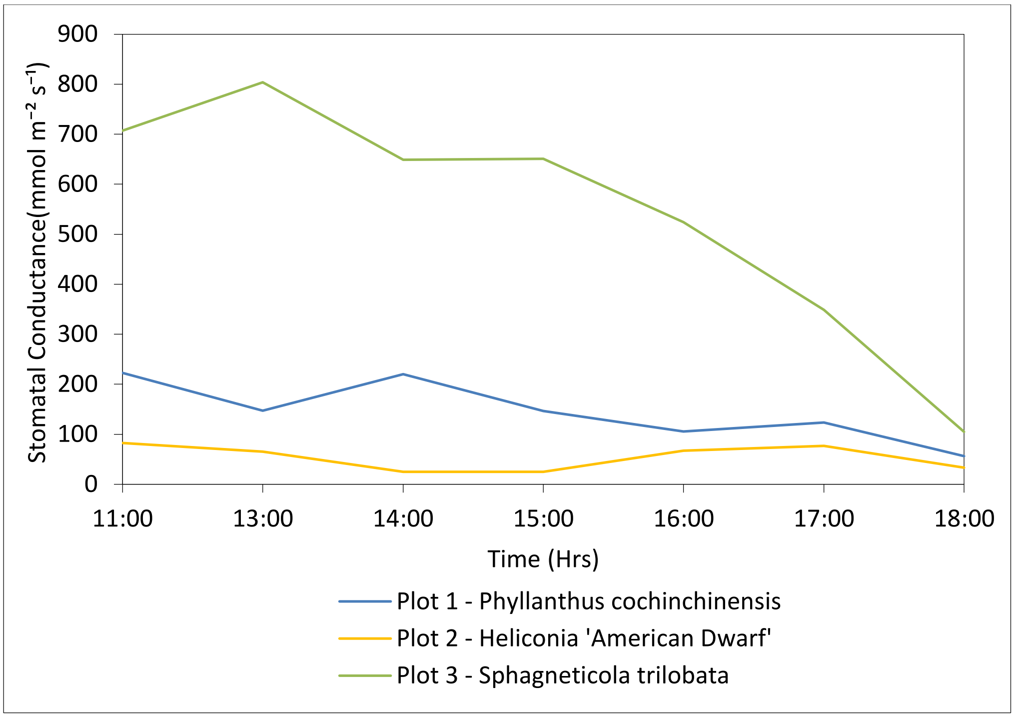

Figure 56: Stomata Conductance (3rd June 2014)

Figure 56 shows stomatal conductance levels from 11:00 hrs to 18:00 hrs on 3rd June 2014. Plot 3 has the highest stomatal conductance level, peaking at 13:00 hrs at a value of 803.7 mmolm^{-2}s^{-1}, while Plot 1 and Plot 2 are greatly lower. Stomatal conductance levels for all plots are drastically reduced in the later part of the day. This corresponds to the reduction of evapotranspiration rate after 17:00 hrs shown in Figure 48.

4.1.1.5.6 Leaf surface temperature

4.1.1.5.6.1 Leaf surface measurement

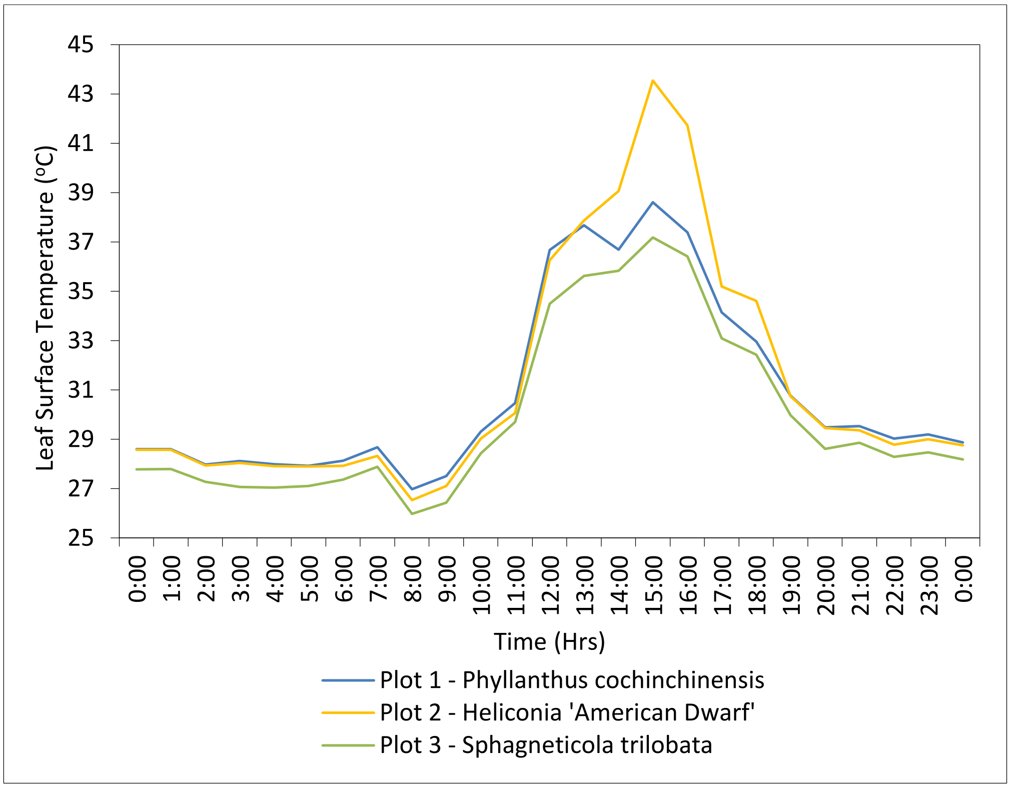

Figure 57. Average leaf surface temperature profiles for Plots 1, 2 and 3 (24th June 2014)

Figure 57 shows average leaf surface temperatures for the 3 plots on 24th June 2014. Leaf surface temperature for plots 1 and 3 are similar while plot 2 shows a higher temperature with greater fluctuation from 12:00 hrs to 16:00 hrs. The highest temperatures recorded at Plot 1, 2 and 3 are 38.4 °C, 44.7 °C and 37.7 °C respectively.

4.1.1.5.6.2 Infrared thermography

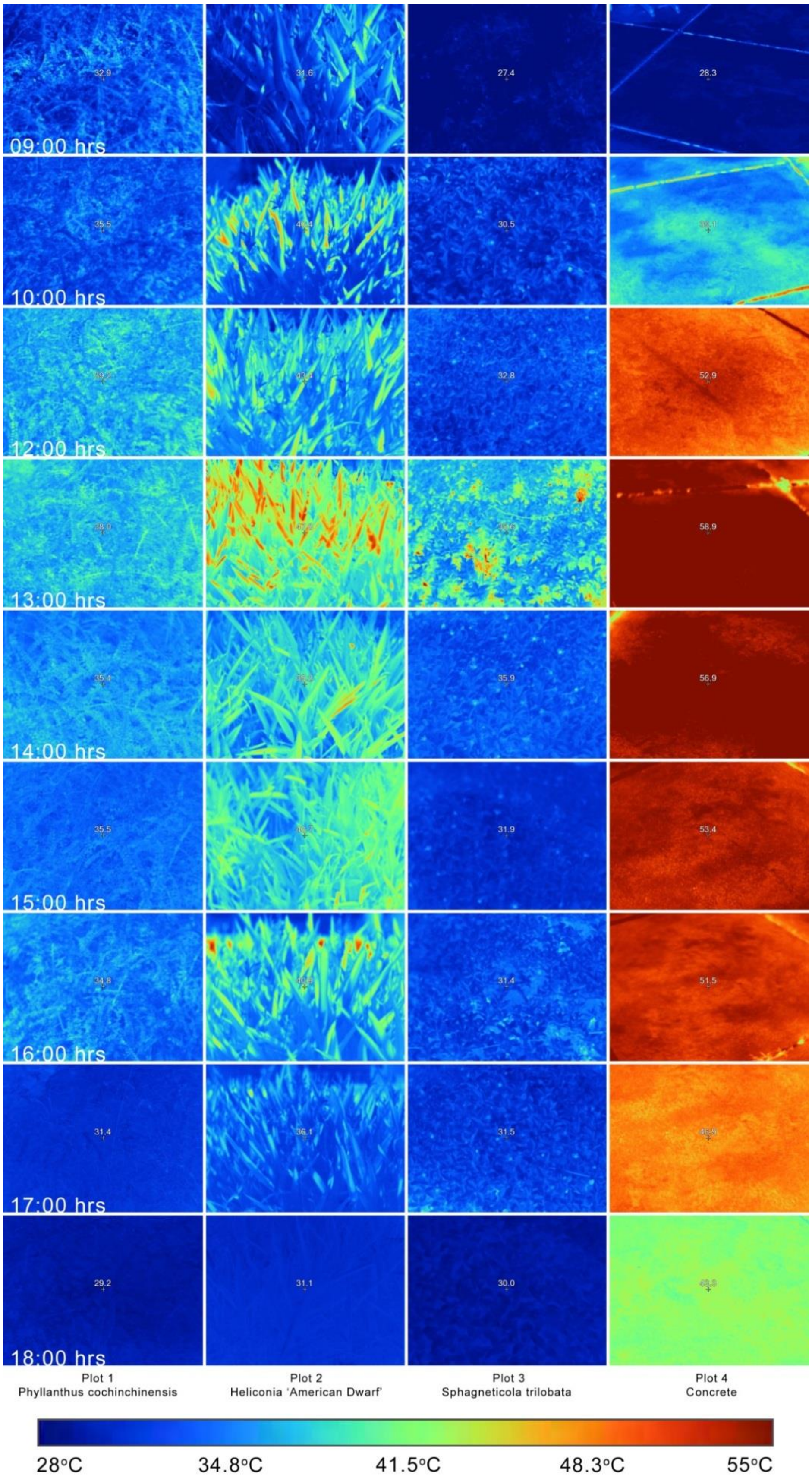

Figure 58: Infrared thermography of green roof plots and concrete

Figure 58 shows infrared thermography of the plots and concrete on a typical clear sky condition day. Results concur with leave surface temperature measurements in Chapter 4.1.1.5.6.1. Surface temperature of concrete is consistently higher than all other plots throughout the day. This is followed by Plot 2 which is higher than Plot 1 and 3 as seen from the brighter colours on the leaf surfaces. Significantly higher temperatures can be seen on the leaf edges for Heliconia 'American Dwarf' (Plot 2).

4.1.1.6 Soil temperature

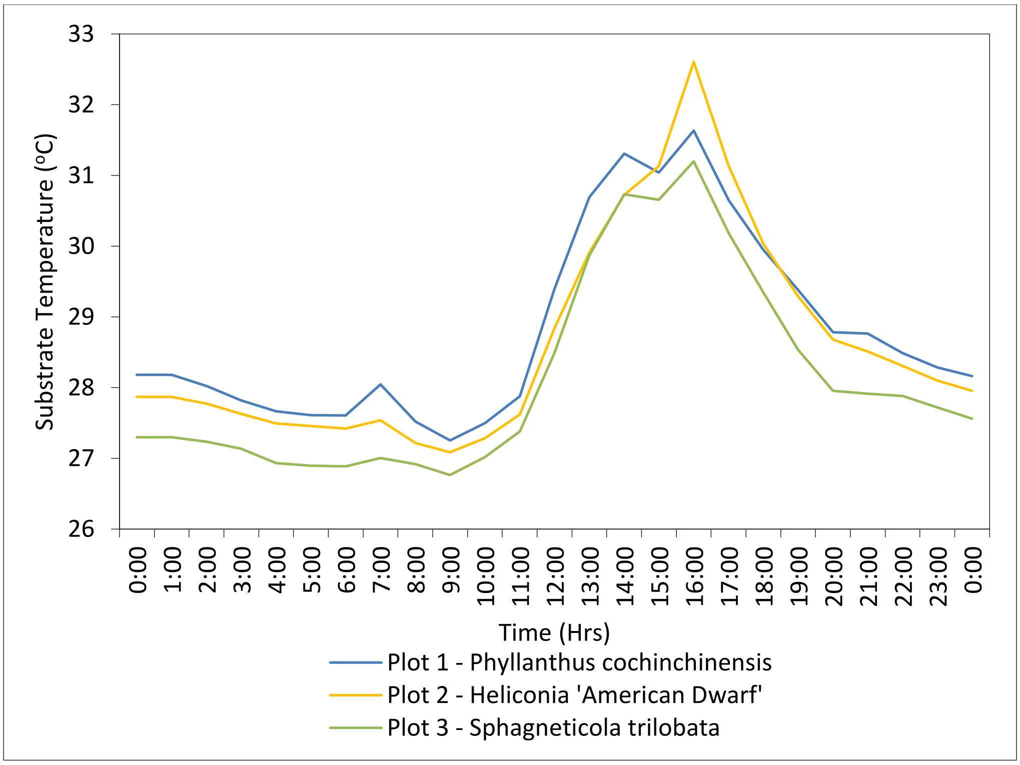

Figure 59. Average soil temperature profiles for Plot 1, 2 and 3 (24th June 2014)

Figure 59 shows average substrate temperatures of the 3 plots on 24th June 2014. Peak temperatures were observed at 16:00 hrs for all three plots with Plot 2 having the highest temperature at 35.7 °C. Plot 1 and Plot 3 shows similar profile and has a peak temperature of 33.9 °C and 34.0 °C. The higher temperature peak for Plot 2 may be explained by the porosity of the Heliconia shrub, compared to Plot 3, where the Sphagneticola trilobata shrub is much more compact. This provides significantly more shade at the soil level.

4.1.1.7 Temperature of concrete under roof garden plots

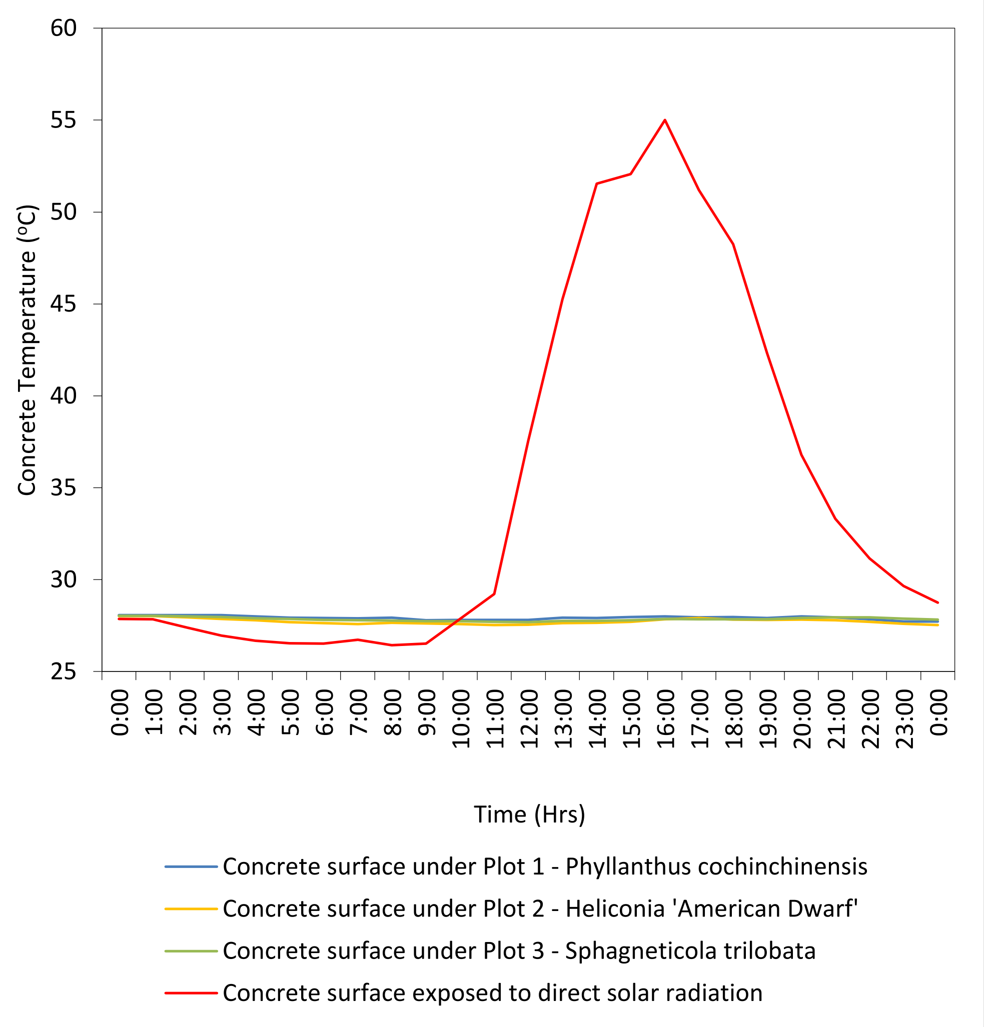

Figure 60. Concrete temperature profiles for Plot 1 to Plot 3 (24th June 2014)

Figure 60 shows concrete temperature profiles beneath all 3 plots on 24th June 2014. The 3 plots show similar profile and temperature ranging from 27.5 °C to 28.1 °C. The concrete temperature is generally lower than the leaf surface temperature and substrate temperature as shown from Figure 57 to Figure 59.

4.1.1.8 Net all-wave radiation

Net all-wave radiation describes the rooftop greenery energy surface budget (in the day) in the form of long and shortwave radiation (Oke, 1988):

$$\begin{aligned} Q^* &= K\downarrow - K\uparrow + L\downarrow - L\uparrow \\ &= K^* + L^* \end{aligned} \qquad [23]$$

Where,

Q^* = Net all-wave radiation (Wm^{-2})

$K\downarrow$ = Incident shortwave radiation (Wm^{-2})

$K\uparrow$ = Reflected shortwave radiation (Wm^{-2})

K^* = Net shortwave radiation (Wm^{-2})

$L\downarrow$ = Incident longwave radiation (Wm^{-2})

$L\uparrow$ = Reflected longwave radiation (Wm^{-2})

L^* = Net longwave radiation (Wm^{-2})

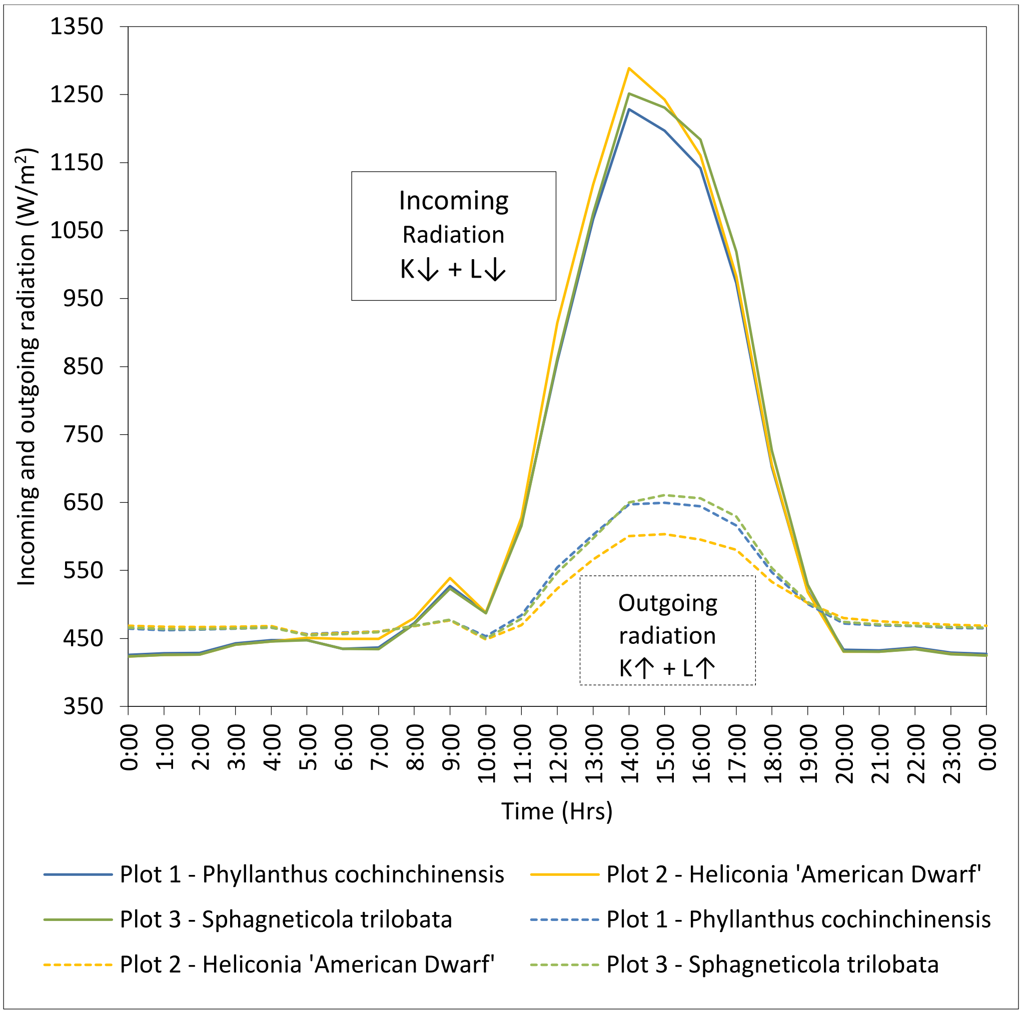

Figure 61: Incoming and outgoing radiation for Plots 1 to 3 (7th July 2014)

Figure 61 shows incoming and outgoing radiation of all 3 plots. Incoming radiation peaked at 14:00 hrs with Plot 2 having the greatest radiation of 1288.9 Wm^{-2} and the lowest for Plot 1 at 1251.5 Wm^{-2}. Outgoing radiation is drastically lower than incoming radiation and peaks were observed much later. Plot 2 shows the lowest outgoing radiation of 603.2 Wm^{-2} while Plot 1 and Plot 3 show similar values of approximately 661.0 Wm^{-2}. Diurnal net all-wave radiation (Q*) profile for Plots 1 to 3 are shown in Figure 62. It can be observed that net all-wave radiation for Plot 2 is higher than that of Plot 1 and Plot 3. This is likely due to the hotter leaf surface temperature (Chapter 4.1.1.5.6) which resulted in higher longwave emission for Plot 2.

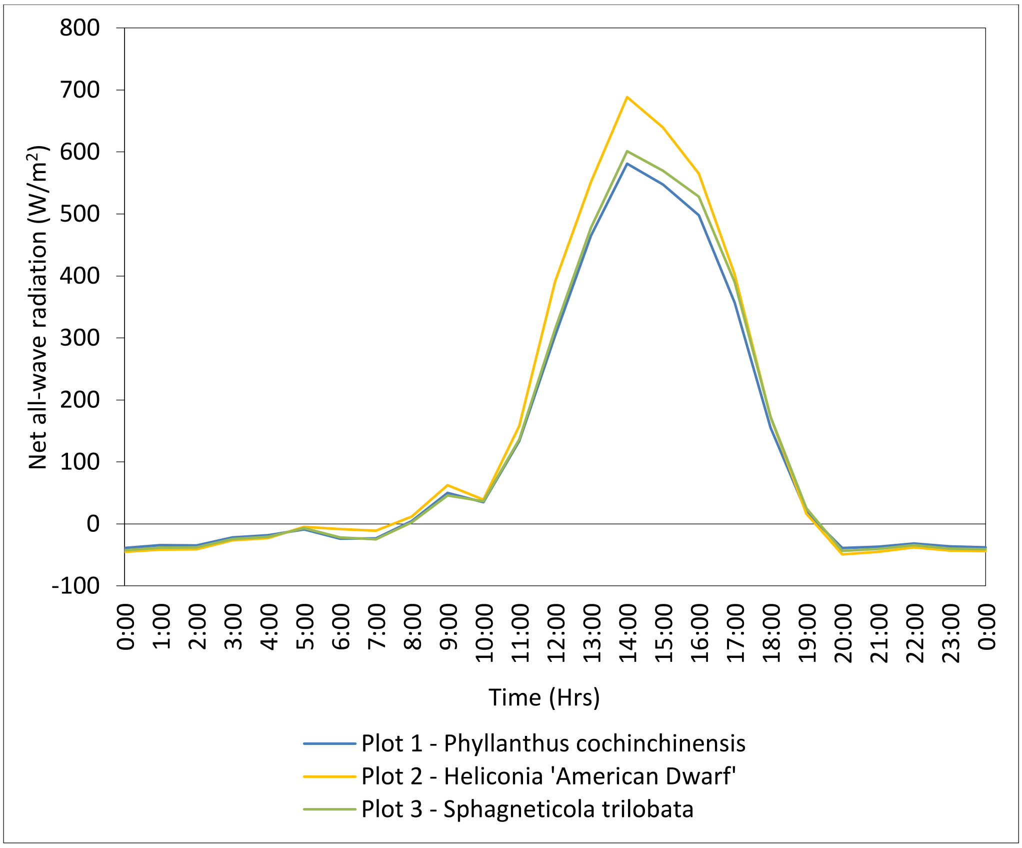

Figure 62. Net all-wave radiation (Q*) for Plots 1 to 3 (7th July 2014)

4.1.1.9 Boundary conditions

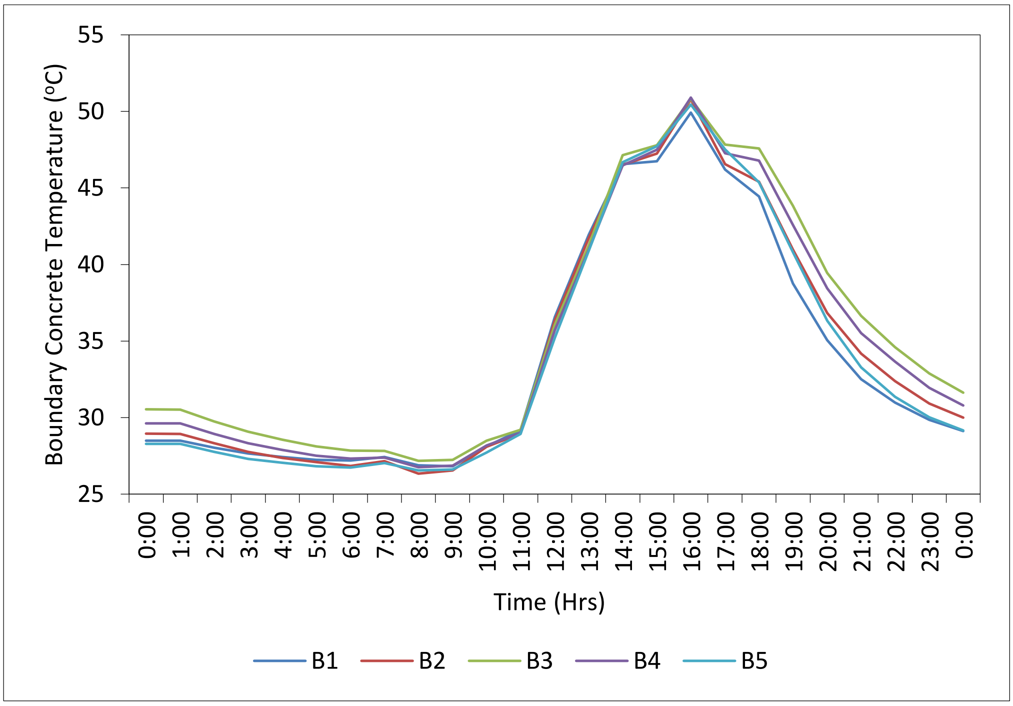

Figure 63. Boundary concrete surface temperature profiles (24th June 2014)

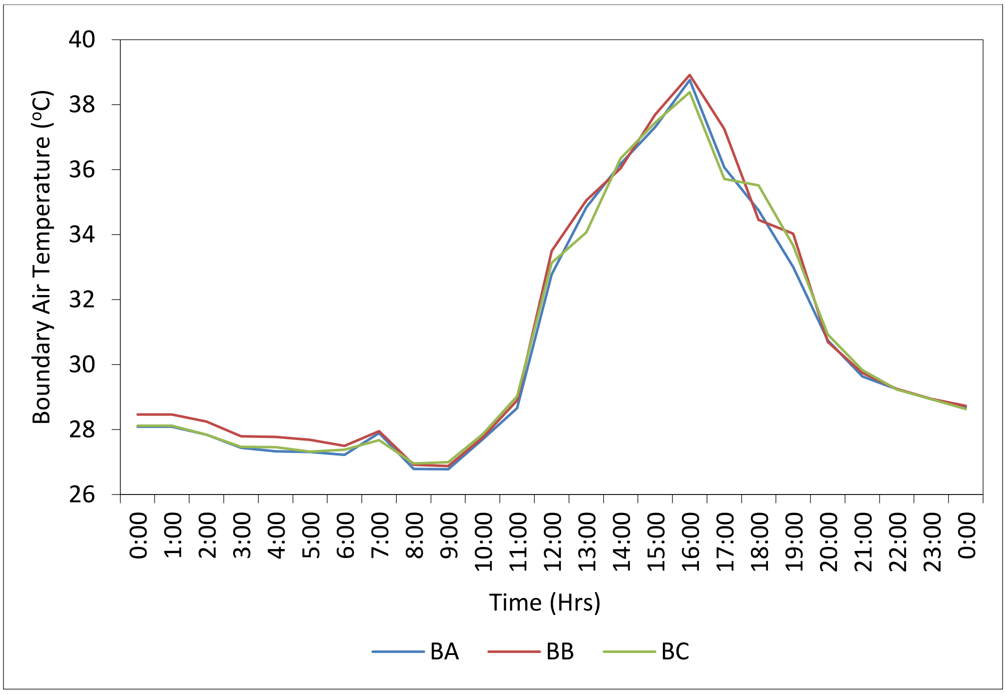

Figure 64. Boundary air temperature profile (24th June 2014)

Figure 63 and Figure 64 represent boundary conditions for the setup. The two figures show that there is no significant difference in the boundary concrete surface temperature and boundary air temperature. Thus, it is reasonable to state that there is little external influence to the experimental setup.

4.1.2 Analysis

4.1.2.1 Impact of rooftop greenery on air temperature

Measurements from the rooftop greenery study described in Chapter 4 show that there is significant difference in air temperature above concrete and greenery. The difference in air temperature between concrete and rooftop greenery plots range from 0.7 °C to 1.4 °C during peak air temperature (Table 10). Air temperature at the soil layer is approximately 3 °C to 4 °C lower than above concrete. One reason for the air temperature at the soil layer for Plot 3 to be 4.6 °C lower than concrete is that leaves of the sphagneticola trilobata plant are able to shield the soil layer effectively. In addition, the stems multiply to form a thick undergrowth that aids in trapping cool air within the canopy. It is noteworthy that the difference between air temperature within and above canopies varies significantly. It can be observed that air temperature within the canopy for Plot 2 and Plot 3 are lower than above it but the reverse is observed for Plot 1 (Figure 65).

Table 10. Peak air temperature values of rooftop greenery plots on 26th July 2014

Location		**Peak air temperature (°C)**	**Air temperature difference when compared to concrete (°C)**
Above concrete		33.8	-
Above canopy	Plot 1	32.5	1.3
	Plot 2	32.4	1.4
	Plot 3	33.1	0.7
Within canopy	Plot 1	32.1	1.7
	Plot 2	33.2	0.6
	Plot 3	33.4	0.4
Soil layer	Plot 1	30.6	3.2
	Plot 2	30.5	3.3
	Plot 3	29.2	4.6

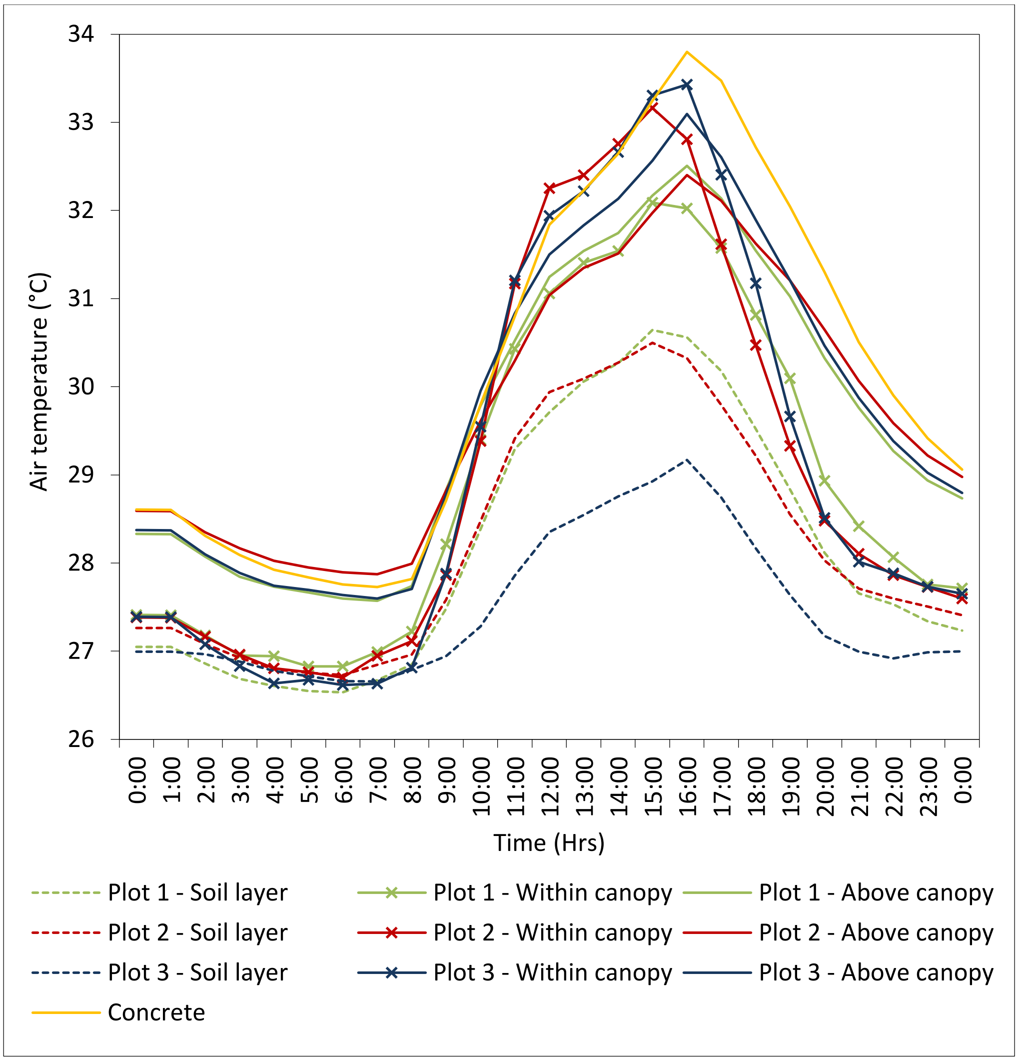

Figure 65. Air temperature profiles of rooftop greenery plots on 26th July 2014

Previous studies on greenery (Table 11) show that reduction of air temperature due to rooftop greenery (shrubs only, without tree canopy shade) can be as high as 4 °C. Results from this field measurement (0.7 °C to 1.4 °C above shrubbery) are within the range found in reviewed literature. Even in the absence of tree canopy shade, introduction of shrubbery can lead to significant reduction in air temperature.

Table 11. Studies on air temperature reduction due to greenery

Focus of study	Finding	Author
Measurement of air temperature reduction due to trees	2 °C to 3.8 °C reduction	Sitawati et al., 2011
Measurement of air temperature along reduced-scale street canyon with green wall and green roof	1.5 °C reduction for street with green wall	Djedjig et al., 2013
Measurement of air temperature under tree canopies	2 °C cooler on average under tree canopy	Taha et al., 1991
Measurement of air temperature above rooftop greenery	4.2 °C cooler than concrete roof at 300mm above greenery	Wong et al., 2003a
Measurement of air temperature above rooftop greenery at multi-storey carpark	6.1 °C to 5.5 °C at 300 mm 3.8 °C to 4.3 °C at 1200 mm	Wong et al., 2007
Measurement of air temperature in parks	Up to 3.5 °C reduction	Bernatzky, 1982
Measurement of air temperature in a garden	Up to 6.9 °C reduction	Oliveira et al., 2011

It can be observed from Figure 66 that plant air temperature is not closely correlated to plant evapotranspiration rate and shrub albedo.

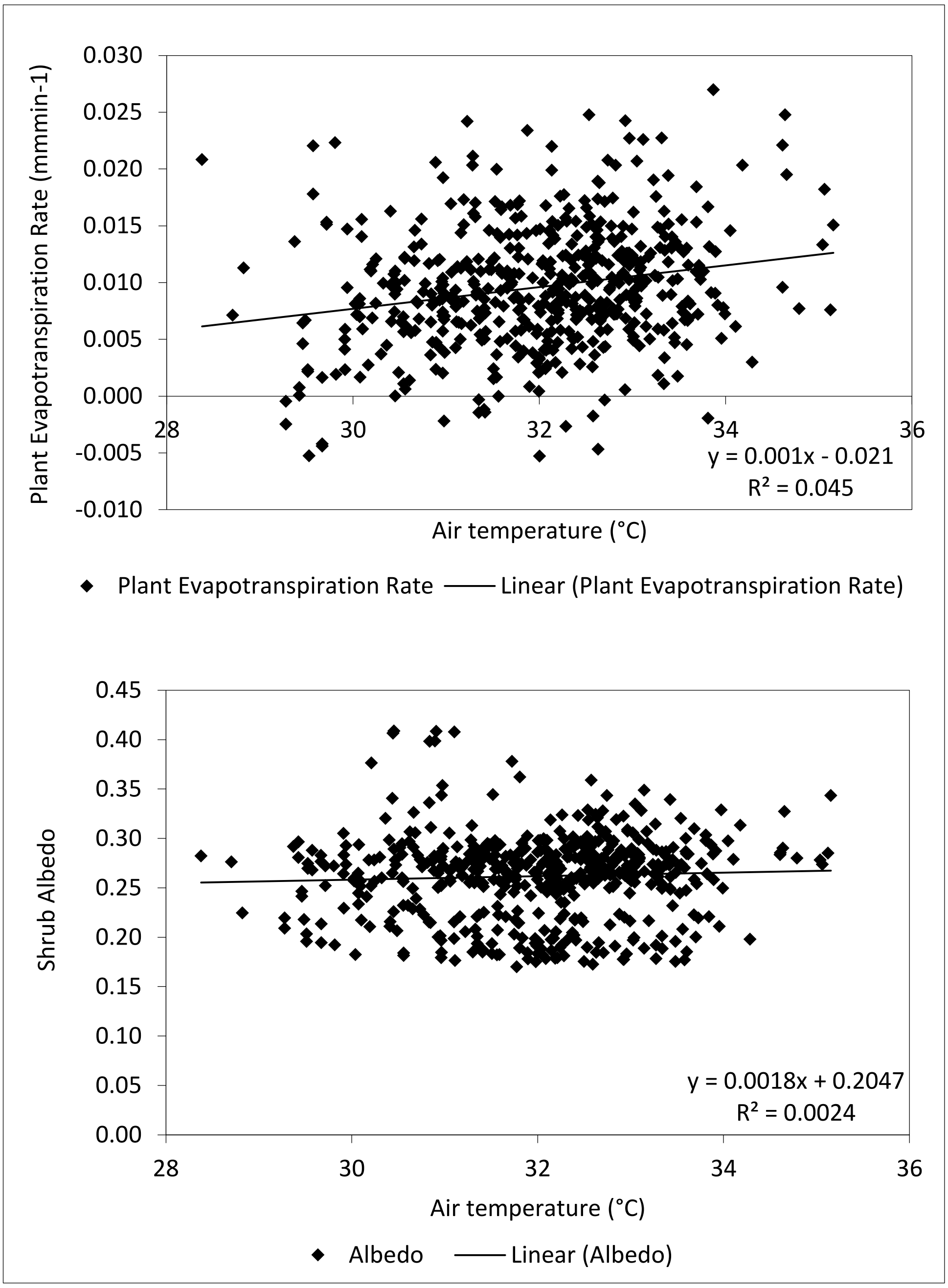

Figure 66. Scatter plots of Plant ET and Albedo on Plant air temperature

4.1.2.2 Impact of rooftop greenery on mean radiant temperature

Results from Chapter 4.1.1.1 show that there is significant reduction in t_{mrt} above the roof surface due to the introduction of plants. This study further explores the magnitude in reduction of different plant types by means of statistical approach to evaluating t_{mrt} reduction against specific plant characteristics. Chapter 5 outlines the statistically derived regression model and concludes the significance of plant characteristics such as plant evapotranspiration rate and shrub albedo in the reduction of t_{mrt}. The coefficient of determination (R^2) of both the regression model (0.850) as well as data used for validation (0.8179) indicates a good fit and reliability of the plant t_{mrt} prediction model.

Figure 67 provides insight into the role of plant evapotranspiration rate (ET) in air and mean radiant temperature reduction. At 12:00 hrs, when average plant ET is approximately 0 $mmmin^{-1}$, it can be observed that there is an average reduction of approximately 3.4 °C for t_{mrt} and 0.7 °C for t_a. At this point, the reduction in temperature can be contributed almost exclusively to plant shade. Thereafter, reductions in t_{mrt} and t_a can be attributed to both plant ET and plant shade.

It is important to note that this is data for one typical day with clear sky conditions and a limitation is that it may not represent a general characteristic of the plants.

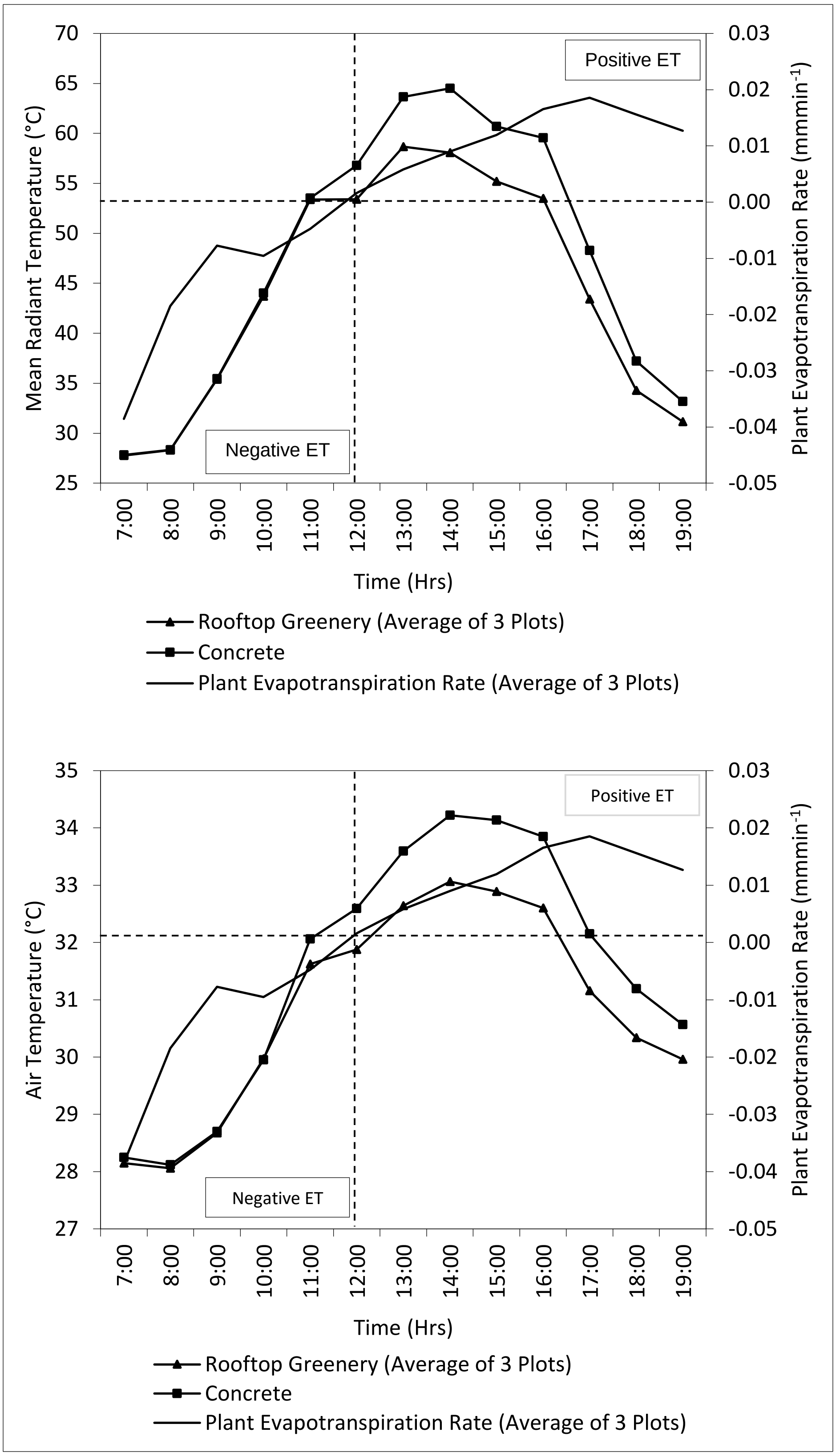

Figure 67. Air and mean radiant temperature profile plotted against plant ET from 07:00 hrs to 19:00 hrs (13th June 2014)

Results from Chapter 4.1.1 show that air and mean radiant temperature can be reduced significantly in the presence of rooftop greenery. Meteorological factors play an important role in temperature reduction, as evident in Chapter 4.1.1.4. A similar trend can be observed in a separate measurement conducted for vertical greenery outlined in Appendix 10.3.1. The potential for cooling by plants in the absence of substantial solar exposure is minimal. This is largely due to the process of plant evapotranspiration, which is light-dependent. A separate study on the impact of height stratification on mean radiant temperature above plant canopies is further explored in Appendix 10.2.

Measurements of shrub characteristics show that plant evapotranspiration rate can vary significantly between plant types. This is verified by measurements of leaf stomata conductance. Similarly, diurnal shrub albedo profiles are observed to vary between plant types. The two factors contribute to lower shrub temperature, which can be observed in Chapter 4.1.1.5.6. This leads to lower longwave emission from the plants to the environment. This is verified by measurements of shortwave and longwave radiation.

Comparisons of LAI values with temperature do not show a correlation of LAI with rooftop greenery cooling potential. Although Heliconia ‘American Dwarf’ has a high LAI value of 7.21, it exhibits the least cooling potential. This may be due to the large leaf area and shrub size of the Heliconia plant, which impedes the delivery of water from soil to leaf. This results in higher leaf surface temperatures, as evident in infrared thermal images shown in Chapter 4.1.1.5.6.2. A more detailed discussion is presented in Chapter 6.1.4.

5 ROOFTOP GREENERY MEAN RADIANT TEMPERATURE PREDICTION MODEL

5.1 Methodology and selection of variables for model development

Parts of Chapter 4.1.1, 5.1 and 5.2 have been published in the Journal of Building and Environment, for which I am the main author:

Tan, C.L., Wong, N.H., Tan, P.Y., Jusuf, S.K., Chiam, Z.Q., 2015, Impact of plant evapotranspiration rate and shrub albedo on temperature reduction in the tropical outdoor environment, *Building and Environment* 94:206-217.

This chapter discusses the development of an empirically derived prediction model that can be utilised to evaluate the impact of rooftop greenery on mean radiant temperature (t_{mrt}). Data that has been collected in Chapter 4 is used in the development of the empirical model. Measurement data and period used for modelling is shown in Table 12.

Variables used for regression modelling are based on observations from the preceding chapter as well as reviewed literature.

From Chapter 4.1.1, it can be observed that evapotranspiration rate and shrub albedo are closely correlated to temperature reduction. These variables influence the overall energy balance of the rooftop greenery system and its resultant temperature. Plant attributes such as LAI, which is observed to have little correlation with overall cooling potential, is omitted from the model.

Mean radiant temperature of the point of measurement ($t_{mrt(plant)}$) is calculated as the dependent variable of the prediction model. Independent variables of the models can be categorized into:

1. Reference mean radiant temperature ($t_{mrt(\mathrm{ref})}$);
2. Plant EvapoTranspiration (ET) rate; and
3. Shrub albedo (SA).

Reference mean radiant temperature ($t_{mrt(\text{ref})}$) is defined as the mean radiant temperature 0.3 m above the concrete surface.

Methodology for measurement of all variables is outlined in Chapter 3.2.3.

A total of 675 data points were used. 525 data points were used for regression modelling. 150 points were used for validation and to test for variability in plant measurement.

A total of 236 days were collected in all. Of the 236 days, 35 days were used for regression modelling and 12 days were used for validation. Data from 188 days were omitted due to one or more of the following reasons:

1. Periods of rain that occurs at any time during 04:00 hrs to 19:00 hrs; and
2. Periods where any equipment used for data collection of the proposed variables is faulty.

Table 12. Variables and days used for regression modelling

Variable	**Total no. of days measured**	**Dates selected for regression modelling (2014)**		**No. of days used for modelling**
Mean radiant temperature above rooftop greenery $t_{mrt(\text{plant})}$ Reference mean radiant temperature $t_{mrt(ref)}$ Plant EvapoTranspiration Rate (ET) Shrub Albedo (SA)	10/05/2014 to 31/12/2014 236 days	May	13, 15, 22, 24, 25, 28, 29	35 days
		June	8, 10, 11, 13, 16, 17, 18, 19, 20, 21, 22, 23, 24, 25	
		July	1, 7, 8, 10, 13, 16, 18, 20, 21, 25, 26	
		August	17	
		September	1, 2	

5.1.1 Model development

Time range of measurements used for modelling is determined based on observations of solar irradiance, mean radiant temperature above concrete and plant evapotranspiration rate. Data from measurements in the absence of sunlight is excluded from consideration. Box plots the three variables are plotted for the period of 07:00 hrs to 19:00 hrs at hourly intervals. Only data from days with clear sky conditions are selected for observation.

From Figure 68, it can be observed that:

1. Significant solar exposure occurs from 10:00 hrs to 17:00 hrs. In this instance, significant solar exposure is defined as solar irradiance that is above 300 Wm^{-2}.
2. Mean radiant temperature of 50 °C occurs from 11:00 hrs to 17:00 hrs.
3. Plant evapotranspiration rate of above 0 $mmmin^{-1}$ occurs from 13:00 hrs to 19:00 hrs.

Figure 34 shows that during the period of 13:00 hrs to 17:00 hrs, significant reductions of t_{mrt} due to rooftop greenery can be observed.

In consideration of the above points, data from the period of 13:00 hrs to 17:00 hrs is used for regression modelling. Data used for modelling is shown in Appendix 10.5.

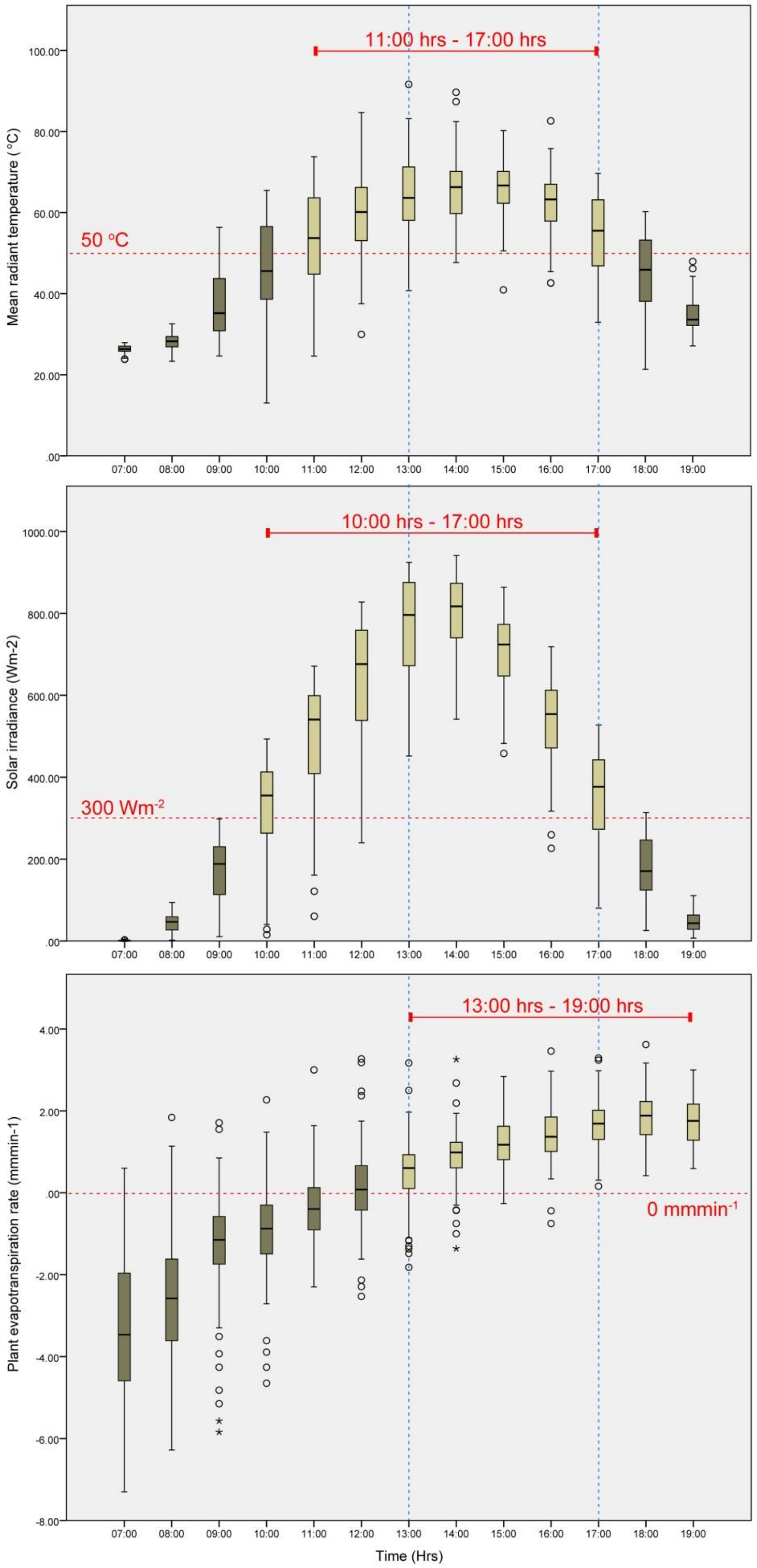

Figure 68. Solar irradiance, plant evapotranspiration rate and t_{mrt} above concrete from 07:00 hrs to 19:00 hrs for days with clear sky conditions

5.1.1.1 Sample characteristics

Visual inspection of normal Q-Q plots, box plots as well as histograms show that all variables are approximately normally distributed (Figure 69).

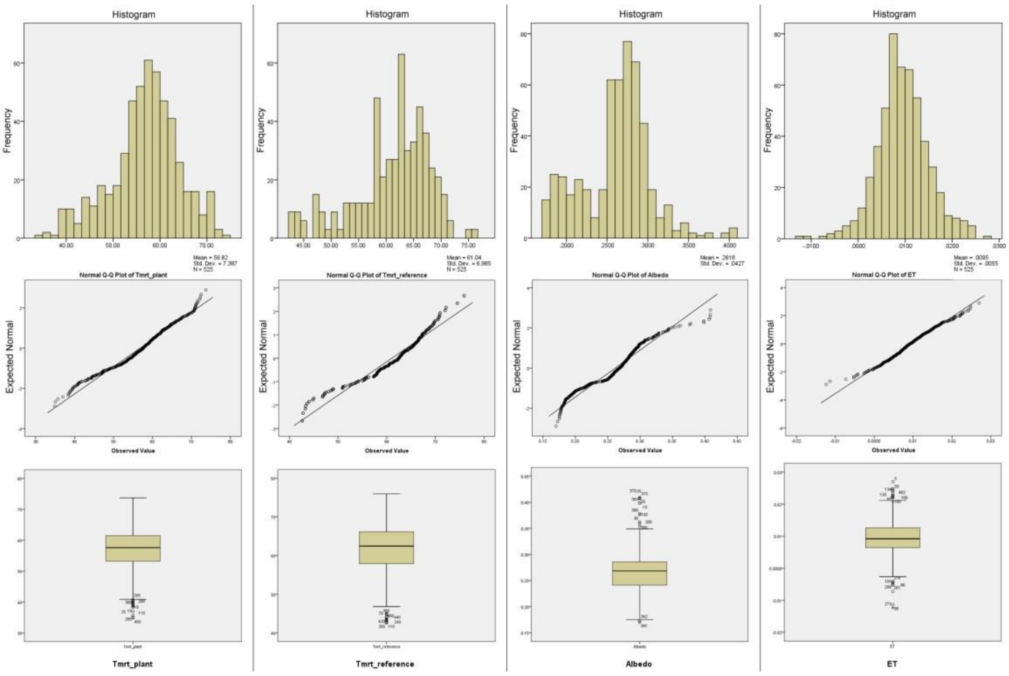

Figure 69. Histograms, Q-Q and box plots for measured variables

5.1.1.2 Correlation analysis

Pearson r correlation analysis is conducted to measure linear correlation between the variables in terms of direction, strength, and significance. Table 13 and Figure 70 shows the relationship between the dependent variable ($t_{mrt(plant)}$) and the independent variables ($t_{mrt(ref)}$, ET and SA). There is significant correlation between independent variables with $t_{mrt(plant)}$ (p<0.01, 2-tailed). Therefore, it can be reasoned that $t_{mrt(plant)}$ can be modelled by using several explanatory variables.

Table 13. Pearson r Correlation Chart

		Tmrt (Reference)	**Plant Evapotranspiration Rate**	**Shrub Albedo**
$t_{mrt(plant)}$	Pearson Correlation (r)	0.824	-0.350	-0.536
	Significance	0.000	0.000	0.000

**All correlations are significant at 0.01 level (2-tailed)*

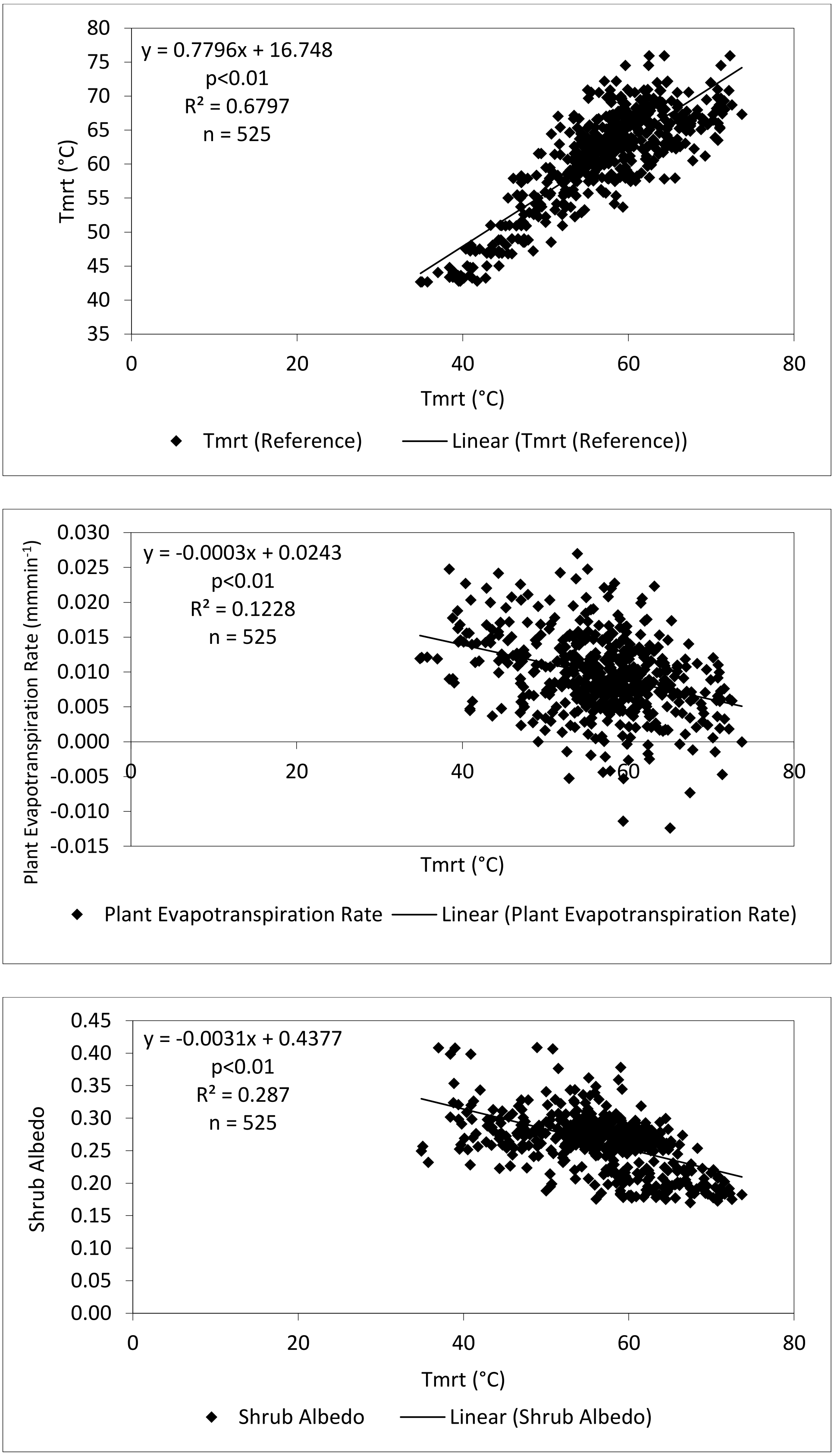

Figure 70. Scatter plots of $t_{mrt(plant)}$ and independent variables

5.1.1.3 Regression model development

Multi-linear regression was conducted using 525 data points. Behavior of variables was analyzed by means of comparing their regression coefficient values (or Beta coefficients) and their correlations (Pearson Correlation or r) with the dependent variable. Observation was made with regards to the significance of the independent variables. Only significant variables ($p<.05$) with beta coefficient signs similar to the Pearson Coefficient (r) were included in the final model. Subsequently, issues with regards to multi-collinearity were addressed by assessing the Variance Inflation Factor (VIF). From published literature, it is recommended for VIF to be lower than the maximum value of 10 (Hair et al., 1995; Kennedy, 1992; Marquardt, 1970; Neter et al., 1989). Another indicator of multi-collinearity is tolerance, where higher levels of tolerance are desired. A value of 0.10 is recommended as the minimum level (Tabachnick and Fidell, 2001). Results of regression modelling is shown in Table 14.

Table 14. Regression summary

Model Summary

R	R Square	Adjusted R Square	Std. Error of the Estimate	Change Statistics		
				R Square Change	F Change	df1
0.923[a]	0.851	0.850	2.85933	0.851	991.983	3

Coefficients[a]

Model	Unstandardized Coefficients		Standardized Coefficients	t	Sig.	Correlations
	B	Std. Error	Beta			Zero-order
(Constant)	26.937	001.479		18.218	0.000	
Tmrt(ref)	0.782	000.018	0.740	42.855	0.000	0.824
SA	-61.011	003.108	-0.353	-19.628	0.000	-0.536
ET	-200.111	023.883	-0.149	-08.379	0.000	-0.350

Coefficients[a]

Model	Correlations		Collinearity Statistics	
	Partial	Part	Tolerance	VIF
(Constant)				
Tmrt(Ref)	0.883	0.725	0.960	1.042
SA	-0.652	-0.332	0.886	1.129
ET	-0.345	-0.142	0.903	1.108

a. Dependent Variable: Tmrt(plant)

Based on results of regression modelling, the mean radiant temperature prediction model can be written as:

$$Tmrt_{\ Plant} = 0.782Tmrt_{ref} - 200.111(°\mathrm{Cmin} \bullet \mathrm{mm}^{-1})ET - 61.011(°\mathrm{C})SA + 26.937(°\mathrm{C})$$

[24]

Where,

$\mathrm{Tmrt}_{\mathrm{Plant}}$ = Mean radiant temperature above rooftop greenery (°C)

$\mathrm{Tmrt}_{\mathrm{Ref}}$ = Mean radiant temperature above concrete (°C)

ET = Plant evapotranspiration rate ($\mathrm{mm{\bullet}min}^{-1}$)

SA = Shrub Albedo

5.1.1.4 Model Validation

Strength and accuracy of the regression model is assessed with several approaches. A total of 150 data points from 12 days were used for validation (Table 15). Figure 71 shows the scatter plot of simulated t_{mrt} values against measured t_{mrt} values. The predicted trend line shows significantly high correlation between measured and simulated values with a high R-squared value.

Table 15. Variables and days used for model validation

Variable	Total no. of days measured	Days selected for validation (2014)		No. of days used for validation
Mean radiant temperature above rooftop greenery $t_{mrt(\mathrm{Plant})}$	10 May 2014	September	7, 8, 10	
Reference mean radiant temperature $t_{mrt(Ref)}$	to	October	2, 3, 9, 10, 19, 20, 23, 25	
Plant EvapoTranspiration Rate (ET)	31 Dec 2014	November	1	12
Shrub Albedo (SA)	236 days	December		

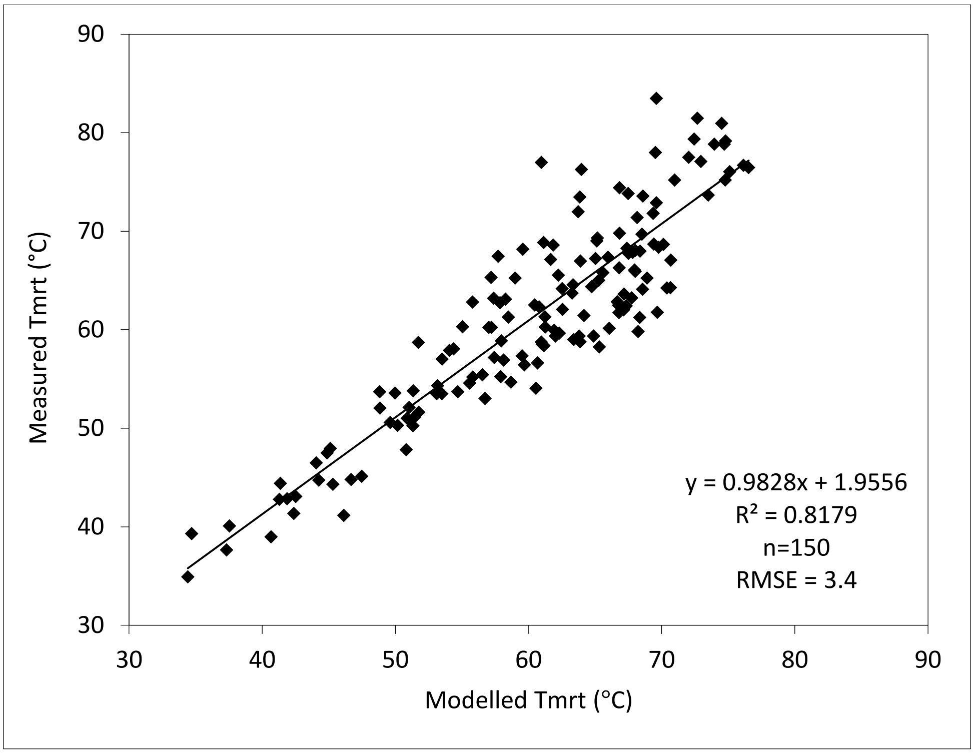

Figure 71. Scatterplot for measured and modelled t_{mrt} values

It can be observed from Figure 71 that the empirical model is able to explain the behavior of t_{mrt} above rooftop greenery plant by considering the proposed independent variables. A box plot of the difference between modelled and measured t_{mrt} values is show in Figure 72. The box plot illustrates the 25th, 50th and 75th percentile of both modelled and measured t_{mrt} values. It can be observed that the difference between modelled and measured data has a mean of close to 0. In addition, the 25th and 75th percentile lie within a range of -4 °C to 2 °C. Therefore, it can be concluded that the empirical model is able to predict plant t_{mrt} with sufficient accuracy.

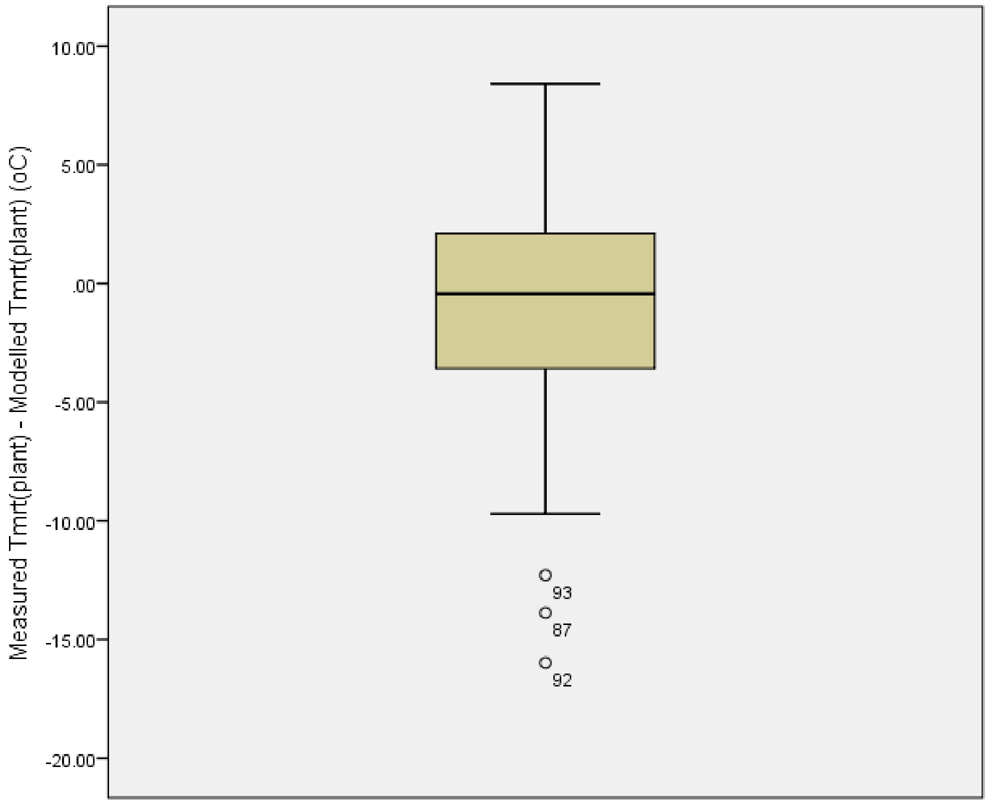

Figure 72. Box plot of modelled and measured t_{mrt} values

By comparing values of modelled and measured t_{mrt} values, it can be concluded that the model is able to explain the behaviour of plant evapotranspiration rate and shrub albedo well in terms of how they can affect rooftop greenery t_{mrt} values.

This chapter has demonstrated how the empirical model can predict rooftop greenery t_{mrt} values. A total of 675 data points from 48 days with clear sky conditions were used to generate a robust and reliable model. The final prediction model work flow can be seen in Figure 73. Co-efficient of determination (R^2) of the empirical model is fairly high (0.85). In addition, analysis has shown that the comparison between modelled and measured t_{mrt} values is similar in terms of magnitude and trend. The following chapter highlights the sensitivity analysis of these models.

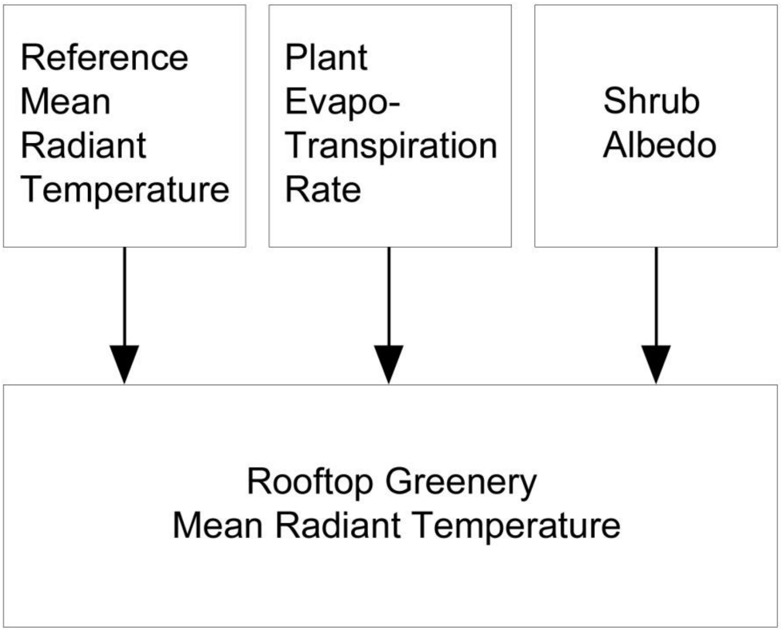

Figure 73. Prediction model workflow

5.2 Sensitivity analysis

The objective of this chapter is to analyze the dependence of rooftop greenery t_{mrt} with regards to variations in each independent variable. Sensitivity analyses were carried out to analyze changes in plant t_{mrt} with certain systematic variations in plant evapotranspiration rate and shrub albedo by using the model developed in Chapter 5.1.

The limit ranges of independent variables are established prior to sensitivity analysis. This is done by creating a matrix comprising of variables and their respective workable range. The variables that are subjected to sensitivity analysis are as follows:

- Reference mean radiant temperature ($t_{mrt(\mathrm{ref})}$);
- Plant evapotranspiration rate (ET);and
- Shrub Albedo (SA).

5.2.1 Establishing range limit for variables

5.2.1.1 Range limit for reference mean radiant temperature

Range limit for reference mean radiant temperature is established by observing the box plot of $t_{mrt(ref)}$ values from 13:00 hrs to 17:00 hrs. It can be observed that the range of 50 °C to 70 °C covers a large portion of upper and lower interquartile ranges of the box plots (Figure 74). This range adequately covers the 25th to 75th percentile of all $t_{mrt(ref)}$ values (Figure 75).

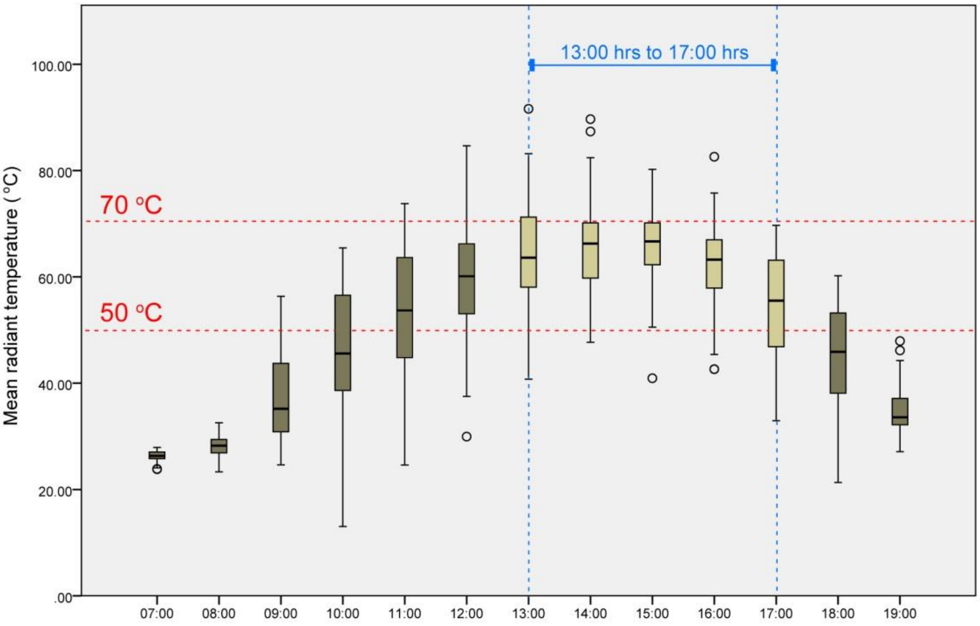

Figure 74. Box plot of Reference t_{mrt} values from 07:00 hrs to 19:00 hrs

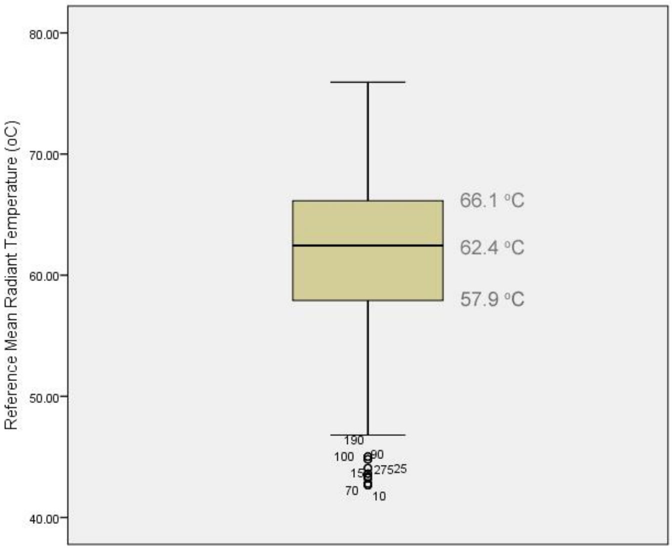

Figure 75. Box plot of Reference t_{mrt} values from 13:00 hrs to 17:00 hrs

5.2.1.2 Range limit for plant evapotranspiration rate

Range limit for plant evapotranspiration rate (ET) is established by first reviewing available literature on plant ET studies. Table 16 shows that plant ET can range from approximately 0.0010 mmmin^{-1} to 0.1110 mmmin^{-1}. It is important to note that most studies measure plant ET in terms of mmday^{-1} or mmhr^{-1}, and values shown in Table 16 have been processed to mmmin^{-1} for ease of comparison. These averaged values assume plant ET rate to be constant throughout the day (1440 minutes), which is highly unlikely due to the fact that transpiration activity takes place mainly in the daytime (approximately 720 minutes) for most plants. It can be expected that actual plant ET values should be noticeably higher during the day. Nonetheless, Table 16 provides a reasonable estimation for the lower limit of plant ET (0.0010 mmmin^{-1}). The higher limit is established by observing the box plot of measured ET rates from Chapter 4. It can be observed from Figure 76 that the 25th to 75th percentile of measured plant ET values ranges from 0.0064 mmmin^{-1} to 0.0126 mmmin^{-1}. Figure 48 shows that measured plant ET can be as high as 0.0200 mmmin^{-1}. Plant ET rates for trees are observed to be significantly higher (0.1110 mmmin^{-1}).

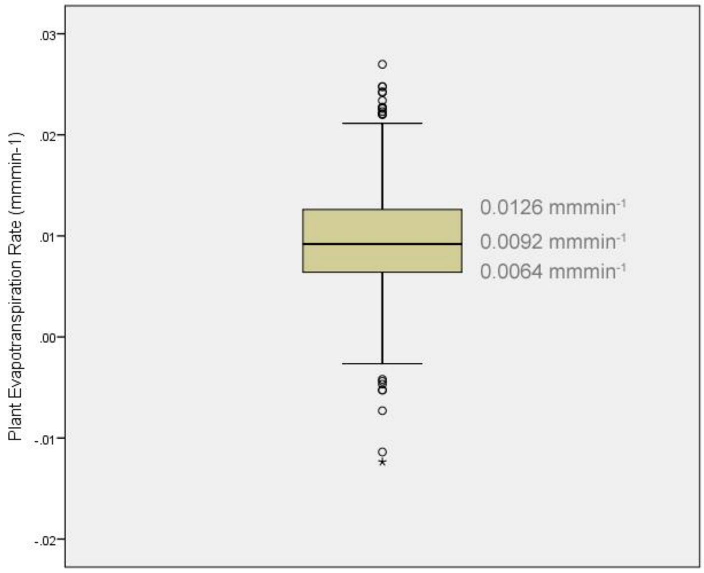

Figure 76. Box plot of plant evapotranspiration rates from 13:00 hrs to 17:00 hrs

Table 16. Plant evapotranspiration rates from reviewed literature

Vegetation	Plant evapotranspiration rate (mmmin^{-1})	Source
Bahiagrass	0.0016	Jia et al., 2009
Bermuda grass overseeded with perennial ryegrass	0.0026 – 0.0032	Devitt et al., 1992
Common Bermuda grass	0.0030 – 0.0033	Carrow, 1995
Buffalo grass	0.0030 to 0.0037	Kim and Beard, 1988
Begonia	0.0033	Baille et al., 1994
Cyclamen	0.0047	
Gardenia	0.0055	
Gloxinia	0.0030	
Hibiscus	0.0055	
Impatiens	0.0063	
Pelargonium	0.0068	
Poinsettia	0.0018	
Schefflera	0.0052	
Carax acutiformis	0.0023	Behrendt et al., 2003
Phragmites australis	0.0030	
Carax disticha	0.0025	
Schoeneplectus lacustris	0.0024	
Thypha latifolia	0.0016	
Willow (Tree)	0.0580 – 0.1110	Guidi et al., 2008
Poplar (Tree)	0.0560 – 0.0670	
Riparian Sandstone Fynbos	0.0028	Dzikiti et al., 2014
Dryland Sandstone Fynbos	0.0010	
Sand Plain Fynbos	0.0020	

5.2.1.3 Range limit for shrub albedo

Range limit for shrub albedo is established by referencing measured albedo values of vegetated surfaces. Reviewed literature suggests that albedo values of vegetated surfaces range from 0.05 to 0.30 (Table 17). Albedo measured in Chapter 4 shows that the 25th to 75th quartile of measured albedo values ranges from 0.24 to 0.29 (Figure 77).

Table 17. Common albedo values of vegetated surfaces

Natural surface type	**Approximated albedo**	**Source**
Forest Grassland and cropland	0.05 - 0.20 0.10 - 0.25	Dobos, 2006
Deciduous forest Tops of oak Pine forest	0.17 0.18 0.14	Kondratiev et al., 1964; Kung et al., 1964
Corn soybean sunflower	0.20 - 0.25 0.21 0.24 - 0.30	Breuer et al., 2003
Evergreen forest (mostly tropical) Deciduous forest Shrub and low tree Tall grass and vegetation Short vegetation, grass, pasture Crop, agriculture	0.125 ± 0.03 0.147 ± 0.03 0.175 ± 0.03 0.175 ± 0.03 0.175 ± 0.03 0.145 ± 0.04	Dickinson and Hanson, 2013
Green roof	0.196	Gaffin et al., 2009
Short turf grass	0.25 – 0.30	Oke, 1988

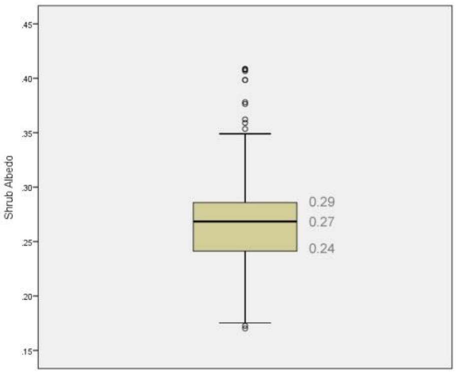

Figure 77. Box plot of shrub albedo values from 13:00 hrs to 17:00 hrs

5.2.2 Sensitivity analysis of prediction model

From the preceding section, the range of values that are used for sensitivity analysis is as follows:

Table 18. Range of values used for sensitivity analysis

Variable	Range			Unit
Reference mean radiant temperature $t_{mrt(Ref)}$	50	-	70	°C
Plant evapotranspiration rate (ET)	0.001	-	0.030	mmmin^{-1}
Shrub albedo (SA)	0.01	-	0.30	-

The proposed ranges reflect values found in review literature as well as those derived from field measurement.

Sensitivity analysis is conducted using the prediction model generated from Chapter 5.1.1.3 using the equation below:

$$Tmrt_{\ Plant} = 0.782Tmrt_{ref} - 200.111ET - 61.011SA + 26.937 \qquad [25]$$

The averaged values of all variables (based on field measurement data) are shown in Table 19. These values are used for sensitivity analysis.

Table 19. Averaged values used for sensitivity

Plant mean radiant temperature $t_{mrt(Plant)}$	Reference mean radiant temperature $t_{mrt(Ref)}$	Plant evapotranspiration rate (ET) (mmmin^{-1})	Shrub albedo (SA)

(°C)	(°C)		
56.8	61.0	0.0095	0.26

5.2.2.1 Reference mean radiant temperature ($t_{mrt(ref)}$)

Sensitivity analysis is conducted for $t_{mrt(ref)}$ using values shown in Table 20. Figure 78 shows the positive linear relationship between $t_{mrt(ref)}$ and $t_{mrt(plant)}$. For every increase of 1 °C for $t_{mrt(ref),}$ there is a corresponding increase of 0.8 °C for $t_{mrt(plant)}$.

Table 20. Values used for Tmrt(Ref) sensitivity analysis

Plant mean radiant temperature $t_{mrt(Plant)}$ (°C)	**Reference mean radiant temperature $t_{mrt(Ref)}$ (°C)**	**Plant evapotranspiration rate (ET) (mmmin^{-1})**	**Shrub albedo (SA)**
56.8	50.0 - 70.0	0.0095	0.26

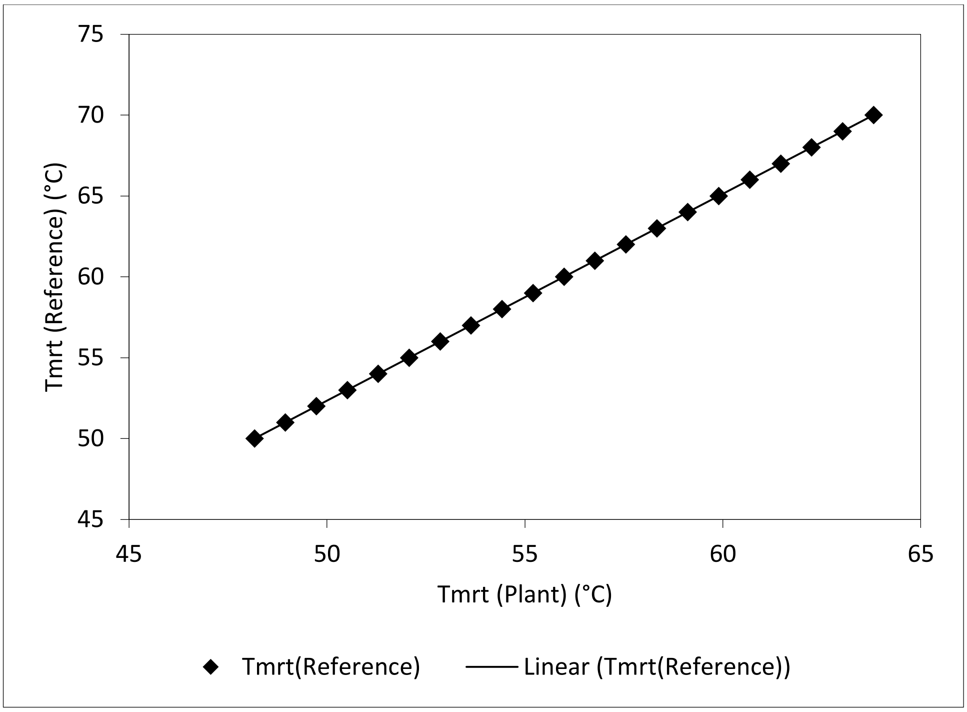

Figure 78. Plot of Plant t_{mrt} and Reference t_{mrt}

5.2.2.2 Plant evapotranspiration rate (ET)

Sensitivity analysis is conducted for plant evapotranspiration rate (ET) using values shown in Table 21. Figure 79 shows the negative linear relationship between plant (ET) and $t_{mrt(plant)}$. For every increase of 0.001 mmmin^{-1} for plant ET, there is a corresponding decrease of 0.2 °C for $t_{mrt(plant)}$.

Table 21. Values used for Plant ET sensitivity analysis

Plant mean radiant temperature $t_{mrt(Plant)}$ (°C)	**Reference mean radiant temperature $t_{mrt(Ref)}$ (°C)**	**Plant evapotranspiration rate (ET) (mmmin^{-1})**	**Shrub albedo (SA)**
56.8	61.0	0.001 – 0.030	0.26

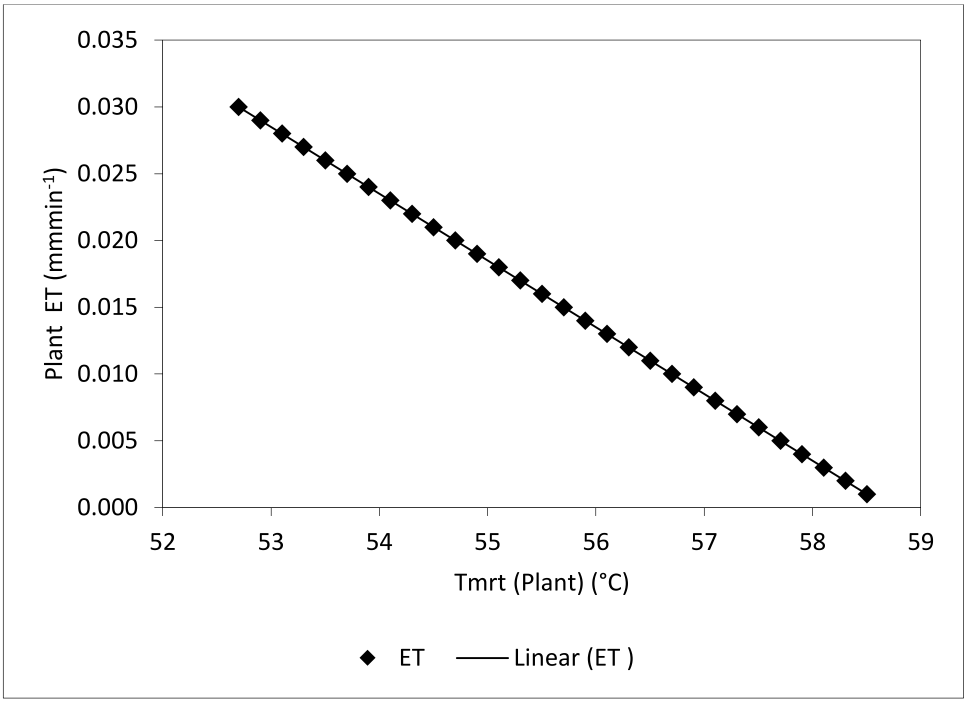

Figure 79. Plot of Plant t_{mrt} and Plant Evapotranspiration Rate

5.2.2.3 Shrub albedo (SA)

Sensitivity analysis is conducted for shrub albedo (SA) using values shown in Table 22. Figure 80 shows the negative linear relationship between (SA) and $t_{mrt(plant)}$. For every increase of 0.01 for SA, there is a corresponding decrease of 0.6 °C for $t_{mrt(plant)}$.

Table 22.Values used for Shrub Albedo sensitivity analysis

Plant mean radiant temperature $t_{mrt(Plant)}$ (°C)	**Reference mean radiant temperature $t_{mrt(Ref)}$ (°C)**	**Plant evapotranspiration rate (ET) (mmmin^{-1})**	**Shrub albedo (SA)**
56.8	61.0	0.0095	0.01 – 0.30

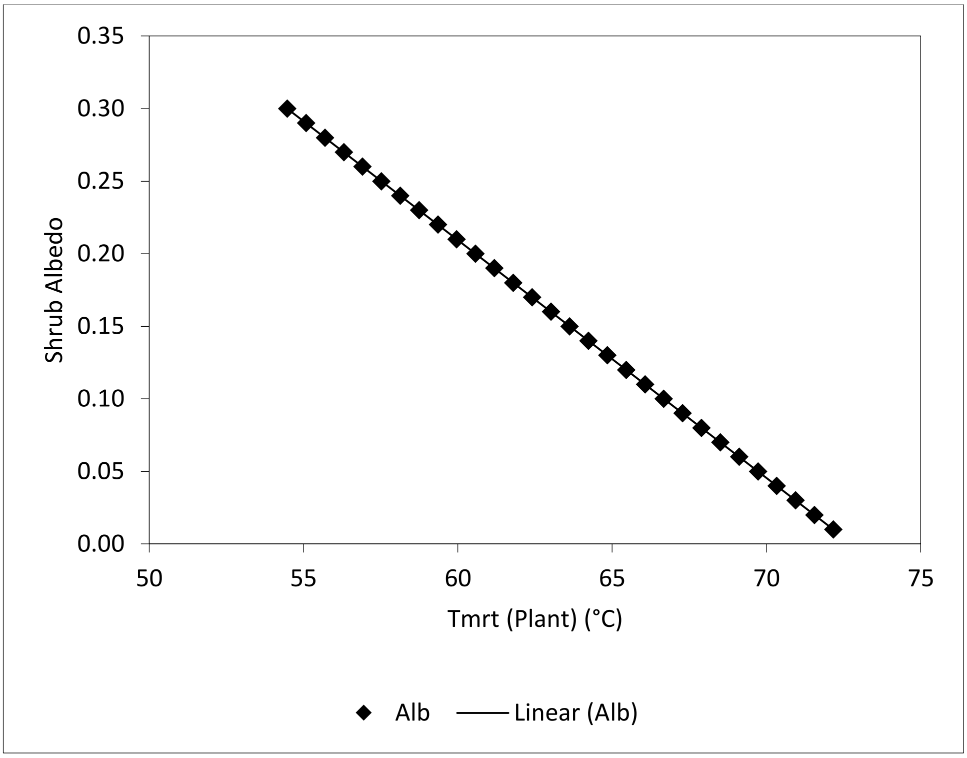

Figure 80. Plot of Plant t_{mrt} and Shrub Albedo

5.2.2.4 Values of $t_{mrt(plant)}$ for $t_{mrt(ref)}$ values of 50 °C to 70 °C

Values of $t_{mrt(plant)}$ are estimated using the empirically derived prediction model for $t_{mrt(ref)}$ values ranging from 50 °C to 70 °C. Results are appended in Chapter 10.8. It can be observed from Table 23 that for the range of 50 °C to 70 °C, reductions in mean radiant temperature can be observed with a minimum albedo of 0.17 and plant ET of 0.029. At peak $t_{mrt(ref)}$ (70 °C), it can be observed that a SA value of 0.19 will result in reduced $t_{mrt(plant)}$ with plant ET as low as 0.001 mmmin^{-1}.

Table 23. Percentage reduction of Tmrt(plant) derived using Tmrt(ref) of 50 °C and 70 °C

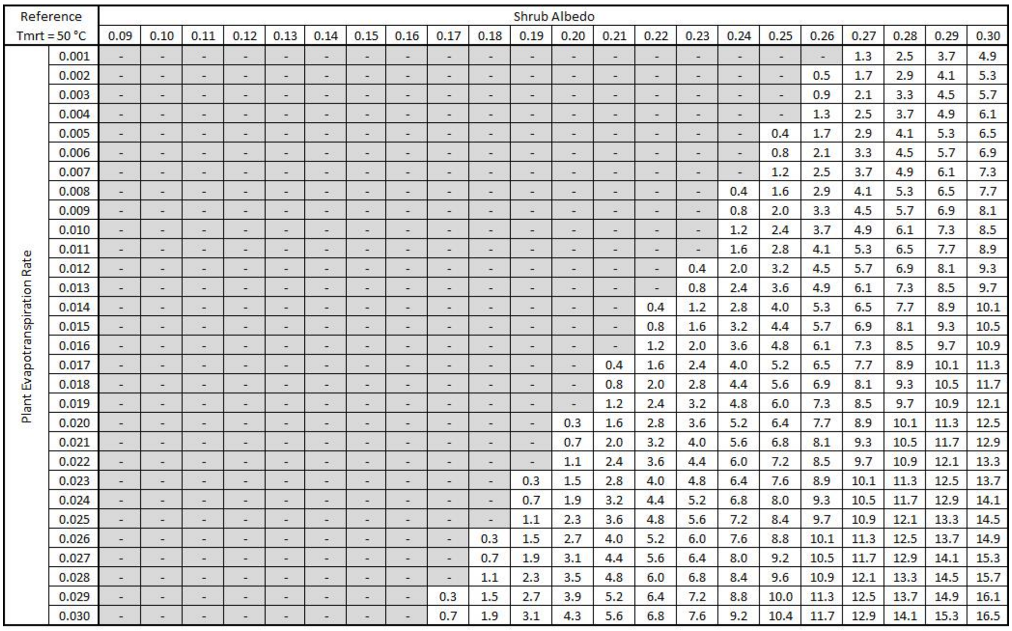

Reference		Shrub Albedo																					
Tmrt = 50 °C		0.09	0.10	0.11	0.12	0.13	0.14	0.15	0.16	0.17	0.18	0.19	0.20	0.21	0.22	0.23	0.24	0.25	0.26	0.27	0.28	0.29	0.30
Plant Evapotranspiration Rate	0.001	-	-	-	-	-	-	-	-	-	-	-	-	-	-	-	-	-	-	1.3	2.5	3.7	4.9
	0.002	-	-	-	-	-	-	-	-	-	-	-	-	-	-	-	-	-	0.5	1.7	2.9	4.1	5.3
	0.003	-	-	-	-	-	-	-	-	-	-	-	-	-	-	-	-	-	0.9	2.1	3.3	4.5	5.7
	0.004	-	-	-	-	-	-	-	-	-	-	-	-	-	-	-	-	-	1.3	2.5	3.7	4.9	6.1
	0.005	-	-	-	-	-	-	-	-	-	-	-	-	-	-	-	-	0.4	1.7	2.9	4.1	5.3	6.5
	0.006	-	-	-	-	-	-	-	-	-	-	-	-	-	-	-	-	0.8	2.1	3.3	4.5	5.7	6.9
	0.007	-	-	-	-	-	-	-	-	-	-	-	-	-	-	-	-	1.2	2.5	3.7	4.9	6.1	7.3
	0.008	-	-	-	-	-	-	-	-	-	-	-	-	-	-	-	0.4	1.6	2.9	4.1	5.3	6.5	7.7
	0.009	-	-	-	-	-	-	-	-	-	-	-	-	-	-	-	0.8	2.0	3.3	4.5	5.7	6.9	8.1
	0.010	-	-	-	-	-	-	-	-	-	-	-	-	-	-	-	1.2	2.4	3.7	4.9	6.1	7.3	8.5
	0.011	-	-	-	-	-	-	-	-	-	-	-	-	-	-	-	1.6	2.8	4.1	5.3	6.5	7.7	8.9
	0.012	-	-	-	-	-	-	-	-	-	-	-	-	-	-	0.4	2.0	3.2	4.5	5.7	6.9	8.1	9.3
	0.013	-	-	-	-	-	-	-	-	-	-	-	-	-	-	0.8	2.4	3.6	4.9	6.1	7.3	8.5	9.7
	0.014	-	-	-	-	-	-	-	-	-	-	-	-	-	0.4	1.2	2.8	4.0	5.3	6.5	7.7	8.9	10.1
	0.015	-	-	-	-	-	-	-	-	-	-	-	-	-	0.8	1.6	3.2	4.4	5.7	6.9	8.1	9.3	10.5
	0.016	-	-	-	-	-	-	-	-	-	-	-	-	-	1.2	2.0	3.6	4.8	6.1	7.3	8.5	9.7	10.9
	0.017	-	-	-	-	-	-	-	-	-	-	-	-	0.4	1.6	2.4	4.0	5.2	6.5	7.7	8.9	10.1	11.3
	0.018	-	-	-	-	-	-	-	-	-	-	-	-	0.8	2.0	2.8	4.4	5.6	6.9	8.1	9.3	10.5	11.7
	0.019	-	-	-	-	-	-	-	-	-	-	-	-	1.2	2.4	3.2	4.8	6.0	7.3	8.5	9.7	10.9	12.1
	0.020	-	-	-	-	-	-	-	-	-	-	-	0.3	1.6	2.8	3.6	5.2	6.4	7.7	8.9	10.1	11.3	12.5
	0.021	-	-	-	-	-	-	-	-	-	-	-	0.7	2.0	3.2	4.0	5.6	6.8	8.1	9.3	10.5	11.7	12.9
	0.022	-	-	-	-	-	-	-	-	-	-	-	1.1	2.4	3.6	4.4	6.0	7.2	8.5	9.7	10.9	12.1	13.3
	0.023	-	-	-	-	-	-	-	-	-	-	0.3	1.5	2.8	4.0	4.8	6.4	7.6	8.9	10.1	11.3	12.5	13.7
	0.024	-	-	-	-	-	-	-	-	-	-	0.7	1.9	3.2	4.4	5.2	6.8	8.0	9.3	10.5	11.7	12.9	14.1
	0.025	-	-	-	-	-	-	-	-	-	-	1.1	2.3	3.6	4.8	5.6	7.2	8.4	9.7	10.9	12.1	13.3	14.5
	0.026	-	-	-	-	-	-	-	-	-	0.3	1.5	2.7	4.0	5.2	6.0	7.6	8.8	10.1	11.3	12.5	13.7	14.9
	0.027	-	-	-	-	-	-	-	-	-	0.7	1.9	3.1	4.4	5.6	6.4	8.0	9.2	10.5	11.7	12.9	14.1	15.3
	0.028	-	-	-	-	-	-	-	-	-	1.1	2.3	3.5	4.8	6.0	6.8	8.4	9.6	10.9	12.1	13.3	14.5	15.7
	0.029	-	-	-	-	-	-	-	-	0.3	1.5	2.7	3.9	5.2	6.4	7.2	8.8	10.0	11.3	12.5	13.7	14.9	16.1
	0.030	-	-	-	-	-	-	-	-	0.7	1.9	3.1	4.3	5.6	6.8	7.6	9.2	10.4	11.7	12.9	14.1	15.3	16.5

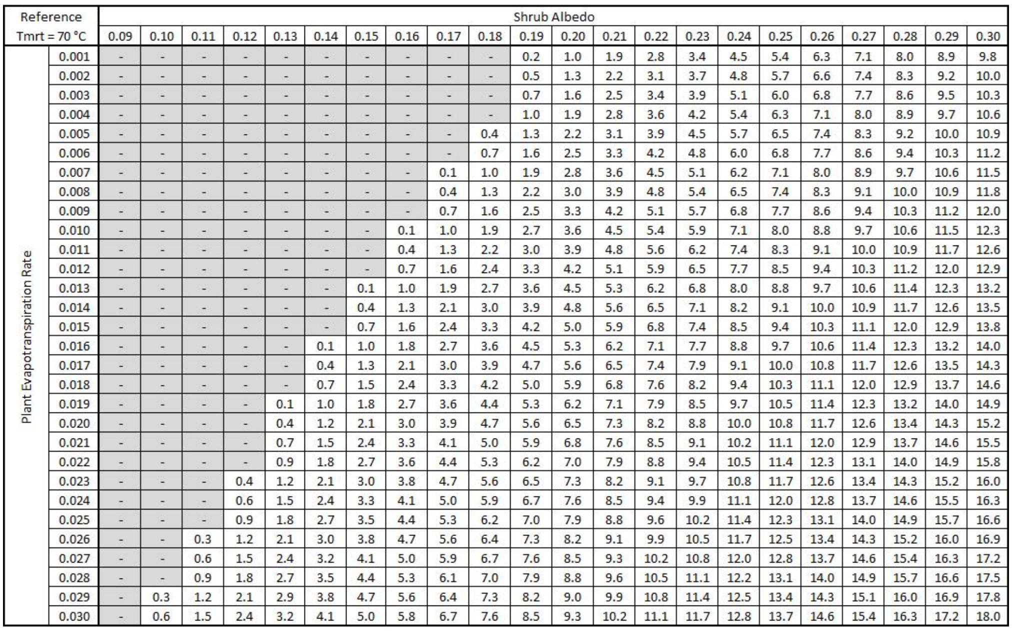

Reference		Shrub Albedo																					
Tmrt = 70 °C		0.09	0.10	0.11	0.12	0.13	0.14	0.15	0.16	0.17	0.18	0.19	0.20	0.21	0.22	0.23	0.24	0.25	0.26	0.27	0.28	0.29	0.30
Plant Evapotranspiration Rate	0.001	-	-	-	-	-	-	-	-	-	-	0.2	1.0	1.9	2.8	3.4	4.5	5.4	6.3	7.1	8.0	8.9	9.8
	0.002	-	-	-	-	-	-	-	-	-	-	0.5	1.3	2.2	3.1	3.7	4.8	5.7	6.6	7.4	8.3	9.2	10.0
	0.003	-	-	-	-	-	-	-	-	-	-	0.7	1.6	2.5	3.4	3.9	5.1	6.0	6.8	7.7	8.6	9.5	10.3
	0.004	-	-	-	-	-	-	-	-	-	-	1.0	1.9	2.8	3.6	4.2	5.4	6.3	7.1	8.0	8.9	9.7	10.6
	0.005	-	-	-	-	-	-	-	-	-	0.4	1.3	2.2	3.1	3.9	4.5	5.7	6.5	7.4	8.3	9.2	10.0	10.9
	0.006	-	-	-	-	-	-	-	-	-	0.7	1.6	2.5	3.3	4.2	4.8	6.0	6.8	7.7	8.6	9.4	10.3	11.2
	0.007	-	-	-	-	-	-	-	-	0.1	1.0	1.9	2.8	3.6	4.5	5.1	6.2	7.1	8.0	8.9	9.7	10.6	11.5
	0.008	-	-	-	-	-	-	-	-	0.4	1.3	2.2	3.0	3.9	4.8	5.4	6.5	7.4	8.3	9.1	10.0	10.9	11.8
	0.009	-	-	-	-	-	-	-	-	0.7	1.6	2.5	3.3	4.2	5.1	5.7	6.8	7.7	8.6	9.4	10.3	11.2	12.0
	0.010	-	-	-	-	-	-	-	0.1	1.0	1.9	2.7	3.6	4.5	5.4	5.9	7.1	8.0	8.8	9.7	10.6	11.5	12.3
	0.011	-	-	-	-	-	-	-	0.4	1.3	2.2	3.0	3.9	4.8	5.6	6.2	7.4	8.3	9.1	10.0	10.9	11.7	12.6
	0.012	-	-	-	-	-	-	-	0.7	1.6	2.4	3.3	4.2	5.1	5.9	6.5	7.7	8.5	9.4	10.3	11.2	12.0	12.9
	0.013	-	-	-	-	-	-	0.1	1.0	1.9	2.7	3.6	4.5	5.3	6.2	6.8	8.0	8.8	9.7	10.6	11.4	12.3	13.2
	0.014	-	-	-	-	-	-	0.4	1.3	2.1	3.0	3.9	4.8	5.6	6.5	7.1	8.2	9.1	10.0	10.9	11.7	12.6	13.5
	0.015	-	-	-	-	-	-	0.7	1.6	2.4	3.3	4.2	5.0	5.9	6.8	7.4	8.5	9.4	10.3	11.1	12.0	12.9	13.8
	0.016	-	-	-	-	-	0.1	1.0	1.8	2.7	3.6	4.5	5.3	6.2	7.1	7.7	8.8	9.7	10.6	11.4	12.3	13.2	14.0
	0.017	-	-	-	-	-	0.4	1.3	2.1	3.0	3.9	4.7	5.6	6.5	7.4	7.9	9.1	10.0	10.8	11.7	12.6	13.5	14.3
	0.018	-	-	-	-	-	0.7	1.5	2.4	3.3	4.2	5.0	5.9	6.8	7.6	8.2	9.4	10.3	11.1	12.0	12.9	13.7	14.6
	0.019	-	-	-	-	0.1	1.0	1.8	2.7	3.6	4.4	5.3	6.2	7.1	7.9	8.5	9.7	10.5	11.4	12.3	13.2	14.0	14.9
	0.020	-	-	-	-	0.4	1.2	2.1	3.0	3.9	4.7	5.6	6.5	7.3	8.2	8.8	10.0	10.8	11.7	12.6	13.4	14.3	15.2
	0.021	-	-	-	-	0.7	1.5	2.4	3.3	4.1	5.0	5.9	6.8	7.6	8.5	9.1	10.2	11.1	12.0	12.9	13.7	14.6	15.5
	0.022	-	-	-	-	0.9	1.8	2.7	3.6	4.4	5.3	6.2	7.0	7.9	8.8	9.4	10.5	11.4	12.3	13.1	14.0	14.9	15.8
	0.023	-	-	-	0.4	1.2	2.1	3.0	3.8	4.7	5.6	6.5	7.3	8.2	9.1	9.7	10.8	11.7	12.6	13.4	14.3	15.2	16.0
	0.024	-	-	-	0.6	1.5	2.4	3.3	4.1	5.0	5.9	6.7	7.6	8.5	9.4	9.9	11.1	12.0	12.8	13.7	14.6	15.5	16.3
	0.025	-	-	-	0.9	1.8	2.7	3.5	4.4	5.3	6.2	7.0	7.9	8.8	9.6	10.2	11.4	12.3	13.1	14.0	14.9	15.7	16.6
	0.026	-	-	0.3	1.2	2.1	3.0	3.8	4.7	5.6	6.4	7.3	8.2	9.1	9.9	10.5	11.7	12.5	13.4	14.3	15.2	16.0	16.9
	0.027	-	-	0.6	1.5	2.4	3.2	4.1	5.0	5.9	6.7	7.6	8.5	9.3	10.2	10.8	12.0	12.8	13.7	14.6	15.4	16.3	17.2
	0.028	-	-	0.9	1.8	2.7	3.5	4.4	5.3	6.1	7.0	7.9	8.8	9.6	10.5	11.1	12.2	13.1	14.0	14.9	15.7	16.6	17.5
	0.029	-	0.3	1.2	2.1	2.9	3.8	4.7	5.6	6.4	7.3	8.2	9.0	9.9	10.8	11.4	12.5	13.4	14.3	15.1	16.0	16.9	17.8
	0.030	-	0.6	1.5	2.4	3.2	4.1	5.0	5.8	6.7	7.6	8.5	9.3	10.2	11.1	11.7	12.8	13.7	14.6	15.4	16.3	17.2	18.0

6 DISCUSSION

This chapter discusses the significance of findings from Chapter 4, as well as a proposed methodology for landscape planning based on results of Chapter 5.

6.1 Impact of plant selection on ambient and mean radiant temperature

6.1.1 Plant evapotranspiration rate

Results from Chapter 4 have shown that plant EvapoTranspiration rate (ET) has a significant effect on mean radiant temperature (t_{mrt}) in the tropical urban outdoor environment. Therefore, in the process of plant selection, it is important to choose plants with high ET rates for the purpose of attaining maximum cooling potential. There is a wide variety of flora available for selection, and a systematic categorization of ET rates for commonly used rooftop greenery plants is necessary. The list of plants to be tested can be referenced from relevant literature such as ‘A selection of plants for green roofs in Singapore’ (Tan and Sia, 2008).

A review of existing literature shows that ET rates of plants range from approximately 0.0010 mmmin^{-1} to 0.1110 mmmin^{-1} (Table 16). However, it is noted that most studies measure plant ET on a daily or monthly basis (Behrendt et al., 2003; Devitt et al., 1992; Dzikiti et al., 2014). This makes it impossible to discern the true impact of ET on cooling effect at specific periods (e.g. 13:00 hrs to 17:00 hrs, the hottest period of the day). Moreover, there is very little ET activity as night for most plants owing to the fact that ET is a photosynthetic process.

This study has also looked into ET rates of plants commonly used for rooftop greenery specifically at minute and hourly intervals so as to observe the behavior of plants in terms of their ET during different parts of the day (Figure 81). Additional measurements of plant ET for different plants show that ET rates can vary significantly for different plant types (Figure 82). Measurements were taken on 13th January 2015, under clear sky conditions with peak solar irradiance of 791.2 Wm^{-2} at 15:00 hrs.

Figure 81. Rooftop greenery panel on load cell

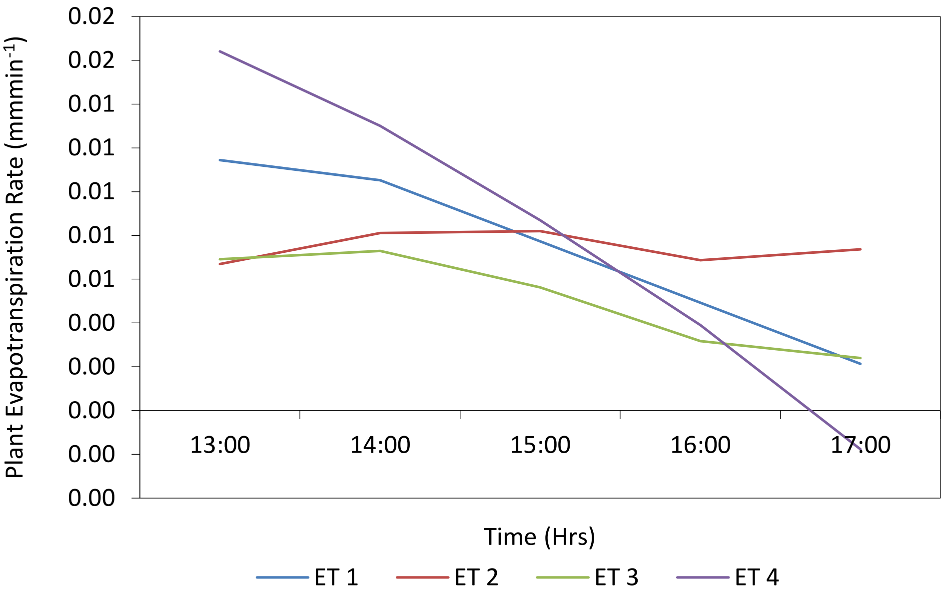

ET	**Plant**	**Average Evapotranspiration Rate (mmmin^{-1}) (13:00 hrs to 17:00 hrs)**
1	Pedilanthus tithymaloides	0.0074
2	Schefflera arboricola	0.0074
3	Euphorbia milii	0.0051
4	Asparagus officinalis	0.0080

For the purpose of optimizing cooling effect, it is recommended that following plants be avoided:

- Crassulacean Acid Metabolism (CAM) plants

  Generally, plants undergoing CAM photosynthesis have leaf stomata fully or partially closed during daytime in order to decrease the rate of ET, but are open during nighttime to receive carbon dioxide (CO_2) (Zeiger et al., 1987). This is a common characteristic in plants found in arid environments (e.g. cacti), where water is limited. While this is an effective water conservation strategy for the plants, it will drastically reduce ET rate during daytime and is therefore unsuitable for rooftop greenery.

- Plants that experience midday stomatal depression

  Midday stomatal closure is common for plants that frequently experience drought stress (e.g. Norway Spruce). It also occurs during periods of high light intensity, which contributes to increases in leaf surface temperature (Tenhunen et al., 1987). Since stomatal closure will result in a halt in ET, the potential of reducing t_{mrt} is significantly reduced and not recommended for rooftop greenery.

6.1.2 Shrub albedo

Results from Chapter 4 have shown that Shrub Albedo (SA) has a significant impact on mean radiant temperature (t_{mrt}) in the tropical urban outdoor environment. Therefore, in the process of plant selection, it is important to select plants with high SA for the purpose of attaining the best cooling potential possible. Table 17 has shown that the albedo of vegetated surfaces range from 0.05 to 0.30. Further measurements conducted within the university campus rooftop gardens showed similar results (Table 24).

An important aspect of mitigating the UHI effect is to increase the albedo of built surface areas. Using materials with high albedo values significantly decreases net solar insolation and reduce surface temperature (Taha et al., 1992). Studies have shown the albedo of highly urbanized areas to be in the range of 0.10 to 0.20 (Dabberdt and Davis, 1978; Kung et al., 1964; Steyn and Oke, 1980), and that areas with vegetation can help to increase albedo value (Taha, 1994; Taha, 1997). A common method of increasing the albedo of rooftop surface is via the usage of cool paint. Studies have shown that cool paint can reduce the temperature of roof surfaces and result in significant building energy savings (Akbari et al., 2001; Rosenfeld et al., 1998). Santamouris et al. (2014) compared the potential of cool roofs and green roofs and observed that when the albedo of cool roofs is equal or higher than

0.7, it has a higher cooling potential than green roofs during the peak period. In general, cool roofs perform better than green roofs in sunny climates. However, deterioration of cool roofs due to weathering (dust, moisture penetration, mircobial growth, etc) can significantly decrease its cooling potential (Cheng et al., 2012; Cheng et al., 2011). Green roofs can also significantly reduce surface temperature, as shown in Chapter 4.1.1.7. Compared to cool roofs, green roofs require more maintenance such as regular pruning and replacement of plants, as well as a reliable irrigation schedule. While the upkeep for rooftop greenery is higher, it offers opportunities for roof spaces to be an appropriate venue for social activities and can improve the aesthetics of the outdoor environment.

Table 24. Albedo spot measurements at 13:00 hrs in National University of Singapore UTown roof gardens

Crinum asiaticum Zoysia japonica Rhododendron macgregoriae Cyanotis cristata D.Don Nephrolepis auriculata

Plant	Upward facing pyranometer (Wm-2)	Downward facing pyranometer (Wm-2)	Albedo
Crinum asiaticum	436	111	0.25
Zoysia japonica	360	107	0.30
Rhododendron macgregoriae F.Muell.	833	292	0.35
Cyanotis cristata D.Don	890	200	0.22
Nephrolepis auriculata	972	267	0.27

6.1.3 Consideration of plant functional traits for plant selection

Chapters 6.1.1 and 6.1.2 have looked into quantifiable aspects of plants (ET and SA) and their impact on mean radiant temperature (t_{mrt}). In the course of field measurement, it was also noted that physical plant traits have a significant impact on resultant plant surface temperature and by extrapolation, mean radiant temperature. It has been observed that Heliconia ‘American Dwarf’ plants (Plot 2) have leaves that are much larger than both Phyllanthus cochinchinensis (Plot 1) and Sphagneticola trilobata (Plot 3) plants (Figure 83). The surface area of its leaves is observed to be much higher than the other plots (Figure 58). The average height of Plot 2 plants is also much higher than Plots 1 and 3. In terms of the plant canopy, Plot 2 is much more porous, compared to Plot 3, which forms a thick, inter-twined undergrowth with its stems. This undergrowth provides excellent shade, which translates to higher reduction in air temperature (Figure 65). Cool air is effectively trapped within the canopy. While there is insufficient data to determine the statistical impact of plant functional traits, there is evidence to suggest that that leaves with smaller surface areas tend to be more effective at reducing t_{mrt}. Therefore, selection of plants with small leaves for the purpose of reducing outdoor t_{mrt} is recommended.

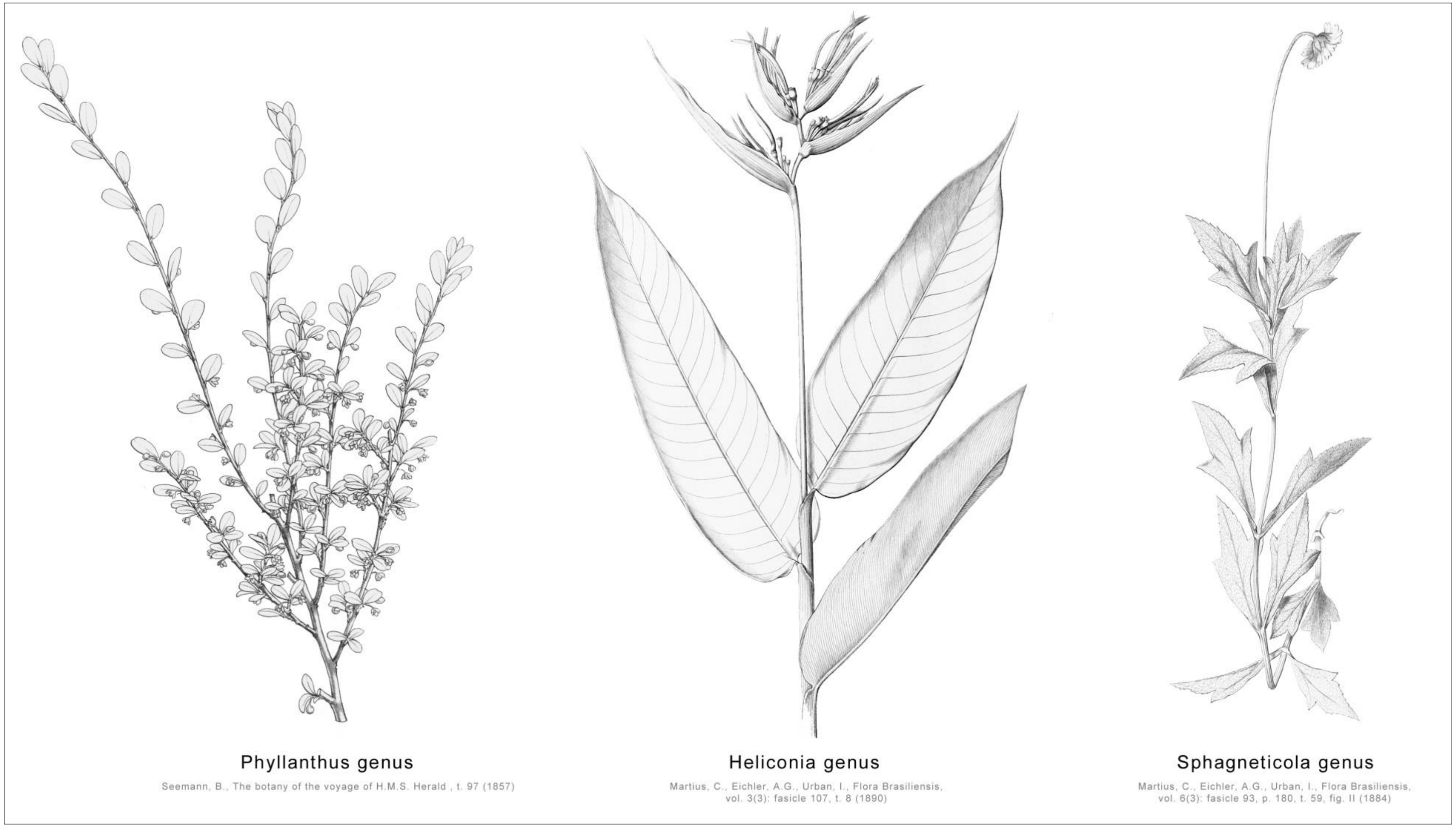

Phyllanthus genus

Seemann, B., The botany of the voyage of H.M.S. Herald , t. 97 (1857)

Heliconia genus

Martius, C., Eichler, A.G., Urban, I., Flora Brasiliensis,
vol. 3(3): fasicle 107, t. 8 (1890)

Sphagneticola genus

Martius, C., Eichler, A.G., Urban, I., Flora Brasiliensis,
vol. 6(3): fasicle 93, p. 180, t. 59, fig. II (1884)

Figure 83. Botanical illustration of plants used for measurement

6.1.4 Leaf Area Index

Numerous studies have shown plant Leaf Area Index to be strongly correlated with temperature reduction. In such cases, temperature reduction is mostly due to shade provided by tree canopy, resulting in reduced heat absorbed by building surfaces, pavements and pedestrians (Fahmy et al., 2010; Gómez-Muñoz et al., 2010; Hardin and Jensen, 2007). Shahidan et al. (2010) found significant correlation between LAI and radiation filtration for M. Ferrea L and H. crepittan (R^2 = 0.96 and 0.95). A higher LAI value will mean more leaves, providing increased reduction of thermal radiation under a tree (Brown and Gillespie, 1995; Kotzen, 2003).

As for the impact of LAI on t_{mrt}, this study has shown that LAI is not strongly correlated with t_{mrt} reduction. Table 9 shows that although the LAI of Plot 2 – Heliconia 'American Dwarf' is 7.21, it is least effective at reducing t_{mrt}. This would suggest that overall radiative qualities of the plant canopy (albedo, absorptance, reflectance, canopy structure) are more substantial at determining its impact on t_{mrt}. It was observed from this study that leaves for Plot 1 and Plot 2 are able to form a compact canopy while leaves for Plot 2 form a porous canopy due to its large vertically-hung leaves.

6.2 Landscape planning guidelines

The underlying objective of this thesis is to discern the impact of plants in the outdoor environment and to explore novel methods of practicing landscape planning to improve outdoor thermal comfort. For the purpose of optimizing the landscape planning process, numerous field measurements were conducted. Data was analyzed with the intention of obtaining insight on how best to improve outdoor thermal conditions based on plants selection and placement. This study defines the optimization of selection and placement processes in the following manner:

- Plant selection

Plants should be selected based on their potential to cool the surrounding environment.

- Plant placement

Plants should be placed in areas where their potential to cool the surrounding environment can be maximized.

The remainder of this chapter summarizes all findings from this study and their implication on plant selection and placement criteria. A framework for landscape planning is proposed, based on these findings. A discussion on relevant tools and technical processes ensues, forming the basis of recommendations on how it can be translated into industry practice.

6.2.1 Recommendations based on quantitative results of study

Chapters 3.2.1 to 10.3 describe the process of recalibrating globe thermometers for use in the tropical outdoor environment, measurement of t_{mrt} in parks and urban areas as well as measurement of t_{mrt} above rooftop greenery. Findings and recommendations are summarized in Table 25.

Table 25. Recommendations for landscape planning

Chapter number	**Title**	**Findings from measurement**	**Recommendation for landscape planning**	**Page**
3.2.1	Calibration of globe thermometers for use in the tropical urban environment	Recalibration of t_{mrt} formula for use in the tropical urban environment	Formula to be used for measurement of t_{mrt} using 40 mm globes	81
4	Measurement of mean radiant temperature on roof garden setting	Rooftop greenery can significantly reduce air and mean radiant temperature. Rooftop greenery can reduce air temperature at night, reducing the impact of the Urban Heat Island effect	Rooftop greenery can be used to improve outdoor thermal comfort and reduce UHI effect	100
		Plant ET and SA characteristics vary significantly from species to species	Selection of plants should take into consideration plant characteristics such as ET and SA. Special attention should be given to plant behavior from 13:00 hrs to 17:00 hrs	113 115
		Leaf Area Index is not strongly correlated with t_{mrt} reduction	In terms of t_{mrt}, LAI should not be used to assess the thermal performance of rooftop greenery	118
		Plant traits such as leaf size and shrub height can affect overall thermal performance	Plants with small leaves and short shrub height should be preferred	122

Chapter number	Title	Findings from measurement	Recommendation for landscape planning	Page
		Surface temperature of concrete is reduced tremendously with rooftop greenery	Rooftop greenery can be used to improve indoor thermal comfort	125
4.1.2	Potential of rooftop greenery for reducing air and mean radiant temperature	Potential of plants to reduce air temperature may be affected by plant functional traits such as shrub structure	Selection of plants should include consideration of shrub structure to optimize cooling potential	131
		Air temperature reduction is poorly related to ET and SA	Selection of plants for temperature reduction should be for t_{mrt} and not for air temperature	133
5	Rooftop greenery mean radiant temperature prediction model	Plant ET and SA are statistically significant functions of t_{mrt} reduction due to rooftop greenery	Selection of plants should include consideration of ET and SA	141
		Development of regression model of t_{mrt} reduction due to rooftop greenery	Impact of rooftop greenery can be assessed using regression model	144
		Development of ET and SA table for plant selection	Plants selected can assessed using selection table	157
6.1	Impact of plant selection on ambient and mean radiant temperature	Rooftop greenery plants have a wide range of ET rates. Some plants with very low ET rates are highlighted	Plants with high ET rates are preferred. Plants such as CAM plants should be avoided	161
		Rooftop greenery plants have a wide range of albedo values	Plants with high SA are preferred	163
		Evidence of plant cooling potential due to plant functional traits	Plants with small leaves and short shrub height should be preferred	164
		Leaf Area Index is poorly correlated with t_{mrt} reduction	In terms of t_{mrt}, LAI should not be used to assess the thermal performance of rooftop greenery	166

Chapter number	Title	Findings from measurement	Recommendation for landscape planning	Page
10.1	Large scale urban mapping of mean radiant temperature	There is little difference between t_{mrt} of urban areas and park areas in the absence of sunlight	Selection and placement of plants need not consider impact at night	218
		Trees can reduce t_{mrt} significantly by means of shade provision.	More trees should be planted on ground level. Trees with large canopies are preferred, as they provide more shade	216
		Sky View Factor (SVF) can be correlated with t_{mrt} reduction	Assessment of shade quality can be done with SVF	222
10.2	Impact of plant height stratification on mean radiant temperature	Temperature stratification above plants vary from species to species	Selection of plants should include consideration of t_{mrt} reduction due to height stratification	227
10.3.1	Impact on vertical greenery on mean radiant temperature	Vertical greenery can reduce air temperature and t_{mrt}	Vertical greenery can be used to improve outdoor thermal comfort	239 241
		Cooling effect of vertical greenery is insignificant when shaded	Vertical greenery should be placed at areas with high exposure to solar irradiance	243
		GIS can be used to generate t_{mrt} map	GIS can be used as a planning/simulation platform for landscape planning	247
10.3.2	Analysis of similar plant types in horizontal and vertical setup	Rooftop greenery is more effective at reducing t_{mrt} than vertical greenery	Rooftop greenery should be preferred to vertical greenery if budget is limited	255
		Westward facing green walls exhibit higher cooling potential compared to eastward facing green walls	Priority should be given to westward-facing facades	256
		Vertical greenery tends to reduce surface albedo	Plants with high SA are preferred	257
		Vertical greenery tends to increase ET rate	Plants with high ET are preferred	260

6.2.2 Plant selection chart

A t_{mrt} reduction chart is derived using the regression model derived in Chapter 5.1.1.3. In addition to recommendations shown in Chapter 6.2.1, plant selection can be conducted by using SA and ET rates of the plant in question to identify the corresponding reduction in t_{mrt}. In this manner, plant performance can be objectively assessed in terms of their t_{mrt} reduction potential.

Although it has been shown that both ET and SA have a direct negative correlation with t_{mrt}, it is important to note that ET and SA are inversely correlated with each other (Seginer, 1969). Selection of plants with high SA may result in a corresponding ET rate that is low. Therefore, ET and SA profiles of commonly used rooftop greenery plants have to be identified and catalogued to find the most suitable plants for use in any given location.

An example of plant selection procedure is shown in Figure 84, where the three types of plants being tested in Chapter 4 are catalogued according to the plant selection chart. The corresponding SA and ET values are derived by averaging all measured values from 13:00 hrs to 17:00 hrs. It can be observed that Heliconia ‘American Dwarf’ (green box) does not provide any reduction in t_{mrt} when the reference temperature is 50 °C. Although it does provide a reduction of 4.8 % when the reference temperature is 70 °C, it is much lower than the reduction potential of Phyllanthus cochinchinensis (red box) and Sphagneticola trilobata (green box), with t_{mrt} reduction potentials of 10.9 % and 10.6 % respectively. Therefore, it can be reasoned that selection of Phyllanthus cochinchinensis or Sphagneticola trilobata is a better choice than Heliconia ‘American Dwarf’.

Since there is lesser chance of reducing t_{mrt} through shade provision by large canopy trees on roof gardens and sky terraces, it is important that the shrubs used can help reduce t_{mrt} as much as possible. The plant selection chart can provide easy reference for landscape architects and help them visualise the impact of their choices.

Reference Tmrt	50°C	Shrub Albedo									
		0.21	0.22	0.23	0.24	0.25	0.26	0.27	0.28	0.29	0.30
Plant Evapotranspiration Rate	0.001	-	-	-	-	-	-	1.3	2.5	3.7	4.9
	0.002	-	-	-	-	-	0.5	1.7	2.9	4.1	5.3
	0.003	-	-	-	-	-	0.9	2.1	3.3	4.5	5.7
	0.004	-	-	-	-	-	1.3	2.5	3.7	4.9	6.1
	0.005	-	-	-	-	0.4	1.7	2.9	4.1	5.3	6.5
	0.006	-	-	-	-	0.8	2.1	3.3	4.5	5.7	6.9
	0.007	-	-	-	-	1.2	2.5	3.7	4.9	6.1	7.3
	0.008	-	-	-	0.4	1.6	2.9	4.1	5.3	6.5	7.7
	0.009	-	-	-	0.8	2.0	3.3	4.5	5.7	6.9	8.1
	0.010	-	-	-	1.2	2.4	3.7	4.9	6.1	7.3	8.5
	0.011	-	-	-	1.6	2.8	4.1	5.3	6.5	7.7	8.9
	0.012	-	-	0.4	2.0	3.2	4.5	5.7	6.9	8.1	9.3
	0.013	-	-	0.8	2.4	3.6	4.9	6.1	7.3	8.5	9.7
	0.014	-	0.4	1.2	2.8	4.0	5.3	6.5	7.7	8.9	10.1
	0.015	-	0.8	1.6	3.2	4.4	5.7	6.9	8.1	9.3	10.5
	0.016	-	1.2	2.0	3.6	4.8	6.1	7.3	8.5	9.7	10.9
	0.017	0.4	1.6	2.4	4.0	5.2	6.5	7.7	8.9	10.1	11.3

Reference Tmrt	70°C	Shrub Albedo									
		0.21	0.22	0.23	0.24	0.25	0.26	0.27	0.28	0.29	0.30
Plant Evapotranspiration Rate	0.001	1.9	2.8	3.4	4.5	5.4	6.3	7.1	8.0	8.9	9.8
	0.002	2.2	3.1	3.7	4.8	5.7	6.6	7.4	8.3	9.2	10.0
	0.003	2.5	3.4	3.9	5.1	6.0	6.8	7.7	8.6	9.5	10.3
	0.004	2.8	3.6	4.2	5.4	6.3	7.1	8.0	8.9	9.7	10.6
	0.005	3.1	3.9	4.5	5.7	6.5	7.4	8.3	9.2	10.0	10.9
	0.006	3.3	4.2	4.8	6.0	6.8	7.7	8.6	9.4	10.3	11.2
	0.007	3.6	4.5	5.1	6.2	7.1	8.0	8.9	9.7	10.6	11.5
	0.008	3.9	4.8	5.4	6.5	7.4	8.3	9.1	10.0	10.9	11.8
	0.009	4.2	5.1	5.7	6.8	7.7	8.6	9.4	10.3	11.2	12.0
	0.010	4.5	5.4	5.9	7.1	8.0	8.8	9.7	10.6	11.5	12.3
	0.011	4.8	5.6	6.2	7.4	8.3	9.1	10.0	10.9	11.7	12.6
	0.012	5.1	5.9	6.5	7.7	8.5	9.4	10.3	11.2	12.0	12.9
	0.013	5.3	6.2	6.8	8.0	8.8	9.7	10.6	11.4	12.3	13.2
	0.014	5.6	6.5	7.1	8.2	9.1	10.0	10.9	11.7	12.6	13.5
	0.015	5.9	6.8	7.4	8.5	9.4	10.3	11.1	12.0	12.9	13.8
	0.016	6.2	7.1	7.7	8.8	9.7	10.6	11.4	12.3	13.2	14.0
	0.017	6.5	7.4	7.9	9.1	10.0	10.8	11.7	12.6	13.5	14.3

🟥 Plot 1 - Phyllanthus cochinchinensis

🟩 Plot 2 - Heliconia 'American Dwarf'

🟦 Plot 3 - Sphagneticola trilobata

Figure 84. Plant selection via chart (Percentage decrease in t_{mrt})

6.2.3 Landscape planning framework

Generally, landscape planning frameworks are concerned with issues such as plant health, maintainability and aesthetic requirements. The purpose of having such frameworks is to ensure comprehensive appraisal and inventory of urban greenery (CTLA, 1992). The criteria for urban greenery assessment may be classified as shown in Table 26.

Table 26. Factors to consider in rating plant species and cultivars (CTLA, 1992)

Factor	
Climate adaptability	Cold hardiness Frost tolerance Drought tolerance Storms: resistance to ice, snow, wind
Growth characteristics	Tolerance to difficult sites Vigour Structural strength Life expectancy
Soil adaptability	Structure and texture Drainage Moisture excess or deficiency Acidity and alkalinity Nutritional deficiencies or excesses
Resistance or tolerance	Diseases Insects Air pollution
Maintenance requirements	Training and pruning Cleanliness: flowers, fruit, leaves, twigs, duration of leaf fall Roof problems Pests Structural problems (cabling and bracing)
Allergenic properties	Pollen Dermal toxins
Aesthetic values	Branches and tree form - growth habit, bark colour and texture Foliage -density, colour texture and duration Flowers – Prominence , fragrance/odor, duration, colour and size Fruit – Prominence, duration, use, colour, size,

fragrance /odour

For the proposed landscape planning workflow, benefits of greenery in terms of how it can improve climatological conditions are factored into the framework. Miller (2007) outlines the positive impacts of urban greenery in terms of their climatological and engineering uses (Table 27).

Table 27. Additional factors in rating plant species (Miller, 2007)

Factor		
Climatological uses	Human comfort	Radiant temperature Air temperature Air movement Humidity and precipitation
	Building energy budgets	Heating Cooling Solar energy and trees
Engineering uses	Sound pollution reduction Air quality control Urban hydrology Erosion control Wastewater treatment Glare and reflection reduction	

This study proposes a landscape planning framework that aims to improve radiant and air temperature conditions of the outdoor landscape (Figure 85). In this case, impact of urban greenery on outdoor climate is considered to be a factor in rating its overall value (specifically, air and mean radiant temperature). The proposed workflow is based on findings shown in Chapters 6.2.1 and 6.2.2.

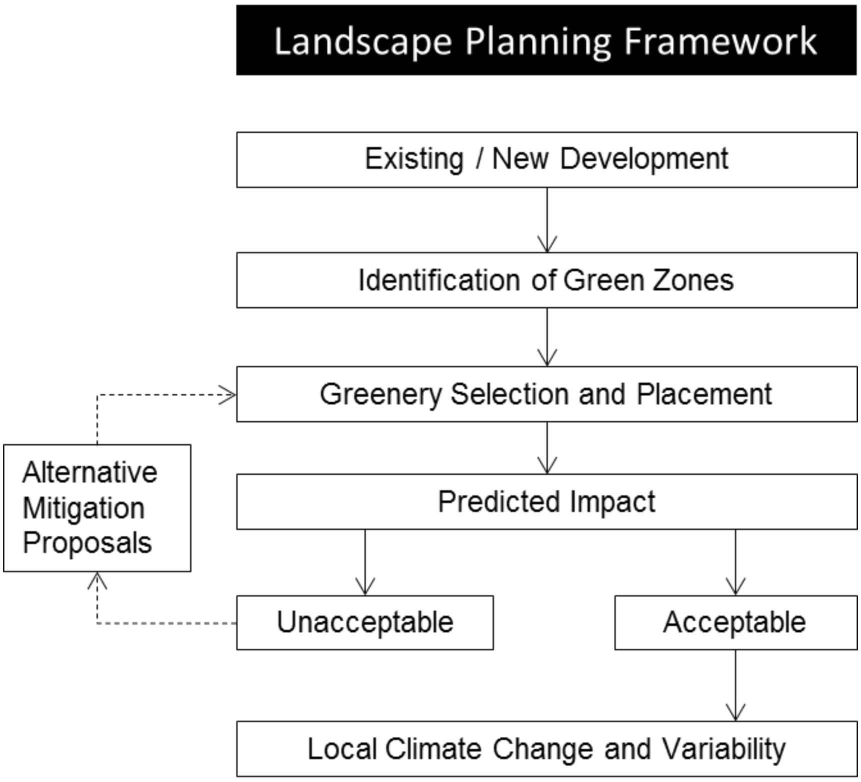

Figure 85. Proposed landscape planning framework

6.2.4 Hypothetical case study illustrating usage of prediction model

A workflow sequence is elaborated, based on the proposed framework (Figure 86). This section outlines the procedure of landscape planning optimization and demonstrates its technical viability with a hypothetical case study.

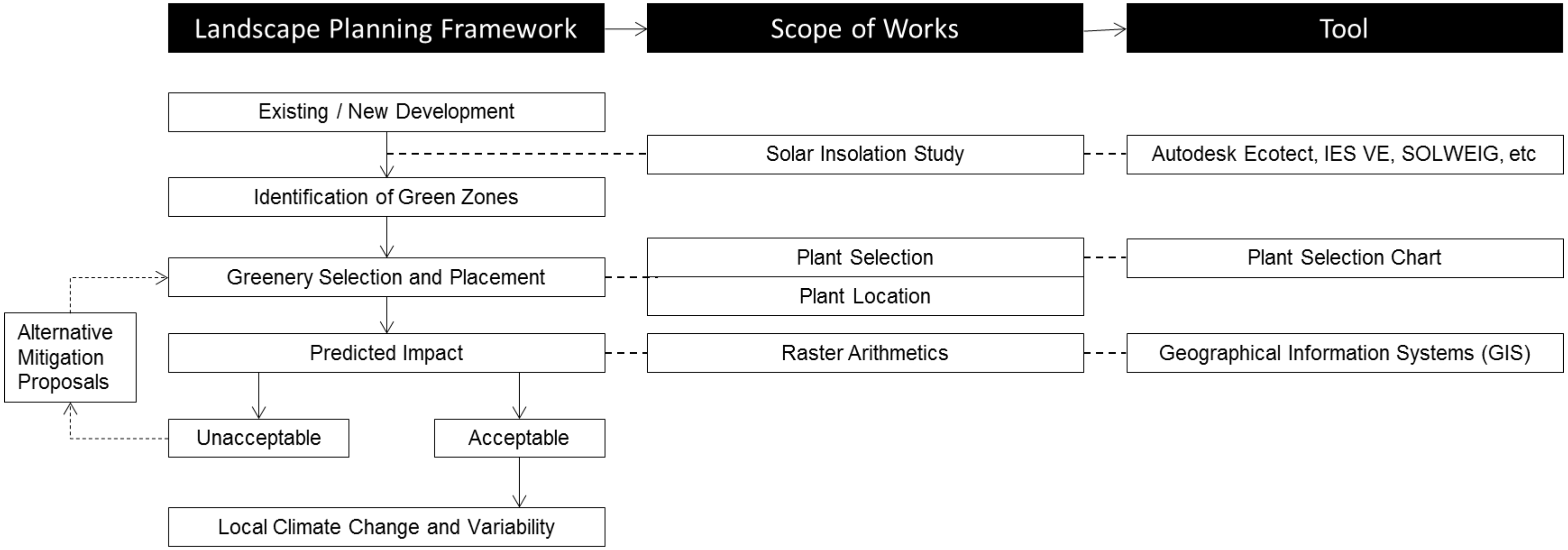

Figure 86. Elaboration of proposed landscape planning framework

6.2.4.1 Hypothetical urban model

A hypothetical scenario is developed to illustrate efficacy of the proposed landscape planning framework (Figure 87). The site measures 400 m by 400 m and is modelled with urban constituents that are representative of a commercial district in a dense urban setting. Common urban morphological parameters such as high-rise commercial buildings, podium blocks, roof gardens and sky terraces are included. A portion of the model is allocated as park space with several low-lying amenity blocks. Areas subjected to the proposed landscape planning methodology are as follows:

1. Pedestrian level; and
2. Building surfaces.

Pedestrian level is defined as 2 m above ground level. Building surfaces include all wall and roof surfaces, as well as building insets. Several iterations of the model are developed to illustrate the capabilities of the landscape planning framework (Table 28).

Table 28. Model properties

Model	**Characteristics**
Iteration 1	Trees with 5 m diameter canopy Generically allocated
Iteration 2	Trees with 15 m diameter canopy Generically allocated
Iteration 3	Trees with 20 m diameter canopy Generically allocated With additional trees in areas exposed to high solar irradiance
Iteration 4	Trees with 20 m diameter canopy Generically allocated With additional trees in areas exposed to high solar irradiance With addition of shurbs and predicted cooling effect

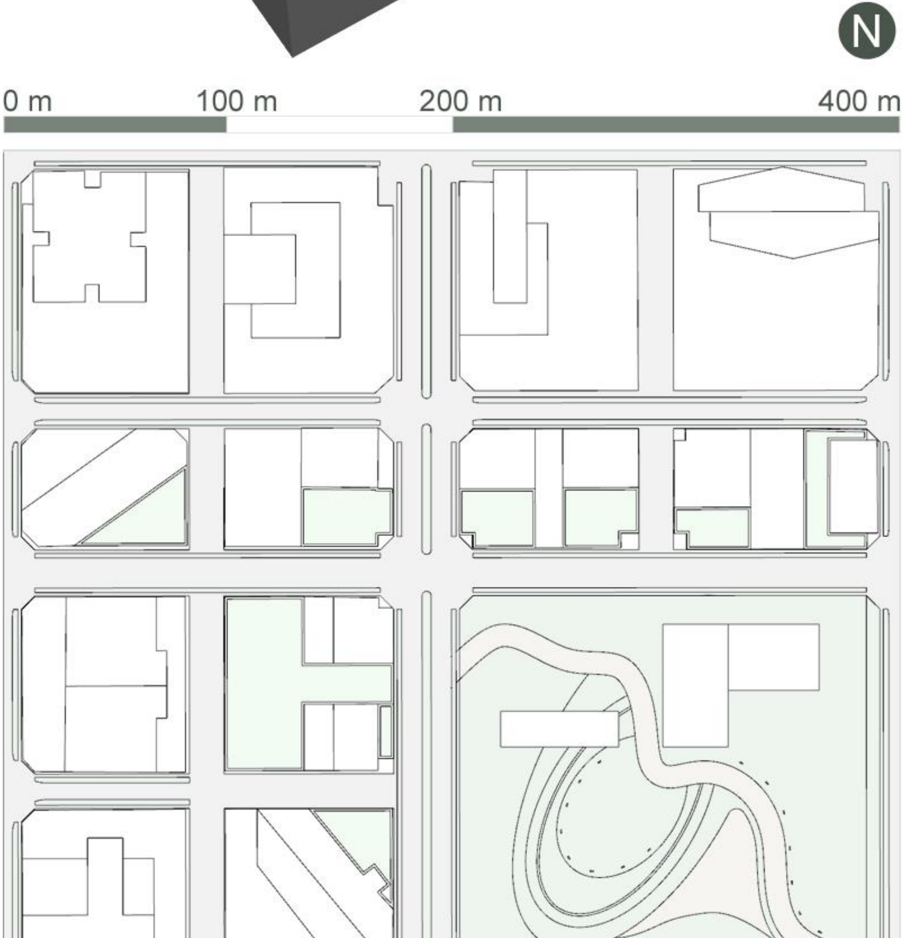
N
0 m
100 m
200 m
400 m

Figure 87. Hypothetical urban model (Baseline)

6.2.4.2 Pedestrian level

In this exercise, the area of interest is a park slated for development with food and beverage outlets. Since a sizable crowd is expected to occupy the open space during events and there is a large pathway that transverses the park diagonally, the proposed landscape planning framework will be utilized to facilitate the landscape design process. The proposed technical workflow is illustrated in Figure 88. Simulation of t_{mrt} is first conducted with tree information (partial plant input) and subsequently completed with shrub information (complete plant input). Cooling effect due to shrubbery is based on the prediction model derived in Chapter 5.

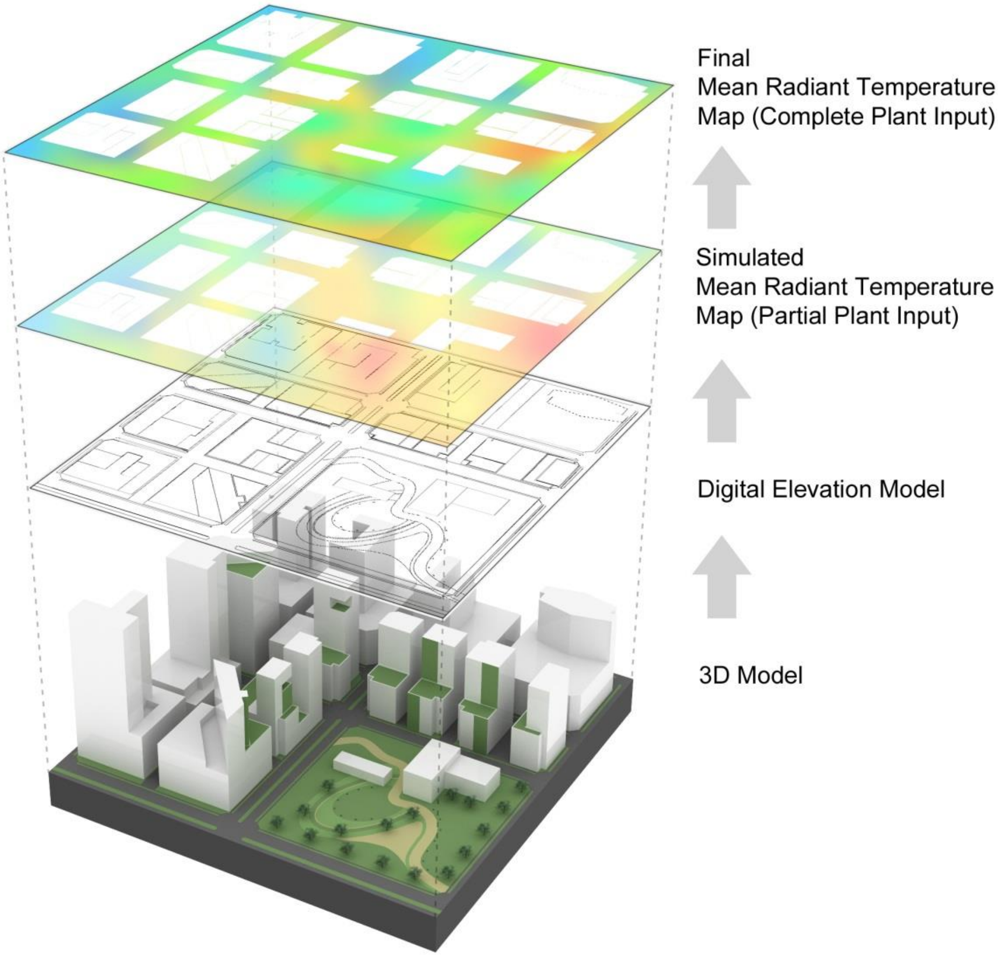

Figure 88. Pedestrain level t_{mrt} modelling hierarchy

6.2.4.2.1 Geographical Information Systems (GIS) as climatic mapping tool

Relevant data is represented through climatic mapping via a GIS platform. Climatic mapping is selected as the mode of presentation as it is already a widely-used tool for urban planning. Climatic maps are able to serve as visualisation aid from micro to macro level. Through the GIS platform, multiple layers of spatial information can be analysed simultaneously. The use of climatic mapping has become a prominent feature in studies of the outdoor climate (Katzschner et al., 2004; Katzschner and Mülder, 2008; Koster, 1998; Stocks and Wise, 2000).

In particular, there has been extensive usage of GIS for the mapping of green spaces. Kamishima et al. (2002) used ADS40 (Airborne Digital Sensor) images to analyse the urban landscape of Tokyo. GIS was used to proximate greenery distribution using the ADS40 images. Subsequently, this information was layered with building data through the GIS platform.

Laing et.al. (2006) measured environmental values of green spaces via GIS spatial analysis for aiding decision in relation to urban green planning. The use of computer visualization provided advances in the presentation and delivery of spatial information.

Table 29 shows software that can be used to facilitate the landscape planning process. Impact of t_{mrt} due to shrub can be attained by using the regression model derived in Chapter 5, with the assumption that temperature reduction of extensive green roof systems are similar to ground level planting conditions. In this exercise, Rhinoceros 3D is used to generate the 3D model, SOLWEIG (Lindberg et al., 2008b) is used to simulate outdoor t_{mrt} conditions and ArcGIS is the GIS platform of choice.

Table 29. Software recommended for simulation

Item	Software
3D Model	Autodesk AUTOCAD, Rhinoceros 3D,or equivalent CAD software
Digital Elevation Model	ArcGIS, or equivalent GIS software
Simulated Mean Radiant Temperature Map	SOLWEIG, Townscope, Thermo Render, or equivalent t_{mrt} simulation software
Final Mean Radiant Temperature Map	ArcGIS, or equivalent GIS software

Figure 89 demonstrates how landscape planning can be conducted systematically via t_{mrt} mapping.

In Iteration 1, trees with small canopies (5 m diameter) are placed at locations designated by the landscape planner.

In Iteration 2, trees with larger canopies are assumed (15 m diameter) at the same spots. The t_{mrt} reduces drastically near the trees.

In Iteration 3, more trees (20 m diameter) are added at areas that are anticipating larger pedestrian flow. As a result, thermal conditions of these areas can be improved.

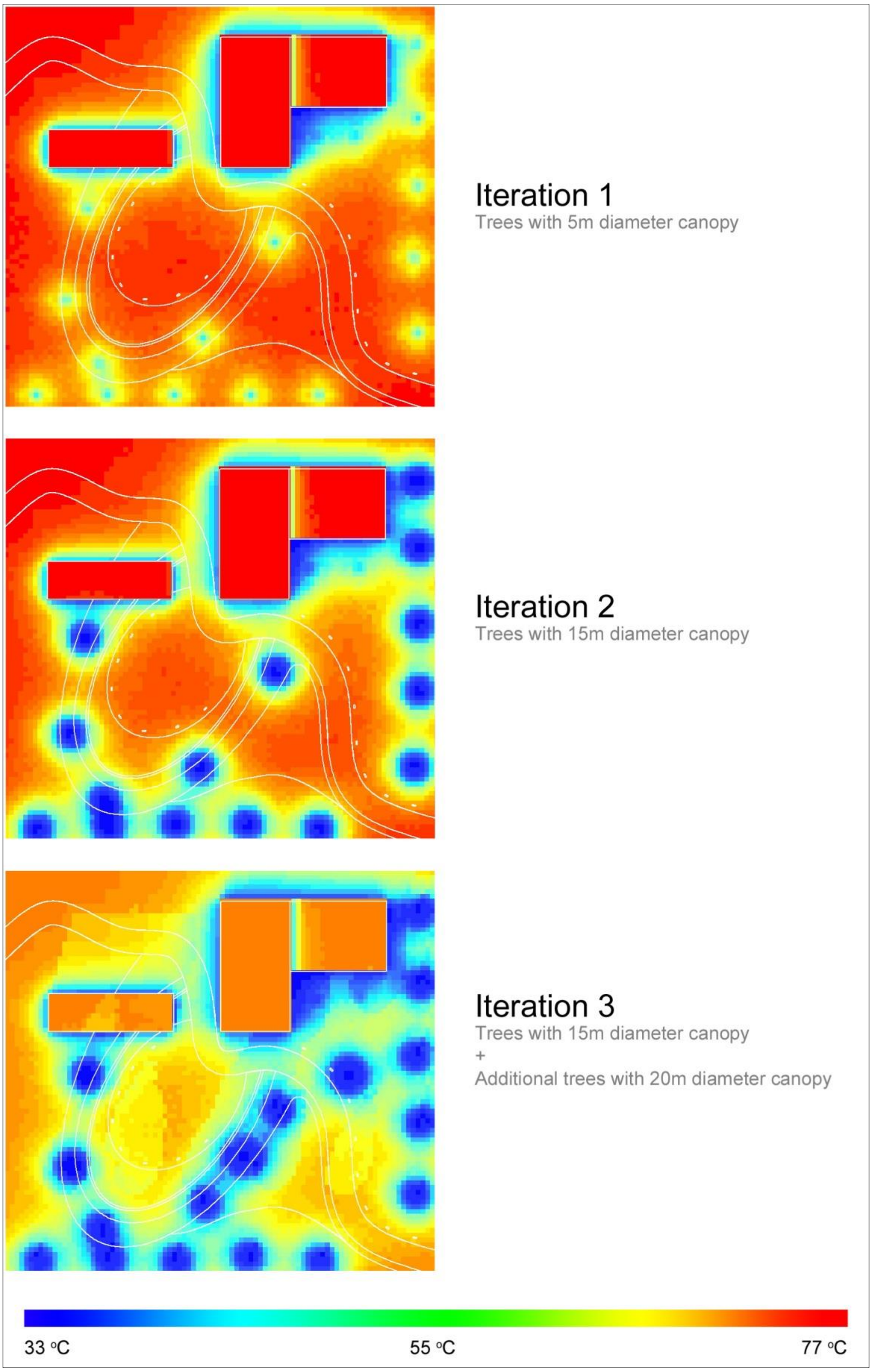

Figure 89. Simulation of t_{mrt} via SOLWEIG and ArcGIS

6.2.4.2.2 Use of prediction model for landscape planning

This section describes how the prediction model derived in Chapter 5 can be used for landscape planning.

Figure 89 has shown how the tree selection and placement process can be optimized through t_{mrt} simulation. In Iteration 3, trees with large canopies are proposed and additional trees are allocated to areas that are exposed to high levels of solar radiation. Although outdoor thermal condition has improved significantly when compared to Iteration 1, the map is incomplete as cooling effect of shrubbery has yet to be considered.

Suppose the landscape planner has reviewed simulation results from Iteration 3 and wishes to improve thermal conditions of Areas A and B, as well as the main pedestrian walkway by planting shrubs (Figure 90). To simulate the cooling effect of shrubs, a fourth iteration is conducted, using the regression model derived in Chapter 5.

Figure 90. Areas where shrubs can be added to reduce t_{mrt}

In the 4th Iteration, cooling effect of shrubbery is considered based on the prediction model derived from Chapter 5:

$$Tmrt_{\ Plant} = 0.782Tmrt_{ref} - 200.111ET - 61.011SA + 26.937 \qquad [25]$$

Where,

$Tmrt_{Plant}$ = Mean radiant temperature above rooftop greenery (°C)

$Tmrt_{Ref}$ = Mean radiant temperature above concrete (°C)

ET = Plant evapotranspiration rate (mm·min^{-1})

SA = Shrub Albedo

The shrub to be used is assumed to have traits similar to Phyllanthus cochinchinensis and allocated as shown in Figure 91:

- Evapotranspiration Rate (ET) of 0.011 mmmin^{-1}; and
- Shrub Albedo (SA) of 0.28.

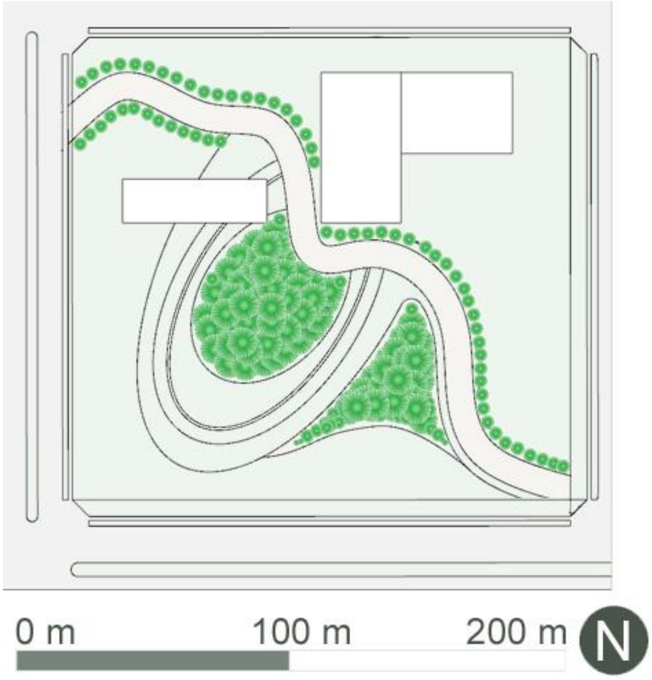

Figure 91. Areas allocated for shrubbery (Highlighted in green)

This information (ET and SA) serves as input variables to Equation (25). Together with values of $t_{mrt(ref)}$ obtained from Iteration 3, resultant t_{mrt} is calculated for every pixel of the simulation map using ArcGIS. Simulation result of Iteration 4 is shown in Figure 92.

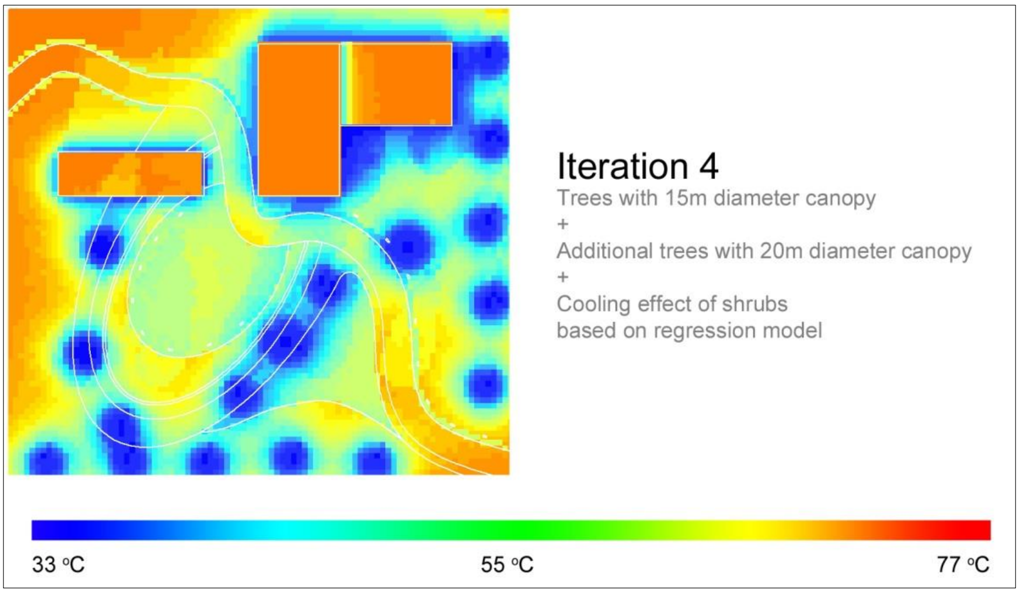

Figure 92. Simulation result with input from regression model

In Iteration 4, thermal effects of shrubbery are factored into the t_{mrt} map via the regression model and plant selection chart derived from this study. Comparison of all four iterations reveals the immense positive impact of tree and shrub allocation using the proposed landscape planning framework (Figure 93). The proposed methodology is an iterative process and can be performed ad infinitum until the desired result is attained.

It is important to note that simulation is currently performed with the assumption that the temperature reduction potential of extensive roof systems is the same as intensive roof systems or shrubbery at ground level. Further study is required to ascertain the actual reduction potential of intensive roof systems and shrubbery at ground level.

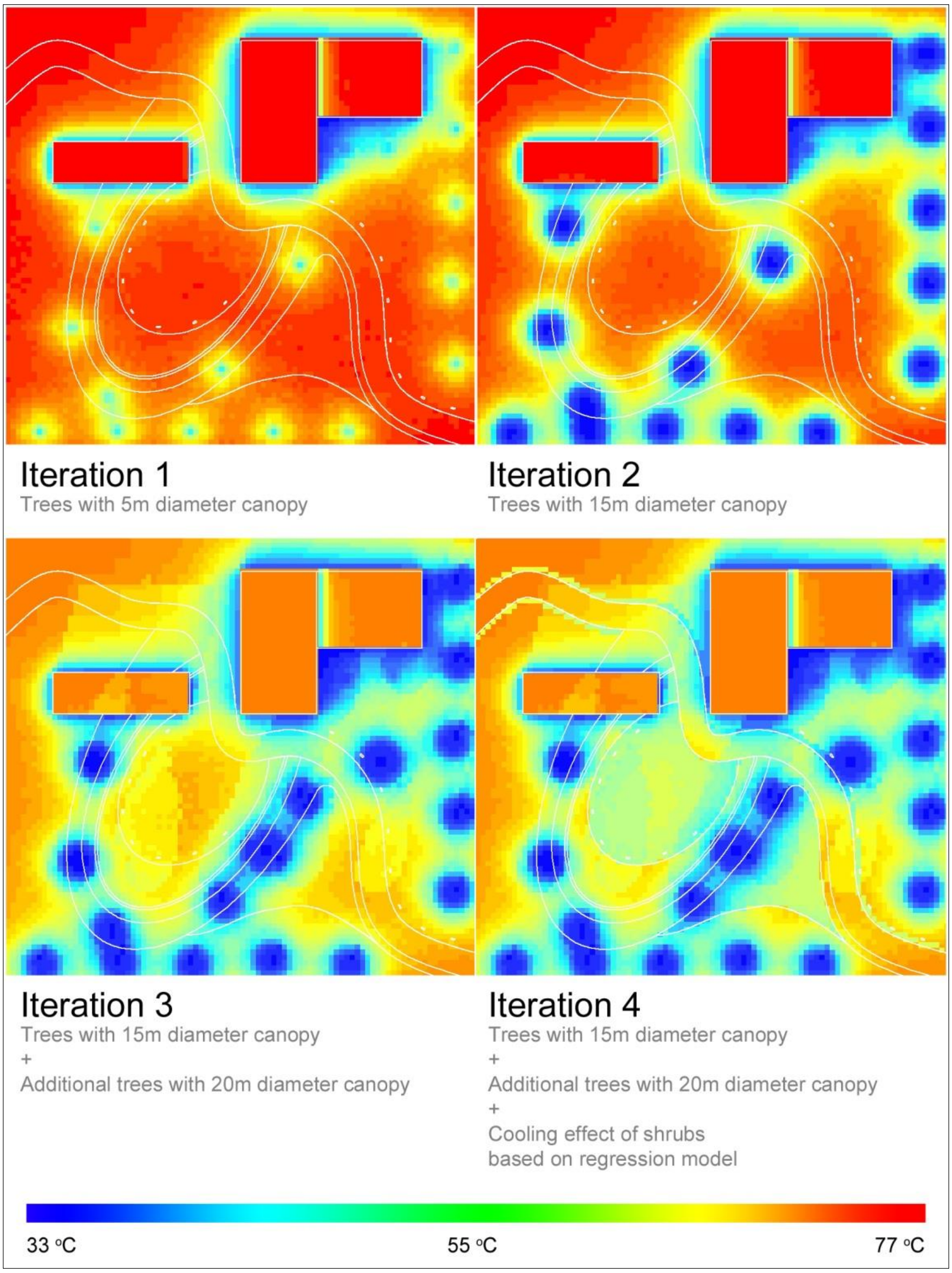

Figure 93. Comparison of T_{mrt} simulation results

6.2.4.3 Building surfaces

In this exercise, the areas of interest are building surfaces. Numerous studies on vertical and rooftop greenery have focused on the issue of heat transmission through building façade and cooling energy (Chen et al., 2013; Cheng et al., 2010; Perini et al., 2011; Wong et al., 2010a). For this study, the emphasis is on identifying suitable areas for plants to be allocated and for them to fully realize their cooling potential on the outdoor environment. Therefore, solar insolation conditions are critically assessed before plants are selected (Figure 94). The list of software recommended for this exercise is shown in Table 30. In this case, Rhinoceros 3D is used for 3D modelling and DIVA (Jakubiec and Reinhart, 2011) is used for solar insolation simulation.

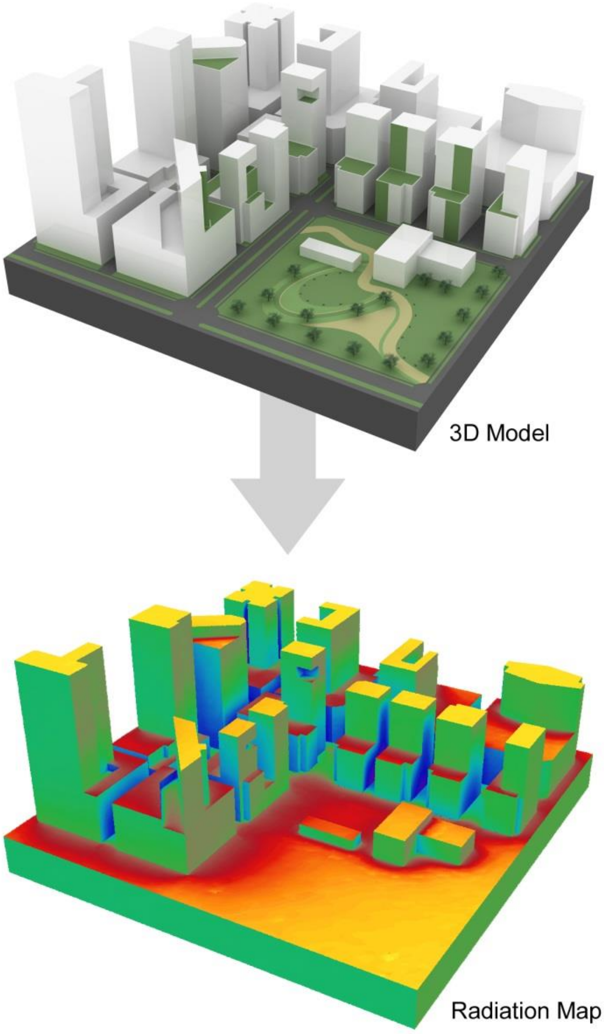

Figure 94. Solar insolation modelling

Table 30. Software recommended for simulation

Item	**Software**
3D Model	Autodesk AUTOCAD, Rhinoceros 3D,or equivalent CAD software
Façade solar insolation map	Autodesk Ecotect, Vasari, IES VE, DIVA, or equivalent software

It can be seen from Figure 95 that solar exposure can vary tremendously for building facades of similar facing and that it is influenced greatly by self-shading and overshadowing of structures in close proximity. For this hypothetical planning exercise, a few building surfaces are selected for assessment (dotted region).

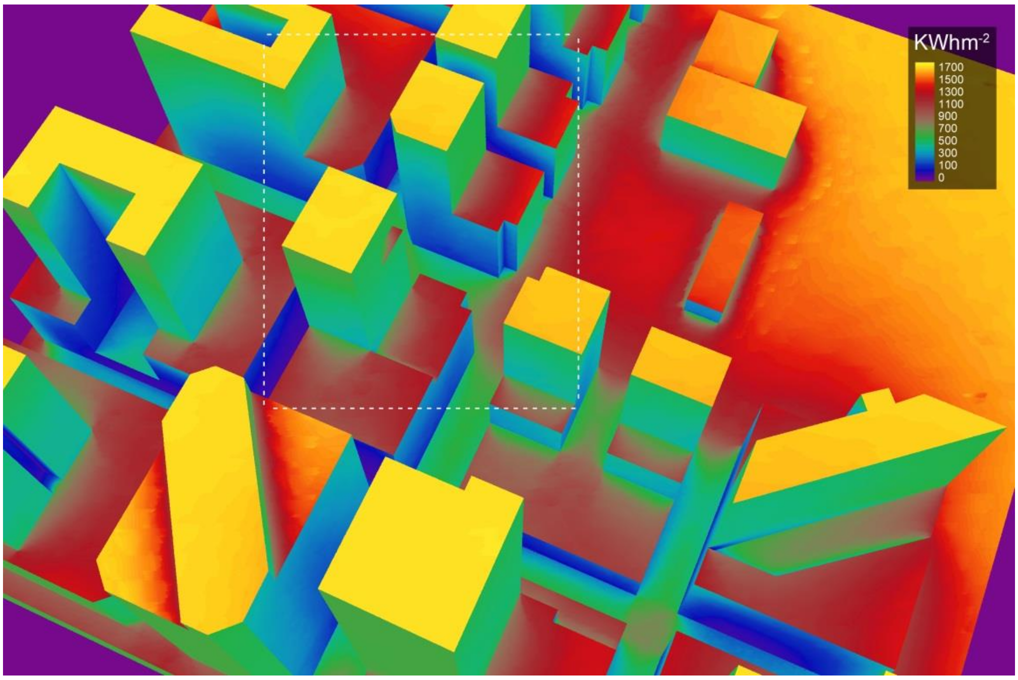

Figure 95. Close-up of solar insolation map

6.2.4.3.1 Use of prediction model for landscape planning

This section describes how the prediction model derived in Chapter 5 can be used for landscape planning. In this instance, landscape planning can be conducted using the plant selection chart derived from the regression model. The proposed methodology for landscape planning of building surfaces is as follows (Figure 96):

1. Simulation of solar insolation of building surfaces.
2. Segregation of building surfaces according to degree of solar exposure.

3. Reference to plant selection chart for allocation of plants to rooftop or vertical greenery.

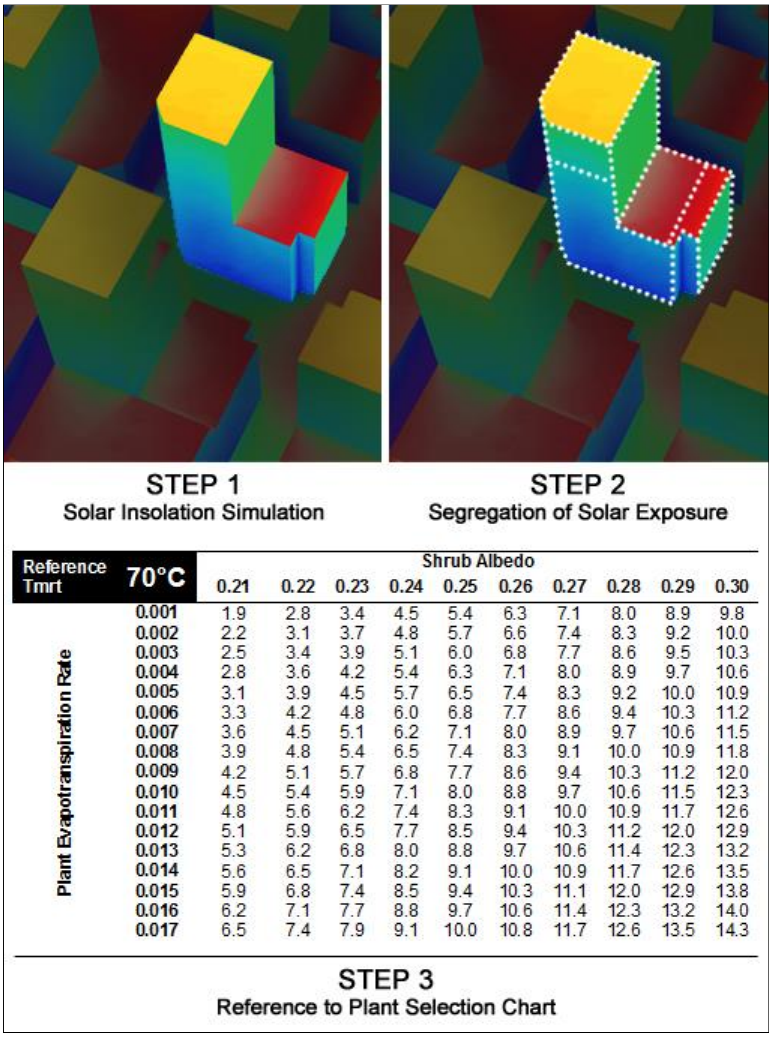

Reference Tmrt	70°C	Shrub Albedo									
		0.21	0.22	0.23	0.24	0.25	0.26	0.27	0.28	0.29	0.30
Plant Evapotranspiration Rate	0.001	1.9	2.8	3.4	4.5	5.4	6.3	7.1	8.0	8.9	9.8
	0.002	2.2	3.1	3.7	4.8	5.7	6.6	7.4	8.3	9.2	10.0
	0.003	2.5	3.4	3.9	5.1	6.0	6.8	7.7	8.6	9.5	10.3
	0.004	2.8	3.6	4.2	5.4	6.3	7.1	8.0	8.9	9.7	10.6
	0.005	3.1	3.9	4.5	5.7	6.5	7.4	8.3	9.2	10.0	10.9
	0.006	3.3	4.2	4.8	6.0	6.8	7.7	8.6	9.4	10.3	11.2
	0.007	3.6	4.5	5.1	6.2	7.1	8.0	8.9	9.7	10.6	11.5
	0.008	3.9	4.8	5.4	6.5	7.4	8.3	9.1	10.0	10.9	11.8
	0.009	4.2	5.1	5.7	6.8	7.7	8.6	9.4	10.3	11.2	12.0
	0.010	4.5	5.4	5.9	7.1	8.0	8.8	9.7	10.6	11.5	12.3
	0.011	4.8	5.6	6.2	7.4	8.3	9.1	10.0	10.9	11.7	12.6
	0.012	5.1	5.9	6.5	7.7	8.5	9.4	10.3	11.2	12.0	12.9
	0.013	5.3	6.2	6.8	8.0	8.8	9.7	10.6	11.4	12.3	13.2
	0.014	5.6	6.5	7.1	8.2	9.1	10.0	10.9	11.7	12.6	13.5
	0.015	5.9	6.8	7.4	8.5	9.4	10.3	11.1	12.0	12.9	13.8
	0.016	6.2	7.1	7.7	8.8	9.7	10.6	11.4	12.3	13.2	14.0
	0.017	6.5	7.4	7.9	9.1	10.0	10.8	11.7	12.6	13.5	14.3

Figure 96. Landscape planning for building surfaces

In this hypothetical scenario, conclusions are drawn based on perspectives of:

- The urban planner

Urban planning is a process that looks into issues such as land use and overall impact to the outdoor environment. Urban planners shape the city though planning guidelines, which are interpreted by the architect and translated into form. From Figure 97, it can be observed that solar insolation levels of higher roofs (R1) are about 20 % more than lower roofs (R2). A green roof on R1 will reduce more heat transmission into the building than the same green roof on R2. Therefore, priority should be given to R1 in terms of green roof allocation. For R2, it can be observed that areas that are further away from S3 receive higher solar exposure. It can therefore be inferred that plants with higher ET and SA can be used to improve radiant conditions at these areas.

Also, building facades along S2 have a higher solar exposure than facades along S1, although they are of the same orientation. The solar insolation diagram can be used as a planning tool to justify the allocation of vertical greenery along S2 rather than S1. Semi-shade or shade tolerant plants can be used for vertical greenery located along S1, and full sun plants can be used for vertical greenery allocated along S2. Plant selection can be done via the selection chart derived from Chapter 5.

While it has been established that westward-facing facades should be retrofitted with vertical greenery to reduce heat gain, Figure 97 shows that it is more effective to allocate vertical greenery on W1 than on W2. This is because W1 has a higher solar exposure level. In this way, policies do not have to be overly generalised (All westward-facing facades must be retrofitted with vertical greenery), but can be optimised by first examining local solar insolation conditions and making an informed judgement based on these examinations.

- The architect or landscape designer

Contrary to urban designers, architects operate at a much finer scale and require an accurate portrayal of form and materiality. In this case, placement of greenery is exact and plant selection is specific to the genus. In this hypothetical scenario, the architect is tasked with selecting an appropriate façade for retrofitting a green wall (W2, S2 or S3). By using the solar insolation diagram, the architect can make an objective decision based on solar exposure. It can be seen that S3 has the highest solar exposure and for the purpose of reducing heat transmission into the building as well as to improve outdoor thermal conditions, S3 is the best candidate for green wall retrofit. Figure 97 also shows that solar insolation need not be homogeneous across a single surface. W2, for instance, will benefit more if a green wall is allocated at the upper portion of the wall (due to higher solar exposure) than if it were to be allocated at the lower portion.

After vertical and rooftop greenery spaces have been allocated, the solar insolation map can be used to identify the type of plants to be used at these areas. Different plants require different light conditions for optimal growth. This is more commonly categorised as full sun, semi-shaded, and fully shaded conditions. The plant selection chart derived from Chapter 5 can be used to select plants based on their evapotranspiration rate and albedo. With the solar insolation map, it is possible to recommend the appropriate type of plants to be allocated based on local insolation levels.

The proposed methodology differs slightly from the preceding section, in that a slightly more qualitative approach to planning and allocation is adopted.

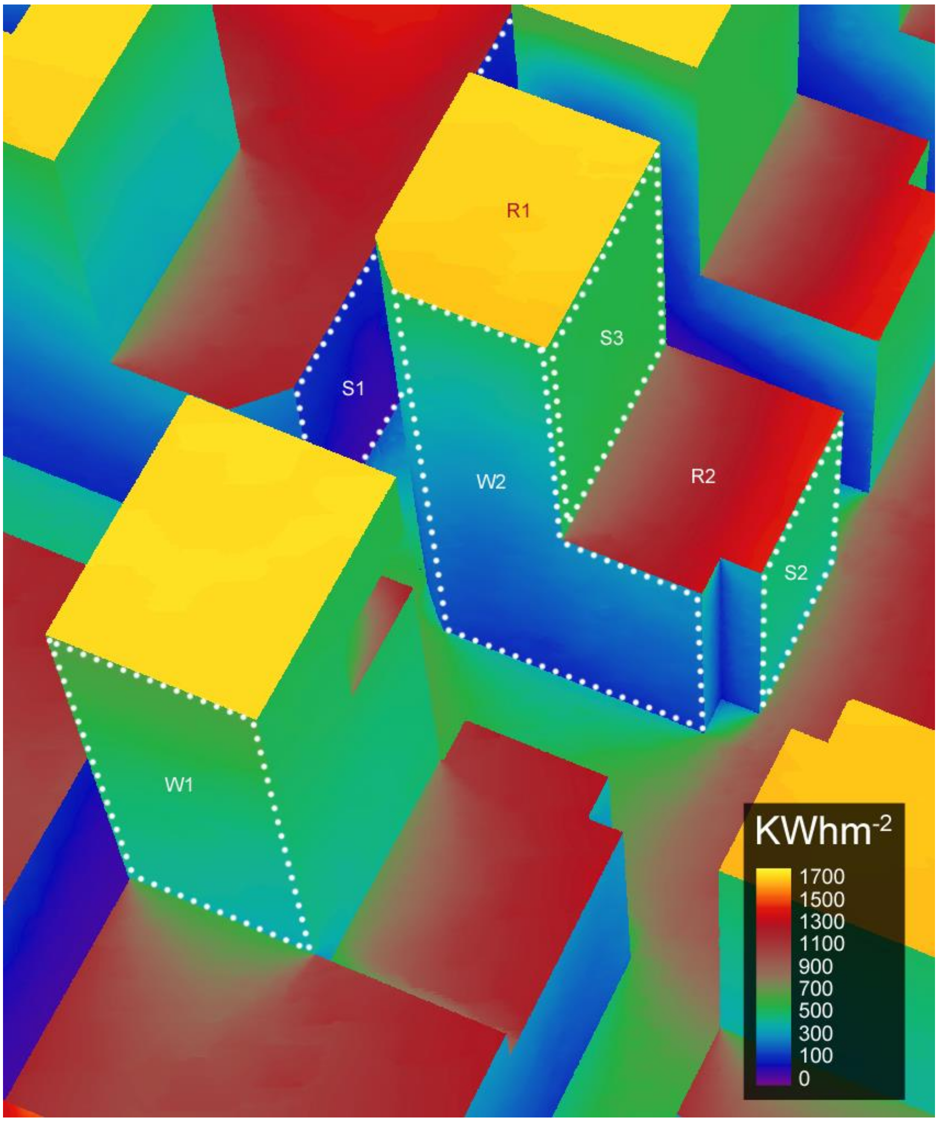

Figure 97. Assessment of building surfaces using solar insolation map

7 CONCLUSION

7.1 Objective 1

The first objective is to quantify the effect of rooftop greenery in the tropical outdoor urban environment. Measurements of air and mean radiant temperature were conducted on a rooftop garden setting and results have shown that they are influenced by both meteorological factors and plant attributes. Plants can reduce air temperature as well as mean radiant temperature, and that certain plant characteristics can affect overall rate of reduction. Solar exposure has been shown to be different at ground level, building envelope and rooftop surfaces. The heterogeneous thermal climate indicated a consequential need for cooling requirements to be uniquely suited to its locality.

7.2 Objective 2

The second objective is to identify relevant plant traits that contribute to temperature reduction and conditions to which the cooling effect can be maximized. Regression modelling was conducted based on measured data. Plant evapotranspiration rate and shrub albedo were identified to be statistically significant variables to mean radiant temperature reduction in the outdoor environment. Other traits such as LAI were found to be poorly correlated to mean radiant temperature reduction. A chart was derived using the regression model with the purpose of aiding the plant selection process.

7.3 Objective 3

The final objective is to propose guidelines for landscape planning based on identified plant traits via this study. A hypothetical case study was used to demonstrate new landscape planning principles derived from findings of this study. The BCA Green Mark Scheme, a local green building rating tool, was reviewed and the role of greenery was concluded to be wanting. Details of the review are presented in Appendix 10.4. It was evident that the numerous benefits of greenery that has been widely acknowledged in the academic realm have yet to be translated into industry practice. Recommendations were made to improve the current assessment criteria, based on results derived from this study as well as reviewed literature.

7.4 Contributions of research

7.4.1 Objective plant selection and placement criteria

This study has shown that it is both possible and beneficial to select and allocate plants based on objective, scientific principles. The proposed series of landscape planning guidelines outline the first steps to optimizing urban greenery as an ecosystem service.

Objective plant selection has become an important criterion in landscape planning. The concept itself is not entirely new: Cameron et al. (2014) showed that different plant species varied distinctively in their cooling capacity and the mechanisms for cooling varied between species. The roles of evapotranspirative cooling and shade cooling were differentiated and it was recommended that plant physiology be considered when selecting plants to maximise the cooling potential of vertical greenery. Fahmy et al. (2010) measured the LAI of *Ficus elastica* and *Peltophorum pterocarpum* trees and concluded a significant correlation between LAI and solar radiation interception. The LAI was used as a criterion for tree selection. Taha et al. (1991) measured meteorological variables in and around an isolated vegetative canopy and showed that extensive planting is not necessary; one or two rows of trees is sufficient to achieve significant cooling. The effects of wind attenuation can also be factored into the landscape proposal.

In practice, plants are already categorised according to various traits and functions. Boo et al. (2014) categorises the functional traits of plants for the purpose of landscape design (Table 31). The emphasis is on maintainability and aesthetics. This study has shown that temperature reduction potential can also be a functional category in plant selection and landscape planning design.

Table 31. Plant categorisation for landscape design (Boo et al., 2014)

Plant habit	**Plant care requirements**	**Plant use characteristics**
Trees	Preference to full-shade condition	Tropical native
Shrub	Preference to semi-shade condition	Suitability for roadside planting
Climbers	Preference to full-sun condition	Suitability for seaside planting
Ferns	Requires occasional spraying	Aquatic plants
Palms	Requires little water for maintenance	Drought tolerant plants
Cycads	Requires moderate watering for maintenance	Indoor plants
	Requires lots of water for maintenance and to be given on a regular basis	Ornamental flowers
		Herbs and spices
		Attracts birds
		Ornamental foliage
		Attracts butterflies

7.4.2 A novel landscape planning and design ethos

One of the aims of this study is to find ways to refine the landscape planning and design process. Scientific objectives are proposed to lend sophistication to the landscape design process and to not let it be limited to aesthetics. This is ever more pertinent in light of the lack of large canopy shade provision by vertical and rooftop greenery. Introduction of solar insolation mapping in this study has highlighted the importance of context and locality. Adjacent buildings can affect solar exposure significantly, thereby influencing the plant selection and placement process, dispelling the common myth that plants can improve the environment by cooling temperature indiscriminately.

In addition to shade provision, this study has highlighted the role of plants as water delivery agents. The efficiency to which water is channelled from soil to leaves can result in significant difference in plant cooling potential.

The proposed landscape planning framework offers a look at how plants can affect the urban environment in an extremely fine spatial and temporal scale. This provides more flexibility in landscape planning, as specific areas can be targeted at specific timings for intervention.

7.4.3 Optimizing the effects of urban greenery

The concept of landscape optimization stems from the simple fact that resources are limited. It is hoped that through the proposed landscape planning framework, urban greenery can be utilized to its full potential. Mean radiant temperature maps can be superimposed with air temperature, wind and relative humidity maps to deduce overall outdoor thermal comfort.

This is can be promoted via building policies as well as a greater part of the Green Mark assessment. An important consideration is whether the proposed landscape planning framework would burden the existing framework in any manner. Chapter 10.4 shows that the proposed framework only requires available information on greenery to be further processed via simulation and does not involve any additional costs for implementation. On the contrary, it can reduce the need for maintenance and significantly lower building energy consumption.

The urban greenery optimization agenda will comprise of many facets of greenery. Cooling potential is but one criterion that will bring about better landscape planning practices. Collaboration between scientists, architects, facility managers and building users is essential for the agenda to be realised to its potential. It is in this light that we can truly partake in climate-responsive landscape design.

7.5 Limitations of study

Limitations of this study are as follows:

- Measurements in Chapter 4 are done for extensive rooftop greenery systems. Cooling effect of intensive rooftop greenery systems and ground level shrubbery may differ in magnitude;
- Plant selection chart is derived using regression model via three types of plants. The study acknowledges limitations in the experiment design in terms of the number of plant species tested as well as space and equipment constraints for replication purposes. Cooling effect reflected on the chart can be more comprehensive if more plants of varying species are used for regression modelling and if replications are permissible; and
- Superimposition of GIS layers outlined in Chapter 6.2.4.2 is made with the assumption that t_{mrt} reduction potential is the same for ground level plantings and that all layers are simulated at the same height above ground.

7.6 Suggestions for further study

Suggestions for further study are as follows:

- The methodology adopted to measure the effects of rooftop greenery and to derive the regression model can be used to determine the effect of vertical greenery on outdoor mean radiant temperature. Several comparative studies of vertical greenery have been conducted in tandem with the main rooftop greenery study and results indicate significant temperature reduction. Details of these studies can be found in Appendix 10.3. A similar plant selection chart can be generated thereafter;

- Plant functional traits such as leaf area and shrub height may be measured to systematically to determine their impact on temperature in the outdoor environment; and
- A more comprehensive urban greenery assessment matrix comprising of existing landscape planning frameworks such as biodiversity quotient, irrigation and maintainability may be developed for use by landscape planners.

8 PUBLICATION AND CONFERENCE LIST

8.1 Conferences

Wong, N.H., Jusuf, S.K., **Tan, C.L**., Tan, E., Nindyani, A.D.S., 2011, Influence of Water bodies on Outdoor Air Temperature in Hot and Humid Climate. *International Conference on Sustainable Design and Construction*, Kansas, USA. Oral Presentation, Published in proceedings.

Wong, N.H., Jusuf, S.K., **Tan, C.L**., 2011, Urban Climatic Map and STEVE Tool for Sustainable Urban Planning in Singapore, *PLEA 2011 - 27th International conference on Passive and Low Energy Architecture*, Louvaine La Nouve, Belgium. Oral Presentation, Published in proceedings.

Wong, N.H., Jusuf, S.K., **Tan, C.L**., 2011, Influence of Urban Morphology on Air Temperature Condition: A Case Study of Eco-Township in Singapore, *18th International Seminar on Urban Form*, Montréal, Canada. Oral Presentation, Published in proceedings.

Jusuf, S.K., Wong, N.H., **Tan, C.L**., Tan, A., 2012, STEVE Tool: Bridging the Gap between Urban Climatology Research and Urban Planning Process, *ICSDC 2011*, Kansas, USA. Oral Presentation, Published in proceedings.

Tan, C.L., 2011, A convenient method for estimating the mean radiant temperature in tropical outdoor urban settings, *Croucher Advanced Study Institute. Urban Climatology on Tropical and Sub-Tropical Regions*. The Chinese University of Hong Kong, Hong Kong. Poster presentation.

Wong, N.H., Jusuf, S.K., **Tan, C.L**., Chia, P.Y., 2012, Outdoor mean radiant temperature measurement in the tropical urban environment, *iNTA 2012*, National University of Singapore, Singapore. Oral Presentation, Published in proceedings.

Wong, N.H., Jusuf, S.K., **Tan, C.L**., Chia, P.Y., 2012, Effects of vertical greenery on mean radiant temperature in the tropical urban environment, *iNTA 2012*, National University of Singapore, Singapore. Oral Presentation, Published in proceedings.

Wong, N.H., Jusuf, S.K., **Tan, C.L**., 2013, Selective placement of vertical and rooftop greenery, SB 13, Marina Bay Sands Expo and Convention Centre, Singapore. Oral Presentation, Published in proceedings.

Wong, N.H., Jusuf, S.K., **Tan, C.L**., 2013, Scientific approaches to landscape design, International Skyrise Greenery Conference, Singapore Expo, Singapore. Poster Presentation.

Wong, N.H., Jusuf, S.K., **Tan, C.L**., Chia, P.Y., 2013, Effect of cool roofs and green roofs on temperature in the tropical urban environment, AIVC 2013, Athens. Oral Presentation by Jusuf, S.K., Published in proceedings.

Tan, C.L., Wong, N.H., Jusuf, S.K., 2015, Plant selection and placement criteria for vertical and rooftop greenery, TAU Conference: Mitigating and Adapting Built Environments for Climate Change in the Tropics. School of Architecture, Tanri Abeng University, Jakarta, Indonesia, Oral Presentation, Published in proceedings.

8.2 Journal publications

Wong, N.H., Jusuf, S.K., **Tan, C.L**., 2011, Integrated urban microclimate assessment method as a sustainable urban development and urban design tool, *Landscape and Urban Planning* 100(4):386-389.

Tan, C.L., Wong, N.H., Jusuf, S.K., 2013, Outdoor mean radiant temperature estimation in the tropical urban environment, *Building and Environment* 64:118-129.

Tan, C.L., Wong, N.H., Jusuf, S.K., 2014, Effects of vertical greenery on mean radiant temperature in the tropical urban environment, *Landscape and urban planning* 127: 52-64.

Tan, C.L., Wong, N.H., Tan, P.Y., Jusuf, S.K., Chiam, Z.Q., 2015, Impact of plant evapotranspiration rate and shrub albedo on temperature reduction in the tropical outdoor environment, *Building and Environment* 94:206-217.

All journal publications are managed by Elsevier.

By choosing to be published under Elsevier, authors agree to transfer copyright to the publisher. However, authors retain rights to use the material under a variety of circumstances. One such scenario is for personal use, which is defined as the inclusion of relevant content in a thesis, on the conditions that the thesis will not be published commercially.

For more information, please visit https://elsevier.com/about/company-information/policies/copyright.

9 REFERENCES

Ahmad, S. B., 1978, Albedo studies of urban and agricultural surfaces near Leeds, University of Leeds.

Ahmad, S. B., Lockwood, J., 1979, Albedo, *Progress in Physical Geography* **3**(4)**:**510-543.

Akbari, H., Bretz, S., Kurn, D. M., Hanford, J., 1997a, Peak power and cooling energy savings of high-albedo roofs, *Energy and Buildings* **25**(2)**:**117-126.

Akbari, H., Konopacki, S. J., 2005, Calculating energy-saving potentials of heat-island reduction strategies, *Energy Policy* **33:**721-756.

Akbari, H., Konopacki, S. J., Eley, C. N., Wilcox, B. A., Van Geem, M. G., Parker, D. S., 1998, Calculations for reflective roofs in support of standard 90.1, *ASHRAE Transactions* **104:**976-987.

Akbari, H., Kurn, D. M., Bretz, S. E., Hanford, J. W., 1997b, Peak power and cooling energy savings of shade trees, *Energy and Buildings* **25**(2)**:**139-148.

Akbari, H., Pomerantz, M., Taha, H., 2001, Cool surfaces and shade trees to reduce energy use and improve air quality in urban areas, *Solar Energy* **70**(3)**:**295-310.

Alexandri, E., Jones, P., 2008, Temperature decreases in an urban canyon due to green walls and green roofs in diverse climates, *Building and Environment* **43**(4)**:**480-493.

Ali-Toudert, F., Mayer, H., 2006, Numerical study on the effects of aspect ratio and orientation of an urban street canyon on outdoor thermal comfort in hot and dry climate, *Building and Environment* **41**(2)**:**94-108.

Ali-Toudert, F., Mayer, H., 2007, Effects of asymmetry, galleries, overhanging facades and vegetation on thermal comfort in urban street canyons, *Solar Energy* **81**(6)**:**742-754.

Allen, R. G., Pereira, L. S., Howell, T. A., Jensen, M. E., 2011, Evapotranspiration information reporting: I. Factors governing measurement accuracy, *Agricultural Water Management* **98**(6)**:**899-920.

Allen, R. G., Pereira, L. S., Raes, D., Smith, M., 1998, Crop evapotranspiration-Guidelines for computing crop water requirements-FAO Irrigation and drainage paper 56, *FAO, Rome* **300:**6541.

Allen, R. G., Pruitt, W. O., Jensen, M. E., 1991, Environmental requirements of lysimeters, *Lysimeters for evapotranspiration and environmental measurements***:**23-25.

Amarakoon, D., Chen, A., McLean, P., 2000, Estimating daytime latent heat flux and evapotranspiration in Jamaica, *Agricultural and Forest Meteorology* **102**(2)**:**113-124.

ASHRAE, 2001a, ASHRAE fundamentals handbook, in: *American Society of Heating, Refrigerating, and Air-Conditioning Engineers,*.

ASHRAE, 2001b, Standard 90.1-2001 (S-I edition)—Energy Standard for Buildings Except Low-Rise Residential Buildings (IESNA cosponsored; ANSI approved; Continuous Maintenance Standard), *SI edition***:**175.

Baik, J.-J., Kwak, K.-H., Park, S.-B., Ryu, Y.-H., 2012, Effects of building roof greening on air quality in street canyons, *Atmospheric Environment* **61:**48-55.

Baille, M., Baille, A., Laury, J. C., 1994, A simplified model for predicting evapotranspiration rate of nine ornamental species vs. climate factors and leaf area, *Scientia Horticulturae* **59**(3–4)**:**217-232.

Bass, B., Baskaran, B., 2003, Evaluating rooftop and vertical gardens as an adaptation strategy for urban areas, Institute for Research and Construction, NRCC-46737, Project no. A020, CCAF

Report B1046. Ottawa, Canada: National Research Council.

BBC, 2013, BBC Bitesize: Making Food.

Behrendt, A., Schalitz, G., Mueller, L., Schindler, U., 2003, Evapotranspiration and Nutrient Leaching of Rewetting, in: *International Soil Tillage Research Organization conference*, University of Queensland, Brisbane, pp. 87-93.

Berkovic, S., Yezioro, A., Bitan, A., 2012, Study of thermal comfort in courtyards in a hot arid climate, *Solar Energy* **86**(5)**:**1173-1186.

Bernatzky, A., 1982, The contribution of trees and green spaces to a town climate, *Energy and Buildings* **5:**1-10.

Bogren, J., Gustavsson, T., Karlsson, M., Postgård, U., 2000, The impact of screening on road surface temperature, *Meteorological Applications* **7**(2)**:**97-104.

Boo, C. M., Chew, S. Y. J., Yong, J. W. H., 2014, Plants in Tropical Cities.

Bowen, I. S., 1926, The ratio of heat losses by conduction and by evaporation from any water surface, *Physical review* **27**(6)**:**779.

Breuer, L., Eckhardt, K., Frede, H.-G., 2003, Plant parameter values for models in temperate climates, *Ecological Modelling* **169**(2–3)**:**237-293.

Brown, R., Gillespie, T., 1990, Estimating radiation received by a person under different species of shade trees, *Journal of Arboriculture* **16**(6)**:**158-161.

Brown, R. D., Gillespie, T. J., 1995, Microclimatic landscape design: creating thermal comfort and energy efficiency, John Wiley & Sons.

Ca, V. T., Asaeda, T., Abu, E. M., 1998, Reductions in air conditioning energy caused by a nearby park, *Energy and Buildings* **29**(1)**:**83-92.

Cameron, R. W. F., Taylor, J. E., Emmett, M. R., 2014, What's 'cool' in the world of green façades? How plant choice influences the cooling properties of green walls, *Building and environment* **73**(0)**:**198-207.

Campbell, G., 1986, Extinction coefficients for radiation in plant canopies calculated using an ellipsoidal inclination angle distribution, *Agricultural and forest meteorology* **36**(4)**:**317-321.

Campbell, G., 1990, Derivation of an angle density function for canopies with ellipsoidal leaf angle distributions, *Agricultural and Forest Meteorology* **49**(3)**:**173-176.

Campbell, G. S., Norman, J. M., 1998, An introduciton to environmental biophysics, Springer-Verlag New York, Inc.

Carlson, R. E., Yarger, D. N., 1971, An Evaluation of Two Methods for Obtaining Leaf Transmissivity from Leaf Reflectivity Measurements1, *Agron. J.* **63**(1)**:**78-81.

Carrow, R. N., 1995, Drought Resistance Aspects of Turfgrasses in the Southeast: Evapotranspiration and Crop Coefficients, *Crop Sci.* **35**(6)**:**1685-1690.

Castleton, H. F., Stovin, V., Beck, S. B. M., Davison, J. B., 2010, Green roofs; building energy savings and the potential for retrofit, *Energy and Buildings* **42**(10)**:**1582-1591.

Chason, J. W., Baldocchi, D. D., Huston, M. A., 1991, A comparison of direct and indirect methods for estimating forest canopy leaf area, *Agricultural and Forest Meteorology* **57**(1–3)**:**107-128.

Chen, H., Ooka, R., Huang, H., Tsuchiya, T., 2009, Study on mitigation measures for outdoor thermal environment on present urban blocks in Tokyo using coupled simulation, *Building and Environment* **44**(11)**:**2290-2299.

Chen, J., Black, T., 1992, Foliage area and architecture of plant canopies from sunfleck size distributions, *Agricultural and Forest Meteorology* **60**(3)**:**249-266.

Chen, J. M., Cihlar, J., 1995, Quantifying the effect of canopy architecture on optical measurements of leaf area index using two gap size analysis methods, *Geoscience and Remote Sensing, IEEE Transactions on* **33**(3)**:**777-787.

Chen, J. M., Rich, P. M., Gower, S. T., Norman, J. M., Plummer, S., 1997, Leaf area index of boreal forests: Theory, techniques, and measurements, *Journal of Geophysical Research: Atmospheres (1984–2012)* **102**(D24)**:**29429-29443.

Chen, Q., Li, B., Liu, X., 2013, An Experimental Evaluation of the Living Wall System in Hot and Humid Climate, *Energy and Buildings* **61:**298-307.

Cheng, C. Y., Cheung, K. K., Chu, L., 2010, Thermal performance of a vegetated cladding system on facade walls, *Building and environment* **45**(8)**:**1779-1787.

Cheng, M.-D., Miller, W., New, J., Berdahl, P., 2012, Understanding the long-term effects of environmental exposure on roof reflectance in California, *Construction and Building Materials* **26**(1)**:**516-526.

Cheng, M.-D., Pfiffner, S. M., Miller, W. A., Berdahl, P., 2011, Chemical and microbial effects of atmospheric particles on the performance of steep-slope roofing materials, *Building and environment* **46**(5)**:**999-1010.

Chua, K.J., Chou, S.K., 2010, An ETTV-based approach to improving the energy performance of commercial buildings, *Energy and Buildings* **42**(4):491-499.

Chudnovsky, A., Ben-Dor, E., Saaroni, H., 2004, Diurnal thermal behavior of selected urban objects using remote sensing measurements, *Energy and Buildings* **36**(11)**:**1063-1074.

Cohen, Y., Fuchs, M., Falkenflug, V., Moreshet, S., 1988, Calibrated heat pulse method for determining water uptake in cotton, *Agronomy Journal* **80**(3)**:**398-402.

Connelly, M., Hodgson, M., 2008, Sound transmission loss of green roofs, in: *Sixth Annual Greening Rooftops for Sustainable Communities*, Baltimore, MD.

Correa, E., Ruiz, M. A., Canton, A., Lesino, G., 2012, Thermal comfort in forested urban canyons of low building density. An assessment for the city of Mendoza, Argentina, *Building and environment* **58:**219-230.

Council of Tree and Landscape Appraisers, 1992, Guide for Plant Appraisal, International Society of Arboriculture, Savoy, Ill.

Cowan, I., 1982, Regulation of water use in relation to carbon gain in higher plants, in: *Physiological Plant Ecology II*, Springer, pp. 589-613.

Crutzen, P. J., 2004, The growing urban heat and pollution ''island'' effect—impact on chemistry and climate, *Atmospheric Environment* **38:**3539–3540.

d'Ambrosio Alfano, F. R., Dell'Isola, M., Palella, B. I., Riccio, G., Russi, A., 2013, On the Measurement of the Mean Radiant Temperature and its Influence on the Indoor Thermal Environment Assessment, *Building and environment* **63:**79-88.

d'Ambrosio Alfano, F. R., Palella, B. I., Riccio, G., 2011a, The role of measurement accuracy on the thermal environment assessment by means of PMV index, *Building and Environment* **46**(7)**:**1361-1369.

d'Ambrosio Alfano, F. R., Palella, B. I., Riccio, G., 2011b, Thermal Environment Assessment Reliability Using Temperature-Humidity Indices, *Industrial health* **49**(1)**:**95-106.

Dabberdt, W., Davis, P., 1978, Determination of energetic characteristics of urban-rural surfaces in the greater St. Louis area, *Boundary-Layer Meteorology* **14**(1)**:**105-121.

Daily, G. C., 1997, Introduction: What are ecosystem services? In: Nature's Services: Societal Dependence on Natural Ecosystems**:**1 - 10.

Daughtry, C. S. T., Goel N.S., Norman, J. M., 1990, Canopy structure: Direct Methods. Instrumentation for studying Vegetation Canopies for Remote Sensing in Optical and Thermal Infrared Regions.**:**66 - 71.

De Dear, R., 1987, Ping-pong globe thermometers for mean radiant temperatures, *Heating and Ventilating Engineer* **60**(681)**:**10-12.

De Groot, R. S., Wilson, M. A., Boumans, R. M., 2002, A typology for the classification, description and valuation of ecosystem functions, goods and services, *Ecological economics* **41**(3)**:**393-408.

Dell'Isola, M., Frattolillo, A., Palella, B., Riccio, G., 2012, Influence of Measurement Uncertainties on the Thermal Environment Assessment, *International Journal of Thermophysics* **33**(8-9)**:**1616-1632.

Devitt, D. A., Morris, R. L., Bowman, D. C., 1992, Evapotransportation, Crop Coefficients, and Leaching Fractions of Irrigated Desert Turfgrass Systems, *Agron. J.* **84**(4)**:**717-723.

Dickinson, R. E., Hanson, B., 2013, Vegetation-Albedo Feedbacks, in: *Climate Processes and Climate Sensitivity*, American Geophysical Union, pp. 180-186.

DiGiovanni, K., Montalto, F., Gaffin, S., Rosenzweig, C., 2013, Applicability of Classical Predictive Equations for the Estimation of Evapotranspiration from Urban Green Spaces: Green Roof Results, *Journal of Hydrologic Engineering* **18**(1):99-107.

Dimoudi, A., Nikolopoulou, M., 2003, Vegetation in the urban environment: microclimatic analysis and benefits, *Energy and buildings* **35**(1)**:**69-76.

Ding, R., Kang, S., Li, F., Zhang, Y., Tong, L., 2013, Evapotranspiration measurement and estimation using modified Priestley–Taylor model in an irrigated maize field with mulching, *Agricultural and forest meteorology* **168:**140-148.

Djedjig, R., Bozonnet, E., Belarbi, R., 2013, Experimental study of the urban microclimate mitigation potential of green roofs and green walls in street canyons, *International Journal of Low-Carbon Technologies*.

Dobos, E., 2006, Albedo, in: *Encyclopedia of Soil Science*.

Donovan, G. H., Butry, D. T., 2009, The value of shade: estimating the effect of urban trees on summertime electricity use, *Energy and Buildings* **41**(6)**:**662-668.

Doughty, C., Field, C., McMillan, A. S., 2011, Can crop albedo be increased through the modification of leaf trichomes, and could this cool regional climate?, *Climatic Change* **104**(2)**:**379-387.

Dugas, W., Fritschen, L., Gay, L., Held, A., Matthias, A., Reicosky, D., Steduto, P., Steiner, J., 1991, Bowen ratio, eddy correlation, and portable chamber measurements of sensible and latent heat flux over irrigated spring wheat, *Agricultural and forest meteorology* **56**(1)**:**1-20.

Dunnett, N., Kingsbury, N., 2008, Planting green roofs and living walls, Portland, USA: Timber Press.

Dzikiti, S., Jovanovic, N., Bugan, R., Israel, S., Le Maitre, D., 2014, Measurement and modelling of evapotranspiration in three fynbos vegetation types, *Water SA* **40:**189-198.

Ehleringer, J., Werk, K., 1986, Modifications of solar-radiation absorption patterns and implications for carbon gain at the leaf level, in: *Givnish TJ (ed) On the economy of plant form and function.*, Cambridge University Press, London.

Eliasson, I., 2000, The use of climate knowledge in urban planning, *Landscape and urban planning* **48**(1)**:**31-44.

Emmanuel, R., Rosenlund, H., Johansson, E., 2007, Urban shading—a design option for the tropics? A study in Colombo, Sri Lanka, *International Journal of Climatology* **27**(14)**:**1995-2004.

Epstein, Y., Moran, D. S., 2006, Thermal comfort and the heat stress indices, *Industrial Health* **44**(3)**:**388-398.

Fahmy, M., Sharples, S., Yahiya, M., 2010, LAI based trees selection for mid latitude urban developments: A microclimatic study in Cairo, Egypt, *Building and environment* **45**(2)**:**345-357.

Falster, D.S., Westoby, M., 2003, Leaf size and angle vary widely across species: what consequences for light interception? *New Phytologist* **158**(3):509-525.

Fanger, P. O., 1972, Thermal comfort. Analysis and applications in environmental engineering, New York: McGraw-Hill.

Flint, A. L., Childs, S. W., 1991, Use of the Priestley-Taylor evaporation equation for soil water limited conditions in a small forest clearcut, *Agricultural and Forest Meteorology* **56**(3)**:**247-260.

Fritschen, L. J., Simpson, J. R., 1989, Surface energy and radiation balance systems-General description and improvements, *Journal of Applied Meteorology* **28:**680-689.

Gaffin, S., Khanbilvardi, R., Rosenzweig, C., 2009, Development of a Green Roof Environmental Monitoring and Meteorological Network in New York City, *Sensors* **9**(4)**:**2647-2660.

Gagge, A., 1971, An effective temperature scale based on a simple model of human physiological regulatory response, *ASHRAE Trans.* **77:**247-262.

Ganesan, S., Lau, S., 2000, Urban challenges in Hong Kong: future directions for design, *Urban Design International* **5**(1)**:**3-12.

Gaspar, A. R., Quintela, D. A., 2009, Physical modelling of globe and natural wet bulb temperatures to predict WBGT heat stress index in outdoor environments, *International journal of biometeorology* **53**(3)**:**221-230.

Gaudet, C. L., Keddy, P. A., 1988, A comparative approach to predicting competitive ability from plant traits, *Nature* **334**(6179)**:**242-243.

Gill, S., Handley, J., Ennos, A., Pauleit, S., 2007, Adapting cities for climate change: the role of the green infrastructure, *Built environment* **33**(1)**:**115-133.

Giridharan, R., Lau, S., Ganesan, S., Givoni, B., 2008, Lowering the outdoor temperature in high-rise high-density residential developments of coastal Hong Kong: The vegetation influence, *Building and Environment* **43**(10)**:**1583-1595.

Givnish, T. J., 1987, Comparative Studies of Leaf Form: Assessing the Relative Roles of Selective Pressures and Phylogenetic Constraints, *New Phytologist* **106**(1)**:**131-160.

Gobster, P. H., 1998, Urban parks as green walls or green magnets? Interracial relations in neighborhood boundary parks, *Landscape and urban planning* **41**(1)**:**43-55.

Goel, N. S., Strebel, D. E., 1984, Simple beta distribution representation of leaf orientation in vegetation canopies, *Agronomy Journal* **76**(5)**:**800-802.

Gómez-Muñoz, V. M., Porta-Gándara, M., Fernández, J., 2010, Effect of tree shades in urban planning in hot-arid climatic regions, *Landscape and urban planning* **94**(3)**:**149-157.

Gómez, F., Tamarit, N., Jabaloyes, J., 2001, Green zones, bioclimatics studies and human comfort in the future development of urban planning, *Landscape and Urban planning* **55**(3)**:**151-161.

Graham, W. G., King, K. M., 1961, Short-wave reflection coefficient for a field of maize, *Quarterly Journal of the Royal Meteorological Society* **87**(373)**:**425-428.

Grahn, P., Stigsdotter, U. K., 2010, The relation between perceived sensory dimensions of urban green space and stress restoration, *Landscape and Urban Planning* **94**(3)**:**264-275.

Greater London Authority, 2004, The London Plan, *London, GLA*.

Grebet, P., Cuenca, R. H., 1991, History of lysimeter design and effects of environmental disturbances, *ASCE, NEW YORK, NY,(USA).*10-18.

Green, S., 1993, Radiation balance, transpiration and photosynthesis of an isolated tree, *Agricultural and forest meteorology* **64**(3)**:**201-221.

Grime, J., 1979, Competition and the struggle for existence, in: *Population Dynamics* (R. M. Anderson, T. B.D., T. L.R., eds.), Blackwell Scientific Oxford.

Guidi, W., Piccioni, E., Bonari, E., 2008, Evapotranspiration and crop coefficient of poplar and willow short-rotation coppice used as vegetation filter, *Bioresource Technology* **99**(11)**:**4832-4840.

Gulyás, Á., Unger, J., Matzarakis, A., 2006, Assessment of the microclimatic and human comfort conditions in a complex urban environment: Modelling and measurements, *Building and Environment* **41**(12)**:**1713-1722.

Gunston, H., Batchelor, C., 1983, A comparison of the Priestley-Taylor and Penman methods for estimating reference crop evapotranspiration in tropical countries, *Agricultural Water Management* **6**(1)**:**65-77.

Gupta, K., Kumar, P., Pathan, S., Sharma, K., 2012, Urban Neighborhood Green Index–A measure of green spaces in urban areas, *Landscape and Urban Planning* **105**(3)**:**325-335.

Hair, J. F. J., Anderson, R. E., Tatham, R. L., Black, W. C., 1995, Multivariate Data Analysis, Macmillan, New York.

Hakim, A. A., Petrovitch, H., Burchfiel, C. M., Ross, G. W., Rodriguez, B. L., White, L. R., Yano, K., Curb, J. D., Abbott, R. D., 1998, Effects of walking on mortality among nonsmoking retired men, *New England Journal of Medicine* **338**(2)**:**94-99.

Hardin, P. J., Jensen, R. R., 2007, The effect of urban leaf area on summertime urban surface kinetic temperatures: A Terre Haute case study, *Urban Forestry & Urban Greening* **6**(2)**:**63-72.

Heilman, J., Brittin, C., Neale, C., 1989, Fetch requirements for Bowen ratio measurements of latent and sensible heat fluxes, *Agricultural and forest meteorology* **44**(3)**:**261-273.

Heisler, G. M., 1986a, Effects of individual trees on the solar radiation climate of small buildings, *Urban Ecology* **9**(3)**:**337-359.

Heisler, G. M., 1986b, Energy savings with trees, *Journal of Arboriculture* **12**(5).

Hillel, D., 1980, Applications of soil physics, Academic Press Inc.(London) Ltd.

Hillel, D., 1998, Environmental soil physics: Fundamentals, applications, and environmental considerations, Academic press.

HKSAR Government, 2010, Greening masterplan.

Hongbing, W., Jun, Q., Yonghong, H., Li, D., 2010, Optimal tree design for daylighting in residential buildings, *Building and Environment* **45**(12)**:**2594-2606.

Honjo, T., Takakura, T., 1991, Simulation of thermal effects of urban green areas on their surrounding areas, *Energy and Buildings* **15**(3)**:**443-446.

Höppe, P., 1999, The physiological equivalent temperature–a universal index for the biometeorological assessment of the thermal environment, *International Journal of Biometeorology* **43**(2)**:**71-75.

Höppe, P., Mayer, H., 1987, Planungsrelevante Bewertung der thermischen Komponente des Stadtklimas, *Landschaft+ Stadt* **19:**22-30.

Hough, M., 2004, Cities and natural process: a basis for sustainability, Psychology Press.

Humphreys, M. A., 1977, The optimum diameter for a globe thermometer for use indoors, *Annals of Occupational Hygiene* **20**(2)**:**135-140.

Hwang, R.-L., Lin, T.-P., Cheng, M.-J., Lo, J.-H., 2010, Adaptive comfort model for tree-shaded outdoors in Taiwan, *Building and Environment* **45**(8)**:**1873-1879.

Hwang, R.-L., Lin, T.-P., Matzarakis, A., 2011, Seasonal effects of urban street shading on long-term outdoor thermal comfort, *Building and environment* **46**(4)**:**863-870.

IPCC, 2007, Report of the nineteenth session of the Intergovernmental Panel on Climate Change Geneva.

ISO 7726, I., 1998, 7726: Ergonomics of the thermal environment–Instruments for measuring physical quantities, *Geneva: International Standard Organization*.

ITTF, 2009, ITTF Technical Leaflet T3: The Ball.

Jacobs, J., 1961, The Death and Life of Great American Cities, West Sussex, UK: John Wiley & Sons, Ltd.

Jakubiec, J. A., Reinhart, C. F., 2011, DIVA-FOR-RHINO 2.0: Environmental parametric modeling in Rhinoceros/Grasshopper using Radiance, Daysim and EnergyPlus, in: *Building Simulation 2011: 12th Conference of International Building Performance Simulation Association*, Sydney, Australia, pp. 2202-2209.

Jauregui, E., 1991, Influence of a large urban park on temperature and convective precipitation in a tropical city, *Energy and buildings* **15**(3)**:**457-463.

Jendritzky, G., de Dear, R., Havenith, G., 2012, UTCI—Why another thermal index?, *International journal of biometeorology* **56**(3)**:**421-428.

Jensen, R. R., Boulton, J. R., Harper, B. T., 2003, The Relationship between Urban Leaf Area and Household Energy Usage in Terre Haute, Indiana, US, *Journal of Arboriculture* **29**(4)**:**226-230.

Jesionek, K., Bruse, M., 2003, Impacts of vegetation on the microclimate: modeling standardized building structures with different greening levels, *ICUC5, Lodz*.

Jia, X., Dukes, M., Jacobs, J., 2009, Bahiagrass crop coefficients from eddy correlation measurements in central Florida, *Irrigation Science* **28**(1)**:**5-15.

Jim, C.Y., 1999, A planning strategy to augment the diversity and biomass of roadside trees in urban Hong Kong, *Landscape and Urban Planning* **44**(1):13-32.

Jim, C. Y., 2012, Effect of vegetation biomass structure on thermal performance of tropical green roof, *Landscape and Ecological Engineering* **8**(2):173-187.

Jim, C.Y., Zhang, H., 2013, Species diversity and spatial differentiation of old-valuable trees in urban Hong Kong, *Urban Forestry & Urban Greening* **12:**171-182.

Johansson, E., 2006, Influence of urban geometry on outdoor thermal comfort in a hot dry climate: A study in Fez, Morocco, *Building and environment* **41**(10)**:**1326-1338.

Jonckheere, I., Fleck, S., Nackaerts, K., Muys, B., Coppin, P., Weiss, M., Baret, F., 2004, Review of methods for in situ leaf area index determination: Part I. Theories, sensors and hemispherical photography, *Agricultural and forest meteorology* **121**(1)**:**19-35.

Jones, H. G., 1992, Plants and microclimate: a quantitative approach to environmental plant physiology, Cambridge University Press.

Jonsson, P., 2004, Vegetation as an urban climate control in the subtropical city of Gaborone, Botswana, *International journal of climatology* **24**(10)**:**1307-1322.

Kamishima, K., Kohmura, K., Mochizuki, K., 2002, The Analysis of Greening Effects on Urban Environment Using GIS, in: *Esri International User Conference*, ESRI, San Diego, CA.

Katzschner, L., Bosch, U., Röttgen, M., 2004, A methodology for bioclimatic microscale mapping of urban spaces, University of Kassel, Kassel, Germany.

Katzschner, L., Mülder, J., 2008, Regional climatic mapping as a tool for sustainable development, *Journal of Environmental Management* **87**(2)**:**262-267.

Kawashima, S., 1991, Effect of vegetation on surface temperature in urban and suburban areas in winter, *Energy and Buildings* **15**(3)**:**465-469.

Kennedy, P., 1992, A Guide to Econometrics, Blackwell, Oxford.

Keuhn, L., Stubbs, R., Weaver, R., 1970, Theory of the Globe Thermometer, DTIC Document.

Kim, K. J., Kil, M. J., Song, J. S., Yoo, E. H., Son, K.-C., Kays, S. J., 2008, Efficiency of volatile formaldehyde removal by indoor plants: contribution of aerial plant parts versus the root zone, *Journal of the American Society for Horticultural Science* **133**(4)**:**521-526.

Kim, K. S., Beard, J. B., 1988, Comparative Turfgrass Evapotranspiration Rates and Associated Plant Morphological Characteristics, *Crop Sci.* **28**(2)**:**328-331.

King, D. A., 1997, The functional significance of leaf angle in Eucalyptus, *Australian Journal of Botany* **45**(4)**:**619-639.

Kipp, Z., 2008, CNR 4 instruction manual 2013.

Kobayashi, H., Suzuki, R., Kobayashi, S., 2007, Reflectance seasonality and its relation to the canopy leaf area index in an eastern Siberian larch forest: Multi-satellite data and radiative transfer analyses, *Remote Sensing of Environment* **106**(2)**:**238-252.

Kondratiev, K. Y., Mironova, Z. F., Otto, A. N., 1964, Spectral albedo of natural surfaces, *pure and applied geophysics* **59**(1)**:**207-216.

Korpela, K., Hartig, T., 1996, Restorative qualities of favorite places, *Journal of Environmental Psychology* **16**(3)**:**221-234.

Koster, E., 1998, Urban morphology and computers, *Urban Morphology* **2**(1)**:**3-7.

Kotzen, B., 2003, An investigation of shade under six different tree species of the Negev desert towards their potential use for enhancing micro-climatic conditions in landscape architectural development, *Journal of Arid environments* **55**(2)**:**231-274.

Kraft, M., Weigel, H.-J., Mejer, G.-J., Brandes, F., 1996, Reflectance measurements of leaves for detecting visible and non-visible ozone damage to crops, *J. Plant Physiol* **145:**148-154.

Kucharik, C.J., Norman, J.M., Gower, S.T., 1998, Measurements of leaf orientation, light distribution and sunlit leaf area in a boreal aspen forest, *Agricultural and Forest Meteorology*, **91**:127-148.

Kuehn, L. A., Stubbs, R. A., Weaver, R. S., 1970, Theory of the globe thermometer, *Journal of Applied Physiology* **29**(5)**:**750-757.

Kung, E. C., Bryson, R. A., Lenschow, D. H., 1964, Study of a continental surface albedo on the basis of flight measurements and structure of the Earth's surface cover over North America, *Monthly Weather Review* **92**(12)**:**543-564.

Kurn, D., Bretz, S., Huang, B., Akbari, H., 1994, The potential for reducing urban air temperatures and energy consumption through vegetative cooling, *ACEEE Summer Study on Energy Efficiency in Buildings, American Council for an Energy Efficient Economy. Pacific Grove, CA*.

La Gennusa, M., Nucara, A., Rizzo, G., Scaccianoce, G., 2005, The calculation of the mean radiant temperature of a subject exposed to the solar radiation—a generalised algorithm, *Building and environment* **40**(3)**:**367-375.

Lagstrom, J., 2004, Do extensive green roofs reduce noise?, International Green Roof Institute.

Laing, R. A., Miller, D., Davies, A.-M., Scott, S., 2006, Urban greenspace: the incorporation of environmental values in a decision support system, *Journal of Information Technology in Construction* **11:**177-196.

Lang, A., 1973, Leaf orientation of a cotton plant, *Agricultural Meteorology* **11:**37-51.

Lang, A. R. G., Goel N.S., Norman, J. M., 1990, An instrument for measuring canopy structure. Instrumentation for studying Vegetation Canopies for Remote Sensing in Optical and Thermal Infrared Regions. **:**66 - 71.

Lemke, B., Kjellstrom, T., 2012, Calculating workplace WBGT from meteorological data: a tool for climate change assessment, *Industrial Health* **50**(4)**:**267-278.

Levent, T. B., Nijkamp, P., 2004, Urban Green Space Policies: A Comparative Study on Performance and Success Conditions in European Cities.

Li, X., Lu, L., Yang, W., Cheng, G., 2012, Estimation of evapotranspiration in an arid region by remote sensing—a case study in the middle reaches of the Heihe River Basin, *International Journal of Applied Earth Observation and Geoinformation* **17:**85-93.

Lin, B., Li, X., Zhu, Y., Qin, Y., 2008, Numerical simulation studies of the different vegetation patterns' effects on outdoor pedestrian thermal comfort, *Journal of Wind Engineering and Industrial Aerodynamics* **96**(10)**:**1707-1718.

Lin, T.-P., Matzarakis, A., Hwang, R.-L., 2010, Shading effect on long-term outdoor thermal comfort, *Building and Environment* **45**(1)**:**213-221.

Lin, T.-P., Tsai, K.-T., Hwang, R.-L., Matzarakis, A., 2012a, Quantification of the effect of thermal indices and sky view factor on park attendance, *Landscape and Urban Planning* **107**(2)**:**137-146.

Lin, T.-P., Tsai, K.-T., Liao, C.-C., Huang, Y.-C., 2012b, Effects of thermal comfort and adaptation on park attendance regarding different shading levels and activity types, *Building and environment* **59:**599-611.

Lindberg, F., Grimmond, C., 2011, The influence of vegetation and building morphology on shadow patterns and mean radiant temperatures in urban areas: model development and evaluation, *Theoretical and applied climatology* **105**(3-4)**:**311-323.

Lindberg, F., Holmer, B., Thorsson, S., 2008a, SOLWEIG 1.0–Modelling spatial variations of 3D radiant fluxes and mean radiant temperature in complex urban settings, *International Journal of Biometeorology* **52**(7)**:**697-713.

Lindberg, F., Holmer, B., Thorsson, S., 2008b, SOLWEIG 1.0 – Modelling spatial variations of 3D radiant fluxes and mean radiant temperature in complex urban settings, *International Journal of Biometeorology* **52**(7)**:**697-713.

Maas, J., Spreeuwenberg, P., Van Winsum-Westra, M., Verheij, R. A., de Vries, S., Groenewegen, P. P., 2009, Is green space in the living environment associated with people's feelings of social safety?, *Environment and planning. A* **41**(7)**:**1763.

Mahmoud, A. H. A., 2011, Analysis of the microclimatic and human comfort conditions in an urban park in hot and arid regions, *Building and Environment* **46**(12)**:**2641-2656.

Makaremi, N., Salleh, E., Jaafar, M. Z., GhaffarianHoseini, A., 2012, Thermal comfort conditions of shaded outdoor spaces in hot and humid climate of Malaysia, *Building and environment* **48:**7-14.

Marquardt, D. W., 1970, Generalized inverses, ridge regression, biased linear estimation and nonlinear estimation, *Technometrics* **12**(3)**:**591-612.

Marshall, J. D., Waring, R. H., 1986, Comparison of methods of estimating leaf-area index in old-growth Douglas-Fir, *Ecology* **67**(4)**:**975-979.

Matzarakis, A., Rutz, F., 2005, Application of RayMan for tourism and climate investigations, *Annalen der Meteorologie* **41**(2)**:**631-636.

Matzarakis, A., Rutz, F., Mayer, H., 2000, Estimation and calculation of the mean radiant temperature within urban structures, in: *Biometeorology and Urban Climatology at the Turn of the Millenium (ed. by RJ de Dear, JD Kalma, TR Oke and A. Auliciems): Selected Papers from the Conference ICB-ICUC*, pp. 273-278.

Matzarakis, A., Rutz, F., Mayer, H., 2010, Modelling radiation fluxes in simple and complex environments: basics of the RayMan model, *International Journal of Biometeorology* **54**(2)**:**131-139.

Mayer, H., 1993, Urban bioclimatology, *Experientia* **49**(11)**:**957-963.

Mayer, H., Höppe, P., 1987, Thermal comfort of man in different urban environments, *Theoretical and Applied Climatology* **38**(1)**:**43-49.

Mazzali, U., Peron, F., Romagnoni, P., Pulselli, R. M., Bastianoni, S., 2013, Experimental investigation on the energy performance of Living Walls in a temperate climate. , *Building and Environment* **64:**57 - 66.

McGill, B. J., Enquist, B. J., Weiher, E., Westoby, M., 2006, Rebuilding community ecology from functional traits, *Trends in Ecology & Evolution* **21**(4)**:**178-185.

McHale, M. R., Gregory McPherson, E., Burke, I. C., 2007, The potential of urban tree plantings to be cost effective in carbon credit markets, *Urban Forestry & Urban Greening* **6**(1)**:**49-60.

McLeod, M. K., Daniel, H., Faulkner, R., Murison, R., 2004, Evaluation of an enclosed portable chamber to measure crop and pasture actual evapotranspiration at small scale, *Agricultural Water Management* **67**(1)**:**15-34.

McPherson, E. G., Herrington, L. P., Heisler, G. M., 1988, Impacts of vegetation on residential heating and cooling, *Energy and Buildings* **12**(1)**:**41-51.

McPherson, E. G., Platt, R. H., Rowntree, R. A., Muick, P. C., 1994, Cooling urban heat islands with sustainable landscapes, The ecological city: preserving and restoring urban biodiversity, Amherst, MA: University of Massachusetts Press**:** 151-172.

McPherson, E. G., Rowntree, R. A., 1988, Geometric solids for simulation of tree crowns, *Landscape and urban planning* **15**(1)**:**79-83.

Miller, R. W., 2007, Urban Forestry: Planning and Managing Urban Greenspaces, Waveland Press, Inc, Illinois

Monteith, J. L., Szeicz, G., 1961, The radiation balance of bare soil and vegetation, *Quarterly Journal of the Royal Meteorological Society* **87**(372)**:**159-170.

Müderrisoğlu, H., Eroğlu, E., Özkan, Ş., Ak, K., 2006, Visual perception of tree forms, *Building and Environment* **41**(6)**:**796-806.

Nasir, R. A., Ahmad, S. S., Ahmed, A. Z., 2012, Psychological Adaptation of Outdoor Thermal Comfort in Shaded Green Spaces in Malaysia, *Procedia-Social and Behavioral Sciences* **68:**865-878.

NEA, 2011, WEATHERWise Singapore, National Environment Agency.

Neter, J., Wasserman, W., Kutner, M. H., 1989, Applied Linear Regression Models, Irwin, Homewood, IL.

Neville, W., 1993, The impact of economic development on land functions in Singapore, *Geoforum* **24**(2)**:**143-163.

Ng, E., Cheng, V., 2012, Urban human thermal comfort in hot and humid Hong Kong, *Energy and Buildings* **55:**51-65.

Niachou, A., Papakonstantinou, K., Santamouris, M., Tsangrassoulis, A., Mihalakakou, G., 2001, Analysis of the green roof thermal properties and investigation of its energy performance, *Energy and Buildings* **33**(7)**:**719-729.

Nichol, J., Wong, M. S., 2005, Modeling urban environmental quality in a tropical city, *Landscape and urban planning* **73**(1)**:**49-58.

Nichol, J. E., 1994, Modelling the relationship between LANDSAT TM thermal data and urban morphology, in: *ACMS/ASPRS Annual Convention and Exposition*, Baltimore, United States.

Nieuwolt, S., 1966, The urban microclimate of Singapore, *The Journal of Tropical Geography* **22:**30-31.

Nikolopoulou, M., Baker, N., Steemers, K., 1999, Improvements to the globe thermometer for outdoor use, *Architectural Science Review* **42**(1)**:**27-34.

Nikolopoulou, M., Lykoudis, S., 2006, Thermal comfort in outdoor urban spaces: analysis across different European countries, *Building and Environment* **41**(11)**:**1455-1470.

Nikolopoulou, M., Lykoudis, S., 2007, Use of outdoor spaces and microclimate in a Mediterranean urban area, *Building and environment* **42**(10)**:**3691-3707.

Nikolopoulou, M., Steemers, K., 2003, Thermal comfort and psychological adaptation as a guide for designing urban spaces, *Energy and Buildings* **35**(1)**:**95-101.

Nkemdirim, L. C., 1972, A Note on the Albedo of Surfaces, *Journal of Applied Meteorology* **11**(5)**:**867-874.

Nobel, P. S., 1983, Biophysical plant physiology and ecology, WH Freeman San Francisco.

Norman, J. M., Campbell, G. S., Pearcy, R., Ehleringer, J., Mooney, H., Rundel, P., 1989, Canopy structure. Plant Physiological Ecology: Field Methods and Instrumentation**:** 301 - 325.

NYC, 2011, plaNYC – A greenery, greater New York.

Oke, T. R., 1988, Boundary layer climates, 2nd edn, Routledge, London.

Oke, T. R., 2006, Towards better scientific communication in urban climate, *Theoretical and Applied Climatology* **84**(1-3)**:**179-190.

Oke, T. R., Crowther, J., McNaughton, K., Monteith, J., Gardiner, B., 1989, The micrometeorology of the urban forest [and discussion], *Philosophical Transactions of the Royal Society of London. B, Biological Sciences* **324**(1223)**:**335-349.

Oliveira, S., Andrade, H., Vaz, T., 2011, The cooling effect of green spaces as a contribution to the mitigation of urban heat: A case study in Lisbon, *Building and environment* **46**(11)**:**2186-2194.

Ong, B. L., 2003, Green plot ratio: an ecological measure for architecture and urban planning, *Landscape and urban planning* **63**(4)**:**197-211.

Palmer, J., Chapman, K., 2000, Direct calculation of mean radiant temperature using radiant intensities, National Inst. of Standards and Technology, Gaithersburg, MD (US).

Panofsky, H. A., Townsend, A., 1964, Change of terrain roughness and the wind profile, *Quarterly Journal of the Royal Meteorological Society* **90**(384)**:**147-155.

Papadakis, G., Tsamis, P., Kyritsis, S., 2001, An experimental investigation of the effect of shading with plants for solar control of buildings, *Energy and Buildings* **33**(8)**:**831-836.

Parizotto, S., Lamberts, R., 2011, Investigation of green roof thermal performance in temperate climate: A case study of an experimental building in Florianópolis city, Southern Brazil, *Energy and Buildings* **43**(7)**:**1712-1722.

Parker, J., 1981, Use of landscaping for energy conservation, *Department of Physical Sciences, Florida International University, Miami, FL*.

Parkhurst, D. F., Loucks, O. L., 1972, Optimal Leaf Size in Relation to Environment, *Journal of Ecology* **60**(2)**:**505-537.

Parsons, K. C., 2003, Human thermal environments: the effect of hot, moderate and cold environments on human health, comfort and performance, *Taylor & Francis, New York*.

Pearcy, R. W., Ehleringer, J. R., Mooney, H. A., Rundel, P. W., 1989, Plant physiological ecology: field methods and instrumentation, Chapman and Hall Ltd.

Peck, S. W., Callaghan, C., Kuhn, M. E., Bass, B., 1999, Greenbacks from green roofs: forging a new industry in Canada, CMHC/SCHL.

Penman, H. L., 1948, Natural evaporation from open water, bare soil and grass, *Proceedings of the Royal Society of London. Series A. Mathematical and Physical Sciences* **193**(1032)**:**120-145.

Pérez-Harguindeguy, N., Díaz, S., Garnier, E., Lavorel, S., Poorter, H., Jaureguiberry, P., Bret-Harte, M. S., Cornwell, W. K., Craine, J. M., Gurvich, D. E., Urcelay, C., Veneklaas, E. J., Reich, P. B., Poorter, L., Wright, I. J., Ray, P., Enrico, L., Pausas, J. G., de Vos, A. C., Buchmann, N., Funes, G., Quétier, F., Hodgson, J. G., Thompson, K., Morgan, H. D., ter Steege, H., van der Heijden, M. G. A., Sack, L., Blonder, B., Poschlod, P., Vaieretti, M. V., Conti, G., Staver, A. C., Aquino, S., Cornelissen, J. H. C., 2013, New handbook for standardised measurement of plant functional traits worldwide, *Australian Journal of Botany* **61**(3)**:**167-234.

Pérez, G., Rincón, L., Vila, A., González, J. M., Cabeza, L. F., 2011, Green vertical systems for buildings as passive systems for energy savings, *Applied energy* **88**(12)**:**4854-4859.

Perini, K., Ottelé, M., Fraaij, A., Haas, E., Raiteri, R., 2011, Vertical greening systems and the effect on air flow and temperature on the building envelope, *Building and Environment* **46**(11)**:**2287-2294.

Picot, X., 2004, Thermal comfort in urban spaces: impact of vegetation growth: Case study: Piazza della Scienza, Milan, Italy, *Energy and Buildings* **36**(4)**:**329-334.

Pieri, P., Fuchs, M., 1990, Comparison of Bowen ratio and aerodynamic estimates of evapotranspiration, *Agricultural and forest meteorology* **49**(3)**:**243-256.

Price, C. A., Symonova, O., Mileyko, Y., Hilley, T., Weitz, J. S., 2011, Leaf Extraction and Analysis Framework Graphical User Interface: Segmenting and Analyzing the Structure of Leaf Veins and Areoles, *Plant Physiology* **155:**236-245.

Priestley, C. H. B., Taylor, R. J., 1972, On the Assessment of Surface Heat Flux and Evaporation Using Large-Scale Parameters, *Monthy Weather Review* **100:**81–92.

Raeissi, S., Taheri, M., 1999, Energy saving by proper tree plantation, *Building and Environment* **34**(5)**:**565-570.

Rana, G., Katerji, N., 2000, Measurement and estimation of actual evapotranspiration in the field under Mediterranean climate: a review, *European Journal of Agronomy* **13**(2)**:**125-53.

Ranson, K. J., Vanderbilt, V., Biehl, L., Robinson, B., Bauer, M., 1981, Soybean canopy reflectance as a function of view and illumination geometry, in: *International Symposium on Remote Sensing of Environment, 15 th, Ann Arbor, MI*, pp. 853-865.

Reich, P. B., Wright, I. J., Cavender-Bares, J., Craine, J. M., Oleksyn, J., Westoby, M., Walters, M. B., 2003, The evolution of plant functional variation : traits, spectra, and strategies, *International Journal of Plant Sciences* **164**(S3)**:**143-164.

Reicosky, D., Peters, D., 1977, A portable chamber for rapid evapotranspiration measurements on field plots, *Agronomy Journal* **69**(4)**:**729-732.

Reicosky, D., Sharratt, B., Ljungkull, J., Baker, D., 1983, Comparison of alfalfa evapotranspiration measured by a weighing lysimeter and a portable chamber, *Agricultural meteorology* **28**(3)**:**205-211.

Rhoads, A. G., Hamburg, S. P., Fahey, T. J., Siccama, T. G., Kobe, R., 2004, Comparing direct and indirect methods of assessing canopy structure in a northern hardwood forest, *Canadian Journal of Forest Research* **34**(3)**:**584-591.

Rich, P. M., 1990, Characterizing plant canopies with hemispherical photographs, *Remote Sensing Reviews* **5:**13-29.

Rosenfeld, A. H., Akbari, H., Romm, J. J., Pomerantz, M., 1998, Cool communities: strategies for heat island mitigation and smog reduction, *Energy and Buildings* **28**(1)**:**51-62.

Roth, M., Oke, T. R., Emery, W. J., 1989, Satellite-derived urban heat islands from three coastal cities and the utilization of such data in urban climatology. , *International Journal of Remote Sensing* **10:**1699-1720.

Royer, D. L., McElwain, J. C., Adams, J. M., Wilf, P., 2008, Sensitivity of leaf size and shape to climate within Acer rubrum and Quercus kelloggii, *New Phytologist* **179**(3)**:**808-817.

Rudie Jr, R. J., Dewers, R. S., 1984, Effects of tree shade on home cooling requirements, *Journal of arboriculture* **10:**320-322.

Ryel, R. J., Beyschlag, W., Caldwell, M., 1993, Foliage Orientation and Carbon Gain in Two Tussock Grasses as Assessed With a New Whole-Plant Gas-Exchanage Model, *Functional Ecology* **7**(1)**:**115-124.

Saadatian, O., Sopian, K., Salleh, E., Lim, C. H., Riffat, S., Saadatian, E., Toudeshki, A., Sulaiman, M. Y., 2013, A review of energy aspects of green roofs, *Renewable and Sustainable Energy Reviews* **23:**155-168.

Sad de Assis, E., Barros Frota, A., 1999, Urban bioclimatic design strategies for a tropical city, *Atmospheric Environment* **33**(24)**:**4135-4142.

Saito, I., Ishihara, O., Katayama, T., 1991, Study of the effect of green areas on the thermal environment in an urban area, *Energy and Buildings* **15**(3)**:**493-498.

Sander, H., Polasky, S., Haight, R. G., 2010, The value of urban tree cover: a hedonic property price model in Ramsey and Dakota Counties, Minnesota, USA, *Ecological Economics* **69**(8)**:**1646-1656.

Santamouris, M., 2014, Cooling the cities–a review of reflective and green roof mitigation technologies to fight heat island and improve comfort in urban environments, *Solar Energy* **103:**682-703.

Seginer, I., 1969, The effect of albedo on the evapotranspiration rate, *Agricultural Meteorology* **6**(1)**:**5-31.

Shahidan, M. F., Jones, P. J., Gwilliam, J., Salleh, E., 2012, An evaluation of outdoor and building environment cooling achieved through combination modification of trees with ground materials, *Building and environment* **58:**245-257.

Shahidan, M. F., Shariff, M. K., Jones, P., Salleh, E., Abdullah, A. M., 2010, A comparison of Mesua ferrea L. and Hura crepitans L. for shade creation and radiation modification in improving thermal comfort, *Landscape and Urban Planning* **97**(3)**:**168-181.

Shashua-Bar, L., Hoffman, M., 2000, Vegetation as a climatic component in the design of an urban street: An empirical model for predicting the cooling effect of urban green areas with trees, *Energy and Buildings* **31**(3)**:**221-235.

Shashua-Bar, L., Hoffman, M., 2002, Quantitative Evaluation of the Effects of Built-Up Geometry and Trees on Diurnal Air Temperature in Canyon-Type Courtyards, *Advances in Building Technology* **2**(3)**:**1493-1500.

Shashua-Bar, L., Hoffman, M. E., 2003, Geometry and orientation aspects in passive cooling of canyon streets with trees, *Energy and Buildings* **35**(1)**:**61-68.

Shashua-Bar, L., Hoffman, M. E., 2004, Quantitative evaluation of passive cooling of the UCL microclimate in hot regions in summer, case study: urban streets and courtyards with trees, *Building and Environment* **39**(9)**:**1087-1099.

Shashua-Bar, L., Tsiros, I. X., Hoffman, M. E., 2010, A modeling study for evaluating passive cooling scenarios in urban streets with trees. Case study: Athens, Greece, *Building and Environment* **45**(12)**:**2798-2807.

Simpson, J. R., 2002, Improved estimates of tree-shade effects on residential energy use, *Energy and Buildings* **34**(10)**:**1067-1076.

Simpson, J. R., McPherson, E. G., 1996, Potential of tree shade for reducing residential energy use in California, *Journal of Arboriculture* **22:**10-18.

Sitawati, S. M. S., Guritno, B., Suryanto, A., 2011, Ability of trees in reducing air temperature, *Journal of Applied Environmental and Biological Sciences* **1**(11)**:**533-537.

Slatyer, R., McIlroy, I., 1961, Practical Microclimatology, *Practical Microclimatology.*

Smit, B., 1993, Adaptation to climatic variability and change, in: *Report of the taskforce on climate adaptation, the Canadian Climate Program*, Department of Geography, University of Guelph.

Smithson, P., Addison, K., Atkinson, K., 2002, Fundamentals of the physical environment, Routledge.

Song, J., 1998, Diurnal asymmetry in surface albedo, *Agricultural and Forest Meteorology* **92**(3)**:**181-189.

Southwood, T. R. E., 1977, Habitat, the template for ecological strategies?, *Journal of Animal Ecology* **46:**337-365.

Stannard, D. I., 1988, Use of a hemispherical chamber for measurement of evapotranspiration, Department of the Interior, US Geological Survey.

Stathopoulos, T., Chiovitti, D., Dodaro, L., 1994, Wind shielding effects of trees on low buildings, *Building and Environment* **29**(2)**:**141-150.

Steele, J., 1997, Sustainable architecture : principles, paradigms, and case studies, McGraw-Hill, New York.

Stewart, J. B., 1971, The albedo of a pine forest, *Quarterly Journal of the Royal Meteorological Society* **97**(414)**:**561-564.

Steyn, D. G., Oke, T. R., 1980, Effects of a small scrub fire on the surface radiation budget, *Weather* **35**(7)**:**212-215.

Stocks, C. E., Wise, S., 2000, The Role of GIS in Environmental Modelling, *Geographical and Environmental Modelling* **4**(2)**:**219-235.

Streiling, S., Matzarakis, A., 2003, Influence of single and small clusters of trees on the bioclimate of a city: a case study, *Journal of Arboriculture* **29**(6)**:**309-316.

Swinbank, W., 1951, The Measurement of Vertical Transfer of Heat and Water Vapor by Eddies in the Lower Atmosphere, *Journal of Atmospheric Sciences* **8:**135-145.

Sydney, C. o., 2011, Greening Sydney plan. 2011.

Tabachnick, B. G., Fidell, L. S., 2001, Using Multivariate Statistics, Allyn and Bacon, Boston, MA.

Taha, H., 1994, Aircraft-based albedo measurements over the south coast air basin in: *Analysis of Energy Efficiency of Air Quality in the South Coast Air Basin* (H. Taha, ed.), Lawrence Berkeley National Laboratory Berkeley, CA, pp. 43-59.

Taha, H., 1997, Urban climates and heat islands: albedo, evapotranspiration, and anthropogenic heat, *Energy and Buildings* **25**(2)**:**99-103.

Taha, H., Akbari, H., Rosenfeld, A., 1991, Heat island and oasis effects of vegetative canopies: Micro-meteorological field-measurements, *Theoretical and Applied Climatology* **44**(2)**:**123-138.

Taha, H., Sailor, D. J., Akbari, H., 1992, High-albedo materials for reducing building cooling energy use, in: *Lawrence Berkeley Laboratory Report 31721 UC-350*, Berkeley, California

Takahashi, K., Yoshida, H., Tanaka, Y., Aotake, N., Wang, F., 2004, Measurement of thermal environment in Kyoto City and its prediction by CFD simulation, *Energy and Buildings* **16:**771–779.

Takano, T., Nakamura, K., Watanabe, M., 2002, Urban residential environments and senior citizens' longevity in megacity areas: the importance of walkable green spaces, *Journal of epidemiology and community health* **56**(12)**:**913-918.

Takebayashi, H., Moriyama, M., 2007, Surface heat budget on green roof and high reflection roof for mitigation of urban heat island, *Building and Environment* **42**(8)**:**2971-2979.

Tan, A., Chiang, K., 2009, Vertical Greenery for the Tropics Centre for Urban Greenery and Ecology, Nparks, Singapore.

Tan, C. L., Wong, N. H., Jusuf, S. K., 2013a, Outdoor mean radiant temperature estimation in the tropical urban environment, *Building and Environment* **64:**118-129.

Tan, P. Y., 2012, Singapore, a vertical Garden City in the making, (Architecture and Urbanism Special Edition)**:**138 - 141.

Tan, P. Y., Sia, A., 2008, A selection of plants for green roofs in Singapore, Centre for Urban Greenery and Ecology.

Tan, P. Y., Sia, A., 2009, Leaf Area Index of tropical plants: A guidebook on its use in the calculation of green plot ratio. , National Parks Board.

Tan, P. Y., Wang, J., Sia, A., 2013b, Perspectives on five decades of the urban greening of Singapore, *Cities* **32:**24-32.

Tanner, C., 1960, Energy balance approach to evapotranspiration from crops, *Soil Science Society of America Journal* **24**(1)**:**1-9.

Tenhunen, J. D., Pearcy, R. W., Lange, O. L., 1987, Diurnal variations in leaf conductance and gas exchange in natural environments, in: *Stomatal Function* (E. Zeiger, G. D. Farquhar, I. R. Cowan, eds.), Stanford University Press, Stanford, California, pp. 312-351.

Thomas, S. C., 1996, Asymptotic Height as a Predictor of Growth and Allometric Characteristics in Malaysian Rain Forest Trees, *American Journal of Botany* **83**(5)**:**556-566.

Thorsson, S., Lindberg, F., Eliasson, I., Holmer, B., 2007, Different methods for estimating the mean radiant temperature in an outdoor urban setting, *International Journal of Climatology* **27**(14)**:**1983-1993.

Tooke, T. R., Coops, N. C., Voogt, J. A., Meitner, M. J., 2011, Tree structure influences on rooftop-received solar radiation, *Landscape and Urban Planning* **102**(2)**:**73-81.

Troy, A., Grove, J. M., 2008, Property values, parks, and crime: A hedonic analysis in Baltimore, MD, *Landscape and Urban Planning* **87**(3)**:**233-245.

Troy, A., Morgan Grove, J., O'Neil-Dunne, J., 2012, The relationship between tree canopy and crime rates across an urban–rural gradient in the greater Baltimore region, *Landscape and Urban Planning* **106**(3)**:**262-270.

Tsiros, I. X., 2010, Assessment and energy implications of street air temperature cooling by shade tress in Athens (Greece) under extremely hot weather conditions, *Renewable Energy* **35**(8)**:**1866-1869.

Uddin, J., Hancock, N., Smith, R., Foley, J., 2013, Measurement of evapotranspiration during sprinkler irrigation using a precision energy budget (Bowen ratio, eddy covariance) methodology, *Agricultural Water Management* **116:**89-100.

UN, 2004, World Urbanization Prospectus 2004.

URA, 2009, Guidelines For Landscape Replacement Areas Within New Developments in (Part) Downtown Core, (Part) Straits View, (Part) Kallang and (Part) Jurong East Planning Areas.

URA, 2014a, Guidelines for landscape replacement areas within new developments and redevelopments.

URA, 2014b, LUSH 2.0: Extending the greenery journey skywards.

Valladares, F., Pugnaire, F. I., 1999, Tradeoffs between irradiance capture and avoidance in semi-arid environments assessed with a crown architecture model, *Annals of Botany* **83**(4)**:**459-469.

Van Elsacker, P., Keppens, H., Impens, I., 1983, A simple photographical method for analyzing the radiation interception by an individual tree, *Agricultural Meteorology* **29**(4)**:**285-298.

Van Renterghem, T., Hornikx, M., Forssen, J., Botteldooren, D., 2012, The potential of building envelope greening to achieve quietness, *Building and environment* **61:**34-44.

VDI, 1994, Environmental meteorology, interactions between atmosphere and surface; calculation of short-and long wave radiation (Part I: Climate, VDI 3789, Part 2: VDI/DIN- Handbuch Reinhaltung der Luft, Band 1b, Düsseldorf.).

Vernon, H. M., 1932, The measurement of radiant temperature in relation to human comfort, *Journal of Industrial Hygiene* **14:**95-111.

Voogt, J. A., 2004, Urban Heat Islands: Hotter Cities, Action BioScience.

Wang, F., 2006, Modelling sheltering effects of trees on reducing space heating in office buildings in a windy city, *Energy and buildings* **38**(12)**:**1443-1454.

Watson, D. J., 1947, Comparative physiological studies on the growth of field crops: I. Variation in net assimilation rate and leaf area between species and varieties, and within and between years, *Annals of Botany* **11**(1)**:**41-76.

Webb, E., 1965, Aerial microclimate, *Meteorological monographs* **6**(28)**:**27-58.

Weiher, E., van der Werf, A., Thompson, K., Roderick, M., Garnier, E., Eriksson, O., 1999, Challenging Theophrastus: A common core list of plant traits for functional ecology, *Journal of Vegetation Science* **10**(5)**:**609-620.

Weihs, P., Staiger, H., Tinz, B., Batchvarova, E., Rieder, H., Vuilleumier, L., Maturilli, M., Jendritzky, G., 2012, The uncertainty of UTCI due to uncertainties in the determination of radiation fluxes derived from measured and observed meteorological data, *International journal of biometeorology* **56**(3)**:**537-555.

Weng, Q., Yang, S., 2004, Managing the adverse thermal effects of urban development in a densely populated Chinese city, *Journal of Environmental Management* **70**(2)**:**145-156.

Werner, C., Ryel, R. J., Correia, O., Beyschlag, W., 2001, Structural and functional variability within the canopyand its relevance for carbon gain and stress avoidance, *Acta Oecologica* **22**(2)**:**129-138.

Westoby, M., Falster, D. S., Moles, A. T., Vesk, P. A., Wright, I. J., 2002, Plant ecological strategies: Some leading dimensions of variation between species, *Annual Review of Ecology and Systematics* **33**(1)**:**125-159.

Westoby, M., Wright, I. J., 2006, Land-plant ecology on the basis of functional traits, *Trends in Ecology & Evolution* **21**(5)**:**261-268.

Wilmers, F., 1991, Effects of vegetation on urban climate and buildings, *Energy and buildings* **15**(3)**:**507-514.

Wilson, J. W., 1959, Analysis of the spatial distribution of foliage by two - dimensional point quadrats, *New phytologist* **58**(1)**:**92-99.

Wilson, J. W., 1965, Point quadrat analysis of foliage distribution for plants growing singly or in rows, *Australian Journal of Botany* **13**(3)**:**405-409.

Wolverton, B., Wolverton, J. D., 1993, Plants and soil microorganisms: removal of formaldehyde, xylene, and ammonia from the indoor environment, *Journal of the Mississippi Academy of Sciences* **38**(2)**:**11-15.

Wolverton, B. C., Douglas, W. L., Bounds, K., 1989, A study of interior landscape plants for indoor air pollution abatement, Stennis Space Center, MS:Science and Technology Laboratory, John C. Stennis Space Center, National Aeronautics and Space Administration.

Wong, N. H., Chen, Y., 2005, Study of green areas and urban heat island in a tropical city, *Habitat International* **29**(3)**:**547-558.

Wong, N. H., Chen, Y., 2006a, A comparison of two rooftop systems in tropical climates, in: *2nd iNTA Conference Proceedings*, Jogjakarta, Indonesia.

Wong, N. H., Chen, Y., 2006b, Thermal benefits of city parks, *Energy and Buildings* **38**(2)**:**105-120.

Wong, N. H., Chen, Y., Ong, C. L., Sia, A., 2003a, Investigation of thermal benefits of rooftop garden in the tropical environment, *Building and environment* **38**(2)**:**261-270.

Wong, N. H., Chen, Y., Wong, V. L., Lee, S. E., Cheong, K. W., Lim, G. T., Ong, C. L., Sia, A., 2002, The thermal effects of plants on buildings, *Architectural Science Review* **45:**1-12.

Wong, N. H., Cheong, D. K. W., Yan, H., Soh, J., Ong, C. L., Sia, A., 2003b, The effects of rooftop garden on energy consumption of a commercial building in Singapore, *Energy and Buildings* **35**(4)**:**353-364.

Wong, N. H., Kwang Tan, A. Y., Chen, Y., Sekar, K., Tan, P. Y., Chan, D., Chiang, K., Wong, N. C., 2010a, Thermal evaluation of vertical greenery systems for building walls, *Building and environment* **45**(3)**:**663-672.

Wong, N. H., Kwang Tan, A. Y., Tan, P. Y., Chiang, K., Wong, N. C., 2010b, Acoustics evaluation of vertical greenery systems for building walls, *Building and environment* **45**(2)**:**411-420.

Wong, N. H., Tan, A. Y. K., Tan, P. Y., Wong, N. C., 2009, Energy simulation of vertical greenery systems, *Energy and buildings* **41**(12)**:**1401-1408.

Wong, N. H., Tan, P. Y., Chen, Y., 2007, Study of thermal performance of extensive rooftop greenery systems in the tropical climate, *Building and environment* **42**(1)**:**25-54.

Woolley, J. T., 1971, Reflectance and transmittance of light by leaves, *Plant Physiol.* **47:**656-662.

Xing, Z., Chow, L., Meng, F.-R., Rees, H. W., Steve, L., Monteith, J., 2008, Validating evapotranspiraiton equations using bowen ratio in New Brunswick, Maritime, Canada, *Sensors* **8**(1)**:**412-428.

Yan, H., Wang, X., Hao, P., Dong, L., 2012, Study on the microclimatic characteristics and human comfort of park plant communities in summer, *Procedia Environmental Sciences* **13:**755-765.

Yeh, G. T., Brutsaert, W., 1971, Sensitivity of the Solution for Heat Flux or Evaporation to Off - Diagonal Turbulent Diffusivities, *Water Resources Research* **7**(3)**:**734-735.

Yoshida, S., 2006, Development of three dimensional plant canopy model for numerical simulation of outdoor thermal environment, in: *the 6th International Conference on Urban Climate (ICUC 6), Goteborg, Sweden, June 12-16, 2006*.

Zeiger, E., Farquhar, G. D., Cowan, I. R., 1987, Stomatal Function, Stanford University Press, Stanford, California.

Zhang, B., Kang, S., Li, F., Zhang, L., 2008, Comparison of three evapotranspiration models to Bowen ratio-energy balance method for a vineyard in an arid desert region of northwest China, *Agricultural and Forest Meteorology* **148**(10)**:**1629-1640.

Zhao, J., 2011, Towards Sustainable Cities in China, Springer.

10 APPENDIX

10.1 Large scale urban mapping of mean radiant temperature

Content from Chapter 10.1 (Pages 212 to 223) has been published in the Journal of Building and Environment, for which I am the main author:

Tan, C.L., Wong, N.H., Jusuf, S.K., 2013, Outdoor mean radiant temperature estimation in the tropical urban environment, *Building and Environment* 64:118-129.

It was also presented in:

Wong, N.H., Jusuf, S.K., **Tan, C.L**., Chia, P.Y., 2012, Outdoor mean radiant temperature measurement in the tropical urban environment, *iNTA 2012*, National University of Singapore, Singapore. Oral Presentation, Published in proceedings.

10.1.1 Objective

The purpose of this study is to observe the diurnal t_{mrt} profile of the outdoor environment and to identify any relation between t_{mrt} and the corresponding urban typology.

10.1.2 Methodology

An urban scale mapping of t_{mrt} is conducted after the recalibration of the t_{mrt} formula with the intention of understanding the diurnal t_{mrt} profile of highly urbanized areas. The measurement areas are categorized into the following:

- Area with high density commercial buildings;
- Area in close proximity to a large water body;
- Area with high density residential buildings;
- Park.

Singapore has a tropical climate. Near-surface air temperature usually ranges from 23 °C to 32 °C. April and May are the warmer months and the monsoon period is from November to March (NEA, 2011) . The first site, Site A, is located in the Central Business District (CBD) of Singapore. The second site, Site B, is in the residential area of eastern Singapore. The locations of the measurement points are shown in Figure 98.

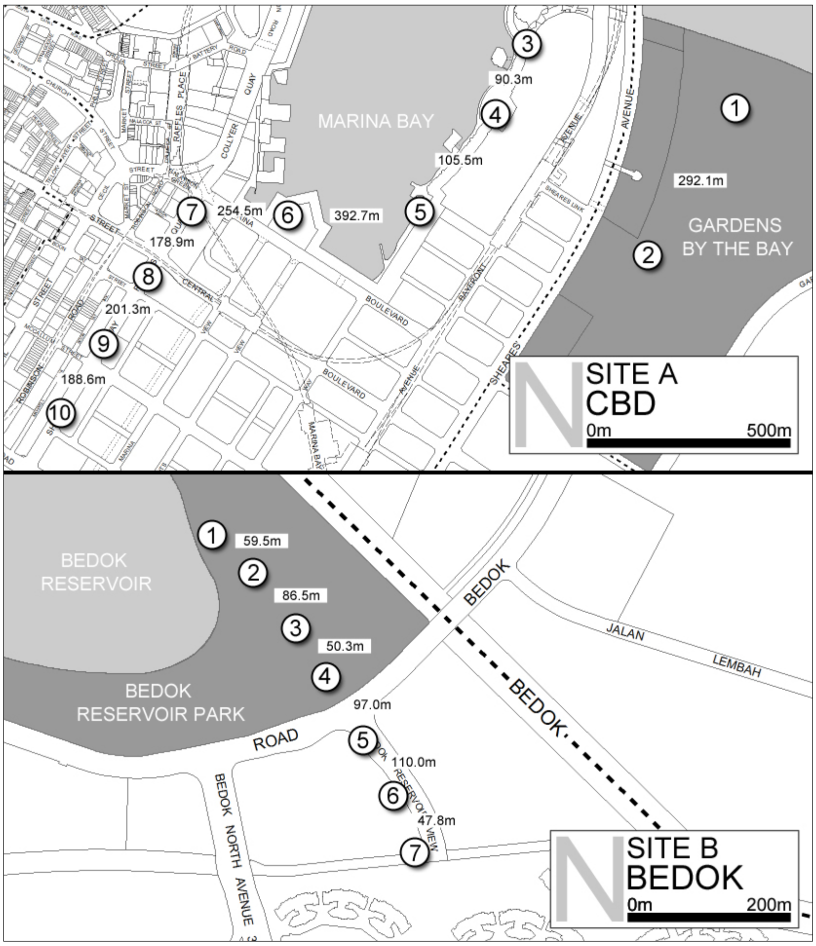

Figure 98. Sites A and B

Characteristics of both sites are shown in Table 32.

Table 32. Site Characteristics

Site	**A**			**B**	
Location	Shenton Way	Marina Bay Sands Casino	Gardens by the Bay	Bedok Reservoir Park	Bedok Reservoir View
Characteristic	High Density Commercial Buildings	Large Waterbody	Park	Park	High Density Residential
Number of measurement points	4	4	2	4	3

Measurements are conducted for a total of four months in 2012. Only days of clear, sunny weather are used for analysis (Table 33). The term clear, sunny weather is defined by scrutinizing the hourly solar irradiance profile and ensuring a smooth curve of at peak of at least 700 Wm^{-2} at the hottest time of the day. Equipment used for measurement is show in Table 8.

Table 33. Measurement period

	Site A	**Site B**
Measurement period	March to April 2012	April to June 2012
Dates used for analysis	15/03/2012 16/03/2012 17/03/2012 01/04/2012 04/04/2012 13/04/2012 15/04/2012 18/04/2012 23/04/2012 -	13/04/2012 16/04/2012 23/04/2012 26/04/2012 27/04/2012 28/04/2012 09/05/2012 10/05/2012 16/05/2012 06/06/2012

10.1.3 Results and discussion

10.1.3.1 Diurnal t_{mrt} profiles of Site A and Site B

Days selected for analysis for both sites are shown in Table 33. Solar irradiance is plotted for all relevant days and the diurnal profile is used to determine the clear, sunny days to be used for analysis.

The diurnal t_{mrt} profiles of all ten measurement points in Site A are shown in Figure 99. Measurements are taken every minute and averaged to one hour intervals. Two distinctive trends can be observed. Points 1 to 6 exhibit significantly higher values of t_{mrt} in the day, especially during the periods of 08:00 hrs to 12:00 hrs and 14:00 hrs to 18:00 hrs. In comparison, Points 7 to 10 recorded lower values of t_{mrt}. The higher values recorded for Points 7 to 10 occur during the period of 11:30 hrs to 14:00 hrs. Points 1 to 6 are situated in the park and near a large water body, whereas Points 7 to 10 are located along a street surrounded by high rise commercial buildings.

The diurnal t_{mrt} profiles of all seven measurement points in Site B are also shown in Figure 99. Measurements are taken every minute and averaged to one hour intervals. Three distinctive trends can be observed. In general, Points 3 and 4 exhibit the lowest t_{mrt} profiles during the day. Points 1 and 2 exhibit slightly higher readings, especially after 12:00 hrs. Points 5 to 7 exhibit the highest readings. Points 1 to 4 are situated in the park, whereas Points 5 to 7 are located along high rise residential buildings.

The measurements are plotted against solar irradiance. The difference in t_{mrt} of the maximum and minimum points for Sites A and B are 23.2 °C and 14.3 °C respectively.

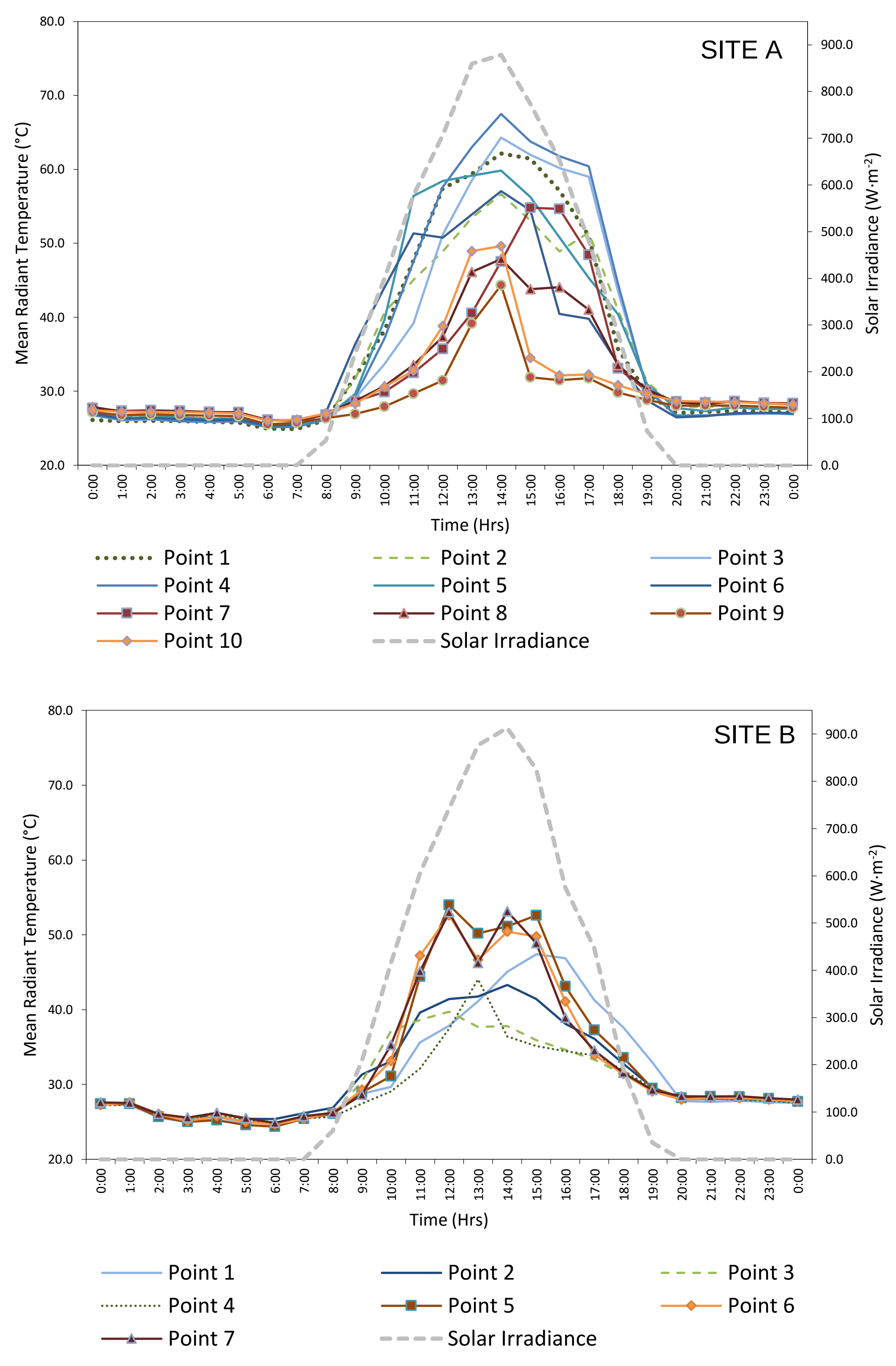

Figure 99. Diurnal profiles of t_{mrt} for Site A and Site B

10.1.3.2 Comparison with Sky View Factor (SVF)

The t_{mrt} profile for both sites are analysed with respect to urban morphology. There is a significant difference in t_{mrt} profile between measurement points along the streets of high rise buildings and the other areas. The Sky View Factor (SVF), which is an indirect representation of built morphology, is used to identify any significant correlation. The SVF value for each measurement point is calculated by first taking a photograph of each point using a fisheye lens. Each photograph is subsequently processed using the RayMan software (Matzarakis et al., 2010).

Values of SVF for all measurement points in Site A and Site B are shown in Table 34. A scatterplot is made for the hottest time of the day for both sites. Scatterplots of the SVF and t_{mrt} values show that there is a correlation between SVF and t_{mrt} (Figure 100).

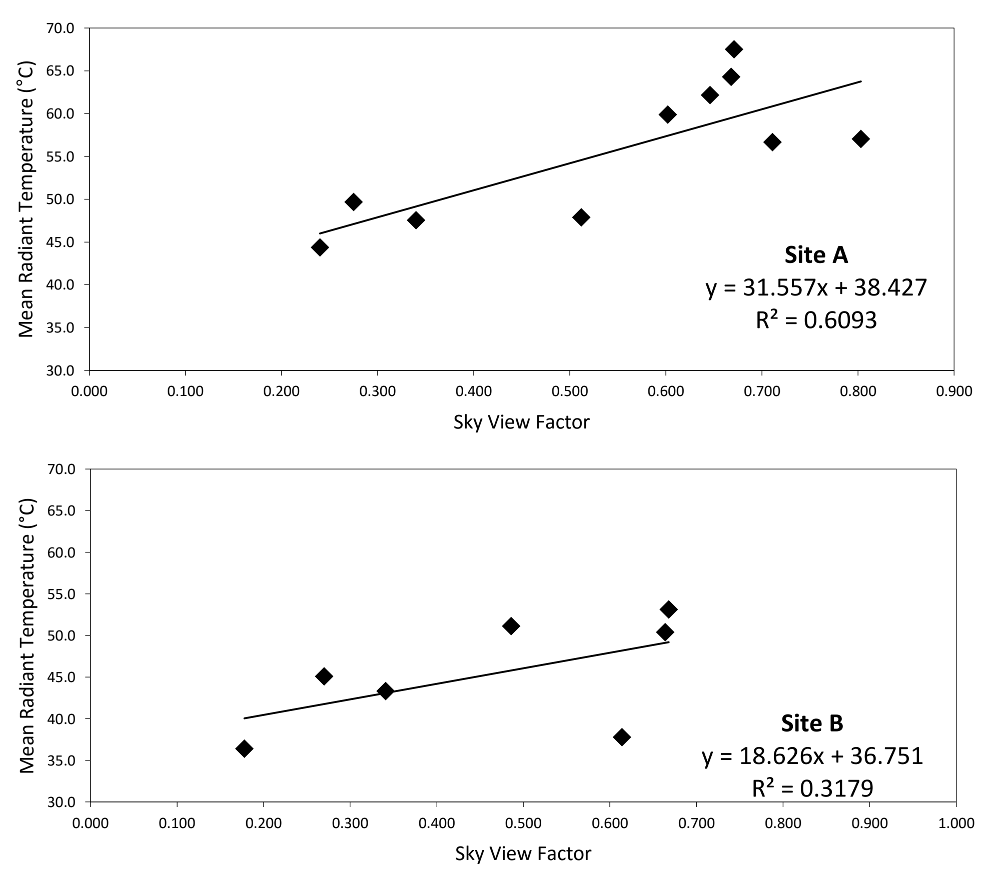

Figure 100. Scatterplots of t_{mrt} and SVF for Site A and Site B at 14:00 hrs

10.1.3.3 Influence of urban constituents on t_{mrt}

Figure 99 shows that buildings affect the t_{mrt} differently for both sites. While the t_{mrt} is the lowest along the high-rise buildings for Site A, the reverse is true for Site B. Although the measurement points are surrounded by high-rise buildings, there is a significant difference between the SVF values for the points in the two sites (Table 34).

Table 34. SVF values for measurement points in Site A and Site B

Measurement Point	Site A	Site B
1	0.646	0.270
2	0.711	0.341
3	0.668	0.614
4	0.671	0.178
5	0.602	0.486
6	0.803	0.664
7	0.340	0.668
8	0.512	-
9	0.240	-
10	0.275	-

The t_{mrt} profile for Site A shows that measurement points near large water bodies actually exhibited the highest t_{mrt} values. Corresponding SVF values are also relatively higher, when compared to the other points. Points 1 and 2 for Site B, while located in the park, show higher t_{mrt} profiles when compared to other measurement points within the park.

Measurement points in Site A show significantly higher readings than those in Site B. This may be due to the fact that there are much more trees in Site B than in Site A, and that the primary function of the trees is to block direct short wave radiation from the sun, rather than reduce the temperature by means of evapotranspiration. The corresponding SVF also supports the correlation between SVF value and t_{mrt}.

10.1.3.4 Estimation of t_{mrt} in the absence of sunlight

In the absence of sunlight, the t_{mrt} values do not fluctuate greatly. This is evident in the diurnal profiles of the two Sites (Figure 99). The difference between the maximum and minimum t_{mrt} values for Site A in the absence of sunlight is 1.3 °C. The difference between the maximum and minimum t_{mrt} values for Site B in the absence of sunlight is 1.0 °C.

The t_{mrt} profile is plotted at 5 minute intervals from 00:00 hrs to 07:00 hrs for both sites (Figure 101). The t_{mrt} profile is fairly constant for Site A, with a slight dip from 05:15 hrs onwards. This dip is observed until 05:35 hrs, and the average decrease in t_{mrt} is 1.6 °C. The dip is more frequent and significant for Site B. The first dip occurred from 01:25 hrs to 01:55 hrs. Point 5 exhibited the largest drop of 4.8 °C. The second dip occurred from 03:50 hrs to 04:15 hrs. Point 5 exhibited the largest drop of 2.2 °C. The final dip occurred from 04:55 hrs to 05:10 hrs. Point 5 exhibited the largest drop of 2.4 °C. Site B was surveyed to understand the drop in t_{mrt} from 01:25 hrs to 01:55 hrs. Wind and air temperature data was observed to have remained constant during the said period. Cloud cover was minimal. Infrared red imaging was used to survey the measurement site for changes in surface temperature. Measurements of the leave surface of trees indicate a slight decrease in temperature of less than 2.0 °C (Figure 102).

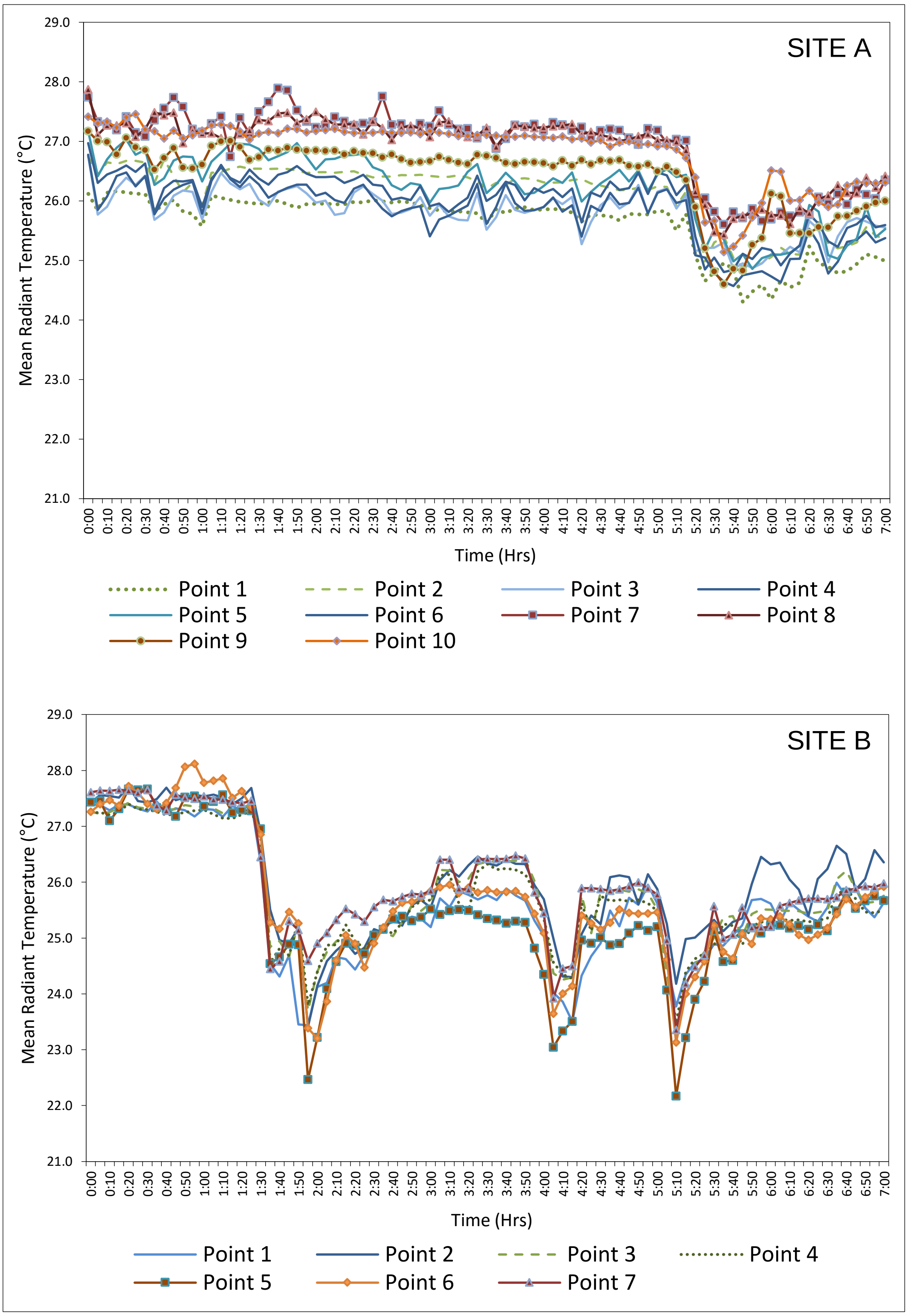

Figure 101. Profiles of t_{mrt} for Site A and Site B from 0:00 hrs to 07:00 hrs

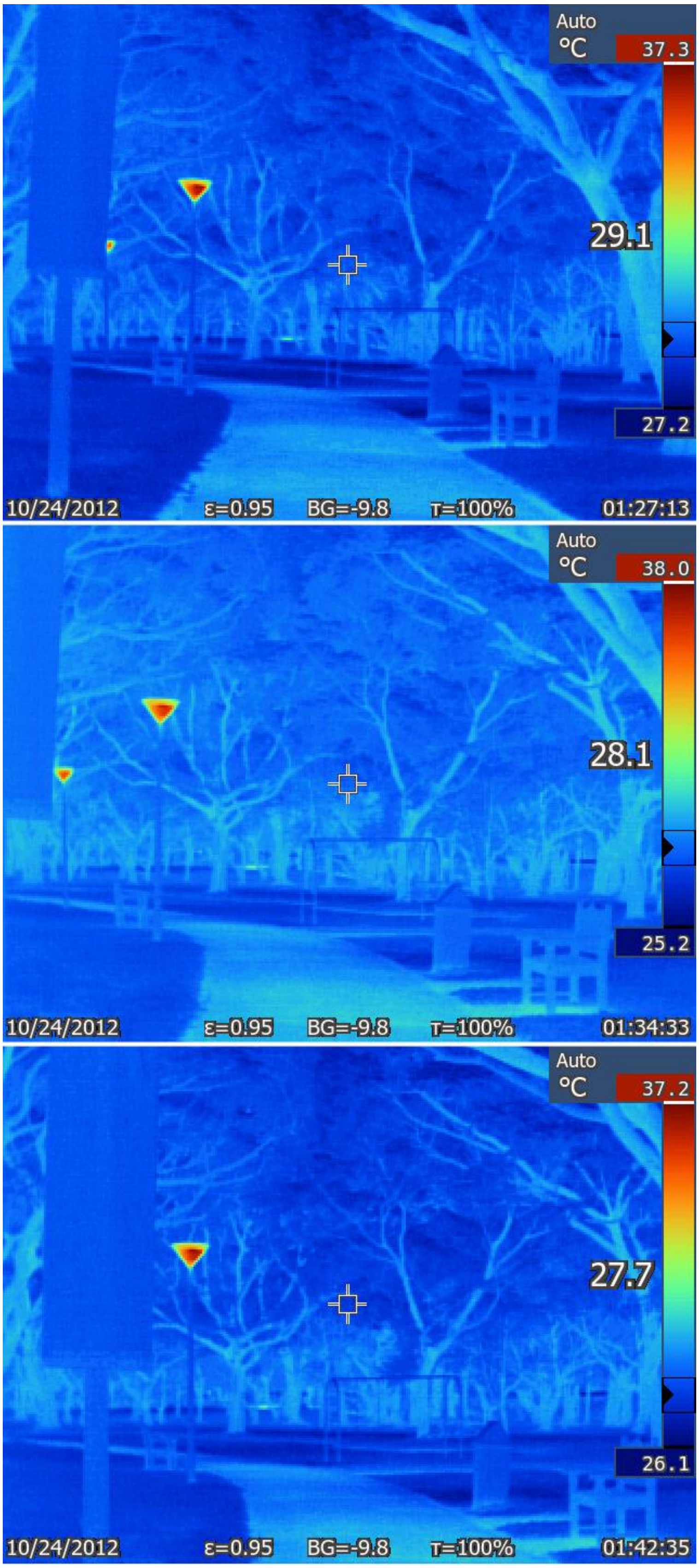

Figure 102. Thermal imaging of tree surface temperature for Site B

10.1.4 Conclusion

10.1.4.1 Characteristics of t_{mrt} profile in the urban environment

The objective of this study is to observe diurnal t_{mrt} behaviour in the urban environment in relation to urban constituents and to determine reasonable expectations for any attempts at reduction. Figure 99 shows that the t_{mrt} profile does not differ significantly in the absence of sunlight. Therefore, any attempt at lowering the t_{mrt} should logically be done only in daytime.

Since reduction of t_{mrt} is subjected to environmental limitations, it is important to identify a reasonable extent of influence to any proposed intervention via passive methods. Figure 99 shows that the peak t_{mrt} at Site A for Point 4 has the potential to be lowered, and by drawing reference to Point 9, a reasonable value would be by around 25 °C to approximately 43 °C. A possible way to quantify the reduction is by comparison of the SVF values of both points (Figure 103), and to propose additions to the landscape to lower the SVF (e.g. planting more trees).

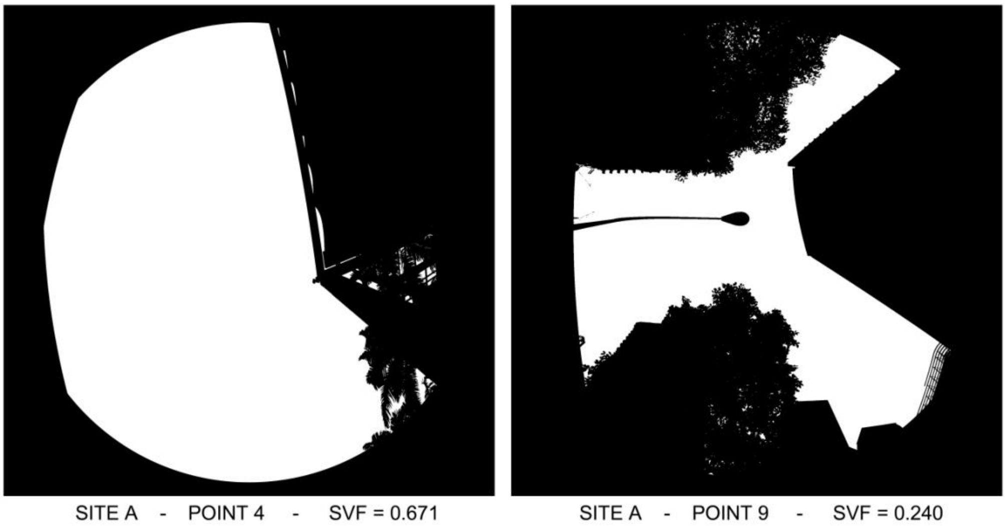

Figure 103. SVF of Point 4 and Point 9

Strategic placement of vegetation is essential for achieving the desired amount of t_{mrt} attenuation. Figure 99 shows that although the type and quantity of trees in Site B are similar throughout the park, the diurnal t_{mrt} profiles can be different. Measurement Point 1 exhibits a higher maximum t_{mrt} value, as well as at a much later time than Measurement Point 3. This may be due to the fact that Measurement Point 1 is next to a large clearing (water body) and is exposed to direct sunlight in the late afternoon. As each measurement point is isolated and analysed, it is possible to critique the t_{mrt} attenuation potential of the surrounding vegetation.

The dip in t_{mrt} profile in the absence of sunlight for Site B may be due to the large amount of vegetation found in Site B. There is a significant amount of vegetation in the park, and the trees may be the cause of the dip. While a slight decrease in surface temperature of the leaves are observed, it may not fully account for the dip. A more detailed study is required to ascertain the cause of the dips.

Most estimations of t_{mrt} are made in the form of spot readings and do not cover large areas. This presents a challenge to the comparison of t_{mrt} in different urban typologies. Diurnal measurements of t_{mrt} can help urban planners to appreciate the quality of outdoor urban spaces in view of thermal comfort. With the customised globe thermometer, air temperature sensor and anemometer, large scale measurements of the urban outdoor environment can be conducted. Measurement points with high values of t_{mrt} can be identified and lowered if necessary, so as to improve the quality of outdoor urban space.

10.2 Impact of plant height stratification on mean radiant temperature

10.2.1 Objective

The objective of this section of study is to observe the effect of height stratification above rooftop greenery plots on mean radiant temperature (t_{mrt}).

10.2.2 Methodology

Measurements of t_{mrt} are made for Plots 1 to 3 from Chapter 4. Measurement points are allocated at intervals above the plots. Details on measurement height are shown in Figure 104. Days used for analysis are shown in Table 35.

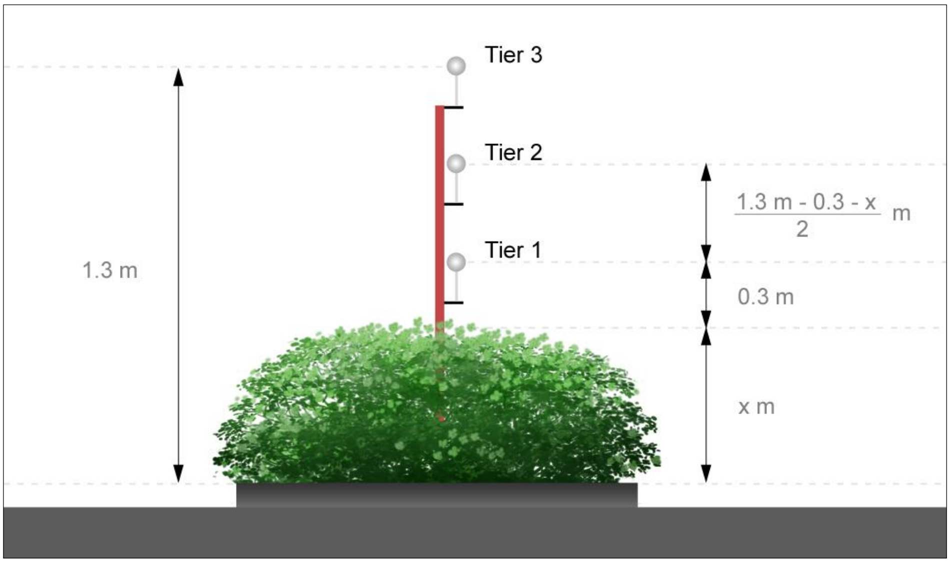

Height (m)	**Plot 1** **Phyllanthus cochinchinensis (m)**	**Plot 2** **Heliconia 'American Dwarf' (m)**	**Plot 3** **Sphagneticola trilobata (m)**	**Plot 4** **Concrete (m)**
x	0.30	1.19	0.46	0.00
Tier 1 x +0.3	0.60	1.49	0.76	0.30
Tier 2 $x + 0.3 + \frac{1.3 - 0.3 - x}{2}$	0.95	N.A.	1.03	0.80
Tier 3	1.30	2.00	1.30	1.30

Figure 104.Measurement points above rooftop greenery plot

Table 35. Days used for analysis

Measurement Period	Dates used for analysis during clear sky conditions
01/10/2013 to 24/01/2014	07/11/2013 08/11/2013 21/11/2013 27/11/2013 28/11/2013 02/01/2014
116 days	6 days

10.2.3 Results and discussion

Figure 105 shows the (6 days) averaged diurnal t_{mrt} profile of the rooftop greenery plots. It can be observed that in general, t_{mrt} for Plot 1 and Plot 2 increases with height. This result is logical as the cooling effect of greenery should naturally diminish with decreasing proximity. It is interesting to note that the t_{mrt} profile for Tiers 2 and 3 of Plot 3 are quite similar. This would suggest that the cooling effect of sphagneticola trilobata is evident for up to 1.3 m. Although the phyllanthus cochinchinensis shrub (Plot 1) is about the same height as sphagneticola trilobata (Plot 3), its cooling potential is significantly diminished beyond the 300 mm level. This makes sphagneticola trilobata a better plant in terms of being able to provide cooling. Therefore, in view of objectifying plant selection for the purpose of improving overall thermal comfort, sphagneticola trilobata may be rationalised as the preferred option.

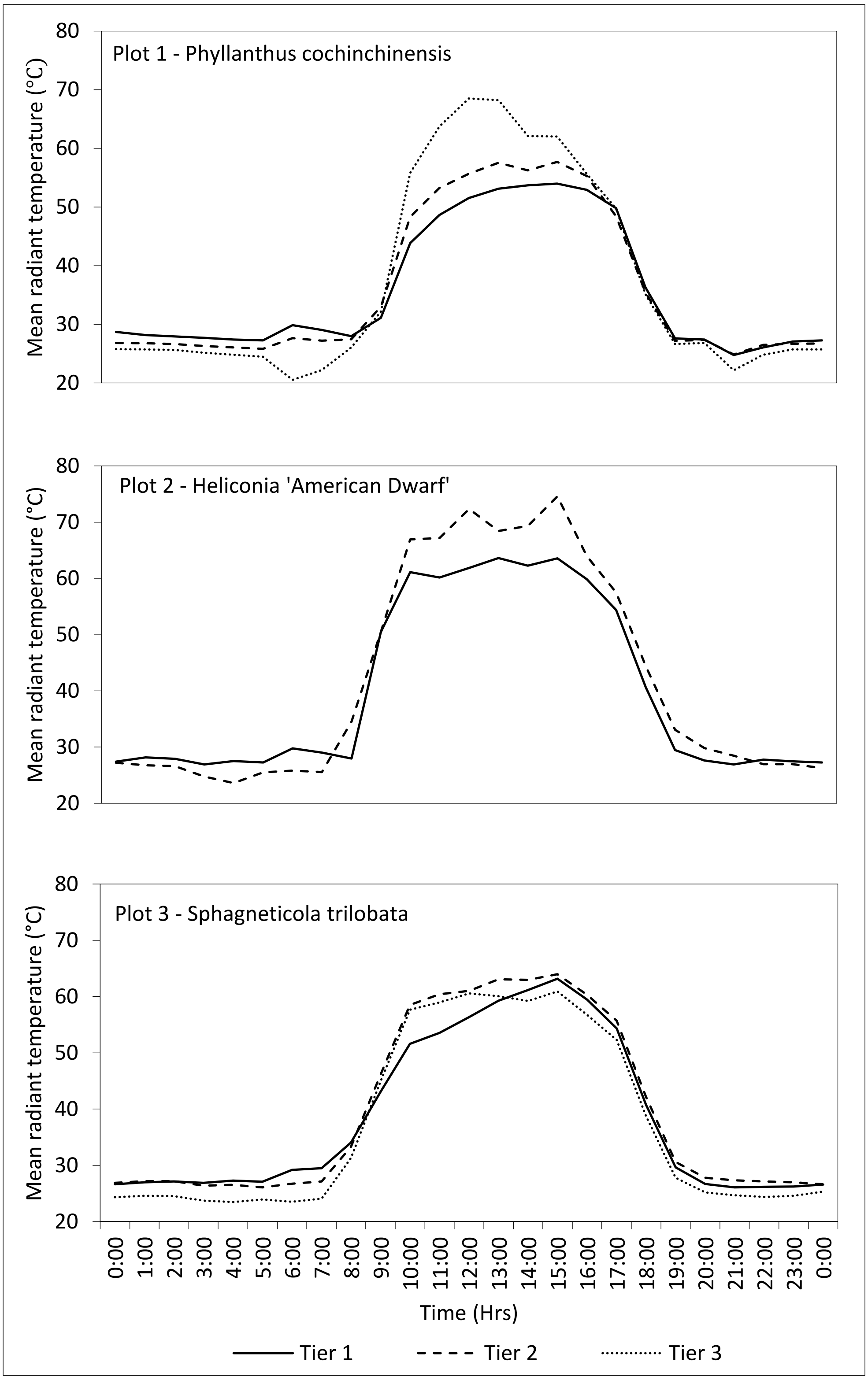

Figure 105. Averaged diurnal t_{mrt} profiles under clear sky conditions

10.3 Comparative studies on vertical greenery

While the focus of this thesis is on rooftop greenery, the study recognizes the impact of vertical greenery as another common alternative to urban greenery design. Many studies have shown vertical greenery to be effective at reducing building envelope temperature and energy consumption (Chen et al., 2013; Cheng et al., 2010; Perini et al., 2011; Wong et al., 2010a). This section seeks to investigate the impact of vertical greenery on outdoor t_{mrt} as well as the effect of using the same type of plants for both vertical and rooftop greenery.

10.3.1 Impact on vertical greenery on mean radiant temperature

Content from Chapter 10.3.1 (Pages 227 to 247) has been published in the Journal of Landscape and Urban Planning, for which I am the main author:

Tan, C.L., Wong, N.H., Jusuf, S.K., 2014, Effects of vertical greenery on mean radiant temperature in the tropical urban environment, *Landscape and urban planning* 127: 52-64.

It was also presented in:

Wong, N.H., Jusuf, S.K., **Tan, C.L.**, Chia, P.Y., 2012, Effects of vertical greenery on mean radiant temperature in the tropical urban environment, *iNTA 2012*, National University of Singapore, Singapore. Oral Presentation, Published in proceedings.

10.3.1.1 Objective

The objective of this study is to quantify the effects on t_{mrt} due to exposure to vertical greenery.

10.3.1.2 Methodology

The first of two sets of data consisted of temperature data collected from two vertical greenery systems (Green Wall A and Green Wall B). Subsequently, Green Wall B was removed. The latter set of data consisted of temperature data from Green Wall A and the concrete wall previously covered by Green Wall B. Measurements are made for the following:

- Air temperature (t_a) in front of the green walls;
- Surface temperature (t_s) of concrete wall behind green walls; and
- Estimation of mean radiant temperature (t_{mrt}) in front of the green walls.

Properties of the two green walls are shown in Table 36. Both green walls are categorised as plant carrier systems. The Suntory Midorie system consists of a lightweight sponge material which is supplemented with nutrients. This system uses a dripping system, where an irrigation pipe is installed on the top most and water slowly drips to the lower part of the wall, such that excess water flows back to the water tank. The light-weight Shimizu Parabienta System is a panel-type wall greening system which uses a dripping system where pipes are connected directly onto each panel of the planting media, and any excess water flows to the drain.

Table 36. Properties of Green walls

	Green Wall A	**Green Wall B**
System	Suntory Midorie System	Shimizu Parabienta System
Dimensions (H X W)	2.27 m X 1.90 m	3.18 m X 2.40 m
Types of plants used	Piper sarmentosum Philodendron Cordyline terminalis Schefflera	Hemigraphis alternata Portulaca grandiflora Nephrolepis acutifolia
LAI	3.8	3.5

The surface temperature of the concrete wall behind the green walls was measured using thermocouples Figure 106. There was a thermocouple wire attached to the concrete wall behind each green wall (Points X1 and Z1), as well as one between the green walls that is directly exposed to the sun (Point Y1). For every point in the exterior, there was a corresponding point on the other side of the wall to measure the temperature on the building interior (Points X2, Y2 and Z2). There was a total of six measurement points.

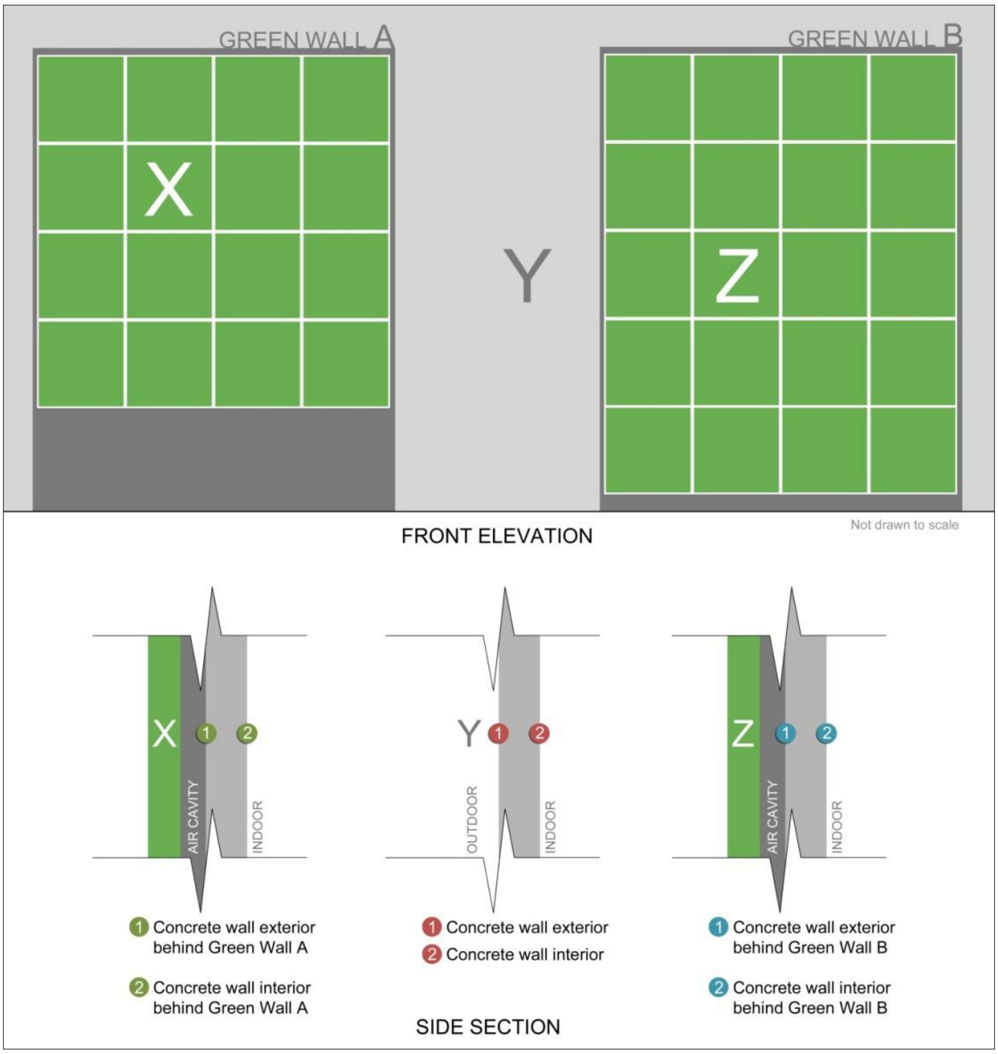

Figure 106. Surface temperature measurement spots

The t_{mrt} and t_a in front of the green walls were estimated in 0.5 m intervals, until 2 m away. The sensors were approximately 1.7 m above ground. Measurement of t_{mrt} is done via the use of a customised globe thermometer. The 38 mm globe thermometer is a common option as the globe used is a table tennis ball, which can be readily purchased and conveniently replaced (Humphreys, 1977). The accuracy of the 38 mm globe thermometer can be adjusted to cater to outdoor conditions by recalibrating the mean convection coefficient. This method has been tested in Sweden (Thorsson et al., 2007) and shown to be effective in outdoor conditions. For this study, t_{mrt} is estimated using customised globe thermometers calibrated for localised usage (Tan et al., 2013a). The LAI of both green walls were calculated by removing a 10 cm by 10 cm segment of the green wall, measuring the total leaf area size with a flatbed scanner and extrapolating it to the size of the green walls. Close-circuit television was used to monitor the effects of shading on estimated t_{mrt}.

Measurements were conducted on the roof top of Block SDE2 in the National University of Singapore, Singapore (1°17′44″N 103°46′36″E). Also known as the Greenery Technology Laboratory (GTL), the site measures approximately 9 m by 9 m (Figure 107). Two green systems were installed on an existing wall. The environment around the green walls is open space, and the room behind the green walls is a smoke-stop lobby that is not mechanically ventilated. There was no machinery or heat generation equipment near the green walls.

Figure 107. Measurement setup. Globe thermometers were attached to poles with white PVC pipes housing surface and air temperature loggers.

For this study, measurements were conducted from 27th September 2011 to 13th March 2012. The measurement period was divided into Period A and B, where Period A denoted the measurement of both green walls, and Period B denoted measurement with Green Wall B removed (Table 37). Only data for clear, sunny days were used for analysis. Selection of the days was based on solar irradiance data measured on-site with a pyranometer. Measurements were made at one minute intervals and averaged to hourly intervals for analysis. A total of 28 points were set up for t_{mrt} and t_a measurement. Each measurement point, which consists of a customised globe thermometer fixed at 1.7 m above ground and an air temperature sensor housed in a PVC pipe, was secured with a concrete footing.

For the purpose of discussion, the measurement points are aligned and named as shown in Figure 108. Air temperature was measured at measurement spots 1 to 28 as well as the weather station.

As the green walls were exposed to self-shading and overshadowing at different periods of the day (Figure 109), daily data were grouped into five periods corresponding to changes in exposure to solar radiation (Table 39).

Table 37. Measurement period

Period	**Measurement duration**	**No. of days measured**	**No. of days used for analysis**	**Dates used for analysis**	**Purpose**
A	27/09/2011 to 03/11/2012	99	5	06/10/2011 13/10/2011 16/10/2011 17/10/2011 25/11/2011	Measurement for Green Wall A and Green Wall B
B	04/01/2012 to 13/03/2012	70	9	15/01/2012 16/01/2012 17/01/2012 21/01/2012 01/02/2012 08/02/2012 10/02/2012 11/02/2012 07/03/2012	Measurement for Green Wall A. Green Wall B is removed

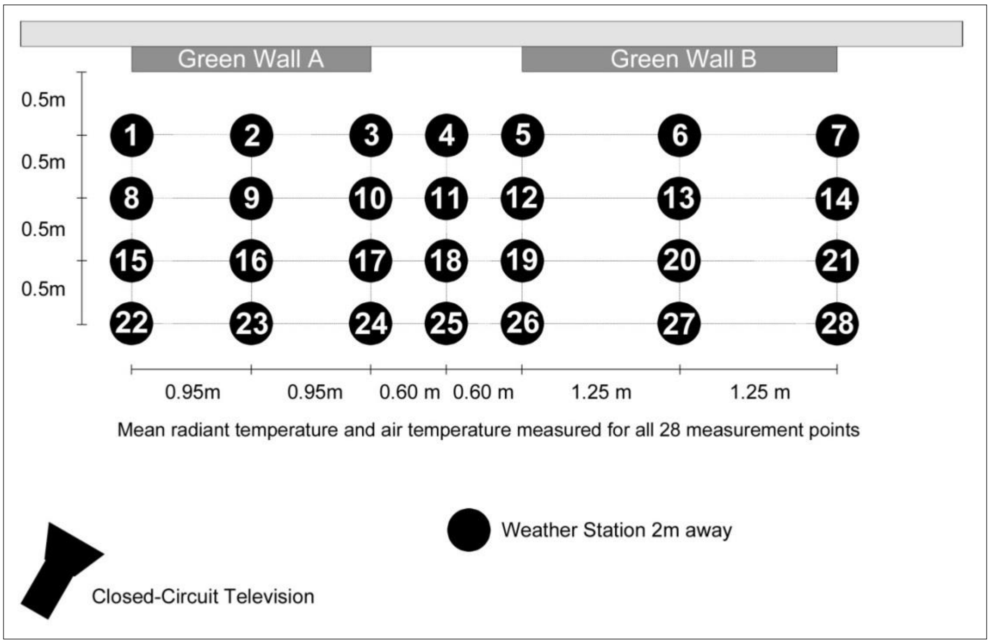

Figure 108. Position of t_{mrt} and t_a measurement points

Table 38. Instruments used for measurement

Variable	**Instrument**
Air temperature, t_a	*HOBO Weatherstation*, H21-001
Globe temperature, t_g	*HOBO Thermocouple Data Logger*, U12-014
Wind speed, V_a	*HOBO Weatherstation*, H21-001
Surface temperature, t_s	*HOBO Thermocouple Data Logger*, U12-014
Shading characteristics	Close-circuit television
Leaf Area Index, LAI	*Canon All-In-One Printer,* MP276

Table 39. Time range used for analysis

Time Range	**Period**	**Condition of wall**
1	0000 hrs – 0700 hrs	Night to Sunrise
2	0700 hrs – 1400 hrs	Self-shaded
3	1400 hrs – 1700 hrs	Exposed to direct sunlight
4	1700 hrs – 1900 hrs	Overshadowing from trees
5	1900 hrs – 0000 hrs	Sunset to night

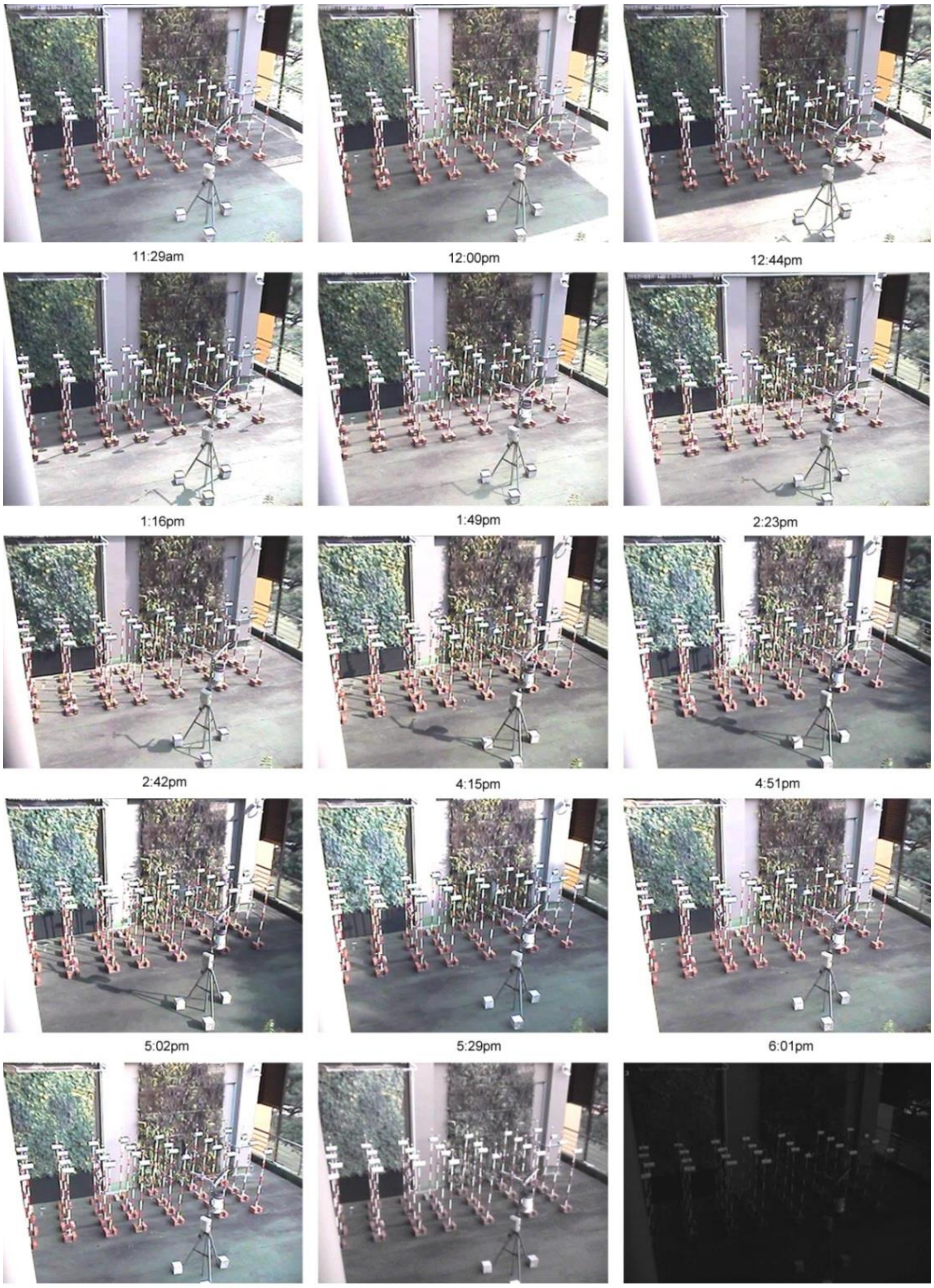
11:29am
12:00pm
12:44pm
1:16pm
1:49pm
2:23pm
2:42pm
4:15pm
4:51pm
5:02pm
5:29pm
6:01pm
6:30pm
7:20pm
7:30pm

Figure 109. CCTV footage of site showing self-shading and overshadowing

10.3.1.3 Results and discussion

10.3.1.3.1 Surface temperature (t_s)

Surface temperatures of the two green walls was compared to a portion of the wall directly exposed to the sun. The aim of this comparison is to determine the surface temperature reduction due to the green walls. Data for five days were used for the analysis of Period A and for nine days were used for the analysis of Period B. The daily data were averaged to produce a single profile for every measurement point.

An increase in surface temperature is observed for Point Z after the removal of Green Wall B. Point Z1 has a flat profile for Period A, but increased steadily to reach a peak of 34.3 °C at 17:00 hrs for Period B. The removal of Green Wall B has resulted in an increase in surface temperature of 6.7 °C. The maximum difference in diurnal surface temperature for the building interior (Point Z2) for Period A was 0.3 °C, but significantly larger for Period B (Up to 3.8 °C). With the exception of Green Wall A, diurnal temperature fluctuations have generally increased.

The exposed concrete surface (Point Y1) exhibited the highest surface temperature for both periods (Figure 110). The highest value for Period A was 35.7 °C at 15:00 hrs. The maximum value was much higher for Period B (44.6 °C at 17:00 hrs) and occurred 2 hours later. The increase in temperature was 8.9 °C. The interior surface temperature (Point Y2) also increased after the removal of Green Wall B. The profile of Point Y2 was relatively flat for Period A, but increased significantly and peaking at 34.6 °C at 19:00 hrs for Period B. The removal of Green Wall B has significantly increased the surface temperature of the exposed concrete wall. The temperature of Y1 is generally much higher than Point Z1. This may be due to the fact that Point Y1 was located closer to a structural concrete column, and thus exposed to a higher thermal mass.

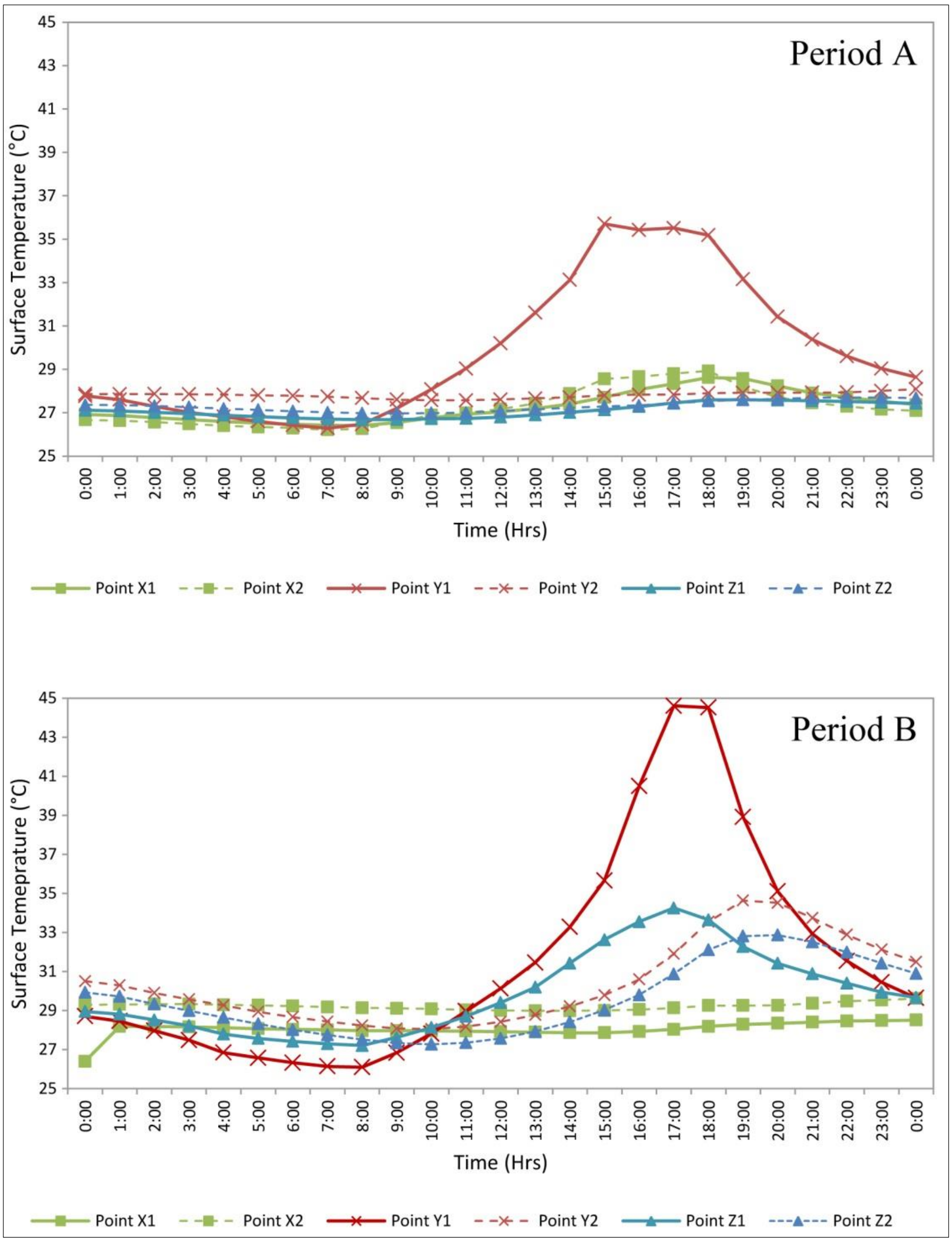

Figure 110. Surface Temperature profiles for Period A and Period B

The surface temperature of Point X2 was similar to Point X1 for Period A but was consistently higher in Period B. No significant fluctuations were observed. The removal of Green Wall B had no significant effect on Green Wall A.

10.3.1.3.2 Air temperature (t_a)

Air temperatures at all 28 measurement points in front of the green walls were analysed. Figure 111 shows that the range of air temperature did not fluctuate greatly. The maximum range recorded was about 1.1 °C for Period A, and increased slightly to 1.5 °C for Period B. This is similar to a study conducted by Wong et al. (2010a), where the ambient temperature range recorded 0.6 m from green walls and a concrete wall was 1.3 °C.

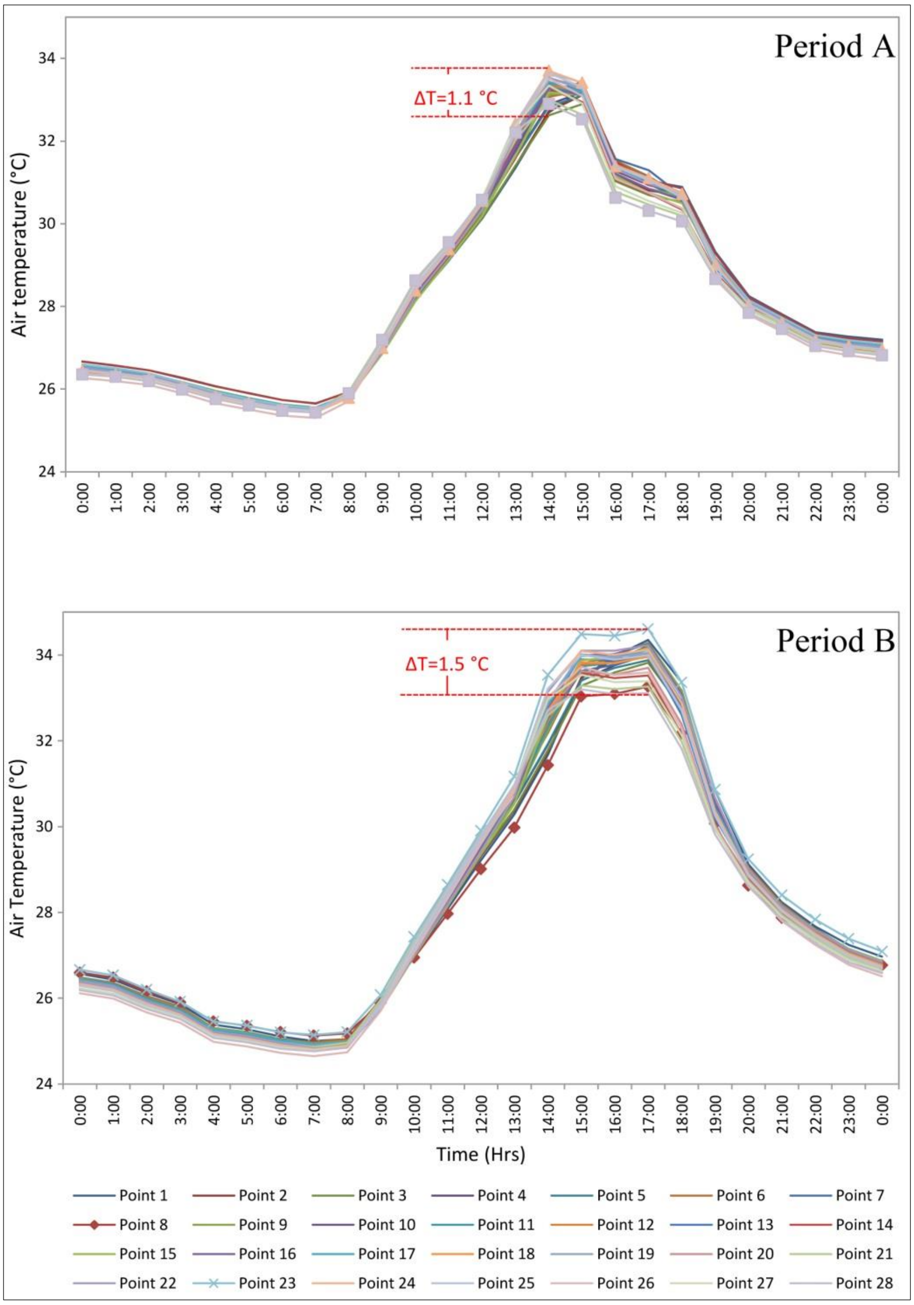

Figure 111. Air temperature profiles for Period A and Period B

10.3.1.3.3 Profile of t_{mrt} across Measurement Points 1 to 7

The t_{mrt} profiles for Period A for Measurement Points 1 to 7 are shown in Figure 112. It can be observed that a portion of the readings near the bottom does not deviate significantly across the 7 points (19:00 hrs to 07:00 hrs). As the sun rised to its zenith, the average t_{mrt} increased steadily, and the difference between the 7 points begin to exhibit increasing amounts of deviation.

A distinct pattern is observed from 15:00 hrs to 17:00 hrs, where most readings peak at Point 4. This pattern exhibits itself most evidently at the highest recorded t_{mrt} at 15:00 hrs. A comparison with Figure 108 shows that Point 4 was the spot that was closest to the part of the wall that was exposed to direct sunlight, whereas the other points are covered with Green Walls A and B. This pattern diminished significantly until the fluctuations cease from approximately 21:10 hrs onwards.

The same patterns were observed for Period B. However, higher peak readings were recorded. This is expected, as there was more concrete surface that was exposed to direct sunlight for Period B. Measurements of Points 5 to 7 are also higher than in Period A during Time Range 3. The difference in t_{mrt} value is clearly only significant during Time Range 3 (14:00 hrs – 17:00 hrs). Outside of this time range, the difference in t_{mrt} between Points 1 to 7 is minimal.

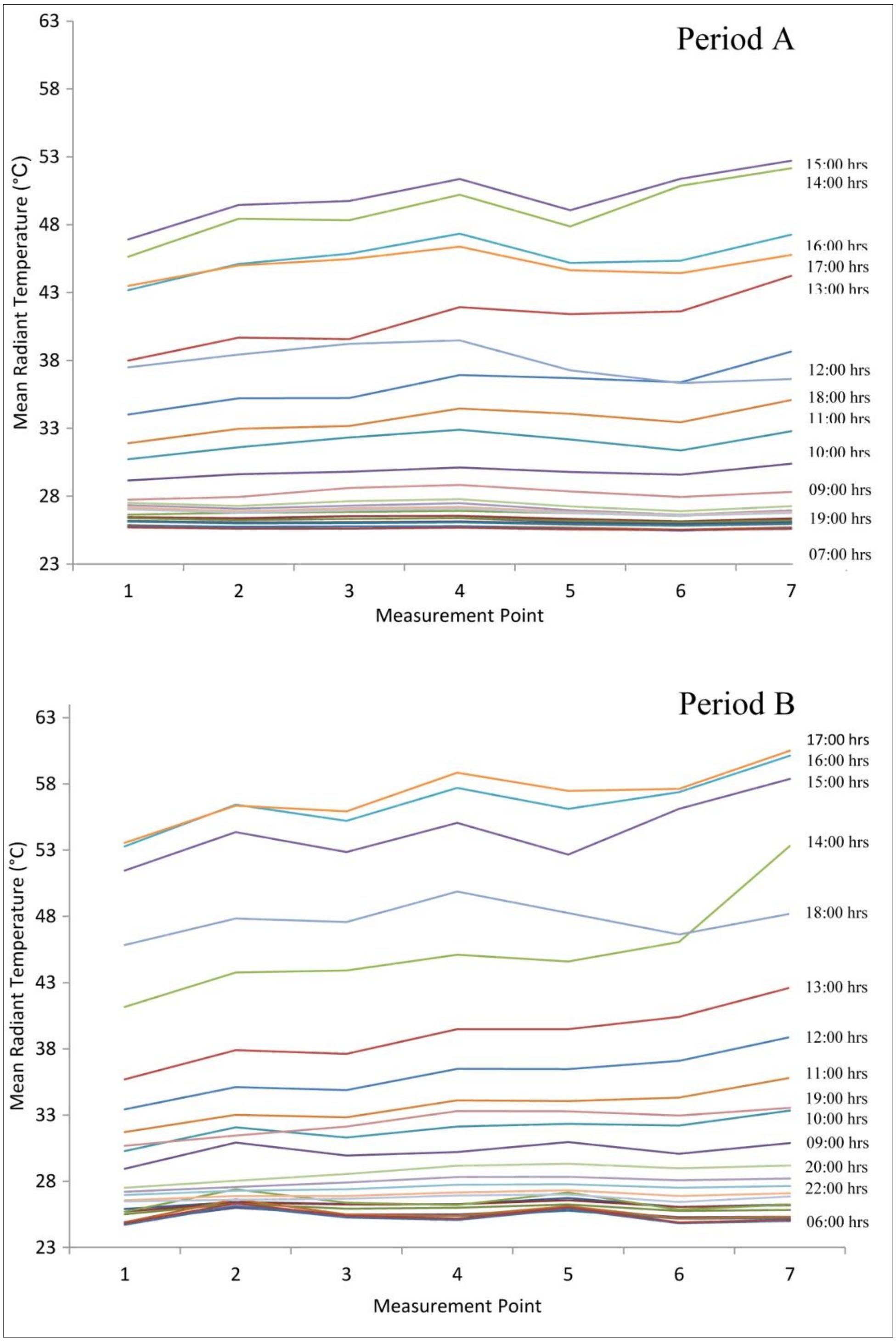

Figure 112. Comparison of t_{mrt} profile for Points 1-7 for Period A and Period B

10.3.1.3.4 Profile of t_{mrt} for Points 2, 4 and 6

The diurnal t_{mrt} profile is compared with the corresponding solar irradiance profile. To simplify the analysis, only 3 points were plotted. The points are show in Figure 113.

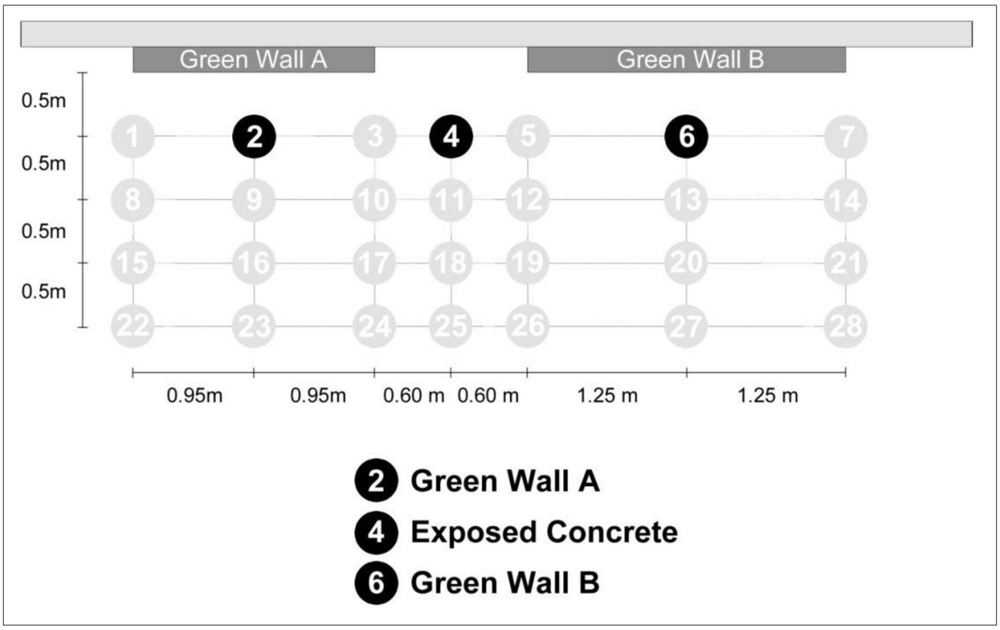

Figure 113. Points 2, 4 and 6

Figure 114 shows the diurnal t_{mrt} plots across Points 2, 4 and 6 for Period A and Period B. Time Ranges 1 and 5 show no relation between the t_{mrt} profile and solar irradiance (due to the absence of sunlight). Time Range 2 shows an increase in t_{mrt} with solar irradiance. Similarly, Time Range 4 shows a similar trend, with t_{mrt} decreasing with solar irradiance correspondingly. It can be seen that the t_{mrt} values correspond to fluctuations of direct and intense solar irradiance (Time Range 3). More importantly, the largest differences in t_{mrt} for the different points occur during periods of peak solar irradiance. In other words, t_{mrt} in front of the Green Walls are reduced during periods of peak solar irradiance.

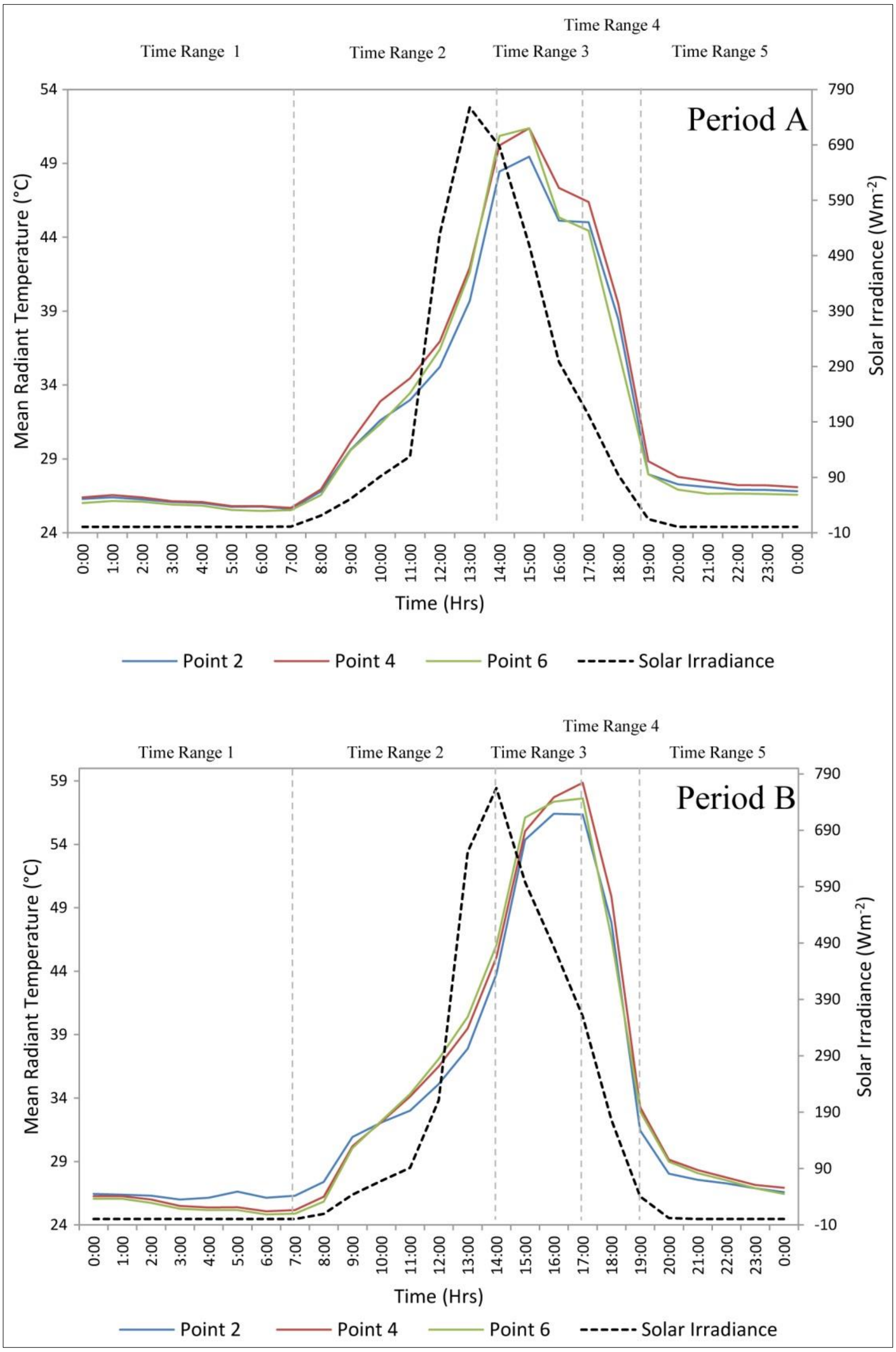

Figure 114. Plot of Points 2,4 and 6 against solar irradiance for Period A and Period B

Similar to Period A, Time Range 1 and the later part of Time Range 5 show no relation between the t_{mrt} profile and solar irradiance (due to the absence of sunlight). Time Range 2 shows an increase in t_{mrt} with solar irradiance. Similarly, Time Range 4 shows a similar trend, with t_{mrt} decreasing with solar irradiance correspondingly. It can be seen from Time Range 3 that the t_{mrt} values reached their peak at approximately 17:00 hrs, and it does not correspond to the solar irradiance peak to the likes of Period A. It would seem that the exposure to increased concrete surface area has resulted in a delay of the diurnal t_{mrt} peak. Increased longwave radiation may have been stored and subsequently emitted by the exposed wall surface, resulting in the time lag.

This time lag is further scrutinised by comparing t_{mrt} profiles at 0.5m intervals away from the wall (Figure 115). It can be seen from Graph A that the t_{mrt} rises rapidly from 14:00 hrs to 15:00 hrs and reaches its peak at 17:00 hrs, when the solar irradiance has passed its peak. As the distance from the wall increases, this phenomenon gradually decreases until the effect cannot be observed on Graph D (2 m away). A comparison shows that the time lag is approximately 2 hours.

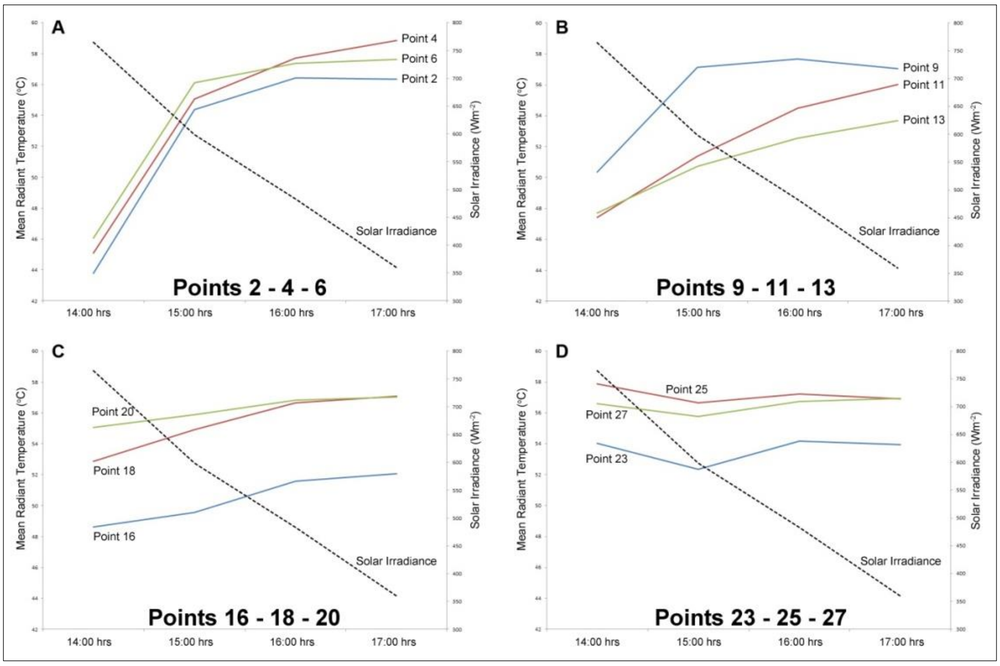

Figure 115. Comparison of tmrt profiles at 0.5 m intervals from the wall for Time Range 3, Period B

10.3.1.3.5 Profile of t_{mrt} plotted against distance from wall

To understand the effect of t_{mrt} with increasing distance from wall, measurements are taken at 0.5 m increments, up to a maximum of 2 m. Figure 116 shows three sets of measurement for Periods A and B. The measurements are positioned at 0.5 m intervals starting from the centre of the green walls and concrete column. The highest t_{mrt} value recorded for Period A is at 13:20 hrs and the highest t_{mrt} value recorded for Period B is at 16:20 hrs. The removal of Green Wall B has caused a general increase to the t_{mrt} profile, especially to the points closest to the wall. There is an increase of 12.7 °C for Point 2, 12.9 °C for Point 4, and 10.9 °C for Point 6. The increase in t_{mrt} for points away from the wall (Points 9 - 16 - 23, Points 11 - 18 - 25 and Points 13 - 20 – 27) ranges from 1.9 °C to 6.4 °C.

The effect on t_{mrt} due to the removal of the wall is most significant within a region of 0.5 m. The highest recorded difference is 12.8 °C for Point 4.

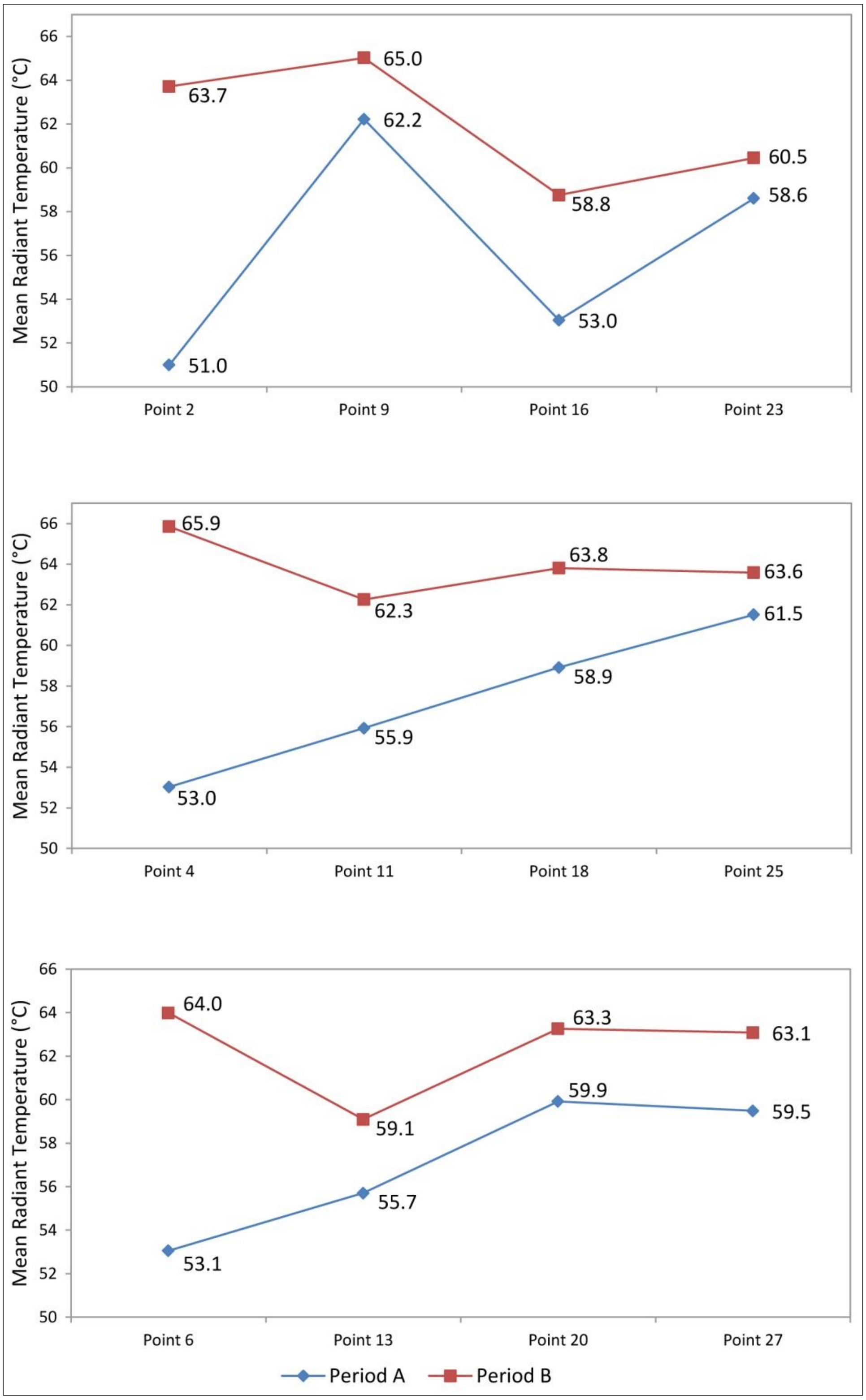

Figure 116. Comparison of points at peak solar irradiance

10.3.1.3.6 Visualisation of t_{mrt} using Geographical Information Systems (GIS)

All 28 points are used for data interpolation using GIS. This facilitates rapid analysis of the conditions of the surveyed area. Hot spots can be identified easily with this method. Measurements for a typical clear sunny day are used for visualisation via GIS. Figure 117 shows the t_{mrt} map of selected timings from 15:55 hrs to 00:35 hrs. It can be seen that the hot spot (dotted circle), which corresponds to Point 4, has a significantly high value compared to the rest of the points. This trend can be observed until approximately 00:00 hrs, although the magnitude of the difference differs drastically across different timings.

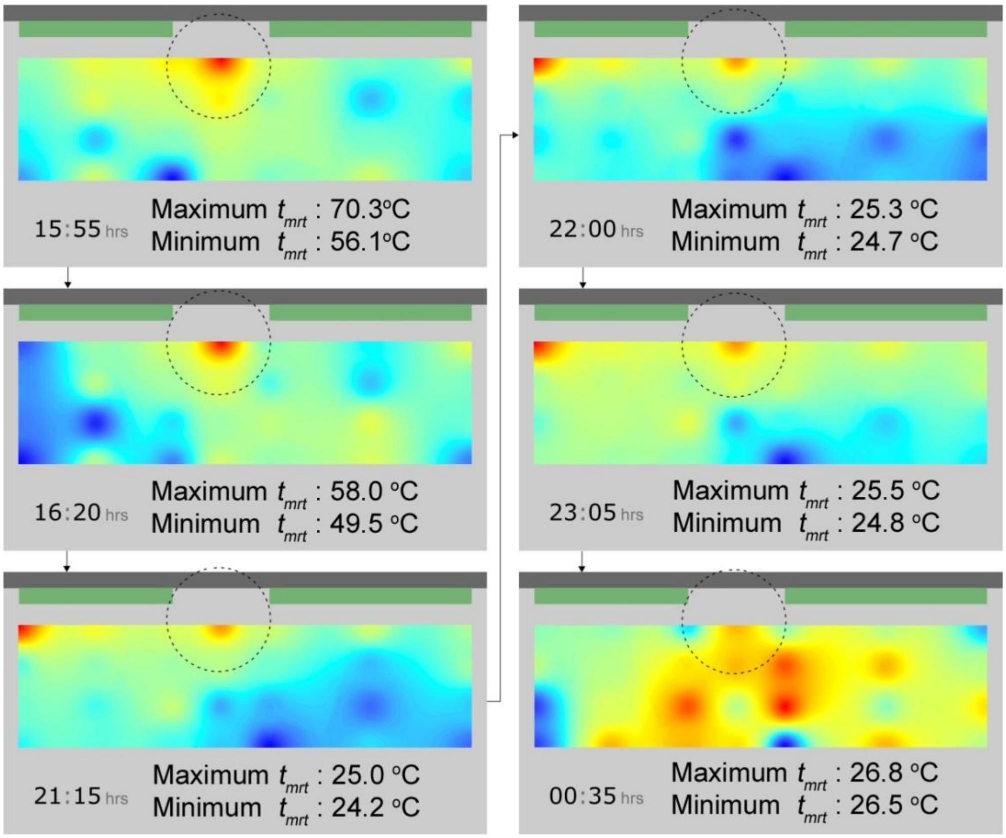

Figure 117. GIS visualisation of t_{mrt}

10.3.1.3.7 Conclusion

The purpose of this study is to observe the effect of green walls on the temperature of a surrounding environment.

Surface temperature measured behind the green walls show that the green wall can reduce the surface temperature of the building envelope. This effect is not restricted to areas covered by the installation of a green wall; areas that are in close proximity to the green wall can also experience a reduction in surface temperature. The implementation of green wall helps to reduce fluctuations of surface temperature. Removal of Green Wall B only resulted in a slight increase in air temperature. However, there is significant difference in the t_{mrt}, especially within 1 m of the green walls. The maximum increase in t_{mrt} after the removal of Green Wall B is 12.8 °C. When one green wall is removed, the effect of time lag can be observed. The peak readings in t_{mrt} are delayed for approximately 2 hours. Since the LAI of both green walls are similar, no significant correlation between LAI and temperature reduction can be ascertained.

Results show that the implementation of vertical greenery can lower the t_{mrt} of its surroundings. The effect of this attenuation is evident for up to 1 m away from the wall. However, this lowering is effective only during periods of intense direct solar exposure. The effect is minimal during times when the green walls experience self-shading or overshadowing. Consideration should be made to the placement of vertical greenery to ensure maximum exposure to direct sunlight so as to take advantage of its t_{mrt} reducing attributes.

This study has shown that the effects of shading provide the optimal form of t_{mrt} reduction. Peak t_{mrt} was recorded at 15:00 hrs in the presence of both green walls. When Green Wall B was removed, peak t_{mrt} occurred significantly later (17:00 hrs) and was 10.9 °C to 12.9 °C higher (0.5 m from the wall). Measurement points further away from the wall also recorded an increase in t_{mrt} ranging from 1.9 °C to 6.4 °C. Areas that do not have access to shade may consider the utilization of green walls, strategically placed to provide further reduction to t_{mrt}. This can help architects and urban planners make informed decisions during design conceptualisation and to achieve better overall outdoor thermal comfort.

The physical dimensions of the green walls are not considered in the analysis, and may become a variable in subsequent attempts at measurement. Similarly, the type of plants used will also be varied to explore the effects of different types of plants on the effects on t_{mrt}.

The use of GIS for data visualisation provides an easy way to comparing temperature profiles across different locations and timings. The interpolated values serve to provide a method to assess the t_{mrt} of any given space that is easily comprehensible to architects and planners. From the figures, it is evident that vertical greenery facilitated the reduction of mean radiant temperature at different magnitudes throughout the day.

This study has shown the feasibility of quantifying thermal effects of greenery on mean radiant temperature in a systematic manner, and can be used for the measurement of other forms of vegetation in the tropical urban context.

10.3.2 Analysis of similar plant types in horizontal and vertical setup

10.3.2.1 Objective

The objective of this study is to investigate the impact of using the same type of plant on vertical and rooftop greenery, and their subsequent impacts on outdoor t_{mrt}. This is done by simultaneously measuring the t_{mrt} of plants above a rooftop greenery plot, as well as two vertical greenery racks over a period of time.

10.3.2.2 Methodology

One specific plant species is selected for green roof and green wall (Table 40). A total of one plot of rooftop greenery and four racks are set up on the rooftop of Block SDE 1, National University of Singapore. Measurements on concrete surfaces are used as experimental control. The racks are labelled as follows:

- Green Wall E denotes a vertical greenery setup that faces East;
- Green Wall W denotes a vertical greenery setup that faces West;
- Concrete Wall E denotes a concrete panel setup that faces East;
- Concrete Wall W denotes a concrete panel setup that faces West.

The racks are insulated in the following sequence:

- One inch extruded foam;
- One inch air gap;
- One inch extruded foam;
- Covered by tarpaulin sheet.

Location of measurement points and setup details are shown in Figure 118, Figure 119 and Table 42. Measurement period and days used for analysis are shown in Table 41. Measurement of t_{mrt} is conducted for a total of six points.

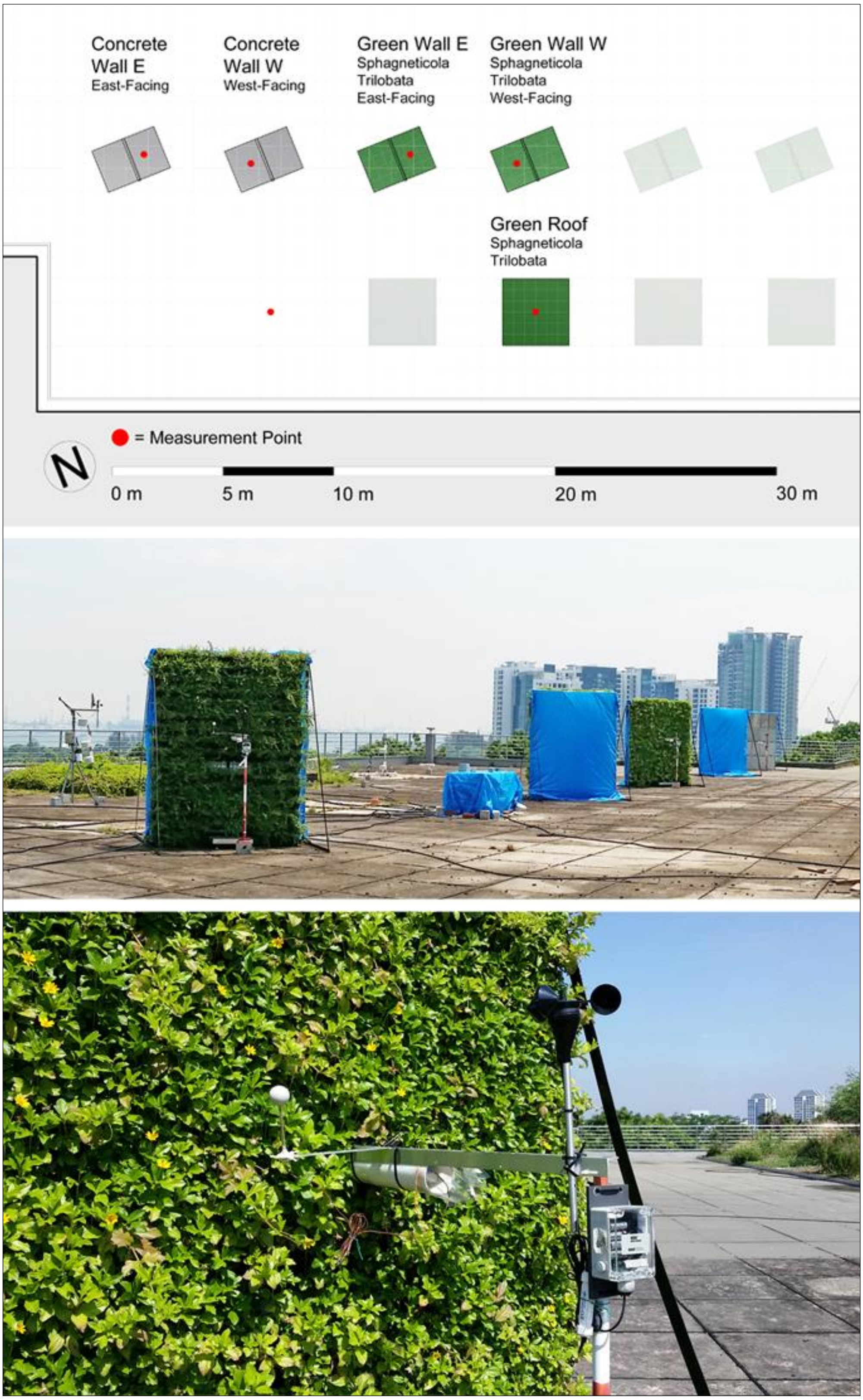

Figure 118. Plan and measurement setup

Figure 119. Setup details

Table 40. Properties of green roof and green walls

	Green Roof	Green Wall E and W	Concrete Wall E and W
Dimensions	3 m X 3 m	2 m X 2.4 m	2 m X 2.4 m
Plant used	Sphagneticola trilobata		

Table 41. Measurement period

Measurement duration	No. of days measured	Date used for analysis
08/05/2014 to 12/06/2014	36	10/06/2014

Table 42. Instruments used for measurement

Variable	Instrument
Air temperature, t_a	*HOBO U12-012 Temp/RH data logger*
Globe temperature, t_g	*HOBO Thermocouple Data Logger*, U12-014
Wind speed, V_a	*Onset Wind Speed Smart Sensor*, S-WSA-M003
Solar irradiance and rainfall	*HOBO Weatherstation*, H21-001
Evapotranspiration Rate (ET)	*HBM Z6FC3 load cell and Quantum X logger*

10.3.2.3 Results and discussion

A typical day with clear sky condition is selected for analysis (Figure 120). Peak irradiance was observed at 14:00 hrs (811.8 Wm^{-2}). The diurnal profile can be observed to closely resemble a symmetrical profile. This is a significant aspect for this study as the walls have direct exposure to solar irradiance for only one half of the day, and irradiance levels need to be similar for both East-facing and West-facing walls on either half.

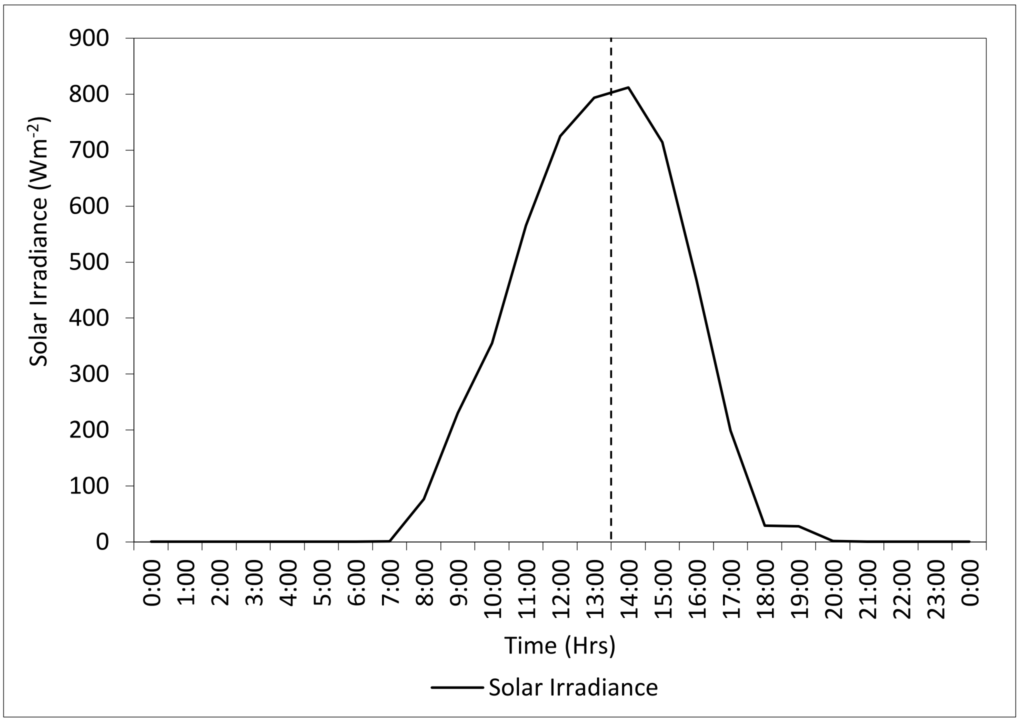

Figure 120. Solar irradiance profile for 10th June 2014

10.3.2.3.1 Air temperature (t_a)

Figure 121 shows diurnal air temperature profiles for green roof, green walls and concrete walls. It can be observed that air temperature near the eastward-facing concrete wall is highest at peak temperature (35.2 °C), followed by air temperature above the concrete roof at 35.1 °C. Air temperature in front of eastward facing walls tends to be higher compared to westward-facing walls. Air temperature above the green roof is similar to air temperature in front of westward-facing walls.

10.3.2.3.2 Mean radiant temperature (t_{mrt})

Figure 122 shows mean radiant temperature (t_{mrt}) profiles for green roof, green walls and concrete walls. It can be observed that t_{mrt} above the concrete roof is highest at peak temperature (15:00 hrs, 66.7 °C). For eastward-facing walls, t_{mrt} is highest around noon, and decreases steadily after noon. This can be attributed to self-shading when the sun is in the West. There is little difference in t_{mrt} between Green Wall E and Concrete Wall E.

In contrast, t_{mrt} profiles for Green Wall W and Concrete Wall W differ significantly. It can be observed that t_{mrt} in front of Green Wall W is lower than Concrete Wall W from 09:00 hrs to 13:00 hrs (about 3 °C cooler), and 15:00 hrs to 16:00 hrs (about 5 °C cooler). Peak t_{mrt} for westward-facing walls (54.6 °C to 59.3 °C) is significantly higher than eastward-facing walls (42.1 °C to 42.3 °C). This would suggest that there is little impact in terms of t_{mrt} due to eastward-facing green walls. From Figure 122, it is clear that the western sun has a much higher impact on t_{mrt} than the eastern sun and the impact of adding green walls is more significant on westward-facing facades. This observation is drastically different from Figure 121, where all six measurement points exhibit similar air temperature profiles.

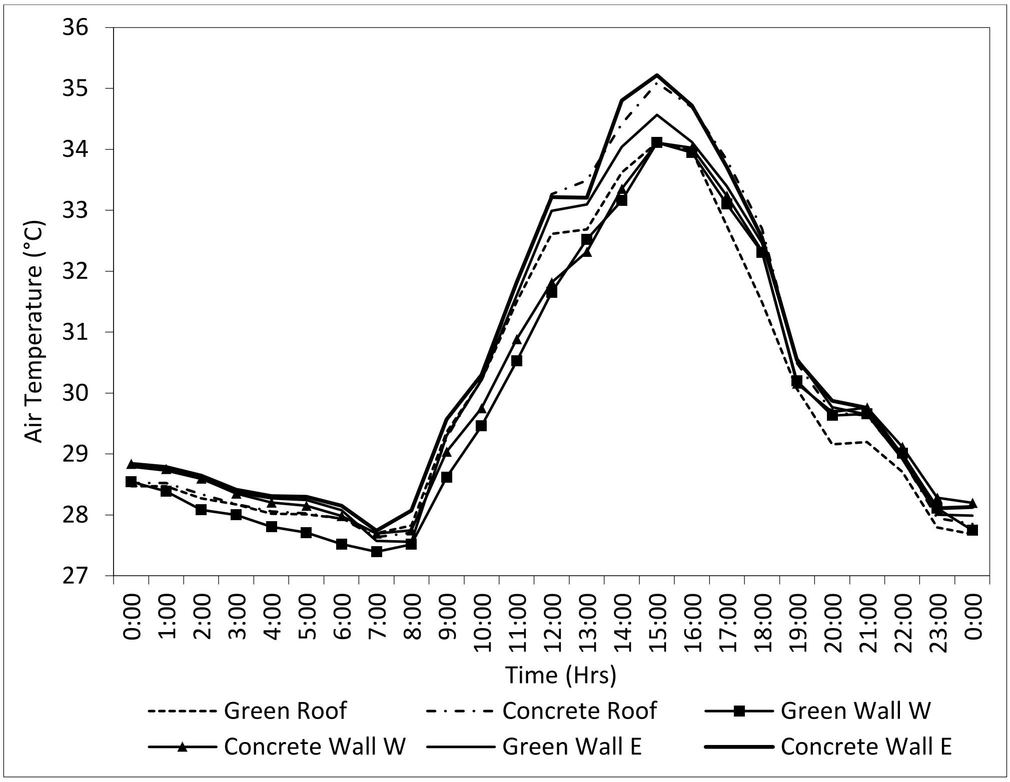

Figure 121. Air temperature profiles for green roof, green walls and concrete walls

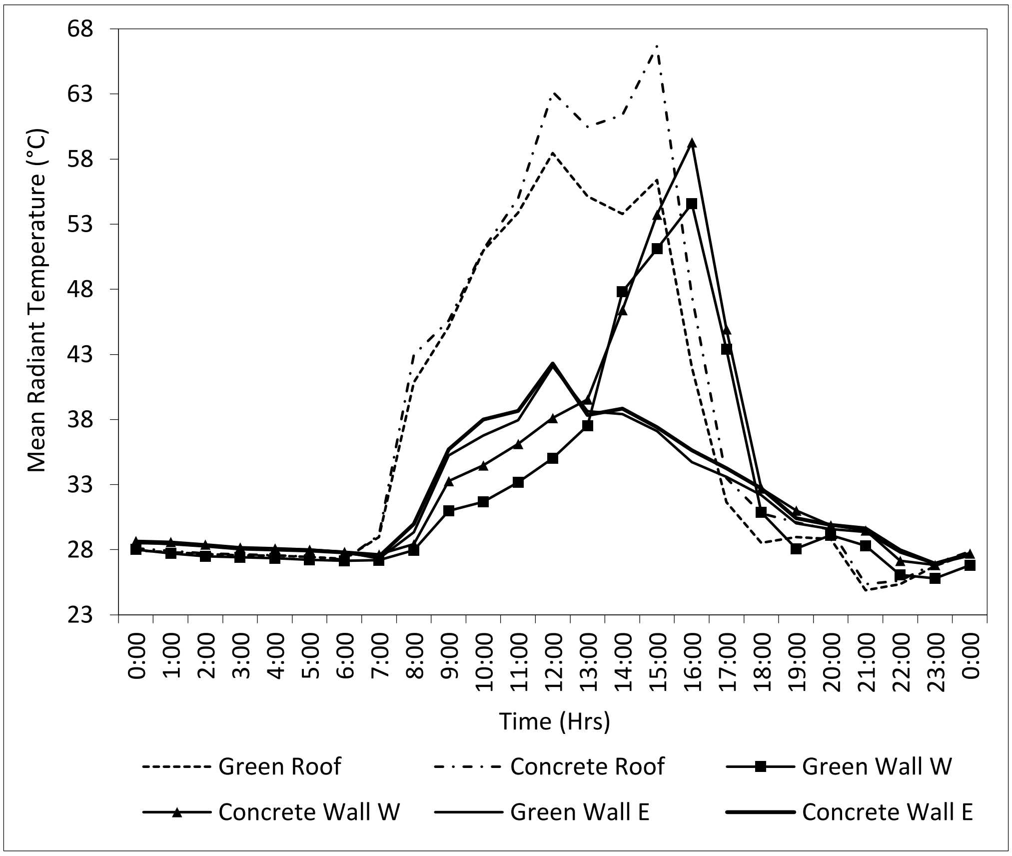

Figure 122. Mean radiant temperature profiles for green roof, green walls and concrete walls

10.3.2.3.3 Comparison of plant albedo

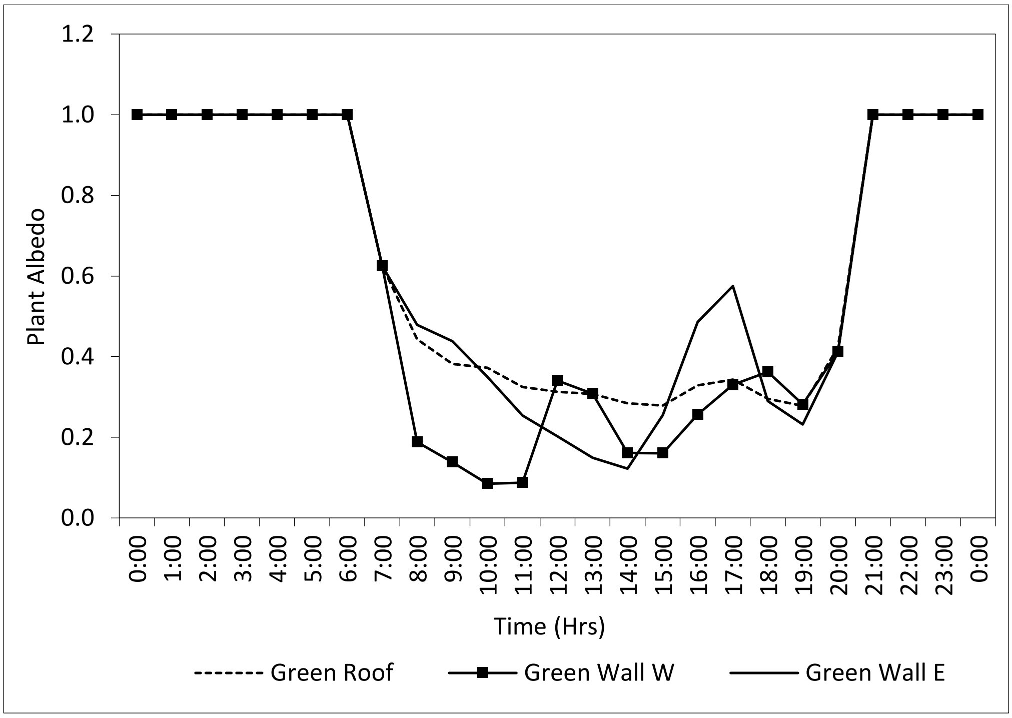

Figure 123. Albedo profiles for green roof and green walls

Figure 123 shows the albedo profile of the green roof and both green walls. Average albedo of the green roof is approximately 0.32 from 10:00 hrs to 17:00 hrs. In comparison, there is significant fluctuation for albedos of Green Wall E and Green Wall W. It can be observed that albedo steadily increases until its peak at 12:00 hrs for Green Wall W and decreases significantly until 14:00 hrs. A steady increase in albedo ensures until sunset. The opposite is observed for Green wall E, where albedo slowly decreases until 14:00 hrs and increases drastically until 17:00 hrs. For the purpose of investigating the impact of green wall albedo, measurements for Green Wall W before noon will have to be disregarded. This is because the sun is behind the Green Wall W before noon, and pyranometer readings do not accurately show the amount of solar radiation that is reflected (Point A on Figure 125). Following this rationale, readings after noon for Green Wall E should also be disregarded from 14:00 hrs onwards.

Albedo values of Green Wall E and Green Wall W are combined and compared with albedo of the green roof (Figure 124). It can be seen that albedo of the green walls are significantly lower that the green roof. This may be explained by the fact that when the sun is at its zenith (14:00 hrs), the direction of solar radiation is almost parallel to the wall surface and reflection is minimal at this point (Point B on Figure 125). Since Chapter 6.1.2 has already highlighted the significance of albedo on t_{mrt} reduction, it follows that vertical greenery may be less effective at reducing t_{mrt} than green roof. This is consistent with measurements shown in Figure 122, where t_{mrt} reduction is significantly higher for green roof compared to both green walls.

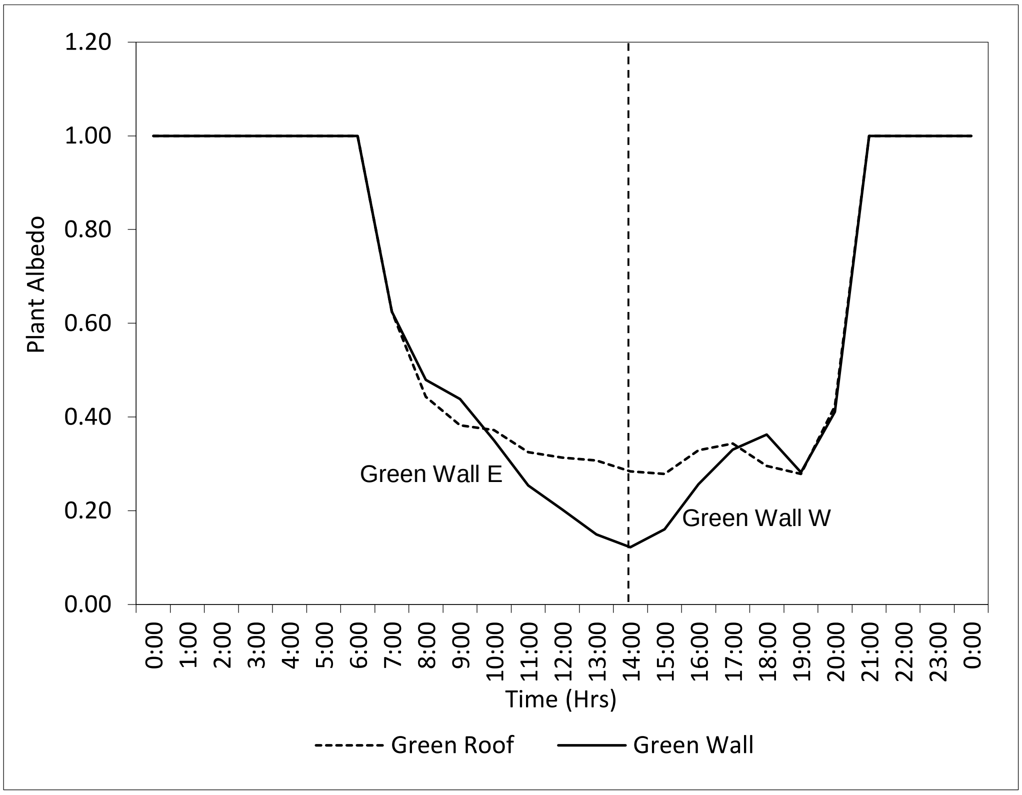

Figure 124. Albedo profiles of Green Roof and Green Walls combined

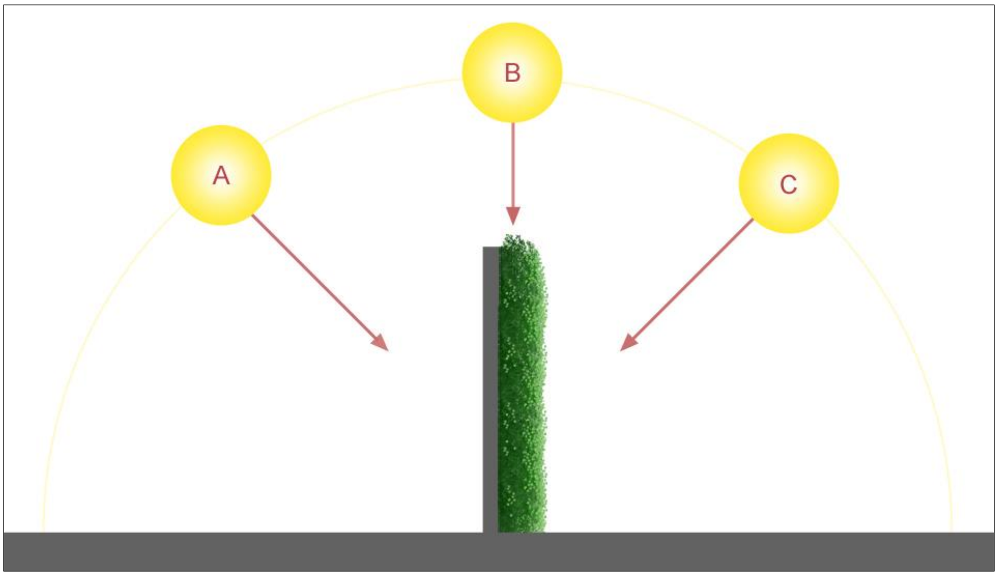

Figure 125. Effect of sun position on albedo

10.3.2.3.4 Comparison of plant Evapotranspiration (ET) rate

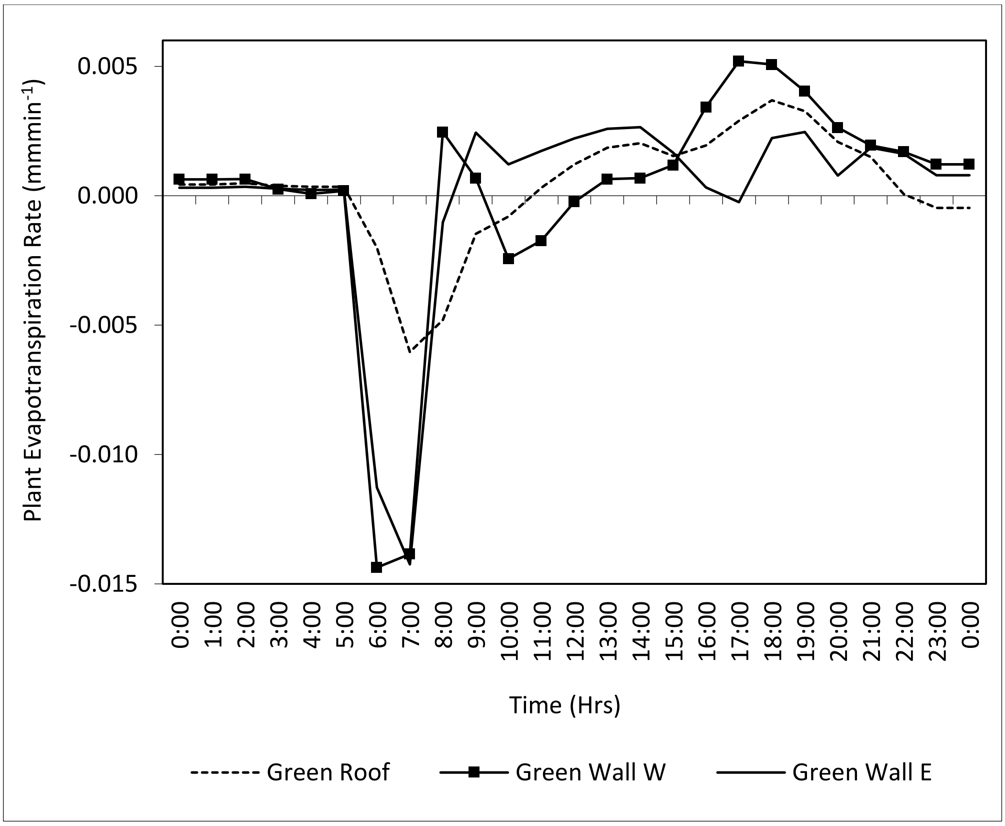

Figure 126. Plant ET profiles for green roof and green walls

Figure 126 shows ET profiles for the green roof and both green walls. For the green roof, ET increases steadily from 10:00 hrs to 17:00 hrs. It can be observed that for Green Wall E, ET is higher than the green roof from sunrise until 15:00 hrs, and decreases significantly thereafter. It is possibly due to higher exposure to direct solar radiation in the morning. Conversely, ET is low for Green Wall W, since it is self-shaded during this period. After 15:00 hrs, ET of Green Wall W increases drastically due to higher exposure to direct solar radiation, and ET of Green Wall E decreases due to self-shade. It can be concluded that ET rate of a plant can be higher in a green wall setting than in a green roof setting.

10.3.2.3.5 Conclusion

The objective of this section of study is to subject the same type of plant simultaneously in both vertical and horizontal arrays and to investigate their corresponding impact on t_{mrt} in the tropical outdoor environment. This chapter has shown that green roofs have a higher potential than green walls in terms of reducing outdoor t_{mrt}. It is observed that for the same plant species, albedo is lower and ET is higher when installed vertically. A comparison of surface temperature via infrared thermography (Figure 127) shows that there can be a difference of about 20 °C for a roof surface with plants and about 7 °C for a wall surface with plants.

Results from this study have also shown that the potential for building surfaces to be retrofitted with vertical greenery can be assessed based on objective criteria such as exposure level to solar radiation and plant functional attributes. Data from t_{mrt} measurements (Chapter 10.3.2.3.2) suggests that retrofitting of vertical greenery should be prioritised for westward-facing walls, as there is evidence of higher potential for t_{mrt} reduction.

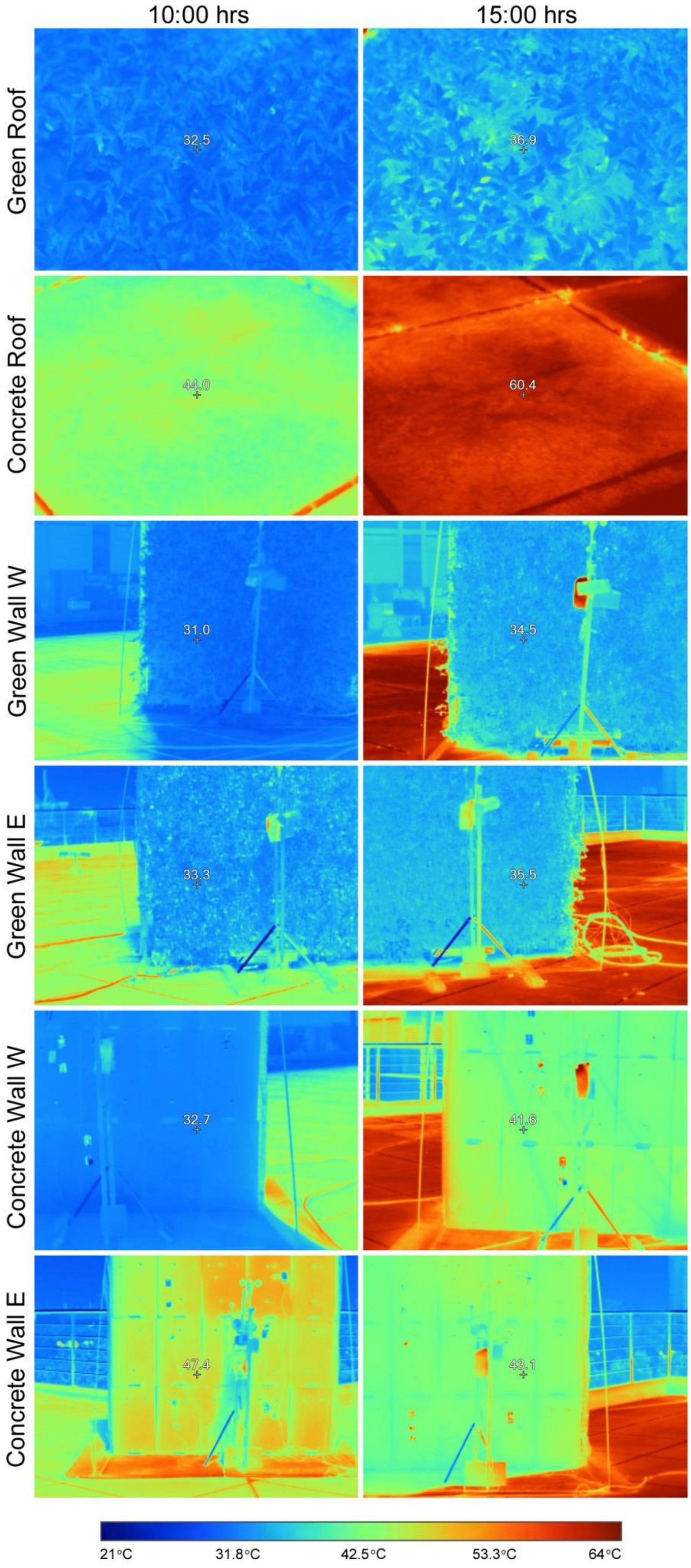

Figure 127. Infrared thermography of green roof plots and concrete (10th June 2014)

10.4 Recommendations for Green Building Rating Tools

10.4.1 Green buildings and Green Building Rating Tools (GBRTs)

Green Building is the practice of building construction with emphasis on efficient use of resources such as energy, construction materials and water. It also strives to exert minimal impact on its surrounding environment as well as to the users of the building throughout the lifespan of the building. This is often achieved through both passive and active intervention by architects, contractors, and users alike. Some methods include a better choice of site, design and construction methods with consideration to the surrounding environment, energy saving operation procedures, and environment friendly removal methods when the building has reached the end of its life-cycle.

The beginnings of green building dates back to the 1970s when activities of the building industry started to be perceived as a significant component in environmental degradation. Rising oil prices in the 1970s resulted in a significant effort to improve energy efficiency and to revise traditional building practices (Steele, 1997). A call for more sustainable measures of building construction spurred the formation of several schools of thought that eventually led to the birth of the Green Building movement.

The earliest attempts with contemporary green building brought to light several important issues, one of which being the need to be able to, in the most objective and unbiased manner, bestow upon a building the status of being Green. One solution that has been put forward is the Green Building Rating system. It is a checklist to which building appraisal is performed, with emphasis on Green Building features. With the checklist, a design approach that is more sensitive to its impact on the environment can be realised. With the formation of the rating tool, the building and construction industry can make an objective assessment of a construction project, from the stage of preliminary design all the way to the stage of operations and maintenance. This system provides an avenue for architects and designers to remain creative and building contractors to maintain the freedom to choose their preferred construction method, without imposing totalitarian regulations in their pursuit of the Green Building agenda.

10.4.2 BCA Green Mark Scheme

In January 2005, the Building and Construction Authority of Singapore (BCA) launched the BCA Green Mark Scheme. It was the Republics' first step in an attempt to promote the practice of Green Building in the construction industry.

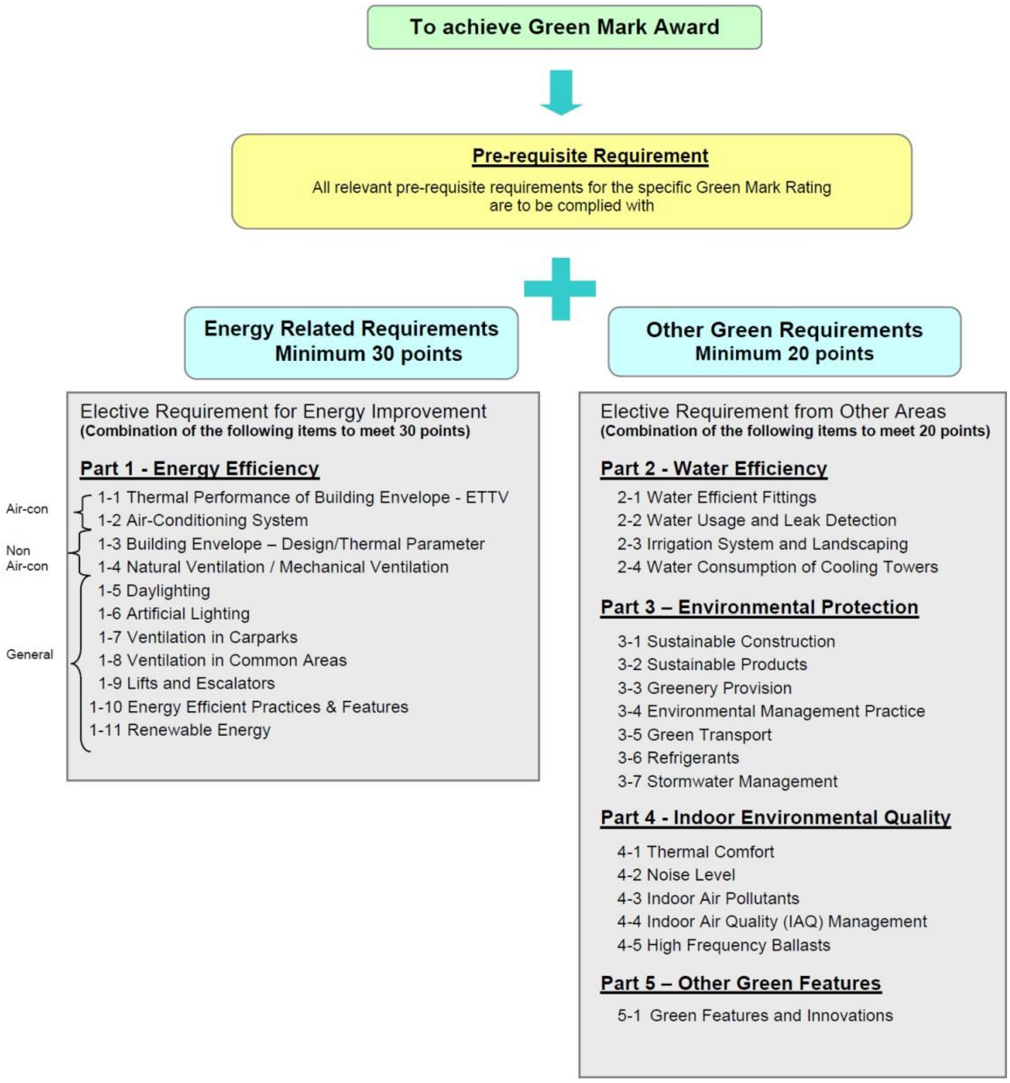

Figure 128. Green Mark award criteria (NRB/4.1)

Under the BCA Green Mark Assessment framework, points are awarded for implementing environment-friendly features in the building proposal (Figure 128). Specific targets are set out and the rationale is that if more targets are met, the building under assessment is likely to be environment-friendlier than buildings which have not considered similar issues. Points are given for targets that are met in the checklist and are collated in the end. The net score is supposed to provide a gauge for the overall environment-friendliness of a building. This minimum environmental sustainability standard reflects the commitment of BCA to push for Green Building in Singapore.

10.4.3 Greenery in Green Mark

The following section outlines the involvement of urban greenery in the Green Mark evaluation process. For the purpose of discussion, BCA Green Mark for New Non-Residential Buildings Version NRB/4.1 will be used as the scheme of interest. Recommendations made in this section are based on reviewed literature as well as findings listed from Chapters 6.2.1 to 6.2.4.

10.4.3.1 Energy Efficiency

It can be observed from Figure 129 that energy efficiency is prominently featured in the Green Mark assessment process. Out of a maximum of 190 points, 116 have been allocated for energy related requirements (61%).

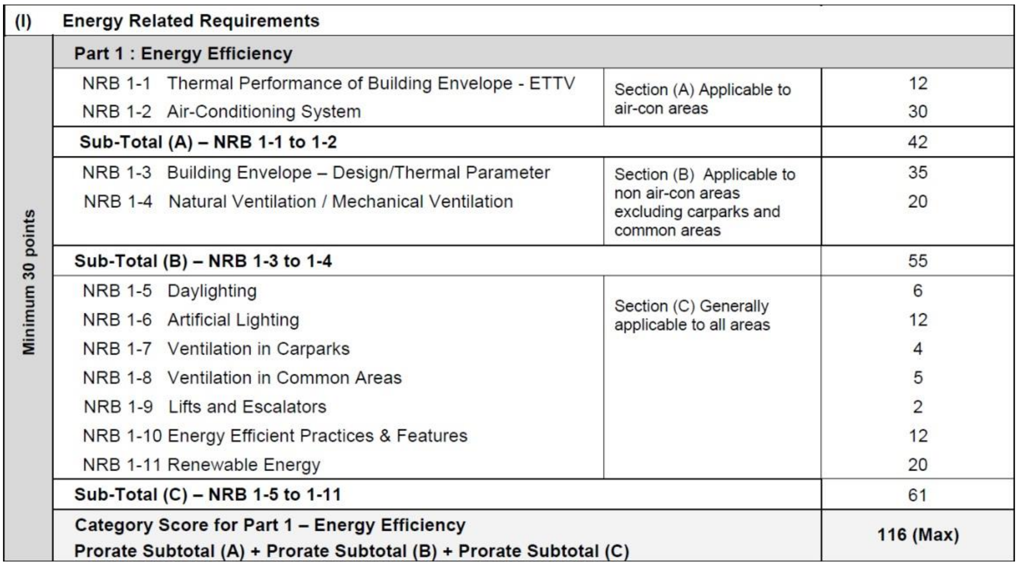

(I)	**Energy Related Requirements**		
Minimum 30 points	**Part 1 : Energy Efficiency**		
	NRB 1-1 Thermal Performance of Building Envelope - ETTV	Section (A) Applicable to air-con areas	12
	NRB 1-2 Air-Conditioning System		30
	Sub-Total (A) – NRB 1-1 to 1-2		42
	NRB 1-3 Building Envelope – Design/Thermal Parameter	Section (B) Applicable to non air-con areas excluding carparks and common areas	35
	NRB 1-4 Natural Ventilation / Mechanical Ventilation		20
	Sub-Total (B) – NRB 1-3 to 1-4		55
	NRB 1-5 Daylighting	Section (C) Generally applicable to all areas	6
	NRB 1-6 Artificial Lighting		12
	NRB 1-7 Ventilation in Carparks		4
	NRB 1-8 Ventilation in Common Areas		5
	NRB 1-9 Lifts and Escalators		2
	NRB 1-10 Energy Efficient Practices & Features		12
	NRB 1-11 Renewable Energy		20
	Sub-Total (C) – NRB 1-5 to 1-11		61
	Category Score for Part 1 – Energy Efficiency **Prorate Subtotal (A) + Prorate Subtotal (B) + Prorate Subtotal (C)**		**116 (Max)**

Figure 129. Energy related requirements

Potential contribution of greenery is outlined in the following requirements:

1. NRB 1-1 Thermal performance of building envelope – Envelope thermal transfer value (ETTV)
2. NRB 1-3 Building envelope – Design / thermal parameters
3. NRB 1-10 Energy efficient practices and features

10.4.3.1.1 NRB 1-1 Thermal performance of building envelope – Envelope thermal transfer value (ETTV)

Figure 130 shows energy requirements for thermal performance of building envelopes. Thermal performance is determined by measuring the Envelope Thermal Transfer Value (ETTV). Developed by Chua and Chou (2010), ETTV describes the amount of heat a building gains via its envelope. Components that are considered for ETTV calculation are as follows:

1. Heat gain through walls and windows;
2. Solar radiation gain through windows.

They are averaged over the building envelope area to derive the ETTV value. The ETTV formula is presented as (Chua and Chou, 2010):

$$ETTV = TD_{eq}(1 - WWR)U_w + \Delta T(WWR)U_f + SF(WWR)(CF)(SC) \qquad [25]$$

Where,

ETTV = Envelope Thermal Transfer Value (Wm^{-2})

TD$_{eq}$ = Equivalent temperature difference (°C)

WWR = Window-to-wall ratio

U$_w$ = Thermal transmittance of opaque wall (Wm^{-2}K)

ΔT = Temperature difference (°C)

U$_f$ = Thermal transmittance of fenestration (Wm^{-2}K)

SF = Solar factor (Wm^{-2})

CF = Solar correction factor for fenestration

SC = Shading coefficient of fenestration

Figure 130 shows that 1.2 points can be earned for every reduction of 1 Wm^{-2} in ETTV from the baseline model. A maximum of 12 points can be attained in this manner. From Equation (26), it can be seen that ETTV can be reduced by decreasing thermal transmittance values of the wall (U_w) and fenestration (U_f), as well as the fenestration shading coefficient (SC).

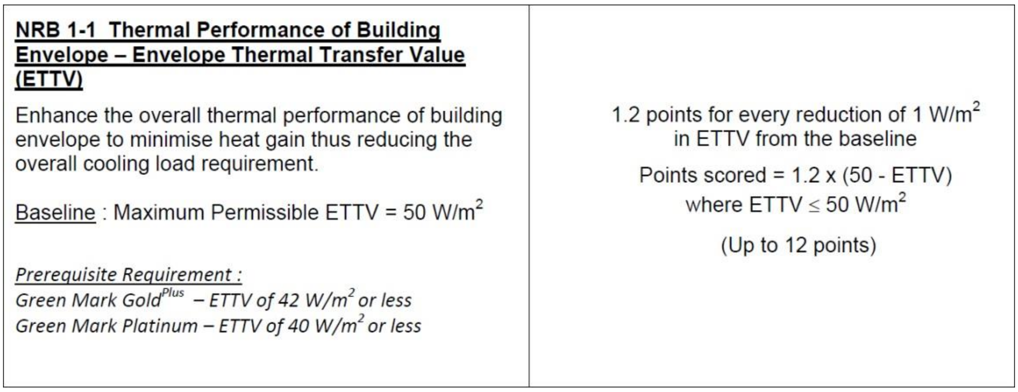

NRB 1-1 Thermal Performance of Building Envelope – Envelope Thermal Transfer Value (ETTV) Enhance the overall thermal performance of building envelope to minimise heat gain thus reducing the overall cooling load requirement. Baseline : Maximum Permissible ETTV = 50 W/m^2 *Prerequisite Requirement :* *Green Mark Gold^{Plus} – ETTV of 42 W/m^2 or less* *Green Mark Platinum – ETTV of 40 W/m^2 or less*	1.2 points for every reduction of 1 W/m^2 in ETTV from the baseline Points scored = 1.2 x (50 - ETTV) where ETTV $\leq$ 50 W/m^2 (Up to 12 points)

Figure 130. NRB 1-1 Thermal performance of building envelope - Envelope thermal transfer value (ETTV)

Many studies have attempted to quantify the reduction of thermal transmittance using vertical greenery. Using field measurement data, Wong et al. (2003b) estimated R-values of various forms of vegetation (tree, shrub and turf) and used those values to simulate the effects of building energy consumption. Wong et al. (2009) used the derived R-values to show that the U-value of walls can be reduced significantly, resulting in lower ETTV values.

An example of a typical wall and green wall construction is shown in Figure 131. It can be seen that U-value of the wall can be reduced by more than 70 % with vertical greenery. Surface temperature reduction is further substantiated by measurements of wall surface temperature shown in Chapter 10.3.1.3.1. The U-value of fenestration (i.e. glass windows) can also be reduced, but to a lesser extent (Wong et al., 2009).

In addition to reducing the U-value of walls, greenery can also reduce the shading coefficient of fenestration, hence lowering heat transmission. Wong et al. (2009) showed that the correlation between plant shading coefficient and LAI can be expressed via the equation below:

$$Plant\ Shading\ Coefficient = -0.3043\ LAI + 0.8112 \qquad [26]$$

Where,

LAI = Leaf Area Index

Assuming an LAI value of 2 is assigned for vertical greenery (Tan and Sia, 2009), Plant Shading Coefficient

= -0.3043 LAI + 0.8112

= -0.3043 X 2 + 0.8112

= 0.2

If we consider a glass fenestration of SC value 0.50,

Overall shading coefficient with windows with greenery in front

= Shading coefficient of windows X Shading coefficient of plants

= 0.50 x 0.2

= 0.10

It can be seen that fenestration SC can be reduced significantly by 80 %. This gives greenery a tremendous ability to in reduce solar penetration into the building.

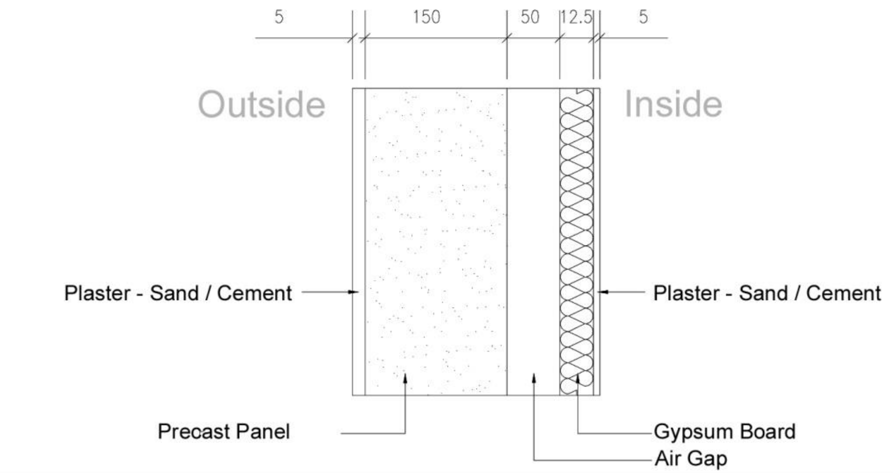

Typical normal wall detail

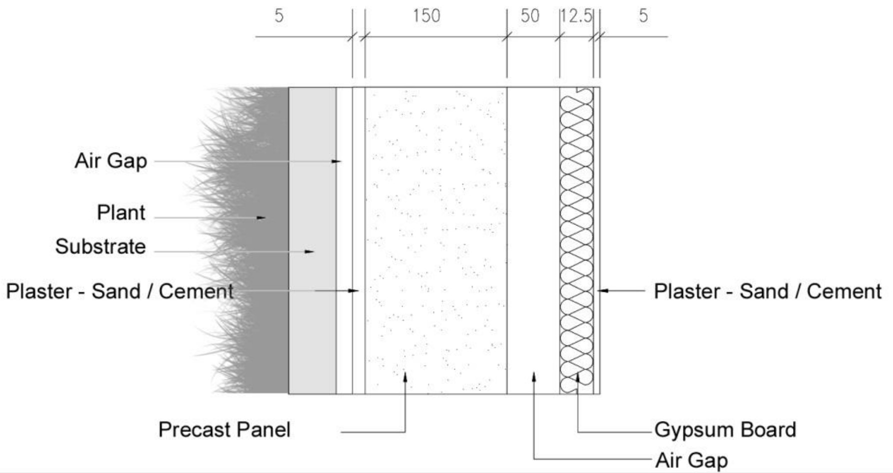

Typical green wall detail

	Typical normal wall composition	**Typical green wall composition**
Component	R-Value	R-Value
Outside air film	0.0440	0.0440
Plant	-	0.3600
Substrate	-	1.9230
Air gap	-	0.1600
Plaster – Sand / Cement	0.0094	0.0094
Precast panel	0.3151	0.3151
Air space	0.1525	0.1525
Gypsum plaster board	0.0735	0.0735
Plaster – Sand / Cement	0.0094	0.0094
Inside surface	0.1200	0.1200
Total R-Value (m^{2}KW^{-1})	0.7239	3.1669
U-Value (Wm-^{2}K^{-1})	1.3814	0.3158

Figure 131. Comparison of U-values for normal wall and green wall

Green wall systems are commonly categorised into carrier (casement/cassette/modular pots) and support systems (creepers) (Tan and Chiang, 2009). Figure 132 illustrates the difference between the two systems.

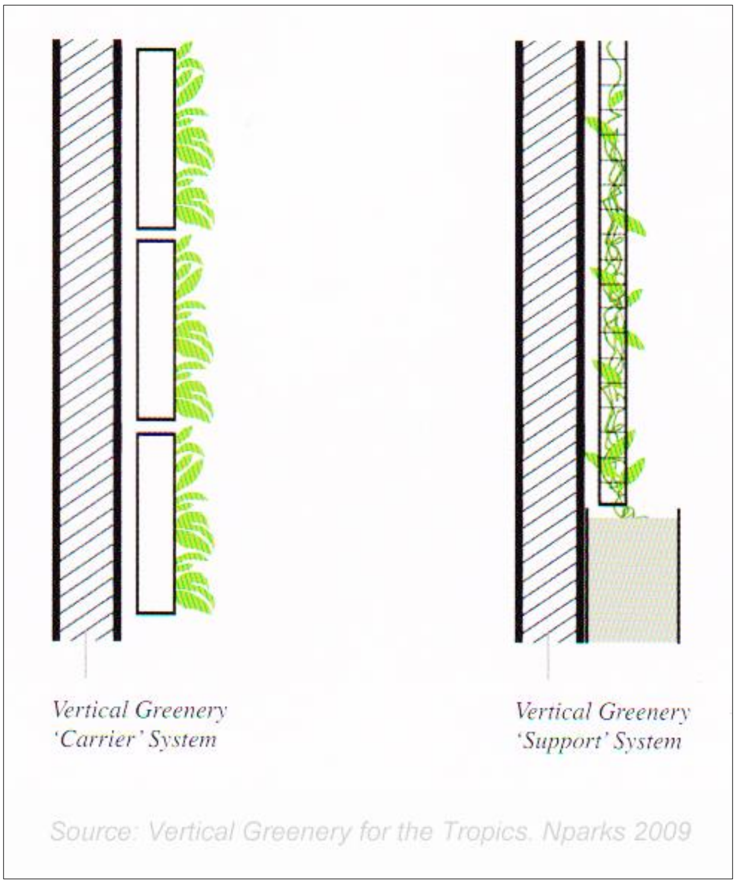

Source: Vertical Greenery for the Tropics. Nparks 2009

Figure 132. Carrier and Support systems

To reduce the SC of building fenestrations, vertical greenery support systems can be used so as not to obstruct views to the exterior completely. An example of vertical greenery in from of a glass façade is shown in Figure 133. Some suggestions for detailing are shown in Figure 134.

Figure 133. An example of greenery in front of glass façade

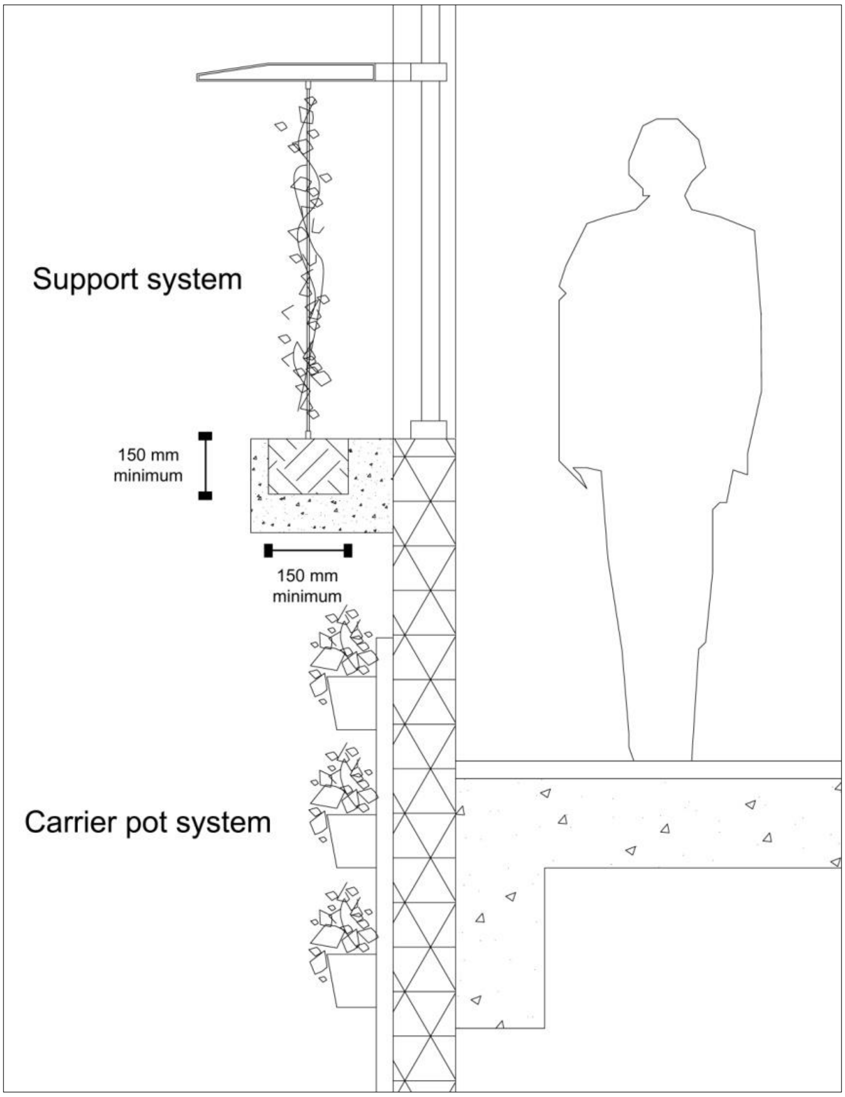

Figure 134. Sketch section of greenery in front of window

Although greenery is not explicitly mentioned in this section, ample evidence has been put forth to suggest that it can reduce solar heat gain into buildings. In addition, as these measurements were conducted in Singapore, R-values derived from these studies are suitable for use in the Green Mark assessment criteria.

Therefore, it is highly recommended that the impact of greenery be considered when calculating U-value and SC.

10.4.3.1.2 NRB 1-3 Building envelope – Design / thermal parameters

Figure 135 shows design and thermal parameters for the building envelope.

Section (c) emphasises on better thermal transmittance (U-value) of external west facing walls, and that U-value of walls should be less than 2 $Wm^{-2}K^{-1}$. The methodology for utilising vertical greenery to improve U-value has been outlined in the previous section.

Section (d) emphasises on better thermal transmittance (U-value) of roof. The U value of roofs can be significantly reduced by adding greenery. (Wong et al., 2003b) showed installation of rooftop greenery can result in 1 % - 15 % savings in annual energy consumption.

Table 43 shows that a reasonable expectation in reduction of U-value is 1.212 Wm^{-2}. Since 1 point is allocated for every 0.1 Wm^{-2} of reduction of green roof U-value, adding rooftop greenery, in addition to lowering energy consumption, can help to improve overall Green Mark score by up to 5 points.

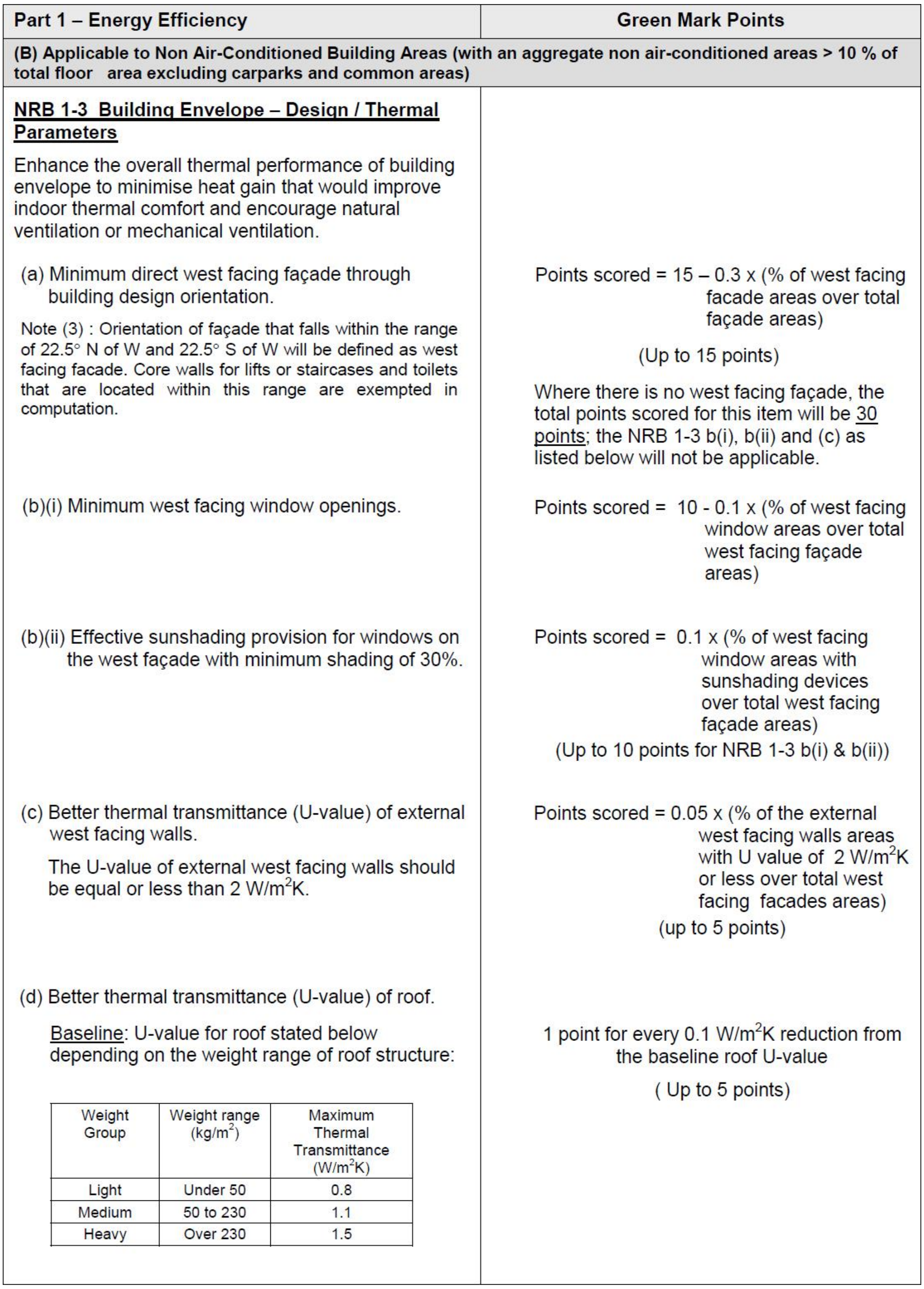

Part 1 – Energy Efficiency	**Green Mark Points**
(B) Applicable to Non Air-Conditioned Building Areas (with an aggregate non air-conditioned areas > 10 % of total floor area excluding carparks and common areas)	
NRB 1-3 Building Envelope – Design / Thermal Parameters Enhance the overall thermal performance of building envelope to minimise heat gain that would improve indoor thermal comfort and encourage natural ventilation or mechanical ventilation.	
(a) Minimum direct west facing façade through building design orientation. Note (3) : Orientation of façade that falls within the range of 22.5° N of W and 22.5° S of W will be defined as west facing facade. Core walls for lifts or staircases and toilets that are located within this range are exempted in computation.	Points scored = 15 – 0.3 x (% of west facing facade areas over total façade areas) (Up to 15 points) Where there is no west facing façade, the total points scored for this item will be 30 points; the NRB 1-3 b(i), b(ii) and (c) as listed below will not be applicable.
(b)(i) Minimum west facing window openings.	Points scored = 10 - 0.1 x (% of west facing window areas over total west facing façade areas)
(b)(ii) Effective sunshading provision for windows on the west façade with minimum shading of 30%.	Points scored = 0.1 x (% of west facing window areas with sunshading devices over total west facing façade areas) (Up to 10 points for NRB 1-3 b(i) & b(ii))
(c) Better thermal transmittance (U-value) of external west facing walls. The U-value of external west facing walls should be equal or less than 2 W/m^2K.	Points scored = 0.05 x (% of the external west facing walls areas with U value of 2 W/m^2K or less over total west facing facades areas) (up to 5 points)
(d) Better thermal transmittance (U-value) of roof. Baseline: U-value for roof stated below depending on the weight range of roof structure:	1 point for every 0.1 W/m^2K reduction from the baseline roof U-value (Up to 5 points)

Weight Group	Weight range (kg/m^2)	Maximum Thermal Transmittance (W/m^2K)
Light	Under 50	0.8
Medium	50 to 230	1.1
Heavy	Over 230	1.5

Figure 135. Energy efficiency checklist

Table 43. U-values of normal roof and green roof (Wong et al., 2003b)

	Typical normal roof composition	**Typical green roof composition**
Component	R-Value	R-Value
Outside air film	0.055	0.055
Turf	-	0.360
Substrate	-	0.063
WOLFIN IB single layer polymerised	0.001	0.001
Cement and sand base screed to fall	0.094	0.094
RC concrete	0.104	0.104
Inside air film	0.162	0.162
Total R-Value (m^2KW^{-1})	0.416	0.839
U-Value ($Wm\text{-}^2K^{-1}$)	2.404	1.192

10.4.3.1.3 NRB 1-10 Energy efficient practices and features

Figure 136 elaborates on energy efficient practices and features. Section (b) awards the use of vertical greenery systems on east and west façade to reduce heat gain through building envelope. Chapter 10.3.2.3.2 has shown that the westward facing wall can be significantly hotter than the eastward facing wall. Therefore, more points should be awarded for adding greenery on westward facing walls. As only a maximum of 1 point is award in this section, there may be little incentive for architects to pay attention to this section. More points may be awarded if more effort is put in by architects to evaluate the impact of greenery placement, such as using the method outlined in Chapter 6.2.4.3 to determine optimal plant selection and allocation.

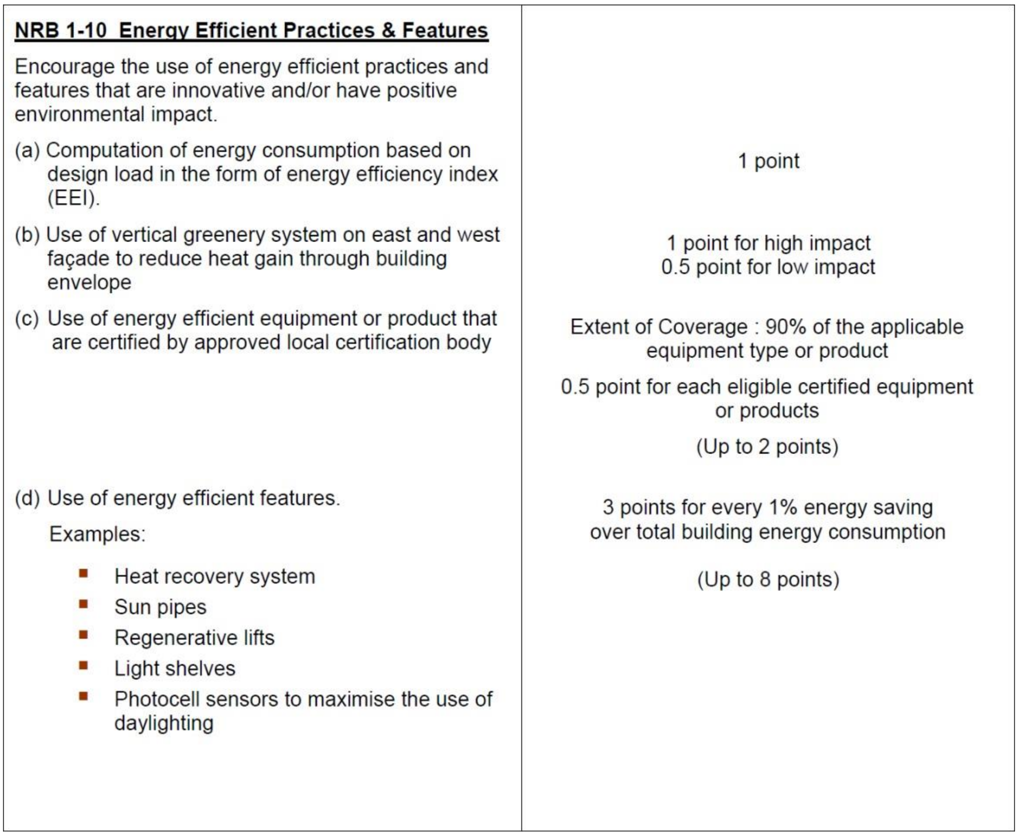

NRB 1-10 Energy Efficient Practices & Features Encourage the use of energy efficient practices and features that are innovative and/or have positive environmental impact.	
(a) Computation of energy consumption based on design load in the form of energy efficiency index (EEI).	1 point
(b) Use of vertical greenery system on east and west façade to reduce heat gain through building envelope	1 point for high impact 0.5 point for low impact
(c) Use of energy efficient equipment or product that are certified by approved local certification body	Extent of Coverage : 90% of the applicable equipment type or product 0.5 point for each eligible certified equipment or products (Up to 2 points)
(d) Use of energy efficient features. Examples: ▪ Heat recovery system ▪ Sun pipes ▪ Regenerative lifts ▪ Light shelves ▪ Photocell sensors to maximise the use of daylighting	3 points for every 1% energy saving over total building energy consumption (Up to 8 points)

Figure 136. NRB 1-10 Energy efficient practices and features

10.4.3.2 Water efficiency

Figure 137 shows water efficiency requirements for Green Mark assessment.

Water efficiency is allocated 17 out of a total of 190 points (8.9 %).

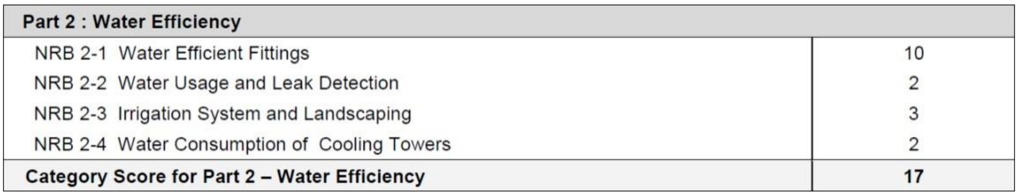

Part 2 : Water Efficiency	
NRB 2-1 Water Efficient Fittings	10
NRB 2-2 Water Usage and Leak Detection	2
NRB 2-3 Irrigation System and Landscaping	3
NRB 2-4 Water Consumption of Cooling Towers	2
Category Score for Part 2 – Water Efficiency	**17**

Figure 137. Water efficiency checklist

Potential contribution of greenery is outlined in the following requirements:

1. NRB 2-3 – Irrigation system and landscaping

10.4.3.2.1 NRB 2-3 Irrigation system and landscaping

Figure 138 shows irrigation system and landscaping requirements. Section (c) awards the use of drought tolerant plants that require minimal irrigation. Chapter 6.1.1 has discussed the merits of choosing plants with high ET rates for the purpose of reducing ambient temperature and outdoor t_{mrt}. The use of drought tolerant plants is discouraged as the ET rate of drought tolerant plants are low and will reduce their cooling potential.

Since the purpose of Section (c) is to minimise water usage, landscape design can be optimised in the following manner:

1. Drought tolerant plants can be used at areas far away from pedestrian pathways; and
2. Plants with high ET rates can be used along pedestrian pathways.

In this manner, water usage can be kept to its minimal without comprising outdoor thermal comfort for pedestrians. Figure 139 illustrates the possible segregation of areas in a hypothesized rooftop garden plan. Areas that are near to designated pedestrian paths (blue) are highlighted in dark green. Drought tolerant plants can be allocated in areas highlighted in light green. An irrigation plan can be set up based on this diagram. Usage of this method may be awarded more points for the intention of optimising urban greenery.

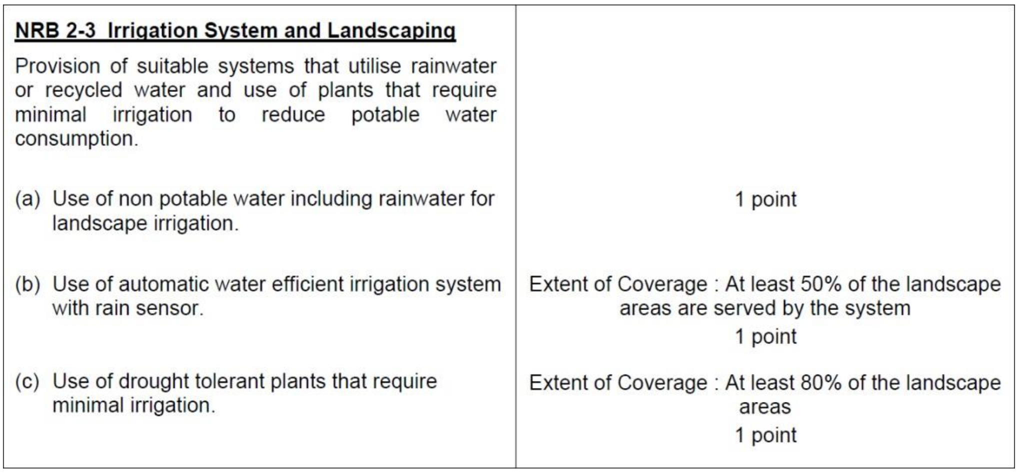

NRB 2-3 Irrigation System and Landscaping Provision of suitable systems that utilise rainwater or recycled water and use of plants that require minimal irrigation to reduce potable water consumption.	
(a) Use of non potable water including rainwater for landscape irrigation.	1 point
(b) Use of automatic water efficient irrigation system with rain sensor.	Extent of Coverage : At least 50% of the landscape areas are served by the system 1 point
(c) Use of drought tolerant plants that require minimal irrigation.	Extent of Coverage : At least 80% of the landscape areas 1 point

Figure 138. NRB 2-3 Irrigation system and landscaping

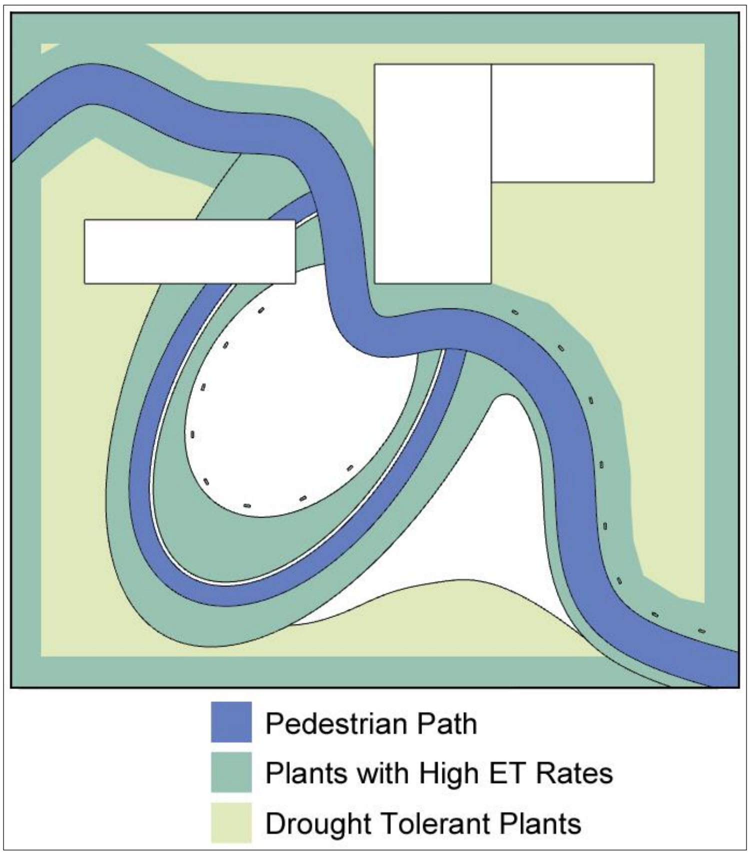

Figure 139. Hypothetical rooftop garden design plan

10.4.3.3 Environmental protection

Figure 140 shows requirements for environmental protection. A total of 42 out of 190 points are allocated (22 %).

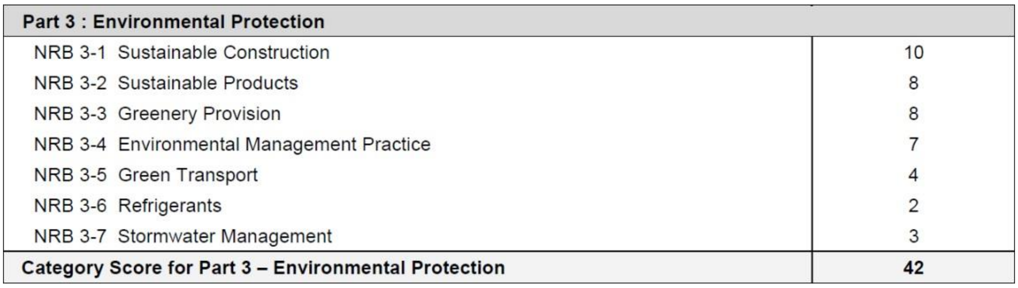

Part 3 : Environmental Protection	
NRB 3-1 Sustainable Construction	10
NRB 3-2 Sustainable Products	8
NRB 3-3 Greenery Provision	8
NRB 3-4 Environmental Management Practice	7
NRB 3-5 Green Transport	4
NRB 3-6 Refrigerants	2
NRB 3-7 Stormwater Management	3
Category Score for Part 3 – Environmental Protection	**42**

Figure 140. Environmental protection checklist

Potential contribution of greenery is outlined in the following requirements:

1. NRB 3-3 – Greenery provision

10.4.3.3.1 NRB 3-3 Greenery provision

Figure 141 shows greenery provision requirements for Green Mark assessment. Section (a) awards up to 6 points for increasing the Green Plot Ratio to 4 and above.

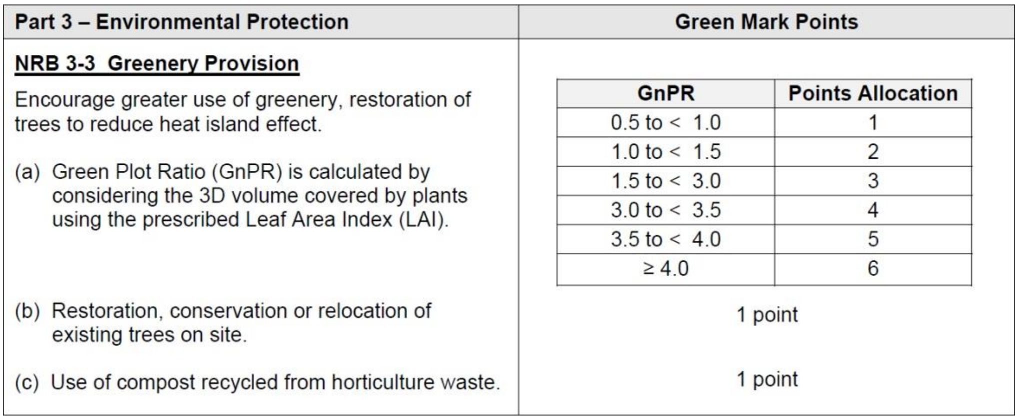

<table>
<tr><th>Part 3 – Environmental Protection</th><th>Green Mark Points</th></tr>
<tr><td>**NRB 3-3 Greenery Provision**
Encourage greater use of greenery, restoration of trees to reduce heat island effect.</td><td></td></tr>
<tr><td>(a) Green Plot Ratio (GnPR) is calculated by considering the 3D volume covered by plants using the prescribed Leaf Area Index (LAI).</td><td>
<table>
<tr><th>GnPR</th><th>Points Allocation</th></tr>
<tr><td>0.5 to < 1.0</td><td>1</td></tr>
<tr><td>1.0 to < 1.5</td><td>2</td></tr>
<tr><td>1.5 to < 3.0</td><td>3</td></tr>
<tr><td>3.0 to < 3.5</td><td>4</td></tr>
<tr><td>3.5 to < 4.0</td><td>5</td></tr>
<tr><td>≥ 4.0</td><td>6</td></tr>
</table>
</td></tr>
<tr><td>(b) Restoration, conservation or relocation of existing trees on site.</td><td>1 point</td></tr>
<tr><td>(c) Use of compost recycled from horticulture waste.</td><td>1 point</td></tr>
</table>

Figure 141. Greenery provision checklist

Green Plot Ratio (GnPR) is defined as the ‘ratio of the total single-side leaf area of the planted landscape to the plot or site area’ (Ong, 2003) and can be expressed as follows:

$$Green\ Plot\ Ratio = \frac{(Total\ Leaf\ Area)}{Site\ Area} = \frac{\sum(LAI\ 1 \times Canopy\ Area\ 1 \ldots + LAI\ N \times Canopy\ Area\ N)}{Site\ Area} \quad [27]$$

Where,

LAI = Leaf Area Index

Figure 142 demonstrates how GnPR is calculated. GnPR is now adopted by Singapore’s National Parks Board (NParks) as a method in quantifying greenery density (Tan and Sia, 2009).

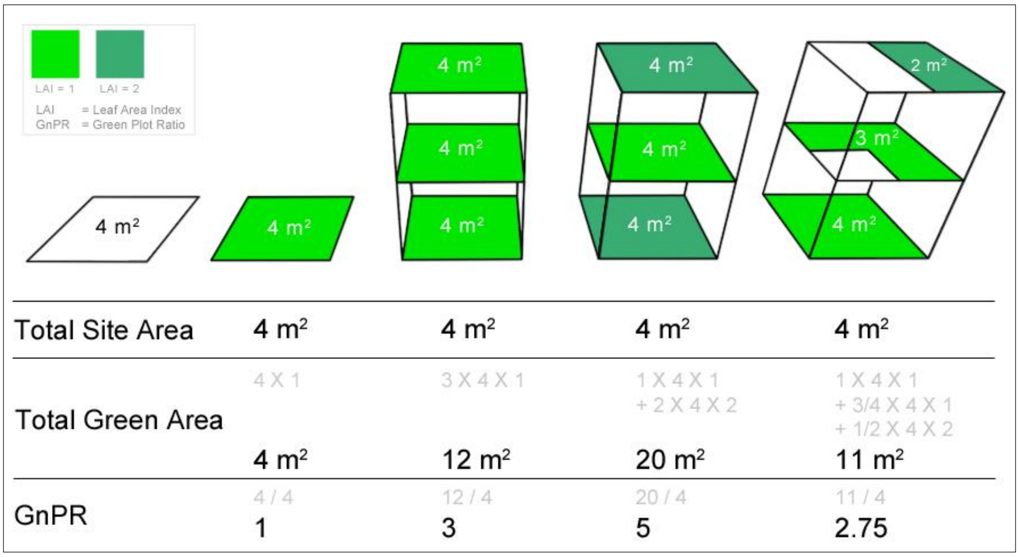

Total Site Area	4 m²	4 m²	4 m²	4 m²
Total Green Area	4 X 1 4 m²	3 X 4 X 1 12 m²	1 X 4 X 1 + 2 X 4 X 2 20 m²	1 X 4 X 1 + 3/4 X 4 X 1 + 1/2 X 4 X 2 11 m²
GnPR	4 / 4 1	12 / 4 3	20 / 4 5	11 / 4 2.75

Figure 142. Illustration of Green Plot Ratio (GnPR) calculation

From Section (a) of Figure 141, it can be deduced that:

1. With a maximum of 6 points to be awarded, the impact of greenery is perceived to be most relevant here compared to other sections;
2. Environmental protection is achieved by reducing the UHI effect;
3. The UHI effect can be mitigated by adding greenery; and
4. More greenery equates to better environmental protection.

Item 4 raises a point of contention, in that it carries the assumption that more greenery will bring about more benefits. It also advocates the belief that plants should only be distinguished by their LAI value, and that other functional traits need not be considered. The limitation of using GnPR as an indicator of plant density and hence level of protection to the environment was recognised by Ong (2003), who acknowledged that GnPR alone cannot indicate relevant environmental factors such as species richness on site. Results from Chapter 4 have also shown that plant traits such as ET and SA contribute significantly to plant cooling potential, and that LAI is poorly correlated with t_{mrt} reduction. Most importantly, this study has shown that plant selection and allocation is not a one-dimensional process and there is a need to consider the effects of context and locality.

Therefore, the study proposes the steps taken in Chapter 6.2, namely the simulation of building and site conditions to locate optimal plant placement spots. More points may be awarded for landscape proposals that take solar insolation into consideration for selection and allocation of plants.

An example is given in Figure 143. More points can be awarded for greenery allocated on building surfaces with higher solar exposure.

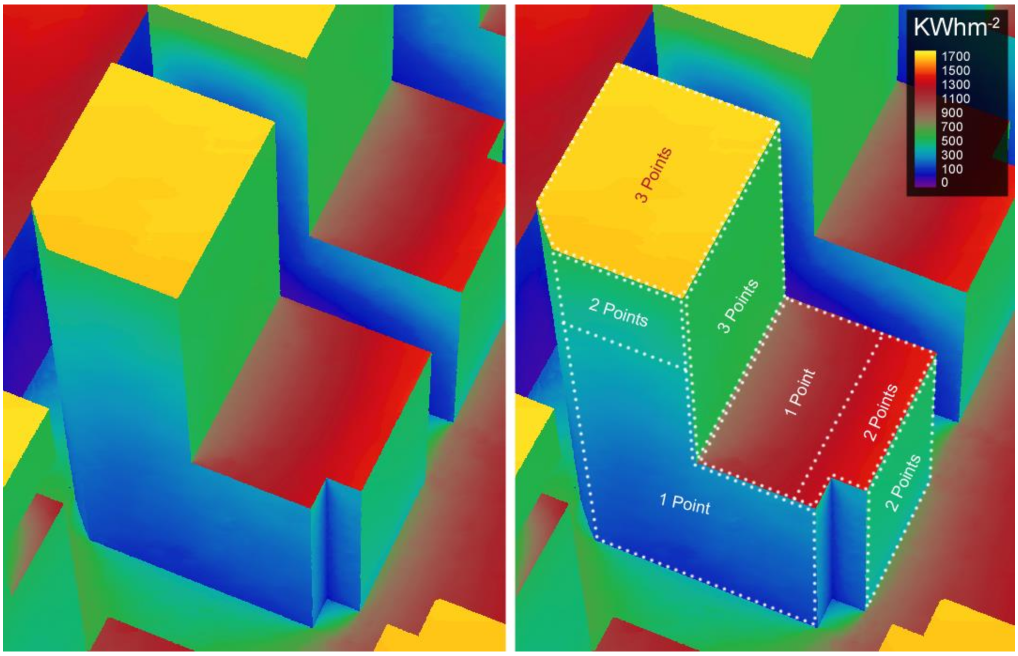

Figure 143. Point allocation based on solar insolation map

This recommendation is not limited to the Green Mark rating tool, as the intention of increasing greenery density is prevalent in other government agencies. For instance, the Urban Redevelopment Authority of Singapore (URA) encourages addition of greenery within the urban environment via its Landscaping for Urban Spaces and High-Rises (LUSH) 2.0 programme (URA, 2014b). One requirement is to ensure that the displaced site area is fully replaced with landscape, with at least 40 % of the development site area comprising of permanent planting (i.e. softscape) (Figure 144)(URA, 2014a).

The Landscape Replacement Areas (LRAs) guidelines are set out to achieve the following objectives (URA, 2009):

1. Using greenery to enhance quality of life;
2. Enhancing image of a city in the tropics by having greenery at ground and above-ground levels; and
3. Improving thermal comfort and air quality through greenery.

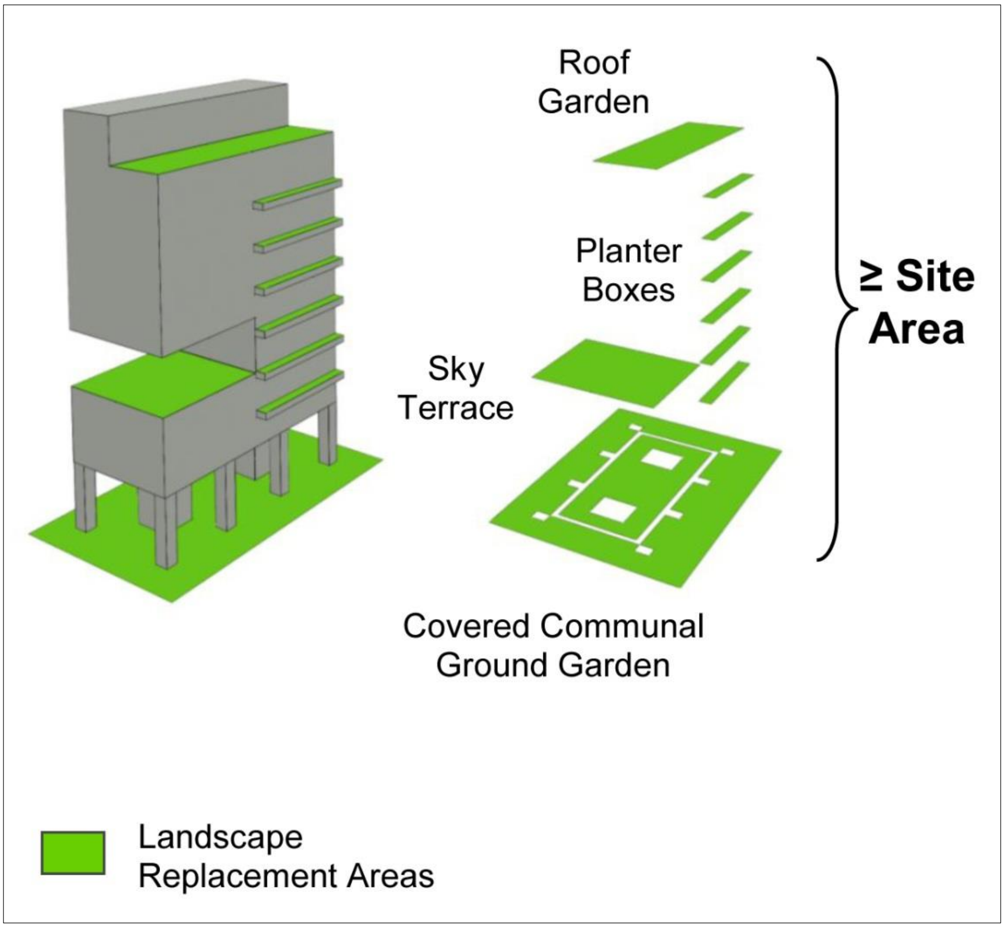

Figure 144. LUSH 2.0 landscape replacement policy

Since the objective of LUSH 2.0 LRA guidelines (Point 3) is similar to BCA Green Mark (NRB 3-3), selection and allocation of plants can follow the methodology proposed in this chapter.

10.4.3.4 Indoor Environmental Quality

Figure 145 shows requirements of indoor environmental quality for Green Mark assessment. A total of 8 out of 190 points is allocated for indoor environmental quality (4 %).

Part 4 : Indoor Environmental Quality	
NRB 4-1 Thermal Comfort	1
NRB 4-2 Noise Level	1
NRB 4-3 Indoor Air Pollutants	2
NRB 4-4 Indoor Air Quality (IAQ) Management	2
NRB 4-5 High Frequency Ballasts	2
Category Score for Part 4 – Indoor Environmental Quality	**8**

Figure 145. Indoor environmental quality checklist

Potential contribution of greenery is outlined in the following requirements:

1. NRB 4-2 – Noise level
2. NRB 4-3 – Indoor air pollutants

10.4.3.4.1 NRB 4-2 Noise level

Figure 146 shows requirements for noise level control.

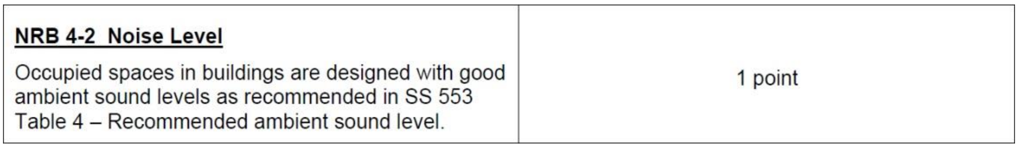

NRB 4-2 Noise Level Occupied spaces in buildings are designed with good ambient sound levels as recommended in SS 553 Table 4 – Recommended ambient sound level.	1 point

Figure 146. NRB 4-2 Noise level

For occupied spaces that are not able to achieve the desired sound level, greenery can be used to improve sound conditions. There have been numerous studies showcasing the acoustic absorbing properties of plants.

Lagstorm (2004) observed that supplementary noise reduction of up to 20 dB could be achieved with the installation of rooftop greenery. This finding was similar to findings by Connelly and Hodgson (2008), who recorded up to 13 dB with an extensive green roof. Wong et al. (2010b) showed that vertical greenery systems can also provide noise reduction capabilities and that the potential is higher with increasing greenery coverage.

10.4.3.4.2 NRB 4-3 Indoor air pollutants

Figure 147 shows requirements for indoor air pollutants.

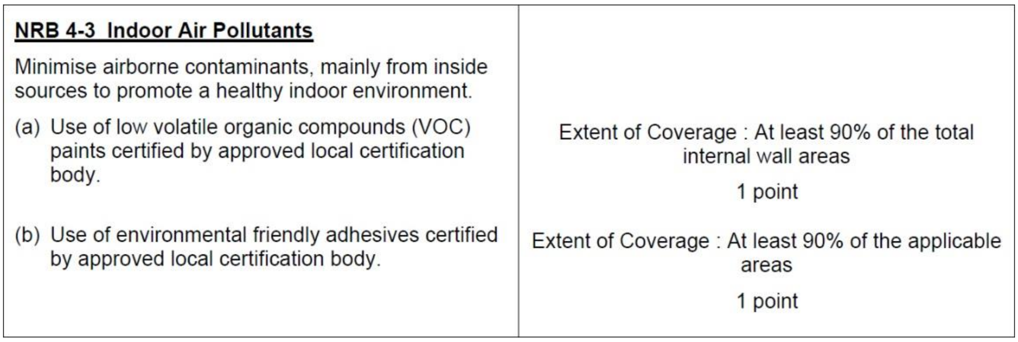

NRB 4-3 Indoor Air Pollutants Minimise airborne contaminants, mainly from inside sources to promote a healthy indoor environment.	
(a) Use of low volatile organic compounds (VOC) paints certified by approved local certification body.	Extent of Coverage : At least 90% of the total internal wall areas 1 point
(b) Use of environmental friendly adhesives certified by approved local certification body.	Extent of Coverage : At least 90% of the applicable areas 1 point

Figure 147. NRB 4-3 Indoor air pollutants

In addition to items highlighted in Sections (a) and (b), plants can be added into the interior design scape to clean the air. Many studies have shown that plants have the ability to improve indoor air quality.

Wolverton et al. (1989) tested twelve indoor plants and showed that reductions in benzene and formaldehyde were significant all plants tested. It was noted that for plant soil to be effective in removing indoor air pollutants, plants must be growing in the soil, pointing to suggestions that indoor air pollution can be removed indirectly though the root/soil pathway.

Kim et al. (2008) measured the removal of volatile formaldehyde by *Fatsia japonica Decne. & Planch* and *Ficus benjamina L*. and observed that formaldehyde concentration is reduced significantly in the root zone of both plants.

Wolverton and Wolverton (1993) showed that commonly used indoor plants can be very effective at removing compounds such as ammonia and formaldehyde from the air. It was observed that *Nephrolepis exaltata "Bostoniensis"* (Boston fern) and *Rhapis excelsa* (Lady palm), both commonly used plants in the local landscaping industry, were effective at removing formaldehyde and ammonia respectively.

10.4.4 Recommendations for improvement

A detailed analysis of the current BCA Green Mark scheme (Chapter 10.4.2) has highlighted the involvement of greenery in the entire assessment process. It is clear that the role of greenery is mainly to reduce the UHI effect. Findings from this study as well as reviewed literature have shown that greenery can be more prominently featured in the areas of energy and water efficiency, as well as indoor environmental quality.

As the building footprint in a city is often limited, building and roof spaces will become increasingly important to improve overall liveability and well-being of its inhabitants. The expectation of urban greenery to enhance the environment will increase in tandem. This may include higher cooling, biodiversity and aesthetic requirements. The proposed recommendations serve to realise the full potential of greenery.

Suggestions for the next version of Green Mark assessment criteria are as follows:

1. Inclusion of thermal transmission of greenery in cooling load simulation (Chapter 10.4.3.1);
2. More points awarded to greenery in the areas of energy and water efficiency, as well as indoor environmental quality; and
3. Use of solar insolation simulation and plant selection chart for landscape plan, in addition to GnPR requirements (Chapter 10.4.3.3).

10.5 Data for regression model

Plot 1 - Phyllanthus cochinchinensis					
Date	Time	Tmrt Plant	Tmrt Reference	Plant ET	Albedo
13-May	13:00	57.09	63.07	0.0076	0.29
	14:00	58.75	67.75	0.0182	0.27
	15:00	57.09	72.22	0.0221	0.29
	16:00	55.07	70.89	0.0248	0.29
	17:00	53.84	65.33	0.0270	0.29
15-May	13:00	53.92	59.68	0.0044	0.28
	14:00	46.55	55.45	0.0127	0.27
	15:00	49.12	61.55	0.0194	0.29
	16:00	46.98	57.89	0.0226	0.33
	17:00	38.39	43.37	0.0248	0.30
22-May	13:00	59.61	57.94	0.0080	0.29
	14:00	54.07	59.34	0.0089	0.27
	15:00	54.08	63.73	0.0087	0.29
	16:00	51.11	61.42	0.0085	0.33
	17:00	38.40	44.80	0.0090	0.40
24-May	13:00	53.33	56.24	0.0084	0.31
	14:00	55.46	63.29	0.0109	0.29
	15:00	47.22	55.44	0.0115	0.30
	16:00	53.46	62.62	0.0098	0.34
	17:00	48.88	58.36	0.0110	0.41
25-May	13:00	55.90	62.17	0.0106	0.29
	14:00	57.92	69.06	0.0106	0.27
	15:00	57.62	69.97	0.0105	0.29
	16:00	45.44	55.02	0.0113	0.30
	17:00	36.98	44.07	0.0119	0.41
28-May	13:00	58.29	64.23	0.0066	0.30
	14:00	54.30	63.11	0.0111	0.28
	15:00	53.73	61.83	0.0141	0.28
	16:00	51.67	62.92	0.0134	0.30
	17:00	55.14	69.69	0.0158	0.36
29-May	13:00	47.44	48.53	0.0050	0.30
	14:00	46.99	51.45	0.0091	0.28
	15:00	54.77	62.66	0.0146	0.30
	16:00	54.85	62.75	0.0184	0.31
	17:00	45.92	49.03	0.0208	0.31
8-Jun	13:00	53.44	58.05	0.0107	0.29
	14:00	51.38	58.14	0.0116	0.28
	15:00	54.04	66.67	0.0118	0.30
	16:00	51.48	67.03	0.0115	0.31
	17:00	53.43	67.16	0.0102	0.32

10-Jun	13:00	56.98	63.15	0.0068	0.30
	14:00	55.24	60.47	0.0096	0.28
	15:00	51.75	61.39	0.0133	0.28
	16:00	53.35	66.68	0.0195	0.33
	17:00	40.37	47.50	0.0227	0.31
11-Jun	13:00	55.48	58.07	-0.0019	0.30
	14:00	57.48	64.20	0.0077	0.28
	15:00	52.90	64.64	0.0151	0.34
	16:00	47.06	57.30	0.0203	0.31
	17:00	51.77	65.43	0.0243	0.32
13-Jun	13:00	55.46	63.62	0.0058	0.29
	14:00	54.29	64.56	0.0110	0.27
	15:00	52.65	60.69	0.0152	0.28
	16:00	50.51	59.49	0.0203	0.30
	17:00	41.01	48.08	0.0203	0.30
16-Jun	13:00	59.57	68.16	0.0072	0.27
	14:00	55.76	62.58	0.0102	0.26
	15:00	57.73	67.17	0.0126	0.27
	16:00	53.96	60.06	0.0158	0.29
	17:00	42.89	46.90	0.0168	0.30
17-Jun	13:00	58.12	67.33	0.0058	0.27
	14:00	57.98	66.26	0.0125	0.26
	15:00	57.93	67.16	0.0157	0.25
	16:00	59.70	68.84	0.0165	0.26
	17:00	59.02	67.86	0.0176	0.25
18-Jun	13:00	57.23	60.49	-0.0022	0.29
	14:00	52.58	58.56	-0.0014	0.25
	15:00	50.86	58.78	0.0042	0.25
	16:00	45.17	50.90	0.0121	0.27
	17:00	40.12	43.26	0.0143	0.27
19-Jun	13:00	49.12	52.24	0.0000	0.29
	14:00	56.04	59.89	0.0004	0.26
	15:00	58.13	62.45	0.0072	0.25
	16:00	52.97	58.52	0.0124	0.25
	17:00	43.39	46.81	0.0142	0.26
20-Jun	13:00	62.10	68.71	0.0079	0.27
	14:00	61.96	68.70	0.0104	0.26
	15:00	61.43	69.48	0.0128	0.25
	16:00	59.43	66.14	0.0163	0.25
	17:00	55.50	61.17	0.0189	0.26
21-Jun	13:00	60.87	67.30	0.0059	0.27
	14:00	58.05	65.61	0.0120	0.26
	15:00	57.31	65.19	0.0150	0.25
	16:00	55.78	62.31	0.0191	0.25

	17:00	58.35	64.54	0.0227	0.26
22-Jun	13:00	59.41	64.85	-0.0053	0.29
	14:00	63.88	70.82	0.0073	0.27
	15:00	54.92	63.40	0.0207	0.28
	16:00	43.37	51.01	0.0200	0.30
	17:00	39.43	43.62	0.0163	0.30
23-Jun	13:00	62.39	67.42	-0.0017	0.28
	14:00	63.04	69.67	0.0130	0.25
	15:00	54.17	60.62	0.0174	0.27
	16:00	49.41	54.09	0.0169	0.26
	13:00	39.69	42.81	0.0168	0.26
24-Jun	13:00	59.37	62.90	-0.0114	0.27
	14:00	56.80	58.02	0.0008	0.28
	15:00	55.76	58.63	0.0064	0.25
	16:00	57.50	60.52	0.0147	0.27
	17:00	42.89	45.03	0.0220	0.29
25-Jun	13:00	52.86	55.86	-0.0052	0.27
	14:00	57.08	60.40	0.0001	0.30
	15:00	57.21	62.27	0.0046	0.24
	16:00	60.58	63.67	0.0096	0.29
	17:00	51.12	53.28	0.0178	0.27
1-Jul	13:00	61.52	63.51	0.0075	0.27
	14:00	61.19	64.88	0.0079	0.27
	15:00	64.57	72.00	0.0076	0.26
	16:00	56.49	63.86	0.0093	0.26
	17:00	35.06	42.66	0.0121	0.26
7-Jul	13:00	58.67	57.82	0.0071	0.28
	14:00	65.11	66.02	0.0081	0.26
	15:00	60.72	66.56	0.0089	0.25
	16:00	60.93	68.33	0.0095	0.25
	17:00	54.72	60.30	0.0085	0.25
8-Jul	13:00	53.01	53.67	0.0023	0.28
	14:00	51.33	54.16	0.0050	0.27
	15:00	48.02	52.88	0.0068	0.27
	16:00	47.34	52.58	0.0079	0.27
	17:00	47.00	53.72	0.0084	0.28
10-Jul	13:00	53.66	55.35	0.0077	0.28
	14:00	64.47	66.47	0.0089	0.30
	15:00	60.47	66.77	0.0073	0.28
	16:00	61.13	65.96	0.0069	0.27
	17:00	47.07	58.28	0.0057	0.25
13-Jul	13:00	62.16	61.19	0.0054	0.27
	14:00	66.13	65.27	0.0067	0.26
	15:00	61.10	66.57	0.0086	0.26

	16:00	46.11	57.92	0.0124	0.25
	17:00	44.30	47.18	0.0158	0.27
16-Jul	13:00	66.50	67.33	0.0041	0.27
	14:00	64.44	68.06	0.0101	0.26
	15:00	65.21	69.31	0.0174	0.26
	16:00	53.70	59.12	0.0234	0.29
	17:00	44.32	48.85	0.0242	0.28
18-Jul	13:00	63.77	65.41	0.0017	0.29
	14:00	57.31	61.50	0.0069	0.25
	15:00	55.80	58.73	0.0082	0.28
	16:00	52.20	55.73	0.0088	0.26
	17:00	59.44	63.16	0.0130	0.26
20-Jul	13:00	61.67	62.23	0.0057	0.28
	14:00	59.29	62.44	0.0085	0.26
	15:00	55.89	58.22	0.0111	0.28
	16:00	50.59	55.72	0.0107	0.25
	17:00	59.10	62.83	0.0113	0.27
21-Jul	13:00	55.14	57.47	0.0011	0.26
	14:00	55.75	57.56	0.0043	0.25
	15:00	60.01	62.27	0.0063	0.26
	16:00	59.52	63.24	0.0107	0.27
	17:00	56.87	60.75	0.0144	0.27
25-Jul	13:00	64.77	63.92	0.0017	0.28
	14:00	62.48	65.82	0.0087	0.26
	15:00	62.57	65.09	0.0139	0.25
	16:00	59.82	66.40	0.0166	0.25
	17:00	61.52	67.96	0.0199	0.26
26-Jul	13:00	60.62	62.57	0.0037	0.29
	14:00	58.33	61.74	0.0057	0.28
	15:00	62.59	66.15	0.0080	0.25
	16:00	59.42	65.69	0.0149	0.26
	17:00	57.94	65.58	0.0220	0.26
17-Aug	13:00	52.37	57.44	0.0056	0.31
	14:00	54.76	59.55	0.0065	0.29
	15:00	54.90	62.78	0.0057	0.29
	16:00	44.68	50.97	0.0048	0.31
	17:00	40.91	47.24	0.0045	0.32
1-Sep	13:00	59.83	66.54	-0.0003	0.27
	14:00	57.38	69.80	0.0052	0.26
	15:00	59.62	74.53	0.0090	0.27
	16:00	55.49	70.58	0.0123	0.31
	17:00	55.29	65.73	0.0118	0.33
2-Sep	13:00	62.33	70.98	0.0043	0.28
	14:00	62.51	75.93	0.0089	0.28

	15:00	56.43	70.54	0.0167	0.29
	16:00	50.68	64.43	0.0169	0.31
	17:00	50.01	59.50	0.0107	0.34

Plot 2-Heliconia 'American Dwarf'					
Date	Time	Tmrt Plant	Tmrt Reference	Plant ET	Albedo
13-May	13:00	66.86	63.07	0.0011	0.20
	14:00	67.03	67.75	0.0072	0.20
	15:00	64.73	72.22	0.0103	0.22
	16:00	61.85	70.89	0.0127	0.26
	17:00	57.66	65.33	0.0167	0.30
15-May	13:00	62.29	59.68	0.0022	0.20
	14:00	50.50	55.45	0.0068	0.19
	15:00	53.45	61.55	0.0126	0.22
	16:00	50.46	57.89	0.0162	0.29
	17:00	39.39	43.37	0.0188	0.32
22-May	13:00	65.63	57.94	0.0069	0.18
	14:00	58.99	59.34	0.0044	0.18
	15:00	59.33	63.73	0.0044	0.20
	16:00	55.58	61.42	0.0034	0.26
	17:00	41.21	44.80	0.0058	0.33
24-May	13:00	56.68	56.24	0.0098	0.19
	14:00	59.00	63.29	0.0100	0.19
	15:00	50.47	55.44	0.0084	0.21
	16:00	56.30	62.62	0.0094	0.27
	17:00	51.46	58.36	0.0116	0.38
25-May	13:00	61.80	62.17	0.0082	0.18
	14:00	64.11	69.06	0.0082	0.18
	15:00	62.21	69.97	0.0051	0.20
	16:00	49.05	55.02	0.0038	0.24
	17:00	38.84	44.07	0.0091	0.35
28-May	13:00	64.67	64.23	0.0050	0.19
	14:00	59.31	63.11	0.0067	0.20
	15:00	57.47	61.83	0.0088	0.22
	16:00	56.28	62.92	0.0108	0.24
	17:00	59.19	69.69	0.0122	0.34
29-May	13:00	50.66	48.53	0.0030	0.20
	14:00	50.01	51.45	0.0034	0.19
	15:00	58.80	62.66	0.0051	0.21
	16:00	59.24	62.75	0.0084	0.25
	17:00	47.39	49.03	0.0132	0.28
8-Jun	13:00	58.99	58.05	0.0164	0.18
	14:00	56.04	58.14	0.0128	0.18
	15:00	61.07	66.67	0.0092	0.21

	16:00	58.15	67.03	0.0083	0.24
	17:00	58.33	67.16	0.0049	0.30
10-Jun	13:00	63.30	63.15	0.0027	0.18
	14:00	60.36	60.47	0.0046	0.18
	15:00	57.48	61.39	0.0030	0.20
	16:00	60.79	66.68	0.0073	0.25
	17:00	43.44	47.50	0.0150	0.29
11-Jun	13:00	60.01	58.07	-0.0026	0.18
	14:00	64.47	64.20	0.0018	0.18
	15:00	61.23	64.64	0.0052	0.23
	16:00	51.99	57.30	0.0079	0.24
	17:00	56.86	65.43	0.0146	0.30
13-Jun	13:00	62.99	63.62	0.0040	0.19
	14:00	62.10	64.56	0.0076	0.19
	15:00	57.88	60.69	0.0106	0.22
	16:00	56.00	59.49	0.0154	0.24
	17:00	45.23	48.08	0.0192	0.25
16-Jun	13:00	70.63	68.16	0.0059	0.18
	14:00	62.22	62.58	0.0069	0.19
	15:00	64.08	67.17	0.0067	0.21
	16:00	57.59	60.06	0.0090	0.24
	17:00	44.71	46.90	0.0126	0.26
17-Jun	13:00	68.19	67.33	0.0021	0.19
	14:00	66.11	66.26	0.0057	0.20
	15:00	65.56	67.16	0.0094	0.20
	16:00	65.88	68.84	0.0107	0.22
	17:00	64.11	67.86	0.0119	0.25
18-Jun	13:00	67.77	60.49	-0.0012	0.19
	14:00	59.31	58.56	0.0009	0.18
	15:00	55.88	58.78	0.0052	0.20
	16:00	47.67	50.90	0.0124	0.22
	17:00	42.76	43.26	0.0142	0.26
19-Jun	13:00	53.54	52.24	0.0021	0.21
	14:00	62.76	59.89	0.0021	0.19
	15:00	64.56	62.45	0.0079	0.20
	16:00	57.92	58.52	0.0126	0.22
	17:00	45.91	46.81	0.0151	0.24
20-Jun	13:00	72.49	68.71	0.0059	0.18
	14:00	70.96	68.70	0.0099	0.18
	15:00	69.43	69.48	0.0103	0.20
	16:00	66.68	66.14	0.0091	0.22
	17:00	60.18	61.17	0.0124	0.26
21-Jun	13:00	70.19	67.30	0.0006	0.18
	14:00	67.49	65.61	0.0059	0.18

	15:00	64.65	65.19	0.0083	0.20
	16:00	62.14	62.31	0.0110	0.22
	17:00	63.74	64.54	0.0153	0.26
22-Jun	13:00	67.45	64.85	-0.0073	0.19
	14:00	72.14	70.82	0.0018	0.19
	15:00	59.56	63.40	0.0147	0.22
	16:00	45.64	51.01	0.0172	0.23
	17:00	40.80	43.62	0.0156	0.23
23-Jun	13:00	71.32	67.42	-0.0047	0.18
	14:00	71.16	69.67	0.0061	0.19
	15:00	59.43	60.62	0.0105	0.21
	16:00	52.27	54.09	0.0123	0.24
	13:00	41.74	42.81	0.0142	0.26
24-Jun	13:00	65.06	62.90	-0.0124	0.19
	14:00	62.53	58.02	-0.0025	0.21
	15:00	60.09	58.63	0.0022	0.20
	16:00	63.04	60.52	0.0086	0.23
	17:00	44.38	45.03	0.0153	0.27
25-Jun	13:00	56.96	55.86	-0.0044	0.21
	14:00	62.37	60.40	-0.0004	0.22
	15:00	63.30	62.27	0.0023	0.20
	16:00	65.90	63.67	0.0070	0.24
	17:00	54.69	53.28	0.0151	0.25
1-Jul	13:00	70.79	63.51	0.0092	0.21
	14:00	66.97	64.88	0.0108	0.22
	15:00	69.94	72.00	0.0089	0.22
	16:00	59.86	63.86	0.0074	0.22
	17:00	35.73	42.66	0.0121	0.23
7-Jul	13:00	64.33	57.82	0.0113	0.22
	14:00	70.84	66.02	0.0110	0.21
	15:00	66.87	66.56	0.0118	0.21
	16:00	65.91	68.33	0.0110	0.22
	17:00	58.31	60.30	0.0076	0.25
8-Jul	13:00	59.31	53.67	0.0067	0.22
	14:00	58.29	54.16	0.0080	0.21
	15:00	54.32	52.88	0.0073	0.23
	16:00	51.99	52.58	0.0082	0.24
	17:00	52.35	53.72	0.0099	0.26
10-Jul	13:00	58.50	55.35	0.0120	0.20
	14:00	70.23	66.47	0.0121	0.22
	15:00	68.91	66.77	0.0048	0.22
	16:00	67.54	65.96	0.0059	0.23
	17:00	57.81	58.28	0.0090	0.23
13-Jul	13:00	69.27	61.19	0.0071	0.18

	14:00	71.02	65.27	0.0058	0.19
	15:00	69.09	66.57	0.0041	0.21
	16:00	57.45	57.92	0.0051	0.22
	17:00	44.35	47.18	0.0099	0.22
16-Jul	13:00	73.70	67.33	0.0000	0.18
	14:00	71.62	68.06	0.0033	0.18
	15:00	71.57	69.31	0.0076	0.20
	16:00	59.78	59.12	0.0157	0.25
	17:00	47.89	48.85	0.0211	0.26
18-Jul	13:00	71.03	65.41	0.0019	0.19
	14:00	63.67	61.50	0.0072	0.18
	15:00	61.55	58.73	0.0097	0.22
	16:00	57.26	55.73	0.0064	0.22
	17:00	64.49	63.16	0.0083	0.26
20-Jul	13:00	67.92	62.23	0.0062	0.18
	14:00	65.22	62.44	0.0074	0.20
	15:00	61.01	58.22	0.0093	0.22
	16:00	55.12	55.72	0.0112	0.21
	17:00	64.41	62.83	0.0109	0.26
21-Jul	13:00	60.26	57.47	0.0006	0.18
	14:00	60.87	57.56	0.0020	0.18
	15:00	65.71	62.27	0.0043	0.20
	16:00	65.35	63.24	0.0066	0.23
	17:00	62.05	60.75	0.0085	0.27
25-Jul	13:00	70.46	63.92	-0.0014	0.19
	14:00	69.57	65.82	0.0024	0.18
	15:00	68.77	65.09	0.0055	0.19
	16:00	67.61	66.40	0.0072	0.22
	17:00	68.32	67.96	0.0112	0.25
26-Jul	13:00	66.22	62.57	-0.0003	0.20
	14:00	64.18	61.74	0.0015	0.19
	15:00	68.97	66.15	0.0029	0.20
	16:00	66.73	65.69	0.0068	0.22
	17:00	64.78	65.58	0.0146	0.25
17-Aug	13:00	57.86	57.44	0.0059	0.22
	14:00	59.82	59.55	0.0066	0.21
	15:00	62.69	62.78	0.0036	0.22
	16:00	52.63	50.97	0.0014	0.23
	17:00	48.79	47.24	0.0027	0.24
1-Sep	13:00	68.74	66.54	0.0034	0.17
	14:00	71.12	69.80	0.0036	0.17
	15:00	72.91	74.53	0.0072	0.19
	16:00	66.25	70.58	0.0141	0.22
	17:00	60.09	65.73	0.0126	0.26

2-Sep	13:00	70.76	70.98	0.0066	0.18
	14:00	72.25	75.93	0.0061	0.18
	15:00	65.90	70.54	0.0101	0.20
	16:00	58.21	64.43	0.0131	0.23
	17:00	54.92	59.50	0.0101	0.26

Plot 3 - Sphagneticola trilobata					
Date	Time	Tmrt Plant	Tmrt Reference	Plant ET	Albedo
13-May	13:00	60.45	63.07	0.0095	0.27
	14:00	59.79	67.75	0.0133	0.26
	15:00	58.54	72.22	0.0140	0.27
	16:00	57.79	70.89	0.0136	0.29
	17:00	55.04	65.33	0.0149	0.31
15-May	13:00	56.11	59.68	0.0097	0.27
	14:00	47.17	55.45	0.0124	0.26
	15:00	49.47	61.55	0.0154	0.27
	16:00	47.83	57.89	0.0171	0.33
	17:00	38.78	43.37	0.0178	0.32
22-May	13:00	57.49	57.94	0.0069	0.27
	14:00	54.49	59.34	0.0057	0.26
	15:00	56.64	63.73	0.0047	0.28
	16:00	54.73	61.42	0.0028	0.32
	17:00	40.89	44.80	0.0047	0.40
24-May	13:00	52.40	56.24	0.0112	0.29
	14:00	55.38	63.29	0.0104	0.27
	15:00	48.58	55.44	0.0066	0.28
	16:00	54.49	62.62	0.0065	0.34
	17:00	50.80	58.36	0.0074	0.41
25-May	13:00	56.42	62.17	0.0083	0.27
	14:00	59.29	69.06	0.0082	0.26
	15:00	59.08	69.97	0.0049	0.27
	16:00	46.97	55.02	0.0042	0.29
	17:00	38.98	44.07	0.0084	0.41
28-May	13:00	58.84	64.23	0.0077	0.29
	14:00	55.74	63.11	0.0074	0.28
	15:00	54.81	61.83	0.0073	0.28
	16:00	54.62	62.92	0.0086	0.30
	17:00	59.01	69.69	0.0086	0.38
29-May	13:00	47.29	48.53	0.0054	0.29
	14:00	47.30	51.45	0.0065	0.27
	15:00	54.96	62.66	0.0067	0.29
	16:00	56.97	62.75	0.0083	0.31

	17:00	46.65	49.03	0.0109	0.32
8-Jun	13:00	55.77	58.05	0.0147	0.30
	14:00	53.22	58.14	0.0124	0.29
	15:00	58.50	66.67	0.0094	0.30
	16:00	57.28	67.03	0.0077	0.32
	17:00	58.76	67.16	0.0048	0.36
10-Jun	13:00	58.45	63.15	0.0075	0.31
	14:00	55.14	60.47	0.0081	0.28
	15:00	53.79	61.39	0.0061	0.28
	16:00	56.39	66.68	0.0078	0.33
	17:00	42.01	47.50	0.0116	0.34
11-Jun	13:00	55.55	58.07	0.0026	0.29
	14:00	58.25	64.20	0.0047	0.28
	15:00	55.87	64.64	0.0064	0.34
	16:00	50.17	57.30	0.0074	0.32
	17:00	56.00	65.43	0.0102	0.35
13-Jun	13:00	57.53	63.62	0.0076	0.29
	14:00	57.81	64.56	0.0085	0.28
	15:00	55.01	60.69	0.0101	0.29
	16:00	53.71	59.49	0.0138	0.31
	17:00	43.58	48.08	0.0161	0.31
16-Jun	13:00	60.90	68.16	0.0099	0.28
	14:00	56.45	62.58	0.0106	0.27
	15:00	59.82	67.17	0.0103	0.27
	16:00	56.30	60.06	0.0104	0.29
	17:00	44.35	46.90	0.0116	0.30
17-Jun	13:00	59.18	67.33	0.0082	0.29
	14:00	59.85	66.26	0.0119	0.28
	15:00	61.31	67.16	0.0136	0.26
	16:00	63.11	68.84	0.0131	0.26
	17:00	62.65	67.86	0.0134	0.25
18-Jun	13:00	57.05	60.49	0.0084	0.31
	14:00	52.80	58.56	0.0083	0.27
	15:00	52.72	58.78	0.0098	0.26
	16:00	46.46	50.90	0.0122	0.28
	17:00	41.13	43.26	0.0140	0.27
19-Jun	13:00	49.99	52.24	0.0070	0.29
	14:00	57.05	59.89	0.0088	0.28
	15:00	58.84	62.45	0.0119	0.27
	16:00	54.05	58.52	0.0139	0.26
	17:00	45.48	46.81	0.0145	0.26
20-Jun	13:00	62.76	68.71	0.0116	0.28
	14:00	63.60	68.70	0.0136	0.26
	15:00	63.17	69.48	0.0130	0.27

	16:00	62.33	66.14	0.0132	0.26
	17:00	59.38	61.17	0.0147	0.26
21-Jun	13:00	60.13	67.30	0.0095	0.29
	14:00	59.95	65.61	0.0131	0.27
	15:00	58.92	65.19	0.0141	0.27
	16:00	58.14	62.31	0.0155	0.27
	17:00	62.23	64.54	0.0176	0.26
22-Jun	13:00	59.00	64.85	0.0024	0.30
	14:00	63.80	70.82	0.0099	0.28
	15:00	55.13	63.40	0.0172	0.28
	16:00	44.51	51.01	0.0170	0.29
	17:00	39.77	43.62	0.0146	0.29
23-Jun	13:00	60.79	67.42	0.0043	0.30
	14:00	62.19	69.67	0.0128	0.26
	15:00	53.25	60.62	0.0152	0.27
	16:00	48.80	54.09	0.0146	0.27
	13:00	39.49	42.81	0.0143	0.25
24-Jun	13:00	57.82	62.90	-0.0042	0.28
	14:00	53.52	58.02	0.0041	0.26
	15:00	54.89	58.63	0.0082	0.26
	16:00	56.12	60.52	0.0122	0.26
	17:00	40.51	45.03	0.0156	0.25
25-Jun	13:00	49.94	55.86	0.0016	0.28
	14:00	54.91	60.40	0.0050	0.31
	15:00	57.72	62.27	0.0081	0.26
	16:00	57.83	63.67	0.0102	0.26
	17:00	48.93	53.28	0.0141	0.26
1-Jul	13:00	57.16	63.51	0.0117	0.29
	14:00	58.03	64.88	0.0120	0.28
	15:00	63.45	72.00	0.0099	0.27
	16:00	55.09	63.86	0.0095	0.26
	17:00	34.89	42.66	0.0119	0.25
7-Jul	13:00	57.59	57.82	0.0208	0.28
	14:00	63.13	66.02	0.0223	0.27
	15:00	61.66	66.56	0.0206	0.27
	16:00	61.97	68.33	0.0173	0.26
	17:00	55.48	60.30	0.0108	0.26
8-Jul	13:00	52.43	53.67	0.0136	0.29
	14:00	52.14	54.16	0.0134	0.28
	15:00	48.72	52.88	0.0101	0.28
	16:00	48.57	52.58	0.0100	0.28
	17:00	49.52	53.72	0.0112	0.28
10-Jul	13:00	52.11	55.35	0.0146	0.30
	14:00	61.48	66.47	0.0154	0.32

	15:00	62.03	66.77	0.0077	0.29
	16:00	61.26	65.96	0.0068	0.28
	17:00	53.59	58.28	0.0068	0.27
13-Jul	13:00	55.82	61.19	0.0095	0.28
	14:00	61.10	65.27	0.0091	0.27
	15:00	62.09	66.57	0.0078	0.27
	16:00	53.41	57.92	0.0080	0.27
	17:00	41.53	47.18	0.0114	0.28
16-Jul	13:00	60.85	67.33	0.0051	0.29
	14:00	61.40	68.06	0.0077	0.28
	15:00	63.80	69.31	0.0113	0.28
	16:00	52.96	59.12	0.0154	0.29
	17:00	44.59	48.85	0.0171	0.28
18-Jul	13:00	59.10	65.41	0.0057	0.30
	14:00	56.09	61.50	0.0092	0.27
	15:00	54.79	58.73	0.0104	0.28
	16:00	52.75	55.73	0.0100	0.28
	17:00	60.16	63.16	0.0104	0.28
20-Jul	13:00	56.58	62.23	0.0070	0.29
	14:00	56.59	62.44	0.0091	0.29
	15:00	53.38	58.22	0.0110	0.28
	16:00	52.33	55.72	0.0118	0.28
	17:00	60.11	62.83	0.0119	0.28
21-Jul	13:00	52.19	57.47	0.0039	0.27
	14:00	53.62	57.56	0.0068	0.26
	15:00	59.18	62.27	0.0095	0.28
	16:00	60.63	63.24	0.0108	0.29
	17:00	57.70	60.75	0.0111	0.29
25-Jul	13:00	60.33	63.92	0.0040	0.29
	14:00	60.30	65.82	0.0078	0.28
	15:00	61.14	65.09	0.0099	0.28
	16:00	61.16	66.40	0.0104	0.28
	17:00	61.88	67.96	0.0121	0.28
26-Jul	13:00	57.74	62.57	0.0039	0.30
	14:00	56.74	61.74	0.0057	0.28
	15:00	62.31	66.15	0.0068	0.28
	16:00	60.83	65.69	0.0097	0.28
	17:00	60.20	65.58	0.0140	0.28
17-Aug	13:00	53.80	57.44	0.0065	0.29
	14:00	56.42	59.55	0.0086	0.28
	15:00	58.36	62.78	0.0049	0.27
	16:00	47.07	50.97	0.0024	0.28
	17:00	43.60	47.24	0.0037	0.28
1-Sep	13:00	56.17	66.54	0.0103	0.26

	14:00	58.10	69.80	0.0102	0.25
	15:00	62.43	74.53	0.0115	0.25
	16:00	60.21	70.58	0.0132	0.27
	17:00	58.74	65.73	0.0118	0.27
2-Sep	13:00	59.88	70.98	0.0068	0.27
	14:00	64.32	75.93	0.0088	0.26
	15:00	60.77	70.54	0.0130	0.27
	16:00	54.27	64.43	0.0151	0.26
	17:00	53.54	59.50	0.0117	0.28

10.6 Data for validation of model

Plot 1 - Phyllanthus cochinchinensis					
Date	Time	Tmrt Plant	Tmrt Reference	Plant ET	Albedo
7-Sep	13:00	54.58	59.03	-0.0006	0.29
	14:00	60.27	66.66	0.0060	0.27
	15:00	58.38	69.56	0.0155	0.28
	16:00	53.52	63.05	0.0210	0.31
	17:00	42.80	49.92	0.0227	0.33
8-Sep	13:00	64.23	77.71	0.0036	0.27
	14:00	61.25	76.88	0.0134	0.26
	15:00	62.48	77.43	0.0181	0.28
	16:00	54.70	70.10	0.0196	0.31
	17:00	53.81	64.21	0.0242	0.34
10-Sep	13:00	64.10	75.88	-0.0002	0.29
	14:00	56.65	68.75	0.0078	0.30
	15:00	58.74	70.23	0.0112	0.31
	16:00	53.51	65.62	0.0206	0.34
	17:00	47.50	56.36	0.0245	0.35
2-Oct	13:00	54.06	68.39	0.0036	0.31
	14:00	53.71	63.31	0.0108	0.32
	15:00	50.28	59.83	0.0159	0.33
	16:00	42.84	50.25	0.0178	0.34
	17:00	40.08	45.82	0.0207	0.35
3-Oct	13:00	60.15	75.81	0.0070	0.31
	14:00	59.37	76.01	0.0122	0.31
	15:00	58.53	75.95	0.0237	0.34
	16:00	55.21	70.47	0.0224	0.36
	17:00	50.59	61.50	0.0150	0.37
9-Oct	13:00	62.04	75.41	-0.0022	0.31
	14:00	61.75	77.27	0.0073	0.31
	15:00	64.38	78.79	0.0182	0.33
	16:00	44.82	59.80	0.0289	0.35

	17:00	34.90	42.26	0.0237	0.34
10-Oct	13:00	59.83	77.54	0.0029	0.31
	14:00	58.25	75.35	0.0110	0.30
	15:00	58.77	76.62	0.0164	0.32
	16:00	56.45	73.97	0.0189	0.35
	17:00	54.33	67.67	0.0226	0.36
19-Oct	13:00	61.44	74.01	0.0095	0.31
	14:00	64.55	72.52	0.0093	0.30
	15:00	56.93	66.54	0.0065	0.32
	16:00	59.01	74.78	0.0059	0.34
	17:00	41.17	53.70	0.0076	0.35
20-Oct	13:00	62.83	77.81	0.0092	0.32
	14:00	58.71	60.84	0.0147	0.33
	15:00	58.06	66.40	0.0176	0.34
	16:00	55.25	72.82	0.0160	0.37
	17:00	53.70	64.19	0.0172	0.41
1-Nov	13:00	58.87	62.47	-0.0151	0.34
	14:00	62.51	67.80	-0.0083	0.35
	15:00	61.27	69.29	0.0046	0.36
	16:00	44.72	54.69	0.0137	0.37
	17:00	39.30	44.16	0.0153	0.39

Plot 2-Heliconia 'American Dwarf'					
Date	Time	Tmrt Plant	Tmrt Reference	Plant ET	Albedo
7-Sep	13:00	59.67	59.03	-0.0003	0.18
	14:00	63.63	66.66	0.0043	0.18
	15:00	62.42	69.56	0.0087	0.20
	16:00	57.33	63.05	0.0123	0.23
	17:00	45.12	49.92	0.0167	0.25
8-Sep	13:00	77.46	77.71	0.0018	0.18
	14:00	75.67	76.88	0.0064	0.18
	15:00	74.30	77.43	0.0092	0.20
	16:00	65.77	70.10	0.0111	0.23
	17:00	57.67	64.21	0.0178	0.26
10-Sep	13:00	75.96	75.88	-0.0026	0.19
	14:00	68.17	68.75	0.0033	0.21
	15:00	68.46	70.23	0.0056	0.21
	16:00	61.22	65.62	0.0148	0.24
	17:00	51.23	56.36	0.0223	0.25
2-Oct	13:00	71.38	68.39	0.0017	0.20
	14:00	68.61	63.31	0.0088	0.21
	15:00	63.21	59.83	0.0135	0.22
	16:00	52.05	50.25	0.0155	0.23
	17:00	46.49	45.82	0.0197	0.24

3-Oct	13:00	78.83	75.81	0.0046	0.19
	14:00	79.34	76.01	0.0097	0.20
	15:00	78.00	75.95	0.0183	0.22
	16:00	71.97	70.47	0.0176	0.24
	17:00	62.80	61.50	0.0137	0.27
9-Oct	13:00	78.83	75.41	-0.0052	0.20
	14:00	80.94	77.27	0.0023	0.20
	15:00	81.47	78.79	0.0115	0.22
	16:00	57.92	59.80	0.0241	0.24
	17:00	38.97	42.26	0.0233	0.24
10-Oct	13:00	76.69	77.54	-0.0005	0.19
	14:00	77.09	75.35	0.0054	0.19
	15:00	77.50	76.62	0.0093	0.21
	16:00	73.81	73.97	0.0131	0.24
	17:00	68.18	67.67	0.0193	0.27
19-Oct	13:00	75.21	74.01	0.0092	0.20
	14:00	83.50	72.52	0.0096	0.20
	15:00	73.47	66.54	0.0087	0.22
	16:00	73.58	74.78	0.0099	0.24
	17:00	51.00	53.70	0.0136	0.25
20-Oct	13:00	79.15	77.81	0.0079	0.19
	14:00	76.97	60.84	0.0095	0.19
	15:00	76.27	66.40	0.0114	0.21
	16:00	74.42	72.82	0.0144	0.23
	17:00	67.44	64.19	0.0169	0.26
1-Nov	13:00	63.65	62.47	-0.0108	0.24
	14:00	67.28	67.80	-0.0062	0.24
	15:00	66.00	69.29	0.0030	0.24
	16:00	51.94	54.69	0.0113	0.26
	17:00	42.36	44.16	0.0138	0.27

Plot 3 - Sphagneticola trilobata					
Date	Time	Tmrt Plant	Tmrt Reference	Plant ET	Albedo
7-Sep	13:00	53.04	59.03	0.0038	0.26
	14:00	59.35	66.66	0.0082	0.25
	15:00	59.36	69.56	0.0120	0.25
	16:00	55.41	63.05	0.0153	0.27
	17:00	44.30	49.92	0.0169	0.28
8-Sep	13:00	67.07	77.71	0.0064	0.26
	14:00	68.67	76.88	0.0116	0.24
	15:00	72.88	77.43	0.0141	0.25
	16:00	64.18	70.10	0.0151	0.27
	17:00	60.25	64.21	0.0179	0.27
10-Sep	13:00	68.69	75.88	0.0032	0.27

	14:00	62.06	68.75	0.0081	0.27
	15:00	66.97	70.23	0.0104	0.26
	16:00	63.09	65.62	0.0155	0.28
	17:00	53.57	56.36	0.0177	0.29
2-Oct	13:00	59.94	68.39	0.0066	0.28
	14:00	60.23	63.31	0.0103	0.28
	15:00	57.04	59.83	0.0134	0.29
	16:00	47.94	50.25	0.0153	0.30
	17:00	44.41	45.82	0.0160	0.30
3-Oct	13:00	66.05	75.81	0.0078	0.27
	14:00	68.05	76.01	0.0110	0.26
	15:00	69.80	75.95	0.0176	0.26
	16:00	67.13	70.47	0.0180	0.27
	17:00	60.31	61.50	0.0132	0.28
9-Oct	13:00	65.24	75.41	-0.0003	0.28
	14:00	68.37	77.27	0.0057	0.27
	15:00	71.82	78.79	0.0123	0.27
	16:00	51.11	59.80	0.0208	0.30
	17:00	37.65	42.26	0.0199	0.31
10-Oct	13:00	61.75	77.54	0.0043	0.28
	14:00	65.92	75.35	0.0076	0.27
	15:00	69.70	76.62	0.0109	0.26
	16:00	69.02	73.97	0.0154	0.27
	17:00	65.25	67.67	0.0179	0.28
19-Oct	13:00	63.22	74.01	0.0106	0.24
	14:00	68.27	72.52	0.0102	0.23
	15:00	65.55	66.54	0.0077	0.25
	16:00	67.99	74.78	0.0063	0.26
	17:00	47.81	53.70	0.0073	0.27
20-Oct	13:00	64.28	77.81	0.0084	0.25
	14:00	65.30	60.84	0.0099	0.25
	15:00	68.86	66.40	0.0117	0.25
	16:00	69.30	72.82	0.0131	0.26
	17:00	62.73	64.19	0.0131	0.27
1-Nov	13:00	61.32	62.47	-0.0071	0.26
	14:00	67.37	67.80	-0.0036	0.24
	15:00	67.22	69.29	0.0034	0.25
	16:00	50.27	54.69	0.0093	0.27
	17:00	43.09	44.16	0.0111	0.27

10.7 Data for sensitivity analysis

Tmrt Plant	Tmrt Reference	Plant ET	Albedo
48.17	50.00	0.0095	0.26
48.95	51.00	0.0095	0.26
49.73	52.00	0.0095	0.26
50.51	53.00	0.0095	0.26
51.29	54.00	0.0095	0.26
52.08	55.00	0.0095	0.26
52.86	56.00	0.0095	0.26
53.64	57.00	0.0095	0.26
54.42	58.00	0.0095	0.26
55.20	59.00	0.0095	0.26
55.99	60.00	0.0095	0.26
56.77	61.00	0.0095	0.26
57.55	62.00	0.0095	0.26
58.33	63.00	0.0095	0.26
59.11	64.00	0.0095	0.26
59.90	65.00	0.0095	0.26
60.68	66.00	0.0095	0.26
61.46	67.00	0.0095	0.26
62.24	68.00	0.0095	0.26
63.02	69.00	0.0095	0.26
63.81	70.00	0.0095	0.26
58.50	61.04	0.0010	0.26
58.30	61.04	0.0020	0.26
58.10	61.04	0.0030	0.26
57.90	61.04	0.0040	0.26
57.70	61.04	0.0050	0.26
57.50	61.04	0.0060	0.26
57.30	61.04	0.0070	0.26
57.10	61.04	0.0080	0.26
56.90	61.04	0.0090	0.26
56.70	61.04	0.0100	0.26
56.50	61.04	0.0110	0.26

56.30	61.04	0.0120	0.26
56.10	61.04	0.0130	0.26
55.90	61.04	0.0140	0.26
55.70	61.04	0.0150	0.26
55.50	61.04	0.0160	0.26
55.30	61.04	0.0170	0.26
55.10	61.04	0.0180	0.26
54.90	61.04	0.0190	0.26
54.70	61.04	0.0200	0.26
54.50	61.04	0.0210	0.26
54.30	61.04	0.0220	0.26
54.10	61.04	0.0230	0.26
53.90	61.04	0.0240	0.26
53.70	61.04	0.0250	0.26
53.50	61.04	0.0260	0.26
53.30	61.04	0.0270	0.26
53.10	61.04	0.0280	0.26
52.90	61.04	0.0290	0.26
52.70	61.04	0.0300	0.26
72.16	61.04	0.0095	0.01
71.55	61.04	0.0095	0.02
70.94	61.04	0.0095	0.03
70.33	61.04	0.0095	0.04
69.72	61.04	0.0095	0.05
69.11	61.04	0.0095	0.06
68.50	61.04	0.0095	0.07
67.89	61.04	0.0095	0.08
67.28	61.04	0.0095	0.09
66.67	61.04	0.0095	0.10
66.06	61.04	0.0095	0.11
65.45	61.04	0.0095	0.12
64.84	61.04	0.0095	0.13
64.23	61.04	0.0095	0.14
63.62	61.04	0.0095	0.15
63.01	61.04	0.0095	0.16
62.40	61.04	0.0095	0.17
61.79	61.04	0.0095	0.18
61.18	61.04	0.0095	0.19
60.57	61.04	0.0095	0.20
59.96	61.04	0.0095	0.21
59.35	61.04	0.0095	0.22
58.74	61.04	0.0095	0.23
58.13	61.04	0.0095	0.24
57.52	61.04	0.0095	0.25

56.91	61.04	0.0095	0.26
56.30	61.04	0.0095	0.27
55.69	61.04	0.0095	0.28
55.08	61.04	0.0095	0.29
54.47	61.04	0.0095	0.30

10.8 Plant selection chart

Reference Tmrt 50 °C		Shrub Albedo											
		0.16	0.17	0.18	0.19	0.20	0.21	0.22	0.23	0.24	0.25	0.26	0.27
Plant Evapotranspiration Rate	0.001	56.1	55.5	54.9	54.2	53.6	53.0	52.4	52.0	51.2	50.6	50.0	49.4
	0.002	55.9	55.3	54.7	54.0	53.4	52.8	52.2	51.8	51.0	50.4	49.8	49.2
	0.003	55.7	55.1	54.5	53.8	53.2	52.6	52.0	51.6	50.8	50.2	49.6	49.0
	0.004	55.5	54.9	54.3	53.6	53.0	52.4	51.8	51.4	50.6	50.0	49.4	48.8
	0.005	55.3	54.7	54.1	53.4	52.8	52.2	51.6	51.2	50.4	49.8	49.2	48.6
	0.006	55.1	54.5	53.9	53.2	52.6	52.0	51.4	51.0	50.2	49.6	49.0	48.4
	0.007	54.9	54.3	53.7	53.0	52.4	51.8	51.2	50.8	50.0	49.4	48.8	48.2
	0.008	54.7	54.1	53.5	52.8	52.2	51.6	51.0	50.6	49.8	49.2	48.6	48.0
	0.009	54.5	53.9	53.3	52.6	52.0	51.4	50.8	50.4	49.6	49.0	48.4	47.8
	0.010	54.3	53.7	53.1	52.4	51.8	51.2	50.6	50.2	49.4	48.8	48.2	47.6
	0.011	54.1	53.5	52.9	52.2	51.6	51.0	50.4	50.0	49.2	48.6	48.0	47.4
	0.012	53.9	53.3	52.7	52.0	51.4	50.8	50.2	49.8	49.0	48.4	47.8	47.2
	0.013	53.7	53.1	52.5	51.8	51.2	50.6	50.0	49.6	48.8	48.2	47.6	47.0
	0.014	53.5	52.9	52.3	51.6	51.0	50.4	49.8	49.4	48.6	48.0	47.4	46.8
	0.015	53.3	52.7	52.1	51.4	50.8	50.2	49.6	49.2	48.4	47.8	47.2	46.6
	0.016	53.1	52.5	51.9	51.2	50.6	50.0	49.4	49.0	48.2	47.6	47.0	46.4
	0.017	52.9	52.3	51.7	51.0	50.4	49.8	49.2	48.8	48.0	47.4	46.8	46.2
	0.018	52.7	52.1	51.5	50.8	50.2	49.6	49.0	48.6	47.8	47.2	46.6	46.0
	0.019	52.5	51.9	51.3	50.6	50.0	49.4	48.8	48.4	47.6	47.0	46.4	45.8
	0.020	52.3	51.7	51.1	50.4	49.8	49.2	48.6	48.2	47.4	46.8	46.2	45.6
	0.021	52.1	51.5	50.9	50.2	49.6	49.0	48.4	48.0	47.2	46.6	46.0	45.4
	0.022	51.9	51.3	50.7	50.0	49.4	48.8	48.2	47.8	47.0	46.4	45.8	45.2
	0.023	51.7	51.1	50.5	49.8	49.2	48.6	48.0	47.6	46.8	46.2	45.6	45.0
	0.024	51.5	50.9	50.3	49.6	49.0	48.4	47.8	47.4	46.6	46.0	45.4	44.8
	0.025	51.3	50.7	50.1	49.4	48.8	48.2	47.6	47.2	46.4	45.8	45.2	44.6
	0.026	51.1	50.5	49.9	49.2	48.6	48.0	47.4	47.0	46.2	45.6	45.0	44.4

	0.027	50.9	50.3	49.7	49.0	48.4	47.8	47.2	46.8	46.0	45.4	44.8	44.2
	0.028	50.7	50.1	49.5	48.8	48.2	47.6	47.0	46.6	45.8	45.2	44.6	44.0
	0.029	50.5	49.9	49.3	48.6	48.0	47.4	46.8	46.4	45.6	45.0	44.4	43.8
	0.030	50.3	49.7	49.1	48.4	47.8	47.2	46.6	46.2	45.4	44.8	44.2	43.6

Percentage reduction in mean radiant temperature

Reference Tmrt 50 °C		Shrub Albedo											
		0.16	0.17	0.18	0.19	0.20	0.21	0.22	0.23	0.24	0.25	0.26	0.27
Plant Evapotranspiration Rate	0.001	-	-	-	-	-	-	-	-	-	-	-	1.3
	0.002	-	-	-	-	-	-	-	-	-	-	0.5	1.7
	0.003	-	-	-	-	-	-	-	-	-	-	0.9	2.1
	0.004	-	-	-	-	-	-	-	-	-	-	1.3	2.5
	0.005	-	-	-	-	-	-	-	-	-	0.4	1.7	2.9
	0.006	-	-	-	-	-	-	-	-	-	0.8	2.1	3.3
	0.007	-	-	-	-	-	-	-	-	-	1.2	2.5	3.7
	0.008	-	-	-	-	-	-	-	-	0.4	1.6	2.9	4.1
	0.009	-	-	-	-	-	-	-	-	0.8	2.0	3.3	4.5
	0.010	-	-	-	-	-	-	-	-	1.2	2.4	3.7	4.9
	0.011	-	-	-	-	-	-	-	-	1.6	2.8	4.1	5.3
	0.012	-	-	-	-	-	-	-	0.4	2.0	3.2	4.5	5.7
	0.013	-	-	-	-	-	-	-	0.8	2.4	3.6	4.9	6.1
	0.014	-	-	-	-	-	-	0.4	1.2	2.8	4.0	5.3	6.5
	0.015	-	-	-	-	-	-	0.8	1.6	3.2	4.4	5.7	6.9
	0.016	-	-	-	-	-	-	1.2	2.0	3.6	4.8	6.1	7.3
	0.017	-	-	-	-	-	0.4	1.6	2.4	4.0	5.2	6.5	7.7
	0.018	-	-	-	-	-	0.8	2.0	2.8	4.4	5.6	6.9	8.1
	0.019	-	-	-	-	-	1.2	2.4	3.2	4.8	6.0	7.3	8.5
	0.020	-	-	-	-	0.3	1.6	2.8	3.6	5.2	6.4	7.7	8.9
	0.021	-	-	-	-	0.7	2.0	3.2	4.0	5.6	6.8	8.1	9.3
	0.022	-	-	-	-	1.1	2.4	3.6	4.4	6.0	7.2	8.5	9.7
	0.023	-	-	-	0.3	1.5	2.8	4.0	4.8	6.4	7.6	8.9	10.1
	0.024	-	-	-	0.7	1.9	3.2	4.4	5.2	6.8	8.0	9.3	10.5
	0.025	-	-	-	1.1	2.3	3.6	4.8	5.6	7.2	8.4	9.7	10.9
	0.026	-	-	0.3	1.5	2.7	4.0	5.2	6.0	7.6	8.8	10.1	11.3
	0.027	-	-	0.7	1.9	3.1	4.4	5.6	6.4	8.0	9.2	10.5	11.7
	0.028	-	-	1.1	2.3	3.5	4.8	6.0	6.8	8.4	9.6	10.9	12.1
	0.029	-	0.3	1.5	2.7	3.9	5.2	6.4	7.2	8.8	10.0	11.3	12.5
	0.030	-	0.7	1.9	3.1	4.3	5.6	6.8	7.6	9.2	10.4	11.7	12.9

Reference Tmrt 60 °C		Shrub Albedo											
		0.12	0.13	0.14	0.15	0.16	0.17	0.18	0.19	0.20	0.21	0.22	0.23
Plant Evapotranspiration Rate	0.001	66.3	65.7	65.1	64.5	63.9	63.3	62.7	62.1	61.5	60.8	60.2	59.8
	0.002	66.1	65.5	64.9	64.3	63.7	63.1	62.5	61.9	61.3	60.6	60.0	59.6
	0.003	65.9	65.3	64.7	64.1	63.5	62.9	62.3	61.7	61.1	60.4	59.8	59.4
	0.004	65.7	65.1	64.5	63.9	63.3	62.7	62.1	61.5	60.9	60.2	59.6	59.2
	0.005	65.5	64.9	64.3	63.7	63.1	62.5	61.9	61.3	60.7	60.0	59.4	59.0
	0.006	65.3	64.7	64.1	63.5	62.9	62.3	61.7	61.1	60.5	59.8	59.2	58.8
	0.007	65.1	64.5	63.9	63.3	62.7	62.1	61.5	60.9	60.3	59.6	59.0	58.6
	0.008	64.9	64.3	63.7	63.1	62.5	61.9	61.3	60.7	60.1	59.4	58.8	58.4
	0.009	64.7	64.1	63.5	62.9	62.3	61.7	61.1	60.5	59.9	59.2	58.6	58.2
	0.010	64.5	63.9	63.3	62.7	62.1	61.5	60.9	60.3	59.7	59.0	58.4	58.0
	0.011	64.3	63.7	63.1	62.5	61.9	61.3	60.7	60.1	59.5	58.8	58.2	57.8
	0.012	64.1	63.5	62.9	62.3	61.7	61.1	60.5	59.9	59.3	58.6	58.0	57.6
	0.013	63.9	63.3	62.7	62.1	61.5	60.9	60.3	59.7	59.1	58.4	57.8	57.4
	0.014	63.7	63.1	62.5	61.9	61.3	60.7	60.1	59.5	58.9	58.2	57.6	57.2
	0.015	63.5	62.9	62.3	61.7	61.1	60.5	59.9	59.3	58.7	58.0	57.4	57.0
	0.016	63.3	62.7	62.1	61.5	60.9	60.3	59.7	59.1	58.5	57.8	57.2	56.8
	0.017	63.1	62.5	61.9	61.3	60.7	60.1	59.5	58.9	58.3	57.6	57.0	56.6
	0.018	62.9	62.3	61.7	61.1	60.5	59.9	59.3	58.7	58.1	57.4	56.8	56.4
	0.019	62.7	62.1	61.5	60.9	60.3	59.7	59.1	58.5	57.9	57.2	56.6	56.2
	0.020	62.5	61.9	61.3	60.7	60.1	59.5	58.9	58.3	57.7	57.0	56.4	56.0
	0.021	62.3	61.7	61.1	60.5	59.9	59.3	58.7	58.1	57.5	56.8	56.2	55.8
	0.022	62.1	61.5	60.9	60.3	59.7	59.1	58.5	57.9	57.3	56.6	56.0	55.6
	0.023	61.9	61.3	60.7	60.1	59.5	58.9	58.3	57.7	57.1	56.4	55.8	55.4
	0.024	61.7	61.1	60.5	59.9	59.3	58.7	58.1	57.5	56.9	56.2	55.6	55.2
	0.025	61.5	60.9	60.3	59.7	59.1	58.5	57.9	57.3	56.7	56.0	55.4	55.0
	0.026	61.3	60.7	60.1	59.5	58.9	58.3	57.7	57.1	56.5	55.8	55.2	54.8
	0.027	61.1	60.5	59.9	59.3	58.7	58.1	57.5	56.9	56.3	55.6	55.0	54.6
	0.028	60.9	60.3	59.7	59.1	58.5	57.9	57.3	56.7	56.1	55.4	54.8	54.4
	0.029	60.7	60.1	59.5	58.9	58.3	57.7	57.1	56.5	55.9	55.2	54.6	54.2

	0.030	60.5	59.9	59.3	58.7	58.1	57.5	56.9	56.3	55.7	55.0	54.4	54.0

Percentage reduction in mean radiant temperature

Reference Tmrt 60 °C		Shrub Albedo											
		0.12	0.13	0.14	0.15	0.16	0.17	0.18	0.19	0.20	0.21	0.22	0.23
Plant Evapotranspiration Rate	0.001	-	-	-	-	-	-	-	-	-	-	-	0.3
	0.002	-	-	-	-	-	-	-	-	-	-	-	0.6
	0.003	-	-	-	-	-	-	-	-	-	-	0.3	1.0
	0.004	-	-	-	-	-	-	-	-	-	-	0.6	1.3
	0.005	-	-	-	-	-	-	-	-	-	-	0.9	1.6
	0.006	-	-	-	-	-	-	-	-	-	0.3	1.3	2.0
	0.007	-	-	-	-	-	-	-	-	-	0.6	1.6	2.3
	0.008	-	-	-	-	-	-	-	-	-	0.9	1.9	2.6
	0.009	-	-	-	-	-	-	-	-	0.2	1.3	2.3	3.0
	0.010	-	-	-	-	-	-	-	-	0.6	1.6	2.6	3.3
	0.011	-	-	-	-	-	-	-	-	0.9	1.9	2.9	3.6
	0.012	-	-	-	-	-	-	-	0.2	1.2	2.3	3.3	4.0
	0.013	-	-	-	-	-	-	-	0.6	1.6	2.6	3.6	4.3
	0.014	-	-	-	-	-	-	-	0.9	1.9	2.9	3.9	4.6
	0.015	-	-	-	-	-	-	0.2	1.2	2.2	3.3	4.3	5.0
	0.016	-	-	-	-	-	-	0.5	1.6	2.6	3.6	4.6	5.3
	0.017	-	-	-	-	-	-	0.9	1.9	2.9	3.9	4.9	5.6
	0.018	-	-	-	-	-	0.2	1.2	2.2	3.2	4.3	5.3	6.0
	0.019	-	-	-	-	-	0.5	1.5	2.6	3.6	4.6	5.6	6.3
	0.020	-	-	-	-	-	0.9	1.9	2.9	3.9	4.9	5.9	6.6
	0.021	-	-	-	-	0.2	1.2	2.2	3.2	4.2	5.3	6.3	7.0
	0.022	-	-	-	-	0.5	1.5	2.5	3.6	4.6	5.6	6.6	7.3
	0.023	-	-	-	-	0.8	1.9	2.9	3.9	4.9	5.9	6.9	7.6
	0.024	-	-	-	0.2	1.2	2.2	3.2	4.2	5.2	6.3	7.3	8.0
	0.025	-	-	-	0.5	1.5	2.5	3.5	4.6	5.6	6.6	7.6	8.3

	0.026	-	-	-	0.8	1.8	2.9	3.9	4.9	5.9	6.9	7.9	8.6
	0.027	-	-	0.1	1.2	2.2	3.2	4.2	5.2	6.2	7.3	8.3	9.0
	0.028	-	-	0.5	1.5	2.5	3.5	4.5	5.6	6.6	7.6	8.6	9.3
	0.029	-	-	0.8	1.8	2.8	3.9	4.9	5.9	6.9	7.9	8.9	9.6
	0.030	-	0.1	1.1	2.2	3.2	4.2	5.2	6.2	7.2	8.3	9.3	10.0

Reference Tmrt 70 °C		Shrub Albedo										
		0.09	0.10	0.11	0.12	0.13	0.14	0.15	0.16	0.17	0.18	0.19
Plant Evapotranspiration Rate	0.001	76.0	75.4	74.8	74.2	73.5	72.9	72.3	71.7	71.1	70.5	69.9
	0.002	75.8	75.2	74.6	74.0	73.3	72.7	72.1	71.5	70.9	70.3	69.7
	0.003	75.6	75.0	74.4	73.8	73.1	72.5	71.9	71.3	70.7	70.1	69.5
	0.004	75.4	74.8	74.2	73.6	72.9	72.3	71.7	71.1	70.5	69.9	69.3
	0.005	75.2	74.6	74.0	73.4	72.7	72.1	71.5	70.9	70.3	69.7	69.1
	0.006	75.0	74.4	73.8	73.2	72.5	71.9	71.3	70.7	70.1	69.5	68.9
	0.007	74.8	74.2	73.6	73.0	72.3	71.7	71.1	70.5	69.9	69.3	68.7
	0.008	74.6	74.0	73.4	72.8	72.1	71.5	70.9	70.3	69.7	69.1	68.5
	0.009	74.4	73.8	73.2	72.6	71.9	71.3	70.7	70.1	69.5	68.9	68.3
	0.010	74.2	73.6	73.0	72.4	71.7	71.1	70.5	69.9	69.3	68.7	68.1
	0.011	74.0	73.4	72.8	72.2	71.5	70.9	70.3	69.7	69.1	68.5	67.9
	0.012	73.8	73.2	72.6	72.0	71.3	70.7	70.1	69.5	68.9	68.3	67.7
	0.013	73.6	73.0	72.4	71.8	71.1	70.5	69.9	69.3	68.7	68.1	67.5
	0.014	73.4	72.8	72.2	71.6	70.9	70.3	69.7	69.1	68.5	67.9	67.3
	0.015	73.2	72.6	72.0	71.4	70.7	70.1	69.5	68.9	68.3	67.7	67.1
	0.016	73.0	72.4	71.8	71.2	70.5	69.9	69.3	68.7	68.1	67.5	66.9
	0.017	72.8	72.2	71.6	71.0	70.3	69.7	69.1	68.5	67.9	67.3	66.7
	0.018	72.6	72.0	71.4	70.8	70.1	69.5	68.9	68.3	67.7	67.1	66.5
	0.019	72.4	71.8	71.2	70.6	69.9	69.3	68.7	68.1	67.5	66.9	66.3
	0.020	72.2	71.6	71.0	70.4	69.7	69.1	68.5	67.9	67.3	66.7	66.1
	0.021	72.0	71.4	70.8	70.2	69.5	68.9	68.3	67.7	67.1	66.5	65.9
	0.022	71.8	71.2	70.6	70.0	69.3	68.7	68.1	67.5	66.9	66.3	65.7
	0.023	71.6	71.0	70.4	69.8	69.1	68.5	67.9	67.3	66.7	66.1	65.5
	0.024	71.4	70.8	70.2	69.6	68.9	68.3	67.7	67.1	66.5	65.9	65.3
	0.025	71.2	70.6	70.0	69.4	68.7	68.1	67.5	66.9	66.3	65.7	65.1
	0.026	71.0	70.4	69.8	69.2	68.5	67.9	67.3	66.7	66.1	65.5	64.9

	0.027	70.8	70.2	69.6	69.0	68.3	67.7	67.1	66.5	65.9	65.3	64.7
	0.028	70.6	70.0	69.4	68.8	68.1	67.5	66.9	66.3	65.7	65.1	64.5
	0.029	70.4	69.8	69.2	68.6	67.9	67.3	66.7	66.1	65.5	64.9	64.3
	0.030	70.2	69.6	69.0	68.4	67.7	67.1	66.5	65.9	65.3	64.7	64.1

Percentage reduction in mean radiant temperature

Reference Tmrt 70 °C		Shrub Albedo										
		0.09	0.10	0.11	0.12	0.13	0.14	0.15	0.16	0.17	0.18	0.19
Plant Evapotranspiration Rate	0.001	-	-	-	-	-	-	-	-	-	-	0.2
	0.002	-	-	-	-	-	-	-	-	-	-	0.5
	0.003	-	-	-	-	-	-	-	-	-	-	0.7
	0.004	-	-	-	-	-	-	-	-	-	-	1.0
	0.005	-	-	-	-	-	-	-	-	-	0.4	1.3
	0.006	-	-	-	-	-	-	-	-	-	0.7	1.6
	0.007	-	-	-	-	-	-	-	-	0.1	1.0	1.9
	0.008	-	-	-	-	-	-	-	-	0.4	1.3	2.2
	0.009	-	-	-	-	-	-	-	-	0.7	1.6	2.5
	0.010	-	-	-	-	-	-	-	0.1	1.0	1.9	2.7
	0.011	-	-	-	-	-	-	-	0.4	1.3	2.2	3.0
	0.012	-	-	-	-	-	-	-	0.7	1.6	2.4	3.3
	0.013	-	-	-	-	-	-	0.1	1.0	1.9	2.7	3.6
	0.014	-	-	-	-	-	-	0.4	1.3	2.1	3.0	3.9
	0.015	-	-	-	-	-	-	0.7	1.6	2.4	3.3	4.2
	0.016	-	-	-	-	-	0.1	1.0	1.8	2.7	3.6	4.5
	0.017	-	-	-	-	-	0.4	1.3	2.1	3.0	3.9	4.7
	0.018	-	-	-	-	-	0.7	1.5	2.4	3.3	4.2	5.0
	0.019	-	-	-	-	0.1	1.0	1.8	2.7	3.6	4.4	5.3
	0.020	-	-	-	-	0.4	1.2	2.1	3.0	3.9	4.7	5.6
	0.021	-	-	-	-	0.7	1.5	2.4	3.3	4.1	5.0	5.9
	0.022	-	-	-	-	0.9	1.8	2.7	3.6	4.4	5.3	6.2
	0.023	-	-	-	0.4	1.2	2.1	3.0	3.8	4.7	5.6	6.5
	0.024	-	-	-	0.6	1.5	2.4	3.3	4.1	5.0	5.9	6.7
	0.025	-	-	-	0.9	1.8	2.7	3.5	4.4	5.3	6.2	7.0
	0.026	-	-	0.3	1.2	2.1	3.0	3.8	4.7	5.6	6.4	7.3
	0.027	-	-	0.6	1.5	2.4	3.2	4.1	5.0	5.9	6.7	7.6

	0.028	-	-	0.9	1.8	2.7	3.5	4.4	5.3	6.1	7.0	7.9
	0.029	-	0.3	1.2	2.1	2.9	3.8	4.7	5.6	6.4	7.3	8.2
	0.030	-	0.6	1.5	2.4	3.2	4.1	5.0	5.8	6.7	7.6	8.5

10.9 Specifications for green roof

10.9.1 Green roof panel

Material – Polypropylene

Depth – 70 mm

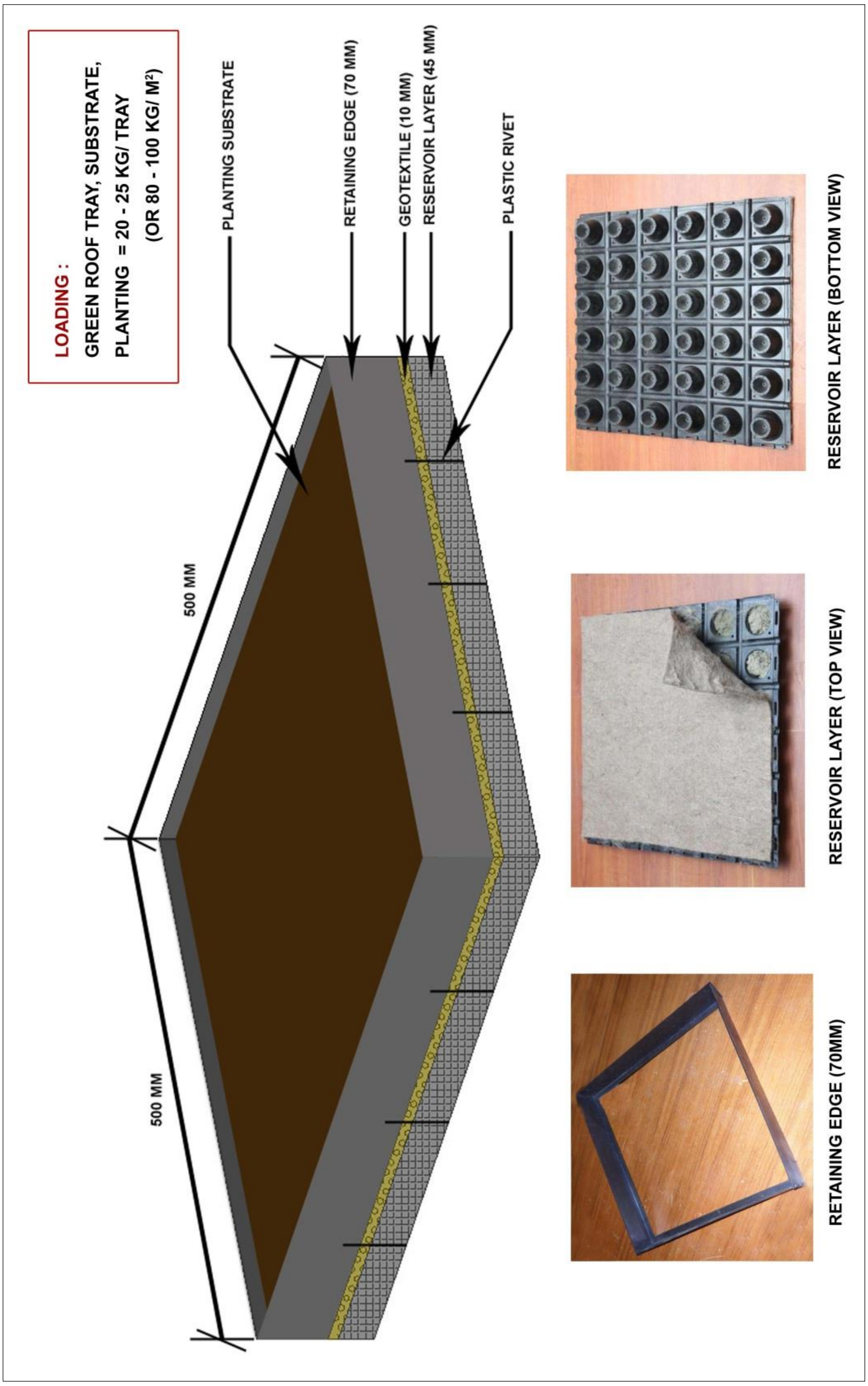

Figure 148. Green roof panel specifications

10.9.2 Substrate

Composition – pumice

Weight of substrate per unit panel – 10 Kg

10.9.3 Irrigation

Automatic drip irrigation system

Emitter flow rate – 1.0 Litre per hour

Battery powered controller used to control irrigation

Irrigation timing – 06:00 hrs to 07:00 hrs daily

Amount of water supplied to single 500 mm X 500 mm green roof panel – 1.16 Kg

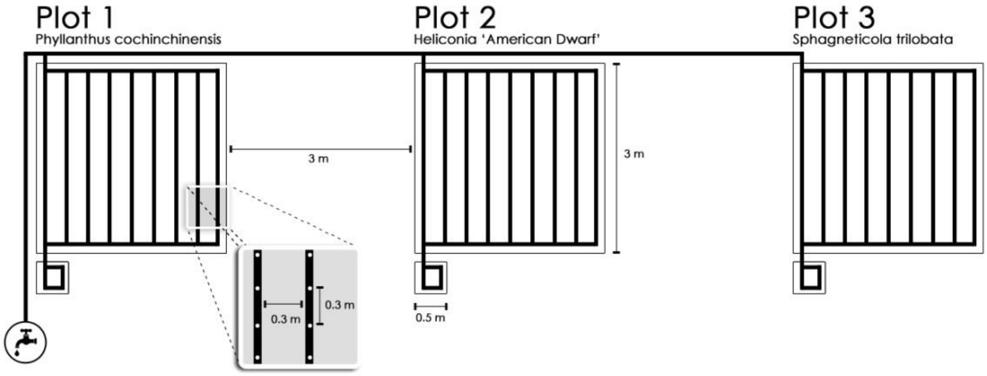

Figure 149. Irrigation plan

10.10 BCA Green Mark for New Non-Residential Buildings Version NRB/4.1

BCA GREEN MARK

BCA Green Mark for New Non-Residential Buildings
Version NRB/4.1

Framework - BCA Green Mark for New Non-Residential Buildings (Version NRB/4.1)

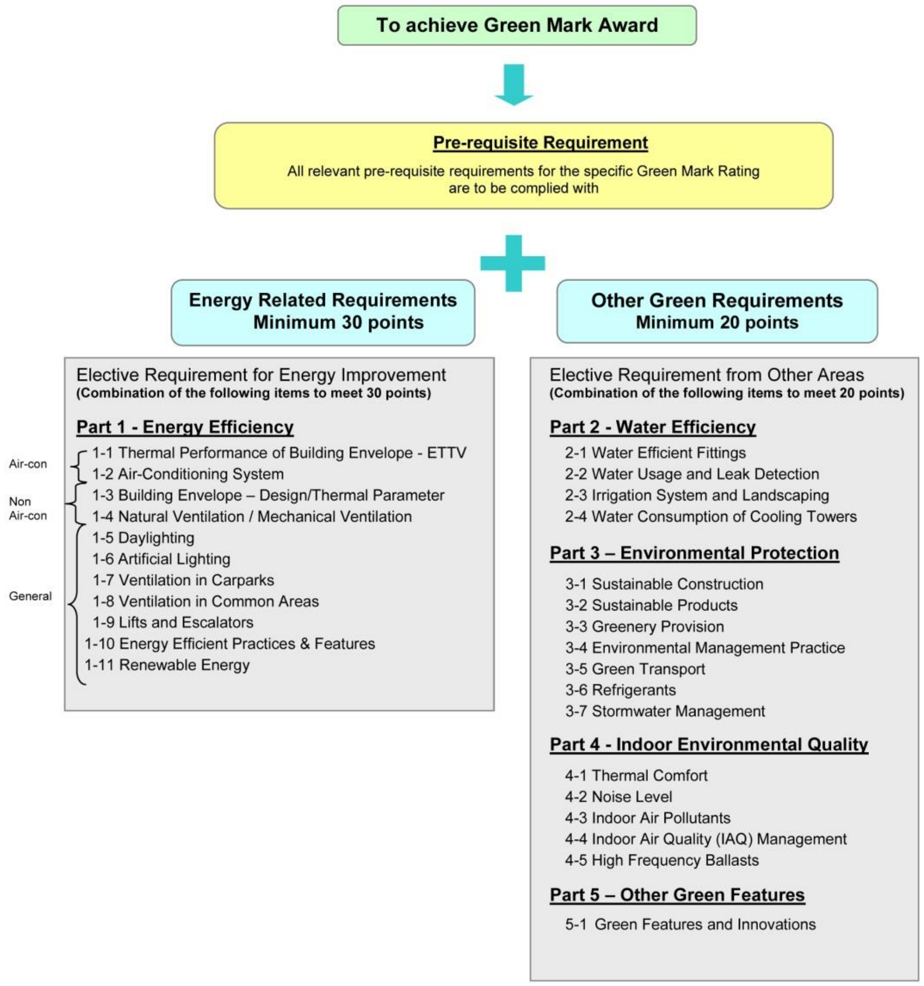

To achieve Green Mark Award

Pre-requisite Requirement

All relevant pre-requisite requirements for the specific Green Mark Rating are to be complied with

Energy Related Requirements
Minimum 30 points

Other Green Requirements
Minimum 20 points

Elective Requirement for Energy Improvement
(Combination of the following items to meet 30 points)

Part 1 - Energy Efficiency

Air-con
- 1-1 Thermal Performance of Building Envelope - ETTV
- 1-2 Air-Conditioning System

Non Air-con
- 1-3 Building Envelope – Design/Thermal Parameter
- 1-4 Natural Ventilation / Mechanical Ventilation

General
- 1-5 Daylighting
- 1-6 Artificial Lighting
- 1-7 Ventilation in Carparks
- 1-8 Ventilation in Common Areas
- 1-9 Lifts and Escalators
- 1-10 Energy Efficient Practices & Features
- 1-11 Renewable Energy

Elective Requirement from Other Areas
(Combination of the following items to meet 20 points)

Part 2 - Water Efficiency

- 2-1 Water Efficient Fittings
- 2-2 Water Usage and Leak Detection
- 2-3 Irrigation System and Landscaping
- 2-4 Water Consumption of Cooling Towers

Part 3 – Environmental Protection

- 3-1 Sustainable Construction
- 3-2 Sustainable Products
- 3-3 Greenery Provision
- 3-4 Environmental Management Practice
- 3-5 Green Transport
- 3-6 Refrigerants
- 3-7 Stormwater Management

Part 4 - Indoor Environmental Quality

- 4-1 Thermal Comfort
- 4-2 Noise Level
- 4-3 Indoor Air Pollutants
- 4-4 Indoor Air Quality (IAQ) Management
- 4-5 High Frequency Ballasts

Part 5 – Other Green Features

- 5-1 Green Features and Innovations

Point Allocations - BCA Green Mark for New Non-Residential Buildings (Version NRB/4.1)

	Category		Point Allocations
(I)	**Energy Related Requirements**		
Minimum 30 points	**Part 1 : Energy Efficiency**		
	NRB 1-1 Thermal Performance of Building Envelope - ETTV	Section (A) Applicable to air-con areas	12
	NRB 1-2 Air-Conditioning System		30
	Sub-Total (A) – NRB 1-1 to 1-2		42
	NRB 1-3 Building Envelope – Design/Thermal Parameter	Section (B) Applicable to non air-con areas excluding carparks and common areas	35
	NRB 1-4 Natural Ventilation / Mechanical Ventilation		20
	Sub-Total (B) – NRB 1-3 to 1-4		55
	NRB 1-5 Daylighting	Section (C) Generally applicable to all areas	6
	NRB 1-6 Artificial Lighting		12
	NRB 1-7 Ventilation in Carparks		4
	NRB 1-8 Ventilation in Common Areas		5
	NRB 1-9 Lifts and Escalators		2
	NRB 1-10 Energy Efficient Practices & Features		12
	NRB 1-11 Renewable Energy		20
	Sub-Total (C) – NRB 1-5 to 1-11		61
	Category Score for Part 1 – Energy Efficiency **Prorate Subtotal (A) + Prorate Subtotal (B) + Prorate Subtotal (C)**		**116 (Max)**
(II)	**Other Green Requirements**		
Minimum 20 points	**Part 2 : Water Efficiency**		
	NRB 2-1 Water Efficient Fittings		10
	NRB 2-2 Water Usage and Leak Detection		2
	NRB 2-3 Irrigation System and Landscaping		3
	NRB 2-4 Water Consumption of Cooling Towers		2
	Category Score for Part 2 – Water Efficiency		**17**
	Part 3 : Environmental Protection		
	NRB 3-1 Sustainable Construction		10
	NRB 3-2 Sustainable Products		8
	NRB 3-3 Greenery Provision		8
	NRB 3-4 Environmental Management Practice		7
	NRB 3-5 Green Transport		4
	NRB 3-6 Refrigerants		2
	NRB 3-7 Stormwater Management		3
	Category Score for Part 3 – Environmental Protection		**42**
	Part 4 : Indoor Environmental Quality		
	NRB 4-1 Thermal Comfort		1
	NRB 4-2 Noise Level		1
	NRB 4-3 Indoor Air Pollutants		2
	NRB 4-4 Indoor Air Quality (IAQ) Management		2
	NRB 4-5 High Frequency Ballasts		2
	Category Score for Part 4 – Indoor Environmental Quality		**8**
	Part 5 : Other Green Features		
	NRB 5-1 Green Features & Innovations		7
	Category Score for Part 5 – Other Green Features		**7**
		Green Mark Score :	**190 (Max)**

BCA Green Mark Award Rating and Prerequisite Requirements

Green Mark Score	Green Mark Rating
90 and above	Green Mark Platinum
85 to < 90	Green Mark Gold$^{\text{Plus}}$
75 to < 85	Green Mark Gold
50 to <75	Green Mark Certified

Prerequisite Requirements for Non-Residential Building Criteria

Air-Conditioned Buildings

Related Criteria

(1) Building envelope design with Envelope Thermal Transfer Value (ETTV) computed based on the methodology and guidelines stipulated in the Code on Envelope Thermal Performance for Buildings and this Standard.

Green Mark Gold$^{\text{Plus}}$ – ETTV of 42 W/m^2 or lower

Green Mark Platinum – ETTV of 40 W/m^2 or lower

NRB 1-1 – Thermal Performance of Building Envelope

(2) To demonstrate the stipulated energy savings over its reference model using the energy modeling framework set out in Appendix E of the Certification Standard. Details and submission requirements on energy modeling can be found in Appendix E.

Green Mark Gold$^{\text{Plus}}$ – At least 25% energy savings based on energy efficiency measures and improvements that reduce cooling load requirements

Green Mark Platinum – At least 30% energy savings based on energy efficiency measures and improvements that reduce cooling load requirements

(3) Prescribed Design System Efficiency (DSE) of building cooling systems to be as follows:

NRB 1-2(a) – Air–Conditioning System

(i) For Buildings using Water-Cooled Chilled-Water Plant:

Green Mark Rating	Peak Building Cooling Load (RT)	
	< 500	≥ 500
	Minimum Design System Efficiency(1) DSE (kW/RT)	
Certified	0.80	0.70
Gold	0.80	0.70
Gold$^{\text{Plus}}$	0.70	0.65
Platinum	0.70	0.65

Prerequisite Requirements for Non-Residential Building Criteria – *Cont'd*

(ii) For Buildings using Air Cooled Chilled-Water Plant or Unitary Air-Conditioners:

Green Mark Rating	Peak Building Cooling Load (RT)	
	< 500	≥ 500
	Minimum Design System Efficiency(1) DSE (kW/RT)	
Certified	0.90	0.80
Gold	0.90	Not applicable(2)
Gold^{Plus}	0.85	
Platinum	0.78	

Important notes :

(1) The efficiency of the overall air-conditioning system shall meet its design system efficiency as well as the corresponding minimum DSE stipulated for the respective air-conditioning system and Green Mark rating during the building operating hours specified below:

Office Buildings: Monday to Friday : 9 a.m. to 6 p.m.	**Hotels:** Monday to Sunday : 24 Hours
Retail Malls : Monday to Sunday :10 a.m. to 9 p.m.	**Other Building Types:** To be determined based on operating hours

(2) For building with peak building cooling load of more than 500 RT, the use of air cooled chilled-water plant or unitary air-conditioners are not applicable for Gold and higher ratings. In general, the system efficiency of the air cooled central chilled-water plant and other unitary air-conditioners are to be comparable with the stipulated efficiency for water-cooled central chilled-water plant. Buildings that are designed with air cooled systems and for higher Green Mark rating will be assessed on a case by case basis.

Related Criteria

NRB 1-2(b) – Air–Conditioning System

(4) Instrumentation for monitoring the water cooled chilled-water plant efficiency is to be provided in accordance with the requirement set in the criteria.

NRB 1-2(d) – Air–Conditioning System

(5) Minimum score under NRB 3-1 Sustainable Construction
Green Mark Gold^{Plus} ≥ 3 points
Green Mark Platinum ≥ 5 points

NRB 3-1 – Sustainable Construction

(6) Minimum score under NRB 3-2 Sustainable Products
Green Mark Gold^{Plus} ≥ 3 points
Green Mark Platinum ≥ 4 points

NRB 3-2 – Sustainable Products

Prerequisite Requirements for Non-Residential Building Criteria – *Cont'd*

Non Air-Conditioned Buildings

Related Criteria

(7) To be eligible for Green Mark Platinum rating, it is a requirement to use ventilation simulation modeling and analysis to identify the most effective building design and layout. The simulation results and the recommendations derived are to be implemented to ensure good natural ventilation with minimum weighted average wind velocity of 0.6 m/s within the units. Details and submission requirements on ventilation simulation can be found in Appendix C of the Certification Standard.

NRB 1-4(a)(ii) – Natural Ventilation

(8) Minimum score under NRB 3-1 Sustainable Construction

Green Mark Gold^{Plus} ≥ 3 points

Green Mark Platinum ≥ 5 points

NRB 3-1 – Sustainable Construction

(9) Minimum score under NRB 3-2 Sustainable Products

Green Mark Gold^{Plus} ≥ 3 points

Green Mark Platinum ≥ 4 points

NRB 3-2 – Sustainable Products

Building Developments with more than 30% Non Air-Conditioned Spaces

(10) Prerequisite requirement for building developments with a combination of ventilation mode and with aggregate non-air-conditioned spaces of more than 30% of the total constructed floor areas (excluding carparks and common areas) are as follows :

Aggregate Non Air-Conditioned Spaces (m^2)	**Aggregate Air-Conditioned Spaces (m^2)**	**Ventilation Simulation Requirement** See Note (a)	**Energy Modeling Requirement** See Note (b)	**Justification on Energy Savings** See Note (c)
≥ 2000	≥ 5000	Yes	Yes	No
< 2000	≥ 5000	No	Yes	No
≥ 2000	< 5000	Yes	No	Yes
< 2000	< 5000	No	No	Yes

Important Notes :

(a) Ventilation requirement stated paragraph (7) is a pre-requisite requirement to attain Green Platinum rating.

(b) The stipulated energy savings and Design System Efficiency (DSE) of cooling system stated in paragraph (2) and (3) are pre-requisites to attain Green Mark Gold^{Plus} and Platinum rating.

(c) Detailed calculations to be provided to justify the savings in energy consumption from the use of salient energy efficient features /equipment. Energy savings will be based on the energy efficiency measures and improvements over the reference model established for similar building types. The reference ACMV system will be of the same type as the proposed system. The baseline used for the equipment will be in accordance with the minimum efficiency requirement stipulated in SS 530. For VRF system, the baseline COP of 3.37 shall be adopted. The stipulated energy savings stated in paragraph (2) are pre-requisites to attain Green Mark Gold^{Plus} and Platinum rating.

(d) Other pre-requisite stated paragraph (1), (4), (5), (6), (8) and (9) are applicable where relevant.

<table>
<tr><th>Part 1 – Energy Efficiency</th><th>Green Mark Points</th></tr>
<tr><td colspan="2">(A) Applicable to Air-Conditioned Building Areas (with an aggregate air-conditioned areas > 500 m^2)</td></tr>
<tr><td><u>NRB 1-1 Thermal Performance of Building Envelope – Envelope Thermal Transfer Value (ETTV)</u>
Enhance the overall thermal performance of building envelope to minimise heat gain thus reducing the overall cooling load requirement.
<u>Baseline</u> : Maximum Permissible ETTV = 50 W/m^2
<i><u>Prerequisite Requirement :</u></i>
<i>Green Mark Gold^{Plus} – ETTV of 42 W/m^2 or less</i>
<i>Green Mark Platinum – ETTV of 40 W/m^2 or less</i></td><td>1.2 points for every reduction of 1 W/m^2 in ETTV from the baseline
Points scored = 1.2 x (50 - ETTV) where ETTV ≤ 50 W/m^2
(Up to 12 points)</td></tr>
<tr><td><u>NRB 1-2 Air-Conditioning System</u>
Encourage the use of better energy efficient air-conditioned equipment to minimise energy consumption.
(a) Water-Cooled Chilled-Water Plant :
• Water-Cooled Chiller
• Chilled-Water Pump
• Condenser Water Pump
• Cooling Tower
<table>
<tr><td rowspan="2">Baseline</td><td colspan="2">Peak Building Cooling Load</td></tr>
<tr><td>≥ 500 RT</td><td>< 500 RT</td></tr>
<tr><td><i><u>Prerequisite Requirements</u></i>
Minimum Design System Efficiency (DSE) for central chilled-water plant</td><td>0.70 kW/RT</td><td>0.80 kW/RT</td></tr>
</table>
<i><u>Prerequisite Requirements for Higher Green Mark Rating :</u></i>
<i>Green Mark Gold^{Plus} & Platinum : Minimum Design System Efficiency (DSE) of 0.65 kW/RT for peak building cooling load ≥ 500 RT and 0.7 kW/RT for peak building cooling load < 500 RT</i>

(b) Air Cooled Chilled-Water Plant / Unitary Air-Conditioners
Air Cooled Chilled-Water Plant :
• Air-Cooled Chiller
• Chilled-Water Pump
Unitary Air-Conditioners :
• Variable Refrigerant Flow (VRF) system
• Single-Spilt Unit
• Multi-Spilt Unit</td><td><u>(a) Water-Cooled Chilled-Water Plant</u>
Peak building cooling load ≥ 500 RT
15 points for meeting the prescribed chilled-water plant efficiency of 0.70 kW/RT
0.25 point for every percentage improvement in the chilled-water plant efficiency over the baseline
Points scored = 0.25 x (% improvement)
Peak building cooling load < 500 RT
12 points for meeting the prescribed chilled-water plant efficiency of 0.80 kW/RT
0.45 point for every percentage improvement in the chilled-water plant efficiency over the baseline
Points scored = 0.45 x (% improvement)
(Up to 20 points)

<u>(b) Air Cooled Chilled-Water Plant/ Unitary Air-Conditioners</u>
Peak building cooling load ≥ 500 RT
12 points for meeting the prescribed air-conditioning system efficiency of 0.80 kW/RT
1.3 points for every percentage improvement in the air-conditioning system efficiency over the baseline
Points scored = 1.3 x (% improvement)</td></tr>
</table>

Part 1 – Energy Efficiency | **Green Mark Points**

(A) Applicable to Air-Conditioned Building Areas (with an aggregate air-conditioned areas > 500 m^2)

(b) Air Cooled Chilled-Water Plant / Unitary Air-Conditioners – *Cont'd*

Baseline	Peak Building Cooling Load	
	≥ 500 RT	< 500 RT
Prerequisite Requirements Minimum Design System Efficiency (DSE) for air cooled chilled-water plant or unitary conditioners	0.80 kW/RT	0.90 kW/RT

Prerequisite Requirements for Higher Green Mark Rating :
Green Mark Gold^{Plus} : Minimum Design System Efficiency (DSE) of 0.85kW/RT for peak building cooling load < 500 RT
Green Mark Platinum: Minimum DSE of 0.78kW/RT for peak building cooling load < 500 RT

Note (1) : Where there is a combination of central chilled water plant with unitary conditioners, the points scored will only be based on the air-conditioning system with a larger aggregate capacity.

(c) Air Distribution System :
- Air Handling Units (AHUs)
- Fan Coil Units (FCUs)

Option 1 – Fan System Motor Nameplate Power

Baseline : SS553:2009 Table 2 – Fan power limitation and as prescribed below :

Baseline Air Distribution System Type	Allowable Motor Nameplate Power	
	(kW/m^3/s)	(W/CMH)
AHUs/FCUs ≥ 4kW (Constant Volume)	1.7	0.47
AHUs ≥ 4kW (Variable Volume)	2.4	0.67
Fan systems with nameplate motor power < 4 kW	No baseline	

Option 2 – Fan System Input Power

Baseline : ASHRAE 90.1:2010 Clause 6.5.3.1 and as prescribed below :

Baseline Air Distribution System Type	Allowable Fan System Input Power*	
	(kW/m^3/s)	(W/CMH)
AHUs/FCUs ≥ 4kW (Constant Volume)	1.5	0.42
AHUs ≥ 4kW (Variable Volume)	2.1	0.58
Fan systems with nameplate motor power < 4 kW	0.6	0.17

* Applicable pressure drop adjustments can be considered based on ASHRAE 90.1 Table 6.5.3.1.1B and are subject to BCA's evaluation

Note (2) : For buildings with cooling provision from a licensed District Cooling System (DCS) supplier where the plant efficiency data is not available, the point scored for NRB 1-2(a) and (b) will be pro-rated based on the air distribution system efficiency under NRB 1-2(c).

Peak building cooling load < 500 RT

10 points for meeting the prescribed air-conditioning system efficiency of 0.90 kW/RT

0.6 point for every percentage improvement in the air-conditioning system efficiency over the baseline

Points scored = 0.6 x (% improvement)

(Up to 20 points)

(c) Air Distribution System

0.2 point for every percentage improvement in the air distribution system efficiency over the baseline

Points scored = 0.2 x (% improvement)

(Up to 6 points)

Part 1 – Energy Efficiency	Green Mark Points
(A) Applicable to Air-Conditioned Building Areas (with an aggregate air-conditioned areas > 500 m^2)	
(d) *Prerequisite Requirements :* Provision of permanent measuring instruments for monitoring of water-cooled chilled-water plant efficiency. The installed instrumentation shall have the capability to calculate a resultant plant efficiency (i.e. kW/RT) within 5 % of its true value and in accordance with ASHRAE Guide 22 and AHRI Standard 550/590. The following instrumentation and installation are also required to be complied with : (i) Location and installation of the measuring devices to meet the manufacturer's recommendation. (ii) Data acquisition system with a minimum resolution of 16 bit. (iii) All data logging with capability to trend at 1 minute sampling time interval. (iv) Flow meters are to be provided for chilled-water and condenser water loop and shall be of ultrasonic / full bore magnetic type or equivalent. (v) Temperature sensors are to be provided for chilled water and condenser water loop and shall have an end-to-end measurement uncertainty not exceeding ± 0.05 °C over the entire measurement or calibration range. All thermo-wells shall be installed in a manner that ensures that the sensors can be in direct contact with fluid flow. Provisions shall be made for each temperature measurement location to have two spare thermo-wells located at both side of the temperature sensor for verification of measurement accuracy. (vi) Dedicated power meters are to be provided for each of the following groups of equipment : chillers, chilled water pumps, condenser water pumps and cooling towers.	Applicable only to buildings with provision of water cooled chilled-water plant 1 point
(e) Verification of central water cooled chilled-water plant instrumentation : Heat balance – substantiating test for water cooled chilled-water plant to be computed in accordance with AHRI 550/590	1 point
(f) Provision of variable speed controls for chiller plant equipment such as chilled-water pumps and cooling tower fans to ensure better part-load plant efficiency.	1 point
(g) Sensors or similar automatic control devices are used to regulate outdoor air flow rate to maintain the concentration of carbon dioxide in accordance with Table 1 – Recommended IAQ Parameters of SS 554. Carbon dioxide acceptable range: ≤ 700 ppm above outdoor.	1 point
Exception: For buildings that are underground, NRB 1-1 may be excluded in the computation. The score under NRB 1-2 will be pro-rated accordingly.	
Sub-Total (A) :	Sum of Green Mark Points obtained from NRB 1-1 to 1-2

Part 1 – Energy Efficiency	Green Mark Points

(B) Applicable to Non Air-Conditioned Building Areas (with an aggregate non air-conditioned areas > 10 % of total floor area excluding carparks and common areas)

NRB 1-3 Building Envelope – Design / Thermal Parameters

Enhance the overall thermal performance of building envelope to minimise heat gain that would improve indoor thermal comfort and encourage natural ventilation or mechanical ventilation.

(a) Minimum direct west facing façade through building design orientation.

Note (3) : Orientation of façade that falls within the range of 22.5° N of W and 22.5° S of W will be defined as west facing facade. Core walls for lifts or staircases and toilets that are located within this range are exempted in computation.

Points scored = 15 – 0.3 x (% of west facing facade areas over total façade areas)

(Up to 15 points)

Where there is no west facing façade, the total points scored for this item will be 30 points; the NRB 1-3 b(i), b(ii) and (c) as listed below will not be applicable.

(b)(i) Minimum west facing window openings.

Points scored = 10 - 0.1 x (% of west facing window areas over total west facing façade areas)

(b)(ii) Effective sunshading provision for windows on the west façade with minimum shading of 30%.

Points scored = 0.1 x (% of west facing window areas with sunshading devices over total west facing façade areas)

(Up to 10 points for NRB 1-3 b(i) & b(ii))

(c) Better thermal transmittance (U-value) of external west facing walls.

The U-value of external west facing walls should be equal or less than 2 W/m^{2}K.

Points scored = 0.05 x (% of the external west facing walls areas with U value of 2 W/m^{2}K or less over total west facing facades areas)

(up to 5 points)

(d) Better thermal transmittance (U-value) of roof.

Baseline: U-value for roof stated below depending on the weight range of roof structure:

Weight Group	Weight range (kg/m^2)	Maximum Thermal Transmittance (W/m^{2}K)
Light	Under 50	0.8
Medium	50 to 230	1.1
Heavy	Over 230	1.5

1 point for every 0.1 W/m^{2}K reduction from the baseline roof U-value

(Up to 5 points)

Exception : For existing buildings, NRB 1-3(a) may be excluded in computation, the total score obtained under NRB 1-3 (b), (c) and (d) will be prorated accordingly.

Part 1 – Energy Efficiency	**Green Mark Points**
(B) Applicable to Non Air-Conditioned Building Areas (with an aggregate non air-conditioned areas > 10 % of total floor area excluding carparks and common areas)	

NRB 1-4 Natural Ventilation / Mechanical Ventilation

(a) Natural Ventilation

Encourage building design that facilitates good natural ventilation.

(i) Proper design of building layout that utilises prevailing wind conditions to achieve adequate cross ventilation.

1 point for every 10% of units/rooms with window openings facing north and south directions
Points scored = 1 x (% of units/10)
(Up to 10 points)

(ii) Use of ventilation simulation modeling and analysis or wind tunnel testing to identify the most effective building design and layout to ensure good natural ventilation.

5 points

Additional 5 points
if the recommendations are implemented and meet the air-flow requirement
(Up to 10 points)

Prerequisite Requirement :
Green Mark Platinum : Ventilation simulation modeling and analysis are to be carried out to ensure good natural ventilation with minimum weighted average wind velocity of 0.6 m/s within the functional spaces or units.

(b) Mechanical Ventilation

Encourage energy efficient mechanical ventilation system design as the preferred ventilation mode to minimise air-conditioned spaces.

0.6 point for every percentage improvement in the mechanical ventilation system efficiency over the baseline

Points scored = 0.6 x (% improvement)

(Up to 15 points)

Option 1 – Fan System Motor Nameplate Power

Baseline : SS553:2009 Table 8 – Fan power limitation and as prescribed below :

Baseline Air Distribution System Type	Allowable Motor Nameplate Power	
	(kW/m^3/s)	(W/CMH)
AHUs/FCUs ≥ 4kW (Constant Volume)	1.7	0.47
Fan systems with nameplate motor power < 4 kW	No baseline	

Option 2 – Fan System Input Power

Baseline : ASHRAE 90.1 : 2010 Clause 6.5.3.1 and as prescribed below :

Baseline Air Distribution System Type	Allowable Fan System Input Power *	
	(kW/m^3/s)	(W/CMH)
AHUs/FCUs ≥ 4kW (Constant Volume)	1.5	0.42
Fan systems with nameplate motor power < 4 kW	0.6	0.17

* Applicable pressure drop adjustments can be considered based on ASHRAE 90.1 Table 6.5.3.1.1B and are subject to BCA's evaluation

Note (4) : Where there is a combination of naturally ventilated and mechanical ventilated spaces, points scored will be based on the predominant ventilation modes of normally occupied spaces.

Sub-Total (B) :	Sum of Green Mark Points obtained from NRB 1-3 to 1-4

<table>
<tr><th>Part 1 - Energy Efficiency</th><th>Green Mark Points</th></tr>
<tr><td colspan="2">(C) General</td></tr>
<tr><td><u>NRB 1-5 Daylighting</u>
Encourage design that optimises the use of effective daylighting to reduce energy use for artificial lighting.
(a) Use of daylighting and glare simulation analysis to verify the adequacy of ambient lighting levels in meeting the illuminance level and Unified Glare Rating (UGR) stated in SS 531:Part 1:2006 – Code of Practice for Lighting of Work Places.
(b) Daylighting for the following common areas:
(i) Toilets
(ii) Staircases
(iii) Corridors
(iv) Lift Lobbies
(v) Atriums
(vi) Carparks
Note (5) : All daylit areas must be integrated with automatic electric lighting control system.</td>
<td>Extent of coverage: At least 75% of the units with daylighting provisions meet the minimum illuminance level and are within the acceptable glare exposure.
Points scored based on the extent of perimeter daylight zones
<table>
<tr><th>Distance from the Façade Perimeters (m)</th><th>Points Allocation</th></tr>
<tr><td>≥ 3.0</td><td>1</td></tr>
<tr><td>4.0 – 5.0</td><td>2</td></tr>
<tr><td>> 5.0</td><td>3</td></tr>
</table>
(Up to 3 points)
Extent of Coverage : At least 80 % of each applicable area
0.5 point each
(Up to 3 points)</td></tr>
<tr><td><u>NRB 1-6 Artificial Lighting</u>
Encourage the use of energy efficient lighting to minimise energy consumption from lighting usage while maintaining proper lighting level.
<u>Baseline</u> : Maximum lighting power budget stated in SS 530</td>
<td>0.3 point for every percentage improvement in lighting power budget
Points scored = 0.3 x (% improvement)
(Including tenant lighting provision)
(Up to 12 points)
(Excluding tenant lighting provision)
(Up to 5 points)</td></tr>
<tr><td><u>NRB 1-7 Ventilation in Carparks</u>
Encourage the use of energy efficient design and control of ventilation systems in carparks.
(a) Carparks are designed with natural ventilation.
(b) CO sensors are used to regulate the demand for mechanical ventilation (MV).
Note (6) : Where there is a combination of different ventilation mode adopted for carpark design, the points obtained under NRB 1-7 will be prorated accordingly.</td>
<td>Naturally ventilated carparks – 4 points
Points scored based on the mode of mechanical ventilation provided
Fume extract – 2.5 points
MV with or without supply - 2 points
(Up to 4 points)</td></tr>
</table>

Part 1 - Energy Efficiency	**Green Mark Points**
(C) General	
<u>NRB 1-8 Ventilation in Common Areas</u> Encourage the use of energy efficient design and control of ventilation systems in the following common areas : (a) Toilets (b) Staircases (c) Corridors (d) Lift lobbies (e) Atrium	Extent of Coverage : At least 90 % of each applicable area Points scored based on the mode of ventilation provided in applicable areas Natural ventilation – 1.5 points for each area Mechanical ventilation – 0.5 point for each area (Up to 5 points)
<u>NRB 1-9 Lifts and Escalators</u> Encourage the use of energy efficient lifts and escalators. Lifts and/or escalators with AC variable voltage and variable frequency (VVVF) motor drive and sleep mode features.	Extent of Coverage : All lifts and escalators Lifts – 1 point Escalators – 1 point
<u>NRB 1-10 Energy Efficient Practices & Features</u> Encourage the use of energy efficient practices and features that are innovative and/or have positive environmental impact.	
(a) Computation of energy consumption based on design load in the form of energy efficiency index (EEI).	1 point
(b) Use of vertical greenery system on east and west façade to reduce heat gain through building envelope	1 point for high impact 0.5 point for low impact
(c) Use of energy efficient equipment or product that are certified by approved local certification body	Extent of Coverage : 90% of the applicable equipment type or product 0.5 point for each eligible certified equipment or products (Up to 2 points)
(d) Use of energy efficient features. Examples: ▪ Heat recovery system ▪ Sun pipes ▪ Regenerative lifts ▪ Light shelves ▪ Photocell sensors to maximise the use of daylighting	3 points for every 1% energy saving over total building energy consumption (Up to 8 points)

<table>
<tr><th>Part 1 – Energy Efficiency</th><th>Green Mark Points</th></tr>
<tr><td colspan="2">(C) General</td></tr>
<tr><td><u>NRB 1-11 Renewable Energy</u>
Encourage the application of renewable energy sources in buildings.</td><td>Point scored based on the expected energy efficiency index (EEI) and % replacement of electricity by renewable energy source
<table>
<tr><th rowspan="2">Expected Energy Efficiency Index (EEI)</th><th colspan="2">Every 1% replacement of electricity (based on total building electricity consumption) by renewable energy source</th></tr>
<tr><th>Include tenant's usage</th><th>Exclude tenant's usage</th></tr>
<tr><td>≥ 30 kWh/m²/yr</td><td>5 points</td><td>3 points</td></tr>
<tr><td>< 30 kWh/m²/yr</td><td>3 points</td><td>1.5 points</td></tr>
</table>
(Up to 20 Points)
<i>Condition : The points scored for renewable energy provision shall not result in a double grade jump in the GM rating (i.e. from GM Certified to Gold^{Plus} or Gold to Platinum rating).</i></td></tr>
<tr><td>Sub-Total (C) :</td><td>Sum of Green Mark Points obtained
from NRB 1-5 to 1-11</td></tr>
<tr><td>PART 1 – ENERGY EFFICIENCY
CATEGORY SCORE :</td><td>

$$\text{Sub-Total (A)} \times \frac{\text{Air-Conditioned Building Floor Area}}{\text{Total Floor Area}} + \text{Sub-Total (B)} \times \frac{\text{Non Air-Conditioned Building Floor Area}}{\text{Total Floor Area}} + \text{Sub-Total (C)}$$

where Sub-Total (A) = Sum of Green Mark Points obtained under Section (A) NRB 1-1 to 1-2
Sub-Total (B) = Sum of Green Mark Points obtained under Section (B) NRB 1-3 to 1-4
Sub-Total (C) = Sum of Green Mark Points obtained under Section (C) NRB 1-5 to 1-11</td></tr>
</table>

<table>
<tr><th>Part 2 – Water Efficiency</th><th colspan="3">Green Mark Points</th></tr>
<tr><td rowspan="4"><u>NRB 2-1 Water Efficient Fittings</u>
Encourage the use of water efficient fittings covered under the Water Efficiency Labelling Scheme (WELS).
(a) Basin taps and mixers
(b) Flushing cistern
(c) Shower taps, mixers or showerheads
(d) Sink/Bib taps and mixers
(e) Urinals and urinal flush valve</td><td colspan="2">Rating based on Water Efficiency Labelling Scheme (WELS)</td><td rowspan="4">Points scored based on the number and water efficiency rating of the fitting type used
(Up to 10 points)</td></tr>
<tr><td>Very Good</td><td>Excellent</td></tr>
<tr><td colspan="2">Weightage</td></tr>
<tr><td>8</td><td>10</td></tr>
<tr><td><u>NRB 2-2 Water Usage and Leak Detection</u>
Promote the use of sub-metering and leak detection system for better control and monitoring.
(a) Provision of private meters to monitor the major water usage such as irrigation, cooling tower and tenants' usage.
(b) Linking all private meters to the Building Management System (BMS) for leak detection.</td><td colspan="3">1 point
1 point</td></tr>
<tr><td><u>NRB 2-3 Irrigation System and Landscaping</u>
Provision of suitable systems that utilise rainwater or recycled water and use of plants that require minimal irrigation to reduce potable water consumption.
(a) Use of non potable water including rainwater for landscape irrigation.
(b) Use of automatic water efficient irrigation system with rain sensor.
(c) Use of drought tolerant plants that require minimal irrigation.</td><td colspan="3">1 point
Extent of Coverage : At least 50% of the landscape areas are served by the system
1 point
Extent of Coverage : At least 80% of the landscape areas
1 point</td></tr>
<tr><td><u>NRB 2-4 Water Consumption of Cooling Tower</u>
Reduce potable water use for cooling purpose.
(a) Use of cooling tower water treatment system that can achieve 7 or better cycles of concentration at acceptable water quality.
(b) Use of NEWater or on-site recycled water from approved sources.</td><td colspan="3">1 point
1 point</td></tr>
<tr><td>PART 2 – WATER EFFICIENCY
CATEGORY SCORE :</td><td colspan="3">Sum of Green Mark Points obtained from NRB 2-1 to 2-4</td></tr>
</table>

<table>
<tr><th>Part 3 – Environmental Protection</th><th>Green Mark Points</th></tr>
<tr><td>
<u>NRB 3-1 Sustainable Construction</u>
Encourage recycling and the adoption of building designs, construction practices and materials that are environmentally friendly and sustainable

(a) Use of Sustainable and Recycled Materials
(i) Green Cements with approved industrial by-product (such as Ground Granulated Blastfurnace Slag (GGBS), silica fume, fly ash) to replace Ordinary Portland Cement (OPC) by at least 10% by mass for superstructural works.

(ii) Recycled Concrete Aggregates (RCA) and Washed Copper Slag (WCS) from approved sources to replace coarse and fine aggregates for concrete production of main building elements.

Note (7) : For structural building elements, the use of RCA and WCS shall be limited to maximum 10% replacement by mass of coarse/fine aggregates respectively or as approved by the relevant authorities.
</td><td>
1 point

1 point for every incremental of 0.5 times (0.5x) of the usage requirement (Up to 2x)
<table>
<tr><th>Quantity of RCA /WCS (tons)</th><th>Points Allocation</th></tr>
<tr><td>≥ 0.5 x usage requirement</td><td>1</td></tr>
<tr><td>≥ 1.0 x usage requirement</td><td>2</td></tr>
<tr><td>≥ 1.5 x usage requirement</td><td>3</td></tr>
<tr><td>≥ 2.0 x usage requirement</td><td>4</td></tr>
</table>
where usage requirement = 0.03 x (GFA in m^2)
(Up to 5 points for NRB 3-1(a)(i) and (a)(ii))
</td></tr>
<tr><td>
(b) Concrete Usage Index (CUI)
Encourage designs with efficient use of concrete for building components.

<i><u>Prerequisite Requirement:</u></i>
<i>Minimum points to be scored under this criterion:</i>
<i>Green Mark Gold^{Plus} ≥ 3 points</i>
<i>Green Mark Platinum ≥ 5 points</i>
</td><td>
<table>
<tr><th>Project CUI (m^3/m^2)</th><th>Points Allocation</th></tr>
<tr><td>≤ 0.70</td><td>1</td></tr>
<tr><td>≤ 0.60</td><td>2</td></tr>
<tr><td>≤ 0.50</td><td>3</td></tr>
<tr><td>≤ 0.40</td><td>4</td></tr>
<tr><td>≤ 0.35</td><td>5</td></tr>
</table>
</td></tr>
<tr><td>
<u>NRB 3-2 Sustainable Products</u>
Promote use of environmentally friendly products that are certified by approved local certification body and are applicable to non-structural and architectural related building components.

<i><u>Prerequisite Requirement:</u></i>
<i>Minimum score under this criterion:</i>
<i>Green Mark Gold^{Plus} ≥ 3 points</i>
<i>Green Mark Platinum ≥ 4 points</i>
</td><td>
<table>
<tr><th colspan="3">Weightage based on the extent of environmental friendliness of products</th><th rowspan="3">Points scored based on the weightage and the extent of coverage & impact

1 point for high impact item
0.5 point for low impact item

(Up to 8 points)</th></tr>
<tr><th>Good</th><th>Very Good</th><th>Excellent</th></tr>
<tr><td>0.5</td><td>1.5</td><td>2</td></tr>
</table>
</td></tr>
</table>

<table>
<tr><th>Part 3 – Environmental Protection</th><th>Green Mark Points</th></tr>
<tr><td>NRB 3-3 Greenery Provision
Encourage greater use of greenery, restoration of trees to reduce heat island effect.
(a) Green Plot Ratio (GnPR) is calculated by considering the 3D volume covered by plants using the prescribed Leaf Area Index (LAI).</td><td><table>
<tr><th>GnPR</th><th>Points Allocation</th></tr>
<tr><td>0.5 to < 1.0</td><td>1</td></tr>
<tr><td>1.0 to < 1.5</td><td>2</td></tr>
<tr><td>1.5 to < 3.0</td><td>3</td></tr>
<tr><td>3.0 to < 3.5</td><td>4</td></tr>
<tr><td>3.5 to < 4.0</td><td>5</td></tr>
<tr><td>≥ 4.0</td><td>6</td></tr>
</table></td></tr>
<tr><td>(b) Restoration, conservation or relocation of existing trees on site.</td><td>1 point</td></tr>
<tr><td>(c) Use of compost recycled from horticulture waste.</td><td>1 point</td></tr>
<tr><td>NRB 3-4 Environmental Management Practice
Encourage the adoption of environmental friendly practices during construction and building operation.</td><td></td></tr>
<tr><td>(a) Implement effective environmental friendly programmes including monitoring and setting targets to minimise energy use, water use and construction waste.</td><td>1 point</td></tr>
<tr><td>(b) Main builder that has good track records in the adoption of sustainable, environmentally friendly and considerate practices during construction such as the Green and Gracious Builder Award.</td><td>1 point</td></tr>
<tr><td>(c) Building quality assessed under the Construction Quality Assessment System (CONQUAS).</td><td>1 point</td></tr>
<tr><td>(d) Developer, main builder, M & E consultant and architect that are ISO 14000 certified.</td><td>0.25 point for each firm
(Up to 1 point)</td></tr>
<tr><td>(e) Project team comprises Certified Green Mark Manager (GMM), Green Mark Facilities Manager (GMFM) and Green Mark Professional (GMP).</td><td>0.5 point for certified GMM
0.5 point for certified GMFM
1 point for certified GMP
(Up to 1 point)</td></tr>
<tr><td>(f) Provision of building users' guide that should include details of the environmental friendly facilities and features within the building and their functionalities in achieving the intended environmental performance during building operation.</td><td>1 point</td></tr>
<tr><td>(g) Provision of facilities or recycling bins for collection and storage of different recyclable waste such as paper, glass, plastic food waste etc.</td><td>1 point</td></tr>
</table>

Part 3 – Environmental Protection	**Green Mark Points**
NRB 3-5 Green Transport Promote environmental friendly transport options and facilities to reduce pollution from individual car use.	
(a) Good access to nearest MRT/LRT or bus stops.	1 point
(b) Provision of covered walkway to facilitate connectivity and the use of public transport.	1 point
(c) Provision of electric vehicle charging stations and priority parking lots within the development.	Extent of Coverage : Minimum one(1) electric vehicle charging station and priority parking lot for every 100 carpark lots *(Cap at 5)* 1 point
(d) Provision of sheltered bicycle parking lots with adequate shower and changing facilities.	Extent of Coverage : Minimum ten (10) bicycle parking lots *(Cap at 50)* Points scored based on the number of bicycle parking lots provided *(with adequate shower and changing facilities)* 1 point if the number provided ≥ 3% x Gross Floor Area (GFA)/10 0.5 point if the number provided ≥ 1.5% x Gross Floor Area (GFA)/10
NRB 3-6 Refrigerants Reduce the potential damage to the ozone layer and the increase in global warming caused by the release of ozone depleting substances and greenhouse gases.	
(a) Refrigerants with ozone depletion potential (ODP) of zero or with global warming potential (GWP) of less than 100.	1 point
(b) Use of refrigerant leak detection system in critical areas of plant rooms containing chillers and other equipments with refrigerants.	1 point
NRB 3-7 Stormwater Management Encourage treatment of stormwater run-off before discharge to the public drains. Provision of infiltration or design features as recommended in PUB's ABC Waters Design Guidelines : ▪ Bioretention swales/ other bioretention ▪ systems ▪ Rain gardens ▪ Constructed wetlands ▪ Cleansing biotopes ▪ Retention ponds	Points scored based on the extent of stormwater treatment. 3 points for treatment of run-off from more than 35% of total site area or paved area 2 points for treatment of run-off from 10% to 35% of total site area 1 point for treatment of run-off from up to 10% of total site area
PART 3 – ENVIRONMENTAL PROTECTION CATEGORY SCORE :	Sum of Green Mark Points obtained from NRB 3-1 to 3-7

Part 4 – Indoor Environmental Quality	**Green Mark Points**
NRB 4-1 Thermal Comfort Air-conditioning system is designed to allow for cooling load variation due to fluctuations in ambient air temperature and to maintain consistent indoor conditions for thermal comfort. Indoor operative temperature between 24 °C to 26 °C Relative humidity < 65%	1 point
NRB 4-2 Noise Level Occupied spaces in buildings are designed with good ambient sound levels as recommended in SS 553 Table 4 – Recommended ambient sound level.	1 point
NRB 4-3 Indoor Air Pollutants Minimise airborne contaminants, mainly from inside sources to promote a healthy indoor environment. (a) Use of low volatile organic compounds (VOC) paints certified by approved local certification body. (b) Use of environmental friendly adhesives certified by approved local certification body.	Extent of Coverage : At least 90% of the total internal wall areas 1 point Extent of Coverage : At least 90% of the applicable areas 1 point
NRB 4-4 Indoor Air Quality (IAQ) Management Ensure that building ventilation systems are designed and installed to provide acceptable IAQ under normal operating conditions. (a) Provision of filtration media and differential pressure monitoring equipment in Air Handling Units (AHUs) in accordance with SS 554: Clause 4.3.4.5 and its Annex E. (b) Implement effective IAQ management plan to ensure that building ventilation systems are clean and free from residuals left over from construction activities. Internal surface condition tests for ACMV systems are to be included.	1 point 1 point
NRB 4-5 High Frequency Ballasts *Applicable to offices, classrooms and the like* Improve workplace lighting quality by avoiding low frequency flicker associated with fluorescent lighting with the use of high frequency ballasts in the fluorescent luminaries.	Extent of Coverage : At least 90% of all applicable areas that are served by fluorescent luminaries 2 points
PART 4 – INDOOR ENVIRONMENTAL QUALITY CATEGORY SCORE :	Sum of Green Mark Points obtained from NRB 4-1 to 4-5

Part 5 – Other Green Features	Green Mark Points
NRB 5-1 Green Features and Innovations Encourage the use of other green features that are innovative and/or have positive environmental impact. Examples : ▪ Pneumatic waste collection system ▪ Carbon footprint of development ▪ Calculation of Concrete Usage Index (CUI) ▪ Dual chute system ▪ Self cleaning façade system ▪ Conservation of existing building structure	2 points for high impact item 1 point for medium impact item 0.5 point for low impact item (Up to 7 points)
PART 5 – OTHER GREEN FEATURES CATEGORY SCORE :	Sum of Green Mark Points obtained from NRB 5-1

Green Mark Score (Non-Residential)

Green Mark Score (Non-Res) = ∑Category Score [(Part 1 – Energy Efficiency) +
(Part 2 – Water Efficiency) +
(Part 3 – Environmental Protection) +
(Part 4 – Indoor Environmental Quality) +
(Part 5 – Other Green Features)]

where Category Score for Part 1 ≥ 30 points and
∑Category Score for Part 2, 3, 4 & 5 ≥ 20 points

10.11 LUSH 2.0 landscape replacement circular

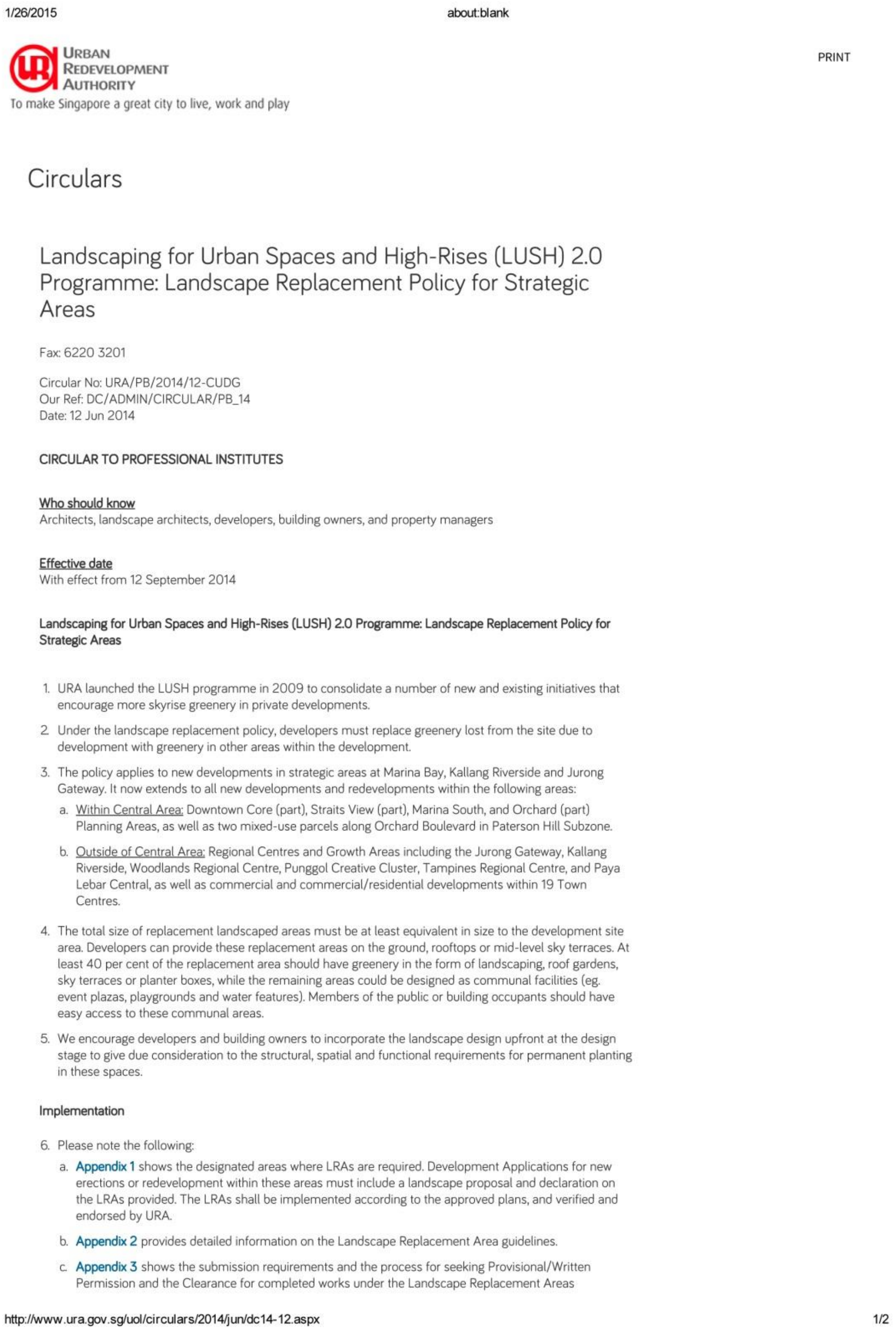

1/26/2015 about:blank

URBAN
REDEVELOPMENT
AUTHORITY
To make Singapore a great city to live, work and play

PRINT

Circulars

Landscaping for Urban Spaces and High-Rises (LUSH) 2.0 Programme: Landscape Replacement Policy for Strategic Areas

Fax: 6220 3201

Circular No: URA/PB/2014/12-CUDG
Our Ref: DC/ADMIN/CIRCULAR/PB_14
Date: 12 Jun 2014

CIRCULAR TO PROFESSIONAL INSTITUTES

Who should know
Architects, landscape architects, developers, building owners, and property managers

Effective date
With effect from 12 September 2014

Landscaping for Urban Spaces and High-Rises (LUSH) 2.0 Programme: Landscape Replacement Policy for Strategic Areas

1. URA launched the LUSH programme in 2009 to consolidate a number of new and existing initiatives that encourage more skyrise greenery in private developments.
2. Under the landscape replacement policy, developers must replace greenery lost from the site due to development with greenery in other areas within the development.
3. The policy applies to new developments in strategic areas at Marina Bay, Kallang Riverside and Jurong Gateway. It now extends to all new developments and redevelopments within the following areas:
   a. Within Central Area: Downtown Core (part), Straits View (part), Marina South, and Orchard (part) Planning Areas, as well as two mixed-use parcels along Orchard Boulevard in Paterson Hill Subzone.
   b. Outside of Central Area: Regional Centres and Growth Areas including the Jurong Gateway, Kallang Riverside, Woodlands Regional Centre, Punggol Creative Cluster, Tampines Regional Centre, and Paya Lebar Central, as well as commercial and commercial/residential developments within 19 Town Centres.
4. The total size of replacement landscaped areas must be at least equivalent in size to the development site area. Developers can provide these replacement areas on the ground, rooftops or mid-level sky terraces. At least 40 per cent of the replacement area should have greenery in the form of landscaping, roof gardens, sky terraces or planter boxes, while the remaining areas could be designed as communal facilities (eg. event plazas, playgrounds and water features). Members of the public or building occupants should have easy access to these communal areas.
5. We encourage developers and building owners to incorporate the landscape design upfront at the design stage to give due consideration to the structural, spatial and functional requirements for permanent planting in these spaces.

Implementation

6. Please note the following:
   a. Appendix 1 shows the designated areas where LRAs are required. Development Applications for new erections or redevelopment within these areas must include a landscape proposal and declaration on the LRAs provided. The LRAs shall be implemented according to the approved plans, and verified and endorsed by URA.
   b. Appendix 2 provides detailed information on the Landscape Replacement Area guidelines.
   c. Appendix 3 shows the submission requirements and the process for seeking Provisional/Written Permission and the Clearance for completed works under the Landscape Replacement Areas

http://www.ura.gov.sg/uol/circulars/2014/jun/dc14-12.aspx 1/2 guidelines. Where relevant, URA's clearance of the completed LRAs is required before the Commissioner of Building Control issues the Temporary Occupation Permit (TOP) or Certificate of Statutory Completion (CSC) if no application is made for TOP.

7. This circular supersedes the earlier circular for Landscape Replacement Areas (LRA) dated 29 Apr 2009 (URA/PB/2009/09-CUDG) and will take effect from 12 Sep 2014 onwards.
8. The revised guidelines will apply to all new applications submitted on or after 12 September 2014[1]. Only formal development applications (excluding Outline Applications) submitted before 12 September 2014 which have already been granted Provisional Permission or which will result in a Provisional Permission, will not be subject to the revised guidelines.
9. I would appreciate it if you could convey the contents of this circular to the relevant members of your organisation. If you or your members have any queries concerning this circular, please contact Ms Ouyang Zhuorui at Tel: 6321 8188 (email: ouyang_zhuorui@ura.gov.sg) or Ms Juliana Tang at Tel: 6671 1044 (email: juliana_tang@ura.gov.sg). For your information, our past circulars and guidelines are available from our website http://www.ura.gov.sg

Thank you.

FUN SIEW LENG (MS)
GROUP DIRECTOR (URBAN PLANNING & DESIGN)
For CHIEF EXECUTIVE OFFICER
URBAN REDEVELOPMENT AUTHORITY

HWANG YU-NING (MS)
GROUP DIRECTOR (PHYSICAL PLANNING)
For CHIEF EXECUTIVE OFFICER
URBAN REDEVELOPMENT AUTHORITY

---

[1] Development applications submitted before the effective date 12 Sep 2014 resulting in an Advice or Refusal of Written Permission (RWP) will be evaluated based on the revised guidelines upon resubmission after the Advice or RWP.

Join URA's mailing list to get the latest updates on current and future plans and developments around Singapore. Click here to subscribe (http://www.ura.gov.sg/uol/Newsletters/Subscribe.aspx)

Back To

CIRCULARS

10.12 Response to comments from examiners

10.12.1 Comments from Examiner 1

Comment:

The link between Knowledge Gap, Research Questions and Objectives are not clear. The candidate needs to rework on this to make the flow of the thesis smoother.

Response:

Knowledge Gap is on page 79

Research Question is on page 22

Objectives is on page 22

Knowledge Gap is elaborated as follows:

"…

1.3 Knowledge Gap

A thorough review of relevant literature reveals that although the benefits of urban greenery have been widely established, there is a lack of objective and systematic methodology for landscape planning based on the temperature reduction potential of plants. While landscape planners and architects may be aware of how greenery can reduce temperature, they are unable to evaluate the temperature reduction potential of their landscape design proposals based on their choice and placement of plants.

The thesis seeks to address this issue by first identifying the appropriate environment component that can be used to evaluate the cooling potential of plants. Thereafter, plant traits that affect temperature reduction are identified and empirically modelled as variables for temperature reduction. The model will be used as a basis for an objective landscape planning framework for landscape design optimisation.

…"

Comment:

Figure 20 on the Research Methodology needs improvement.

Response:

Research methodology (Figure 20) elaborated.

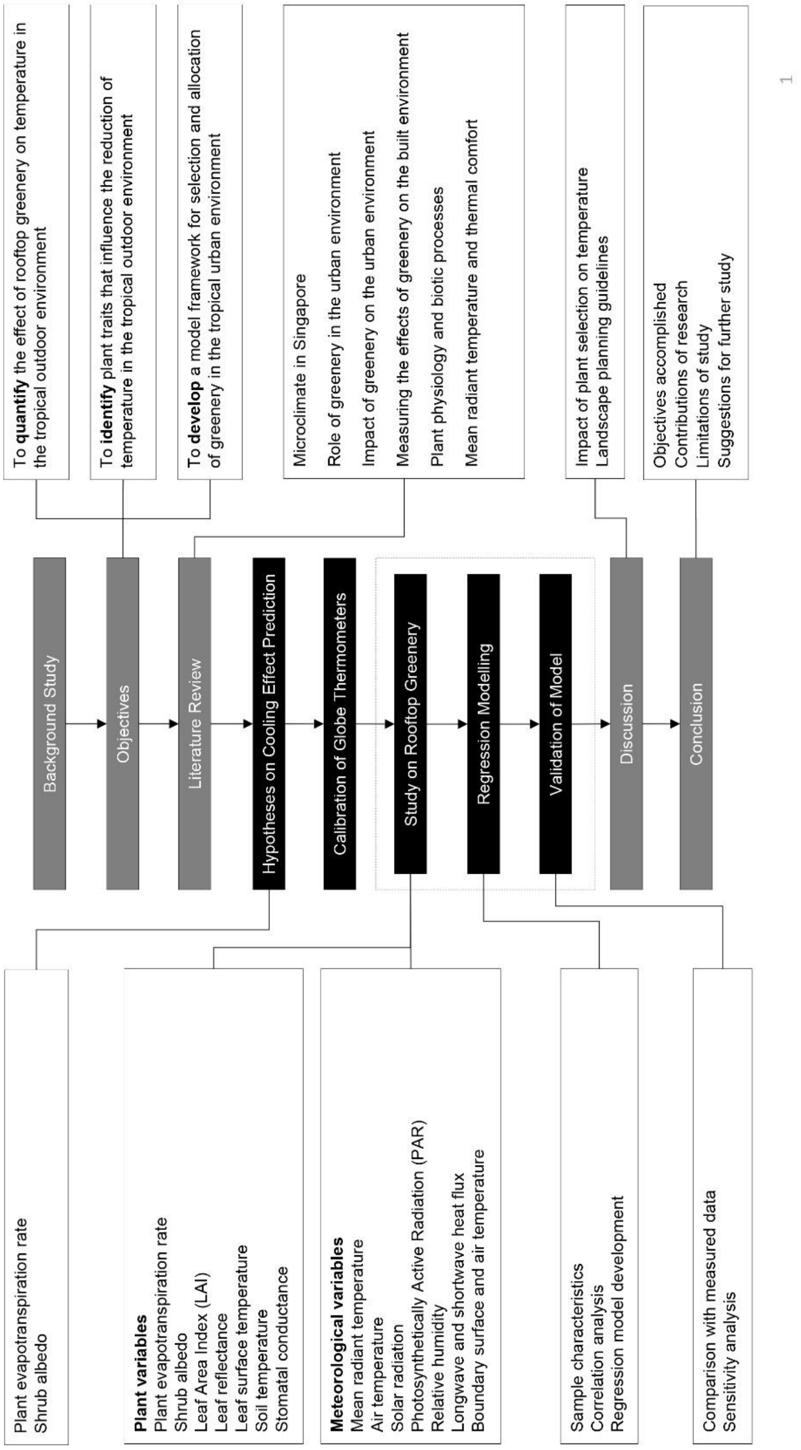

Comment:

The candidate should elaborate on the limitations of the experimental parts to justify the issues with sample size, repeatability and reproducibility. An example is section 3.5.

Response:

Currently, the limitations are as follows:

Structure of the substrate for shrubs on green roofs differs significant from shrubs at ground level. The depth of the substrate at green roofs is typically much shallower than conventional plantings at ground level (Extensive roof garden plots). This will have an impact on the overall evapotranspiration rate for plants.

Studies are conducted in the tropical urban environment. Due to differences in aridity and solar exposure, results may not be valid for temperate regions.

The study assumes all plants of the same genus to have statistically similar physiological attributes.

Limitations to sample size is added as follows:

The sample size is limited to three samples. If more plants of different species are used, the regression model will be representative of a larger spectrum of plants.

The regression model may not be representative of all shrub types. Some shrubs such as CAM plants or plants that experience mid-day stomatal depression plants (Discussed in Chapter 6.1.1) should not be used to construct the regression model.

10.12.2 Comments from Examiner 2

Comment:

In the abbreviation section, only the abbreviations of some commonly used terms are provided. Mathematical abbreviations should also be included to facilitate reading of the thesis.

Response:

Mathematical abbreviations are elaborated below all equations to facilitate reading

Comment:

P.1 5th line: state whether the 48% means the percentage of the world's population.

Response:

Rephrased

Comment:

P.15 last line: indicate where is the green area.

Response:

Amended to "… in forested areas…"

Comment:

P.61 Eqt 15: state the location where the air velocity and temperature are measured when using the equation.

Response:

To be added below Equation 15 "…

t_g = Globe temperature (°C), measured by a temperature sensor placed inside the globe

V_a = Air velocity (ms^{-1}), measured at the level of the globe

t_a = Air temperature (°C), measured near the globe

Comment:

P.76:

1st line: explain how F_i=0.167 is obtained for a sphere or quoted relevant reference.

9th line after Eqt 19: Equation (22) should be Equation (15).

Eqt 20 is the same as Eqt 15 and should be corrected to avoid confusion.

Response:

Value of F_i=0.167 was quoted from Fanger (1972). Citation added.

Equation number amended

Equation number amended

Fanger, P. O., 1972, Thermal comfort. Analysis and applications in environmental engineering, New York: McGraw-Hill.

Comment:

P.77 9th line: explain how the mean wind speed was obtained, for example, state the location where the measurement was conducted.

Response:

Added:

"… Mean wind speed was measured with a weather station that was placed within 10 m of the mean radiant temperature measurement site…"

Comment:

P.92 Table 7: State whether there are any special treatment of data (e.g. discarded) under raining or thunderstorm condition.

Response:

Added:

"… Not all data obtained was used for analysis. For Chapter 4, results shown are representative of typical clear or overcast sky conditions. Rainy days are not used for analysis unless no suitable alternatives are available..."

Comment:

P.103 2nd and 3rd line: it mentioned that the dip in air temperature was observed and is likely due to a short period of rain. If this is the case, it should not be used for analyzing the ambient temperature variation due to the plant species under overcast conditions.

Response:

The 12th of July was used as there were no suitable alternatives to observe the effect of plants on overcast days. It is important to note that rain only occurred for a very short period (06:47 hrs to 06:53 hrs) and should not affect analysis of peak temperature conditions around 16:30 hrs.

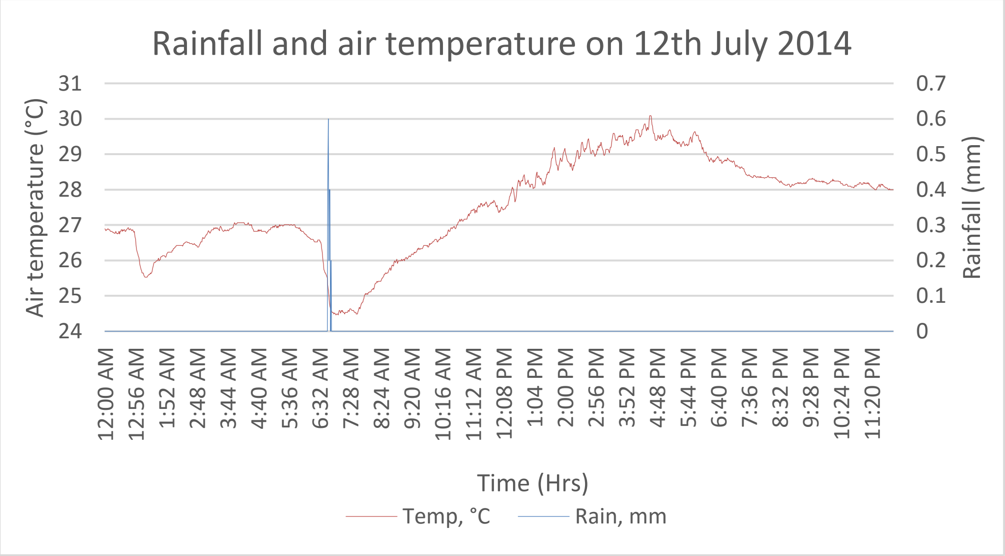

Air temperature for 5th July 2014 was highly erratic due to rain (05:00 hrs to 17:00 hrs) and therefore deemed unsuitable for analysis of air temperature.

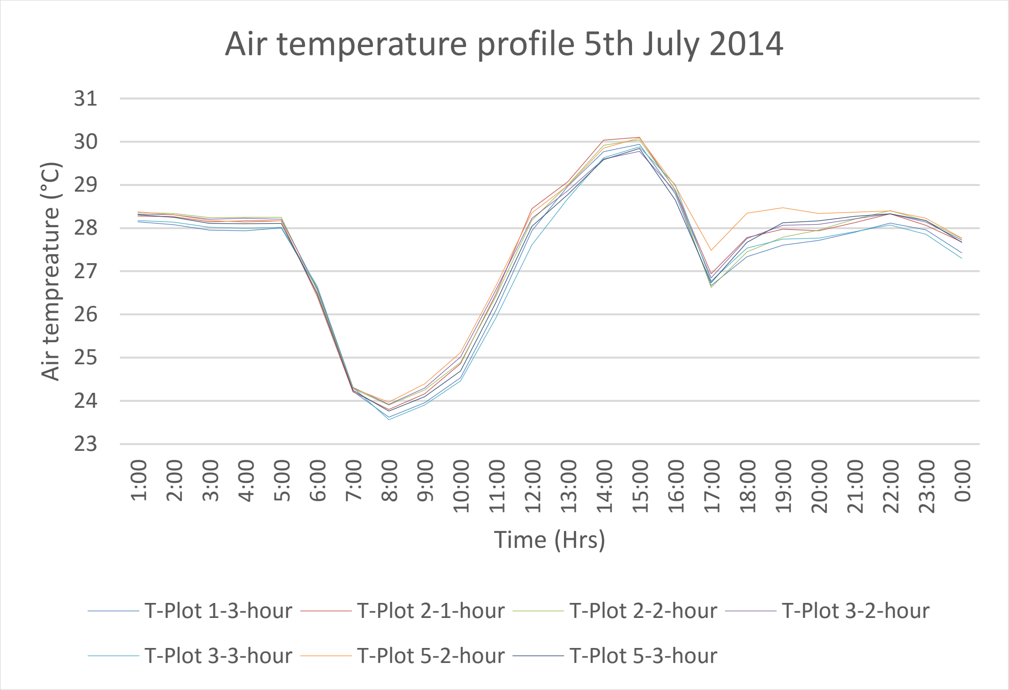

Comment:

P.104 Figure 39: specify the weather condition on 26 July 14 whereas the maximum temperature occurred at 5 pm.

Response:

Weather condition specified below:

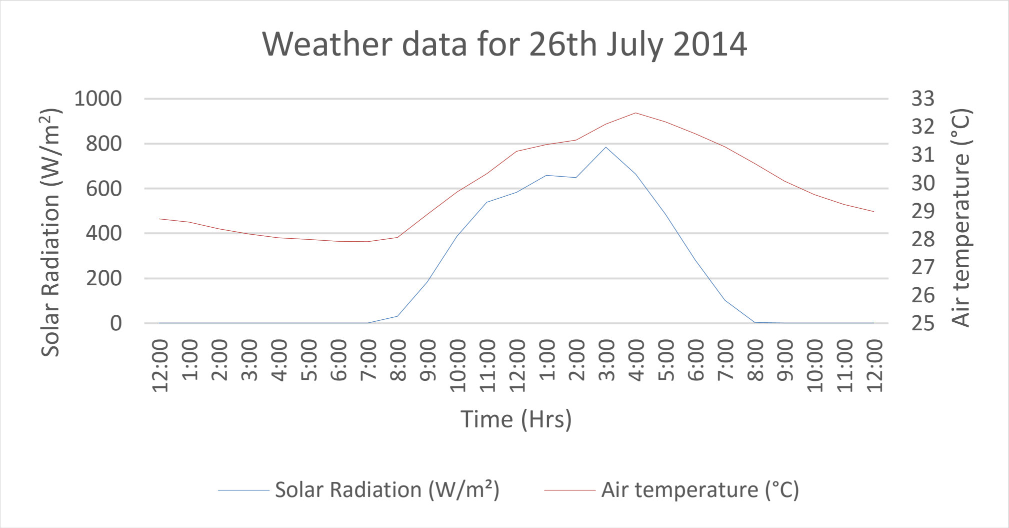

Comment:

P106 last 3rd line: the explanation on the lowered temperature within the canopy for Plot 3 is not reasonable.

Response:

Plot 3 (Sphagneticola trilobatta) provides a lush canopy cover and a thick undergrowth of stems below the canopy. As a result, the undergrowth is very well-shaded from the sun and pockets of air with lower temperature is observed.

Comment:

P.118: there is no deep analysis on the cause of the discrepancy of LAI results obtained from different methods and no determination on whether the indirect or direct measurement result should be adopted or not for analysis. Noted that the results of the indirect method and the literature matched with each other. Furthermore, the result of the soil temperature also matched with the result of LAI determined by the indirect method as shown in Fig. 59 on P.124. However, on P.136 it is concluded that there is no correlation between LAI and the mean radiant temperature. Such a conclusion is not persuasive.

Response:

The purpose of measuring LAI using these different methods is to:

Identify the most accurate value of LAI for the 3 types of plants being studied

To ascertain the influence of LAI in mean radiant temperature reduction using statistical methods

Method 1: Indirect measurement using LAI-2000

Method 2: Direct measurement by plucking leaves and calculating total amount of green pixels

Method 3: Reference to NParks handbook

The most accurate method of LAI measurement is via Method 2. This is because every leaf will be measured at a high degree of precision. However, it is often impractical to employ Method 2 as this is a destructive method and leaves have to be physically removed. Also, it requires extensive manpower to pluck, scan and count the number of green pixels.

Method 1 is a non-destructive and more convenient method of measuring LAI. However, LAI is measured in the form of light attenuation and not actual leaf count. This method is not able to differentiate between light blocked by a single leaf and light blocked by multiple leaves in the canopy. This method is often used to measure LAI of large forested areas and trees with large canopies

Method 3 is a generalised method of assigning LAI values to plants for the purpose of landscape planning.

Values of LAI obtained via Method 2 were deemed to be most accurate.

Values of LAI obtained via Methods 1 and 3 were displayed in Table 9 were used as a comparison. It could be observed that there were significant over and under-estimates of LAI using Methods 1 and 3. LAI for Heliconica (Plot 2) is lower using Method 1 most likely due to the fact that leaves of the Heliconia plant, while large, do not spread horizontally across the shrub and are hanging vertically from the stem. This results in larger open spaces within the canopy, leading to more light captured by the LAI-2000 sensor.

Table: Averaged Leaf Area Indices for Plot 1 to Plot 3

Plot		LAI measurement method					
		Indirect measurement (Using LAI-2000)				Direct measurement (Plucking out leaves in 50 x 50 cm plot, pixel calculation)	Nparks handbook (Tan and Sia, 2009)
		1	2	3	Ave		
1	Phyllanthus cochinchinensis Shrub (Dicot)	4.65	4.22	4.16	4.34	2.78	4.5
2	Heliconia American Dwarf Shrub (Monocot)	3.14	3.69	3.58	3.47	7.21	3.5
3	Sphagneticola trilobata Ground cover	4.70	4.28	4.83	4.60	3.59	4.5

Subsequently, values of LAI obtained via Method 2 were used for analysis.

It can be observed that Plot 2 has the highest LAI of 7.21 from the direct measurement method, which is the most accurate method of measuring LAI. However, the corresponding reduction in T_{mrt} is the lowest. This can be explained by the lack of water transferred to its leaves during periods of high solar irradiance. This results in a higher leaf surface temperature, which can be observed using infrared thermography (figure below).

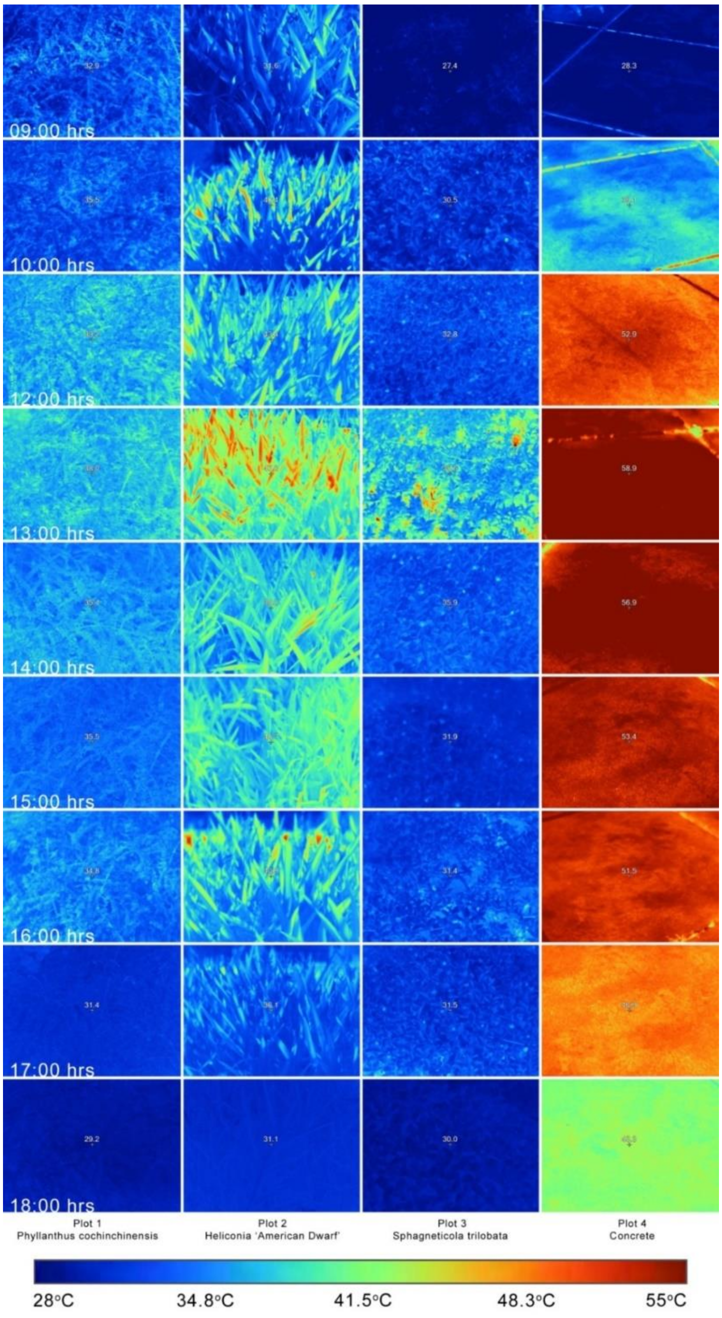

Numerous studies have shown plant Leaf Area Index to be strongly correlated with temperature reduction. In such cases, temperature reduction is mostly due to shade provided by tree canopy, resulting in reduced heat absorbed by building surfaces, pavements and pedestrians (Fahmy et al., 2010; Gómez-Muñoz et al., 2010; Hardin and Jensen, 2007). Shahidan et al. (2010) found a strong correlation between thermal radiation filtration and LAI for M. Ferrea L and H. crepittan (R2 = 0.96 and 0.95). A higher LAI will result in more layers of leaves that will result in reduction thermal radiation under a tree (Brown and Gillespie, 1995; Kotzen, 2003).

However, with regards to the impact of LAI on T_{mrt}, this study has shown that LAI is not strongly correlated with T_{mrt} reduction. On the contrary, temperature is increased with higher LAI. One hypothesis put forth by the author is that as leaf area increases, ease of delivery of water from soil to leaf is reduced. This will result in increased leaf surface temperature. For the same LAI, however, it may be possible to find plants with smaller leaf areas and more leaves. This in turn may result in lower surface temperature for the leaves. Further study is required to validate this assumption. This would suggest that overall radiative qualities of the plant canopy (albedo, absorptance, reflectance, canopy structure) are more substantial at determining its impact on T_{mrt}.

It is the opinion of the author that besides looking solely at LAI, plant functional traits may affect overall temperature reduction potential. This was highlighted in Chapter 6.1.3. A variable that combines values of LAI as well as plant functional traits such as shrub height, leaf dimension, stem structure etc. may provide more insight into how they can provide effective temperature reduction.

References:

Fahmy, M., Sharples, S., Yahiya, M., 2010, LAI based trees selection for mid latitude urban developments: A microclimatic study in Cairo, Egypt, Building and environment 45(2):345-357.

Gómez-Muñoz, V. M., Porta-Gándara, M., Fernández, J., 2010, Effect of tree shades in urban planning in hot-arid climatic regions, Landscape and urban planning 94(3):149-157.

Hardin, P. J., Jensen, R. R., 2007, The effect of urban leaf area on summertime urban surface kinetic temperatures: A Terre Haute case study, Urban Forestry & Urban Greening 6(2):63-72.

Shahidan, M. F., Shariff, M. K., Jones, P., Salleh, E., Abdullah, A. M., 2010, A comparison of Mesua ferrea L. and Hura crepitans L. for shade creation and radiation modification in improving thermal comfort, Landscape and Urban Planning 97(3):168-181.

Brown, R. D., Gillespie, T. J., 1995, Microclimatic landscape design: creating thermal comfort and energy efficiency, John Wiley & Sons.

Kotzen, B., 2003, An investigation of shade under six different tree species of the Negev desert towards their potential use for enhancing micro-climatic conditions in landscape architectural development, Journal of Arid environments 55(2):231-274.

Comment:

P.127 Fig. 61:

I. Give more details on how the incident/reflected shortwave/longwave radiations were measured.

II. It is not understandable why the incoming radiation depends on the plant species.

Response:

I. Figure provided below:

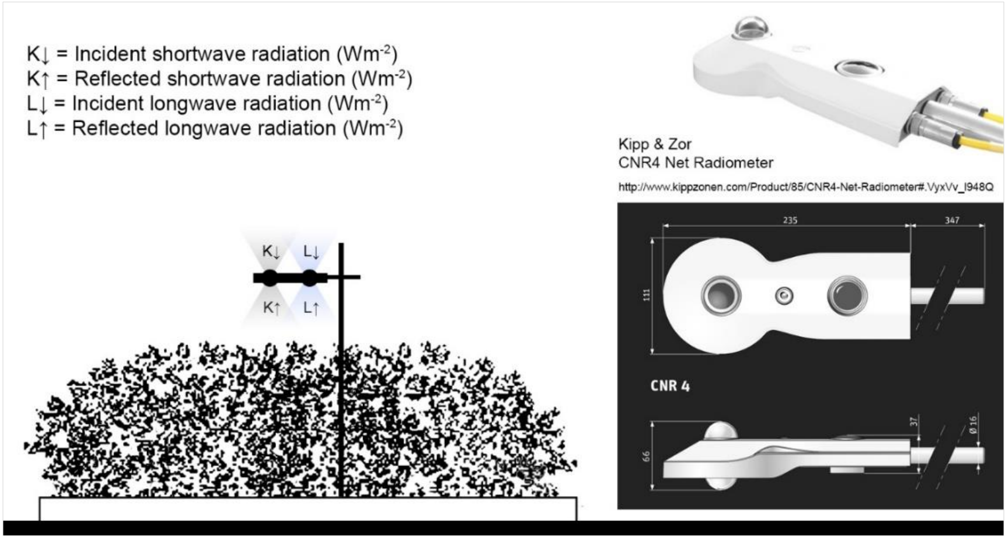

http://www.kippzonen.com/Product/85/CNR4-Net-Radiometer#.VyxVv_I948Q

II. Incoming radiation does not depend on plant species. They are slightly different as they are located 5 to 11 m apart from each other.

Comment:

P.134-135: Comparison of data was done on a specific day only, it is not enough to make a conclusion based on one day's result.

Response:

Added "…It is important to note that this is data for one typical day with clear sky conditions and a limitation is that it may not represent a general characteristic of the plants…"

Comment:

P.137 last 11th line: there is little discussion on LAI in this study. Many studies indicate LAI has strong cooling effect on the environment and it is used as a criterion for tree selection. Inclusion of this parameter may improve the accuracy of the regression equation.

Response:

Please refer to item 11 for explanation of why LAI was not used for regression equation

Comment:

P.138 table 12: the presentation in this table is confusing, as the data in columns 2-5 are referred to all the variables in column one.

Response:

Reformatted to:

Variable	**Total no. of days measured**	**Dates selected for regression modelling (2014)**		**No. of days used for modelling**
Mean radiant temperature above rooftop greenery $t_{mrt(\text{plant})}$ Reference mean radiant temperature $t_{mrt(ref)}$ Plant EvapoTranspiration Rate (ET) Shrub Albedo (SA)	10/05/2014 to 31/12/2014 236 days	May	13, 15, 22, 24, 25, 28, 29	35 days
		June	8, 10, 11, 13, 16, 17, 18, 19, 20, 21, 22, 23, 24, 25	
		July	1, 7, 8, 10, 13, 16, 18, 20, 21, 25, 26	
		August	17	
		September	1, 2	

Comment:

P.142 Fig. 70: from the observation, the correlation between ET and Tmrt and between shrub Albedo and Tmrt are not too high as mentioned, particularly the former one.

Response:

Albedo and Plant ET are hypothesized to be significant variables that can reduce T_{mrt} from reviewed literature.

Although correlation with ET and Albedo are not too high, the two variables exhibit high substantive significance from reviewed literature as well as results from measured data (infrared surface temperature measurements, stomatal conductance measurements, etc.). Results from regression modelling also show that they are significant variables and to omit them would be to commit a Type 2 statistical error.

Comment:

P.160 Figure 82: ET depends on plant species and solar intensity, explain how to determine a representative ET rate and why ET was averaged from 13:00 to 17:00 hrs.

Response:

Reviewed literature shows that ET can be represented in different timescales ($mm \cdot day^{-1}$, $mm \cdot hour^{-1}$, etc). For this case, ET was averaged from 13:00 hrs to 17:00 hrs for the purpose of comparing with ET values used for regression modelling (also average of 13:00 hrs to 17:00 hrs).

Comment:

P.163 last 4th line: the statement “there is evidence to suggest that leaves with smaller …” needs justification or quote relevant reference.

Response:

This is in reference to data obtained from this study. Comparison of leaf size and leaf surface temperature shows that bigger leaves tend to have higher temperatures. Please refer to Figure 58: Infrared thermography of green roof plots and concrete and Figure 83. Botanical illustration of plants used for measurement.

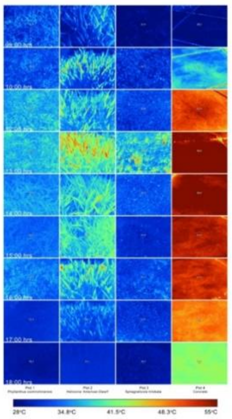

Figure 58

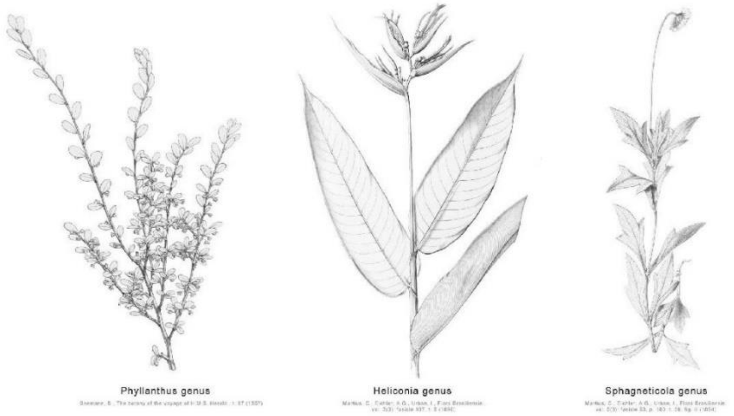

Figure 83

Comment:

P.180: explain how the Tmrt reduction due to the introduction of trees with small canopies, large canopies and more trees can be obtained during the first 3 iterations.

Response:

In Iterations 1 to 3, T_{mrt} is reduced as shortwave radiation is blocked by tree canopies. Trees with bigger canopies provide larger blockage of shortwave radiation and hence provide more reduction to T_{mrt}

Comment:

P.200: this chapter would better be separated into two parts, one is the reference that have been quoted in the manuscript. The other part is the bibliography.

Response:

Chapter renamed as “References”

Typographical and grammatical errors

Check all the equations with proper typing of subscript to avoid confusion.

P.iv 12th line: “quantify air temperature (ta)”.

P.69 4th line: “The variables to be measured ….”.

P.86 5th line: “….the level of uncertainty …”.

P.102 last 4th line: Plot 4 should be Plot 1. Also on last 3rd line: “It can also be ….”.

The title of many figures (e.g. Figs. 42 to 51) should be amended to truly reflect their contents. For example, to reflect the content in Fig. 42, the title should better be hourly variation of solar radiation and mean radiant temperature over the day.

P.124 4th line: “higher than that”.

P.127 last 3rd line: “Plot 2 is higher than that of Plot 2 made Plot 3.”\

P.130 7th line: “…. Lower than that.

P.138 6th line: “due to one or more ….”

P.153 Section 5.2.2 Sensitivity analysis of prediction model: the analysis can be simplified without the need of the graphical determination. The conclusions in this section (e.g. for every increase of 1 oC for tmrt (plant), there is a corresponding increase of 0.8 oC for tmrt (plant)) can be derived directly from Eqt. 25.

Response:

All typographical and grammatical errors have been amended

10.12.3 Comments from Examiner 3

Comment:

Comparative efficacy of rooftop greenery as the background

In the introduction of research question on the page 6, you have question to the efficacy of rooftop greenery to the urban microclimate as the background of this research. However, it is difficult to discuss absolute value of the effect of individual UHI countermeasure because UHI is quite complex phenomenon and each element might influence each other. So, this kind of effect should be discussed under the comparison to other existing countermeasures; for example high-reflection paint, water retention material and so on.

My suggestion is making a simple study on the effect of other countermeasure in the same condition or citing other achievements to clarify the comparative efficacy of rooftop greenery as the background.

Response:

Urban greenery has been proven to be an effective UHI mitigation component. Although this thesis has focused solely on the temperature reduction potential of rooftop greenery, the author fully acknowledges the mitigative impact of other various UHI countermeasures such as cool paint and water retention material. Comparison with other UHI countermeasures have been conducted in the author's capacity as a research assistant. These studies include:

I. Study of temperature reduction potential for rooftop greenery and cool roof
II. Study of temperature reduction potential of rooftop greenery system with water retention layer
III. Study of temperature reduction potential of trees in the urban environment

IV. Study of temperature reduction potential of vertical greenery in the urban environment

These studies have been represented in the following manner:

I. Wong, N.H., Jusuf, S.K., **Tan, C.L**., Chia, P.Y., 2013, Effect of cool roofs and green roofs on temperature in the tropical urban environment, AIVC 2013, Athens. Oral Presentation by Jusuf, S.K., Published in proceedings.

II. Wong, N.H., Tan, P.Y., **Tan, C.L.**, Lim, C.V.J., Chua, H.X.V., Takasuna, H., Kudo, T., Takemasa, Y., 2016, Impact of Soil and Water Retention Characteristics on Green Roof Thermal Performance, 4th International Conference on Countermeasures to Urban Heat Island, 30-31 May and 1 June 2016, National University of Singapore, Singapore.

III. Chapter 10.1 of thesis

IV. Chapter 10.3 of thesis

These studies can help provide a more holistic understanding of common UHI countermeasures.

Comment:

Basis of hypothetical urban model

In the discussion of landscape planning guidelines on the page 177, you suggest hypothetical urban model as a case study. However, it is possible to show different result if the model is different as many past achievement mentioned. This study may have been delivered based on specified idea.

My suggestion is remarking the basis of the model; for example based on the existing urban district, arrangement of preliminary study result, to emphasize specified phenomenon, and so on to clarify significance of the case study.

Response:

The author acknowledges the importance of substantiating simulated results with actual measurements and that subsequent studies on actual sites may be considered should the opportunity arise.

However, the purpose of introducing the hypothetical study is to demonstrate the steps landscape planners can take to understand the thermal impact of their design decisions (Figure 88). These steps are used as a basis for recommendations to improve the existing green building rating tool in Singapore (BCA Green Mark Scheme). To provide simulated results for the purpose of validation against actual results is beyond the scope of this thesis and requires a wholly different methodology.

The objective of this exercise is to show that numerous design iterations can be made with tools that are readily available (Table 29).

Although the model is hypothetical, it is based on actual planning parameters used by the Urban Redevelopment Authority of Singapore (URA). Moreover, the first round of simulation is based on physical (not empirical) modelling. Therefore, simulation results derived from this hypothetical model should resemble actual conditions in a significant manner.